



TARGETING FLATWORM SIGNALING CASCADES FOR THE DEVELOPMENT OF NOVEL
ANTHELMINTHIC DRUGS

SIGNALKASKADEN VON PLATTWÜRMERN ALS ANGRIFFPUNKTE ZUR ENTWICKLUNG NEUER
ANTHELMINTHIKA

Doctoral thesis for a doctoral degree
at the Graduate School of Life Sciences,
Julius-Maximilians-Universität Würzburg,
Section Infection and Immunity

submitted by

VERENA MAGDALENA GELMEDIN

from

SAARBRÜCKEN

Würzburg 2008

Submitted on:

Office stamp

Members of the *Promotionskomitee*:

Chairperson: Prof. Dr. Manfred Gessler

Primary Supervisor: Prof. Dr. Klaus Brehm

Supervisor (Second): Prof. Dr. Roland Benz

Supervisor (Third): Prof. Dr. Joachim Morschhäuser

Date of Public Defence:

Date of receipt of Certificates:

AFFIDAVIT

I hereby declare that my thesis entitled TARGETING FLATWORM SIGNALING CASCADES FOR THE DEVELOPMENT OF NOVEL ANTHELMINTHIC DRUGS is the result of my own work. I did not receive any help or support from third parties, i.e. commercial consultants or others. All sources and/or material are listed and specified in the thesis.

Furthermore, I verify that this thesis, neither in identical nor similar form, has not yet been submitted as part of another examination process.

I confirm that the information which I have given in this application is complete and true.

Würzburg,

DANKSAGUNG

An dieser Stelle möchte ich die Gelegenheit nutzen, mich bei denjenigen zu bedanken, die zum Gelingen dieser Arbeit beigetragen haben – in wahlloser Reihenfolge:

Prof. Dr. Klaus Brehm für die sehr gute Betreuung und permanente Unterstützung dieser Arbeit, die anschaulichen Diskussionen und die enthusiastischen und lebendigen Ausflüge in die Parasitenkunde, aber auch in die Geschichte

Prof. Dr. Matthias Frosch

Prof. Dr. Roland Benz und Prof. Dr. Morschhäuser für die Übernahme der Gutachten und die Teilnahme an der Prüfungskommission

Meiner Trainingsgruppe des internationalen Graduiertenkollegs Würzburg-Nice GCWN 1141

Der Echinokokkenarbeitsgruppe Kerstin Epping, Sabine Lorenz, Dirk Radloff, Sophia Müller, Sarah Hemer, Ferenc Kiss, Markus Spiliotis und denjenigen, die nicht mehr dabei sind, für die angenehme Arbeitsatmosphäre und das Ausstatten meines Arbeitsplatzes, vor allem auch Christian Konrad, Monika Bergmann für die Unterstützung und die fränkischen Weisheiten, Rainer Brand für die tierisch gute Zusammenarbeit, Michael Ullrich für die Hilfsbereitschaft und das stets schnelle Beheben von technischen Defekten, den restlichen Mitarbeitern des Instituts für Hygiene und Mikrobiologie, die mich meine Promotionsstätte in guter Erinnerung behalten lassen

Xenia Schmidt, Valeska Guth und Carmen Ziegler für die langjährige Freundschaft

Meiner Familie

1. Summary	- 1 -
2. Introduction	- 4 -
2.1 Phylogeny and distribution of the genus <i>Echinococcus</i>	- 4 -
2.2 Life cycle of <i>E. multilocularis</i>	- 6 -
2.3 Alveolar echinococcosis	- 8 -
2.3.1 Alveolar echinococcosis and transmission risk	- 8 -
2.3.2 Alveolar echinococcosis and its manifestation	- 8 -
2.3.3 Treatment options and chemotherapy	- 9 -
2.4 Signaling in developmental and proliferation processes	- 10 -
2.4.1 Peptide growth factors and their receptors	- 12 -
2.4.2 The Erk1/2 MAPK module	- 13 -
2.4.3 The p38 MAPK module	- 14 -
2.4.4 The atypical MAPKs	- 15 -
2.4.5 Alternative pathways	- 15 -
2.5 Host-parasite interplay during alveolar echinococcosis	- 16 -
2.5.1 Early molecular and biochemical approaches	- 16 -
2.5.2 <i>In vitro</i> cultivation of <i>E. multilocularis</i>	- 17 -
2.5.3 Genomic sequencing project	- 17 -
2.5.4 Evolutionary conserved signaling in <i>E. multilocularis</i>	- 18 -
2.6 Aim of the project	- 20 -
3. Results	- 21 -
3.1 EmMPK2 – the p38 MAPK orthologue of <i>E. multilocularis</i> as a possible target for the treatment of AE	- 21 -
3.1.1 Identification and characterization of <i>emmpk2</i>	- 21 -
3.1.2 Expression analysis of <i>emmpk2</i> in <i>Echinococcus</i> larval stages	- 26 -
3.1.3 Expression and activity analyses of EmMPK2 in <i>Echinococcus</i> larval stages	- 27 -
3.1.4 EmMPK2 activation in <i>in vitro</i> cultivated metacestode vesicles	- 29 -
3.1.5 EmMPK2 – an enzymatically active MAP kinase	- 31 -
3.1.6 Treatment of <i>in vitro</i> cultivated metacestode vesicles with pyridinyl imidazoles	- 34 -
3.1.7 Treatment of <i>Echinococcus</i> primary cells with pyridinyl imidazoles	- 37 -
3.1.8 Treatment of <i>in vitro</i> cultivated protoscoleces with pyridinyl imidazoles	- 40 -
3.1.9 Effects of pyridinyl imidazoles on mammalian cells	- 42 -
3.2 Treatment of the cestodes <i>E. granulosus</i> and <i>T. crassiceps</i> with pyridinyl imidazoles	- 43 -
3.2.1 Partial characterization of the p38 MAPK homologue of <i>E. granulosus</i>	- 43 -
3.2.2 The p38 MAPK homologue of <i>T. crassiceps</i>	- 43 -
3.3 EmSSY- an unusual MAPK / a new type of MAPK?	- 47 -
3.4 Effects of miltefosine and perifosine on <i>in vitro</i> cultivated parasite material	- 50 -
3.4.1 <i>In vitro</i> treatment of <i>E. multilocularis</i> metacestode vesicles	- 50 -
3.4.2 <i>In vitro</i> treatment of <i>E. multilocularis</i> primary cells	- 51 -
3.5 EmMKK2 - a factor of the <i>E. multilocularis</i> MAP kinase cascade	- 52 -
3.5.1 Classification of EmMKK2 as MAPK kinase on the basis of structural features	- 52 -
3.5.2 Expression of <i>emmkk2</i> in <i>E. multilocularis</i> larvae	- 57 -
3.5.3 Interaction studies between EmMKK2 and potential members of the <i>E. multilocularis</i> MAPK cascade	- 58 -
3.5.4 <i>In vitro</i> activity of the parasite MAPK cascade	- 60 -

3.6 Analysing and targeting the EGF signaling pathway of <i>E. multilocularis</i>	- 60 -
3.6.1 Phosphorylation of Elp in response to host EGF and the effects of inhibitors	- 60 -
3.6.2 Activation of EmMPK1 in response to host EGF	- 61 -
3.6.3 Enhanced proliferation of <i>E. multilocularis</i> in response to host EGF	- 63 -
3.7 <i>In vitro</i> treatment of metacestodes with tyrosine kinase and MAPK cascade inhibitors	- 64 -
3.8 Influence of various host growth factors on vesicle regeneration	- 65 -
3.9 EmMPK3 – a serum sensitive MAPK	- 70 -
3.10 Activity assay for EmER, the EGF receptor of <i>E. multilocularis</i> - Preliminary data	- 72 -
4. Discussion	- 73 -
5. Material and methods	- 86 -
5.1 Material	- 86 -
5.2 Oligonucleotides	- 87 -
5.3 Determination of nucleic acid concentration and purity	- 90 -
5.4 RNA procedures	- 91 -
5.4.1 Isolation of total RNA from mammalian cell lines	- 91 -
5.4.2 Isolation of total RNA from <i>E. multilocularis</i> larvae	- 91 -
5.4.3 Decontamination of isolated RNA	- 91 -
5.4.4 First strand cDNA synthesis	- 91 -
5.4.5 Synthesis of SMART cDNA	- 92 -
5.5 DNA procedures	- 92 -
5.5.1 Isolation of chromosomal DNA from the metacestode larval stage with purification	- 92 -
5.5.2 BrdU-Staining	- 92 -
5.5.3 DAPI staining of DNA blotted on nitrocellulose membrane	- 93 -
5.5.4 Isolation of plasmid DNA from <i>E. coli</i>	- 93 -
5.5.5 Gel electrophoresis of DNA	- 93 -
5.5.6 Purification of DNA	- 94 -
5.5.7 DNA precipitation	- 94 -
5.5.8 Sequencing	- 94 -
5.5.9 Amplification of DNA via PCR	- 94 -
5.5.10 Rapid amplification of cDNA ends (RACE)	- 95 -
5.5.11 Semi-quantitative RT PCR	- 95 -
5.5.12 TA cloning	- 95 -
5.5.13 Colony-PCR	- 95 -
5.5.14 Restriction digest of DNA	- 95 -
5.5.15 Ligation of DNA fragments	- 96 -
5.6 Protein procedures	- 96 -
5.6.1 Determination of protein concentration	- 96 -
5.6.2 <i>In vitro</i> activity assay with myelin basic protein as substrate	- 96 -
5.6.3 <i>In vitro</i> activity assay for the MAPK cascade	- 96 -
5.6.4 Co-immunoprecipitation	- 97 -
5.6.5 SDS-PAGE	- 97 -
5.6.6 Coomassie staining of protein gels	- 98 -
5.6.7 Western blotting	- 98 -
5.7 Working with bacteria	- 99 -
5.7.1 Bacteria strains and media	- 99 -
5.7.2 Chemically competent <i>E. coli</i>	- 100 -
5.7.3 <i>E. coli</i> transformation	- 100 -
5.7.4 Heterologous expression in <i>E. coli</i> and purification of the recombinant proteins	- 100 -

5.8 Working with yeast	- 102 -
5.8.1 Yeast strains and media	- 102 -
5.8.2 Yeast two hybrid analysis	- 103 -
5.9 Working with mammalian cell lines	- 104 -
5.9.1 Cell lines and media	- 104 -
5.9.2 Quantitative live-dead staining of mammalian cell lines	- 104 -
5.9.3 Transfection of HEK293 cells	- 104 -
5.10 Working with <i>E. multilocularis</i>	- 105 -
5.10.1 <i>E. multilocularis</i> isolates	- 105 -
5.10.2 <i>In vivo</i> cultivation of metacystode larvae	- 105 -
5.10.3 Isolation and activation of protoscoleces	- 105 -
5.10.4 <i>In vitro</i> Cultivation of metacystode larvae	- 106 -
5.10.5 Treatment of the metacystode vesicles	- 107 -
5.10.6 Quantitative measurement of <i>E. multilocularis</i> alkaline phosphatase activity	- 107 -
5.10.7 Isolation and cultivation of <i>E. multilocularis</i> primary cells	- 107 -
5.10.8 Treatment of <i>E. multilocularis</i> primary cells	- 108 -
5.11 Computer analyses and statistics	- 108 -
6. Supplements	- 109 -
7. List of abbreviations	- 112 -
8. References	- 113 -
9. Publications	- 123 -
10. Curriculum vitae	- 125 -

1. Summary

Summary

Echinococcus multilocularis is the causative agent of alveolar echinococcosis (AE), a life-threatening disease with limited options of chemotherapeutic treatment. Anti-AE chemotherapy is currently based on a single class of drugs, the benzimidazoles. Although acting parasitocidal *in vitro*, benzimidazoles are merely parasitostatic during *in vivo* treatment of AE and cause severe site effects. In the case of operable lesions, the resection of parasite tissue needs to be supported by a prolonged chemotherapy. Thus, the current treatment options for AE are inadequate and require alternatives.

In the present work, the flatworm signaling pathways were analyzed to establish potential targets for novel therapeutic approaches. I focused on factors that are involved in development and proliferation of *E. multilocularis* using molecular, biochemical and cell biological methods. Among the analysed factors were three MAP kinases of the parasite, EmMPK1, an Erk-1/2 orthologue, EmMPK2, a p38 orthologue and EmMPK3, an Erk7/8 orthologue. Further, I identified and characterized EmMCK2, a MEK1/2 orthologue of the parasite, which, together with the known kinases EmRaf and EmMPK1, forms an Erk1/2-like MAPK module.

Moreover, I was able to demonstrate several influences of host growth factors such as EGF (epidermal growth factor) and insulin on worm signaling mechanisms and larval growth, including the phosphorylation of Eip, an ezrin-radixin-moesin like protein, EmMPK1, EmMPK3 and increased mitotic activity of *Echinococcus* cells. In addition, several substances were examined for their efficacy against the parasite including (i) general tyrosine kinase inhibitors (PP2, leflunamide), (ii) compounds designed to inhibit the activity of receptor tyrosine kinases, (iii) anti-neoplastic agents (miltefosine, perifosine), (iv) serine/threonine kinase inhibitors that have been designed to block the Erk1/2 MAPK cascade and (v) inhibitors of p38 MAPKs.

In these studies, EmMPK2 proved to be a promising drug target for the following reasons. Amino acid sequence analysis disclosed several differences to human p38 MAPKs, which is likely to be the reason for the observed enhanced basal activity of recombinant EmMPK2 towards myelin basic protein in comparison to human recombinant p38 MAPK- α . In addition, the prominent auto-phosphorylation activity of the recombinant EmMPK2 protein together with the absence of an interaction with the *Echinococcus* MKKs suggest a different mechanism of regulation compared to the human enzyme. EmMPK2 activity could be effectively inhibited *in vitro* and in cultivated metacestode vesicles by treatment with SB202190 and ML3403, two ATP-competitive pyridinyl imidazole inhibitors of p38 MAPKs, in a concentration-dependent manner. Moreover, both compounds, in particular ML3403, caused parasite vesicle inactivation at concentrations which did not affect cultured mammalian cells. Likewise, during the cultivation of *Echinococcus* primary cells, the presence of ML3403 prevented the generation of new vesicles.

Targeting members of the EGF signaling pathway, particularly of the Erk1/2-like MAPK cascade, with Raf and MEK inhibitors prevented the phosphorylation of EmMPK1 in metacestodes cultivated *in vitro*. However, although parasite growth was prevented under

these conditions, the structural integrity of the metacystode vesicles maintained during long-term cultivation in the presence of the MAPK cascade inhibitors. Similar results were obtained when studying the effects of other drugs mentioned above.

Taken together, several targets could be identified that reacted with high sensitivity to the presence of inhibitory substances, but did not cause the parasite's death with one exception, the pyridinyl imidazoles. Based on the presented data, I suggest pyridinyl imidazoles as a novel class of anti-*Echinococcus* drugs and imply EmMPK2 as survival signal mediating factor, the inhibition of which could be used for the treatment of AE.

Zusammenfassung

Echinococcus multilocularis verursacht die Alveoläre Echinokokkose (AE), eine lebensbedrohliche Krankheit mit limitierten chemotherapeutischen Möglichkeiten. Die jetzige Anti-AE Chemotherapie basiert auf einer einzigen Wirkstoffklasse, den Benzimidazolen. Obwohl Benzimidazole *in vitro* parasitozid wirken, wirken sie *in vivo* bei AE-Behandlung lediglich parasitostatisch und rufen schwere Nebenwirkungen hervor. In Fällen operabler Läsionen erfordert die Resektion des Parasitengewebes über einen längeren Zeitraum eine chemotherapeutische Unterstützung. Damit sind die jetzigen Behandlungsmöglichkeiten inadäquat und benötigen Alternativen.

In der vorliegenden Arbeit wurden die Signalwege von Plattwürmern analysiert, um potentielle Targets für neue therapeutische Ansätze zu identifizieren. Dabei konzentrierte ich mich unter Anwendung von molekularbiologischer, biochemischer und zellbiologischer Methoden auf Faktoren, die an Entwicklung und Proliferation von *E. multilocularis* beteiligt sind. Darunter waren die drei MAP Kinasen des Parasiten EmMPK1, ein Erk1/2-Ortholog, EmMPK2, ein p38-Ortholog und EmMPK3, ein Erk7/8-Ortholog. Des Weiteren identifizierte und charakterisierte ich EmMCK2, ein MEK1/2-Ortholog des Parasiten, welches zusammen mit den bekannten Kinasen EmRaf und EmMPK1 ein Erk1/2-ähnliches MAPK Modul bildet. Ich konnte zudem verschiedene Einflüsse von Wirtswachstumsfaktoren wie EGF (epidermal growth factor) und Insulin auf die Signalmechanismen des Parasiten und das Larvenwachstum zeigen, darunter die Phosphorylierung von Eip, ein Ezrin-Radixin-Moesin ähnliches Protein, die Aktivierung von EmMPK1 und EmMPK3 und eine gesteigerte mitotische Aktivität der Echinokokkenzellen. Zusätzlich wurden verschiedene Substanzen auf ihre letale Wirkung auf den Parasiten untersucht, darunter befanden sich (1.) generelle Inhibitoren von Tyrosinkinase (PP2, Leflunamid), (2.) gegen die Aktivität von Rezeptor-Tyrosin-Kinasen gerichtete Präparate, (3.) ursprünglich anti-neoplastische Wirkstoffe wie Miltefosin und Perifosin, (4.) Inhibitoren von Serin/ Threonin-Kinasen, die die Erk1/2 MAPK Kaskade blockieren und (5.) Inhibitoren der p38 MAPK.

In diesen Untersuchungen hat sich EmMPK2 aus den folgenden Gründen als vielversprechendes Target erwiesen. Aminosäuresequenz-Analysen offenbarten einige Unterschiede zu menschlichen p38 MAP Kinasen, welche sehr wahrscheinlich die beobachtete gesteigerte basale Aktivität des rekombinanten EmMPK2 verursachen, verglichen mit der Aktivität humaner p38 MAPK- α . Zusätzlich suggerieren die prominente Autophosphorylierungsaktivität von rekombinantem EmMPK2 und das Ausbleiben einer

Interaktion mit den *Echinococcus* MKKs einen unterschiedlichen Regulierungsmechanismus im Vergleich zu den humanen Proteinen. Die Aktivität von EmMPK2 konnte sowohl *in vitro* als auch in kultivierten Metazestodenvesikeln durch die Behandlung mit SB202190 und ML3403, zwei ATP kompetitiven Pyridinylimidazolinhibitoren der p38 MAPK, in Konzentrations-abhängiger Weise inhibiert werden. Zudem verursachten beide Substanzen, insbesondere ML3403 die Inaktivierung von Parasitenvesikeln bei Konzentrationen, die kultivierte Säugerzellen nicht beeinträchtigten. Ebenso verhinderte die Anwesenheit von ML3403 die Generation von neuen Vesikeln während der Kultivierung von *Echinococcus* Primärzellen.

Das Targeting von Mitgliedern des EGF-Signalwegs, insbesondere der Erk1/2-ähnlichen MAPK Kaskade mit Raf- und MEK- Inhibitoren verhinderte die Phosphorylierung von EmMPK1 in *in vitro* kultivierten Metazestoden. Obwohl das Parasitenwachstum unter diesen Konditionen verhindert wurde, blieb die strukturelle Integrität der Metazestodenvesikeln während der Langzeitkultivierung in Anwesenheit der MAPK Kaskade-Inhibitoren erhalten. Ähnliche Effekte wurden beobachtet nach Behandlung mit den anderen zuvor aufgeführten Inhibitoren.

Zusammenfassend lässt sich festhalten, dass verschiedene Targets identifiziert werden konnten, die hoch sensibel auf die Anwesenheit der inhibitorischen Substanzen reagierten, aber nicht zum Absterben des Parasiten führten, mit Ausnahme der Pyridinylimidazolen. Die vorliegenden Daten zeigen, dass EmMPK2 ein Überlebenssignal vermittelnden Faktor darstellt und dessen Inhibierung zur Behandlung der AE benutzt werden könnte. Dabei erwiesen sich p38 MAPK Inhibitoren der Pyridinylimidazolklasse als potentielle neue Substanzklasse gegen Echinokokken.

2. Introduction

Echinococcus multilocularis as causative agent of alveolar echinococcosis (AE)

2.1 Phylogeny and distribution of the genus *Echinococcus*

Platyhelminths of the genus *Echinococcus* belong to the family of Taeniidae that are grouped into the class of Cestoda (Fig. 2.1). Closely related human parasites are the pig tapeworm *Tania solium* and the beef tapeworm *Taenia saginata*. General features of the phylum Platyhelminthes which they share with all protostomes are bilateral symmetry, the formation of three germ layers as well as the development of the mouth near the gut entrance during the gastrulation. The protostomes can be divided into two major branches: Ecdysozoa and Lophotrochozoa. The group of Ecdysozoa covers all moulting animals including the fruit fly *Drosophila melanogaster* and the nematode *Caenorhabditis elegans*. Lophotrochozoa encompass flatworms, annelids as well as molluscs and are characterized particularly by spiral cleavage and a prominent digestion system. The term “helminths” is historically used for all endoparasitic living nematodes and platyhelminths and is not based on phylogenetic findings [1].

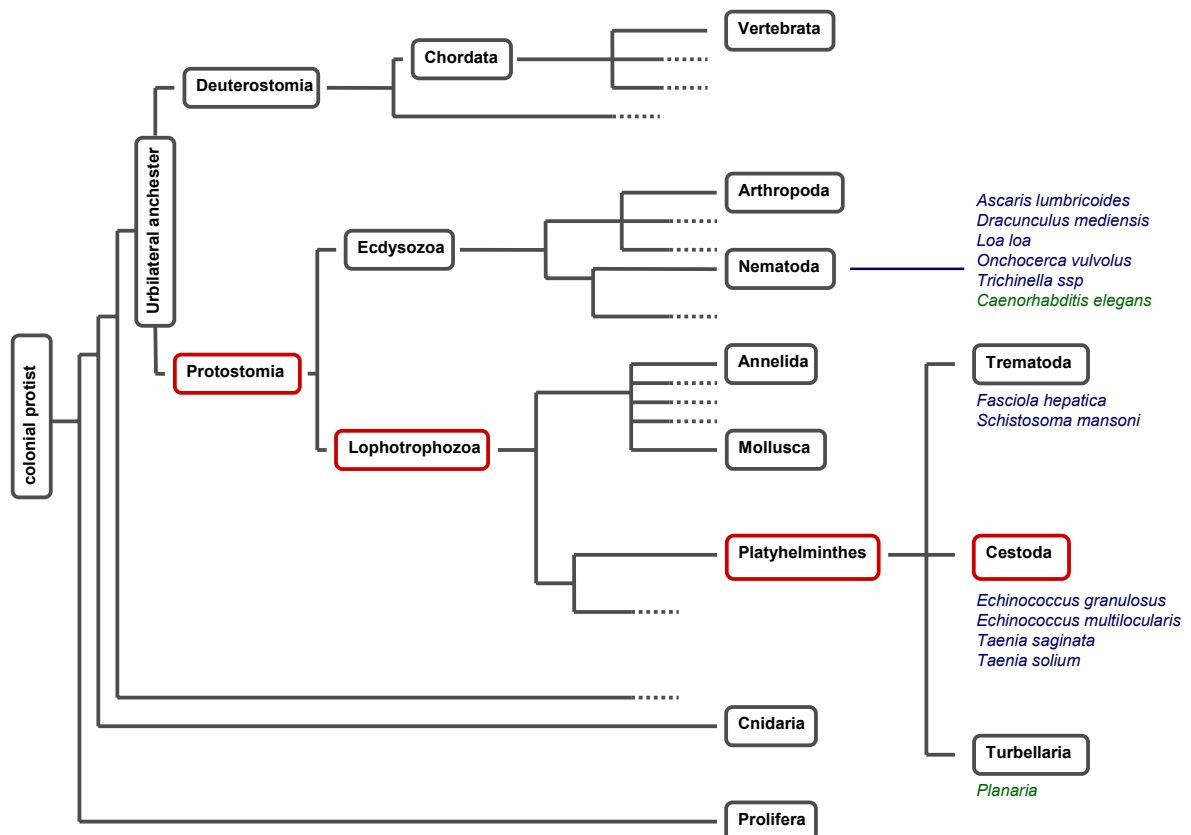


Fig. 2.1: Phylogenetic tree of the animal kingdom. Species highlighted in blue are parasitic living, examples for free living worms are in green [1].

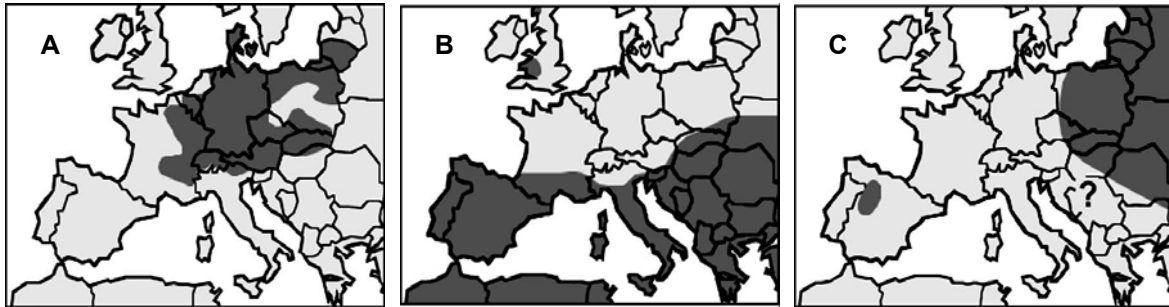


Fig. 2.2: Distribution of *Echinococcus* species in Europe. Endemic area of *E. multilocularis* (A), *E. granulosus* s.s. (B) and *E. granulosus* G7 (pig strain). Romig et al, 2006 [2] .

The genus *Echinococcus* is responsible for a variety of clinical pictures and comprises at least eight species. These are *E. oligarthus*, *E. vogeli*, *E. shiquicus*, the small fox tapeworm *E. multilocularis*, various strains of the dog tapeworm *E. granulosus* and the newly repositioned *E. felidis* from African lions [3]. The *E. granulosus* strains and the small fox tapeworm *E. multilocularis* represent the species with the greatest impact on human and animal health and economic issues. In humans, they cause life-threatening diseases; *E. granulosus* causes cystic echinococcosis (CE) and *E. multilocularis* alveolar echinococcosis (AE). Their management has become increasingly important in Europe in the last two decades [4]. In the following section, particular emphasis will therefore be put on *E. multilocularis* and *E. granulosus*

In recent years, the taxonomic classification of the *E. granulosus* strains (G1-G10) has been modified and some strains were considered as standalone species based on the genetic stability in sympatric areas and the priority for specific hosts. According to that, *E. granulosus* G1 is named *E. granulosus* sensu stricto and separated from G5 *E. ortleppi* and G4 *E. equinus*. The cervid strain G10 and the pig strain G7 including the variant G9 were integrated together with the non-European strain G6 in one monophyletic group [2]. Among them, *E. granulosus* sensu stricto occurs world-wide as concomitant of sheep farming and is distributed in Europe the Mediterranean area, Wales and Bulgaria [5].

In contrast to *E. granulosus*, strain diversity has not yet been found for the fox tapeworm *E. multilocularis*. Since the 1990's, *E. multilocularis* is endemically distributed in arctic and temperate zones of the Northern Hemisphere. Its occurrence has extended in Europe from the south-central to central Europe including Denmark, Flanders, central France, northern Italy to the Balkan states (Fig.1.2) [2]. However, the area might be larger than described due to insufficient data [5-7]. Besides the expansion of the endemic area, an increase of definitive density host has been promoted by rabies vaccination of foxes, which leads to higher survival rates and as a consequence, to an increased infection rate of *E. multilocularis* intermediate hosts (detailed in section 2.3.1) [2, 7].

Two other species, namely *E. oligarthus* and *E. vogeli*, are responsible for polycystic echinococcosis (PE) in South and Central America and breed mostly in sylvatic life cycles.

E. vogeli prefers bush dogs (*Speothos venaticus*) as final host and agoutis (*Dasyprocta* spp.) and pacas (*Cuniculus paca*) as intermediate hosts, whereas *E. oligarthus*' definitive hosts are various species of wild felids. Infections of humans are rare and occur after contact with contaminated domestic animals [8]. *Echinococcus shiquicus* from the Tibetan highlands was recently described and executes preferably fox-lagomorphe cycles [9, 10]. For this species, no case of human infection has been observed yet [10].

2.2 Life cycle of *E. multilocularis*

As a parasitic cestode, *E. multilocularis* has a di-heteroxenous life cycle (Fig.1.3). Preferably wild foxes (*Vulpes* spp.) and raccoon dogs (*Nyctereutes procyonoides*), but also other carnivores like domestic dogs and cats serve as definitive hosts [5, 8]. A wide spectrum of mammals can serve as intermediate hosts, but in the case of a sylvatic cycle, mostly small rodents (especially *Microtus arvalis* and *Arvicola terrestris*) are affected [2, 7].

In the definitive host, *E. multilocularis* settles between the villi of the small intestine. The adult worm is characterized by a size between one and four millimetres and a maximum of five segments, so-called proglottides. Approximately four weeks after its settlement in the small intestine, up to 200 eggs are produced daily in the last proglottide by protandry. Infective eggs contain the multicellular, first larval stage, the oncosphere, and are surrounded by a massive egg shell, primarily made up of carbohydrate compounds. They are released into the environment by shedding the gravid proglottide or the loose eggs together with the faeces. The eggs are considerably resistant against external influences and can protect the oncosphere for months [8]. Upon oral uptake by the intermediate host and subsequent hatching, the oncosphere penetrates the gut epithelium from where it reaches the target organ passively via blood and lymph system. Within the target organ, which is predominantly the liver, the oncosphere differentiates into the second larval stage, designated metacestode. The metacestode grows via exogenous budding into the surrounding host tissue. Therefore, the asexual high-rate proliferation of metacestode tissue is often compared with a sponge-like tumour growth. The metacestode stage of *E. granulosus*, the causative agent of cystic echinococcosis (CE), in the other hand, differs through the formation of a main cyst and endogenous budding [8].

A single metacestode vesicle is built of two layers surrounding the hydatid fluid. The outer, acellular laminated layer (LL) contains high-polymer carbohydrates which are responsible for immune evasion effects [11]. It is formed two to four weeks after the encystment process from components secreted by the vesicle cells comprising the inner germinal layer (GL). Besides germinal cells, the GL is composed of several different cell types including muscle cells, glycogen storage cells and undifferentiated cells. The germinal cells actually represent the only mitotically active cells of the parasite and differentiate into brood capsules within which protoscoleces are formed as third larval stage [12, 13]. The protoscolex consists of the head structure of the adult stage with suckers and hooks and remains initially in a resting form. Due to the space demanding growth of the parasite, the host's organs cannot longer fulfil their functions and the small rodent becomes an easy prey for the final host. During the

digestion processes of the bagged intermediate host by the definitive host, the protoscolex is activated by low pH in the stomach and the influence of bile salts, leading to evagination. Now, the protoscolex is able to persist in the gut and to mature into the adult stage, thus completing the life cycle. It is important to mention that the specific factors influencing the metamorphosis of the larval stages, the host specificity as well as the organ tropism remain to be elucidated.

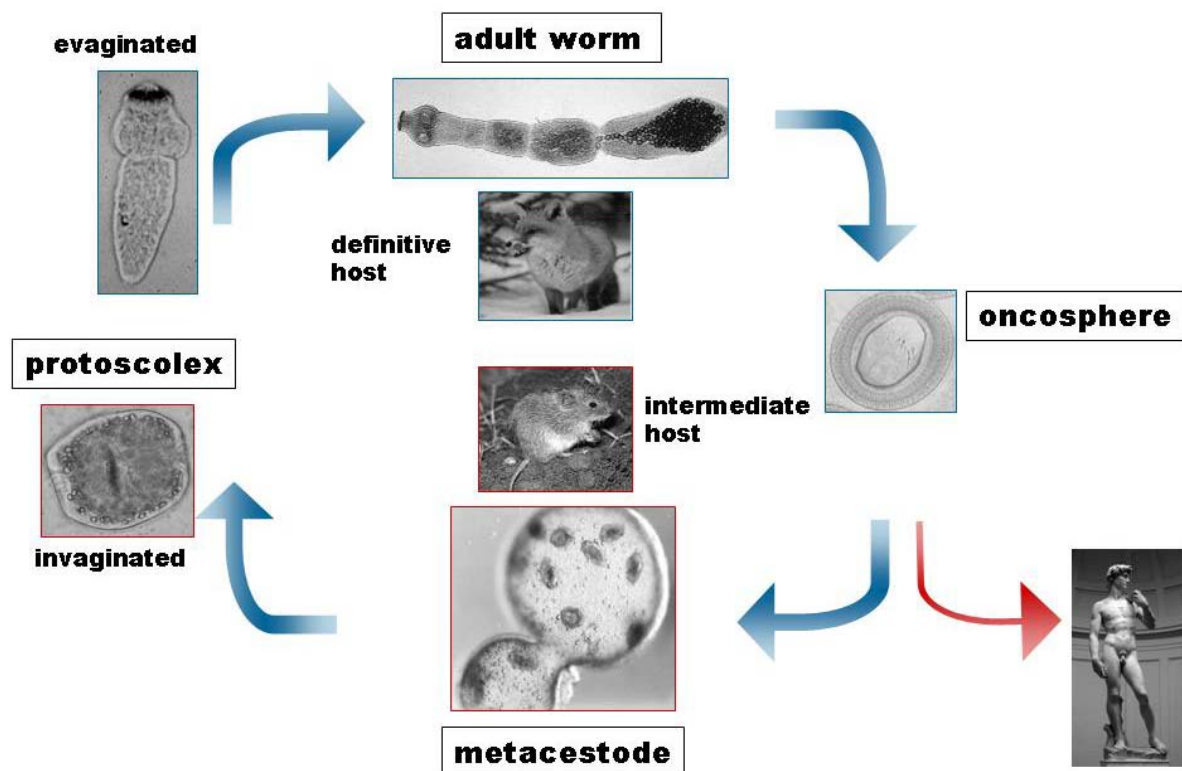


Fig. 2.3: Life cycle of *E. multilocularis*. Foxes and, increasingly, racoon dogs are considered as main spreader of infectious eggs containing the oncospheres in Germany. Upon uptake by small rodents or accidentally humans as intermediate hosts, the oncosphere develops into the second larval stage, the so called metacestode. The establishment of the metacestode tissue takes place predominantly in the liver where growth proceeds without contact inhibition into the host tissue. Then, the third larval stage develops within the brood capsules that are built by differentiated germinal layer cells. The so-called protoscolex larva contains the head structure of the adult worm and remains initially invaginated. After digestion of the intermediate host by the final host, the larva is activated by the passage through the digestion system and turns inside out. Reaching the gut, the evaginated protoscolex develops into a mature adult producing eggs and the life cycle commences again [14].

2.3 Alveolar echinococcosis

2.3.1 Alveolar echinococcosis and transmission risk

The passage of *E. multilocularis* between definitive and intermediate host becomes interrupted when the infectious stage of the worm is accidentally taken up by humans instead of herbivores. The successful development of the metacestode with the accompanying lesion in the host tissue is referred to alveolar echinococcosis (AE). Persons with a high-risk for transmission are humans with close contact to animals and contaminated material, e.g., hunters, farmers, gardeners and mushroom collectors, and in particular dog owners [15].

The transmission ways are difficult to validate because of the large time span between time point of infection and diagnosis of AE. In central Europe, the prevalence of AE is estimated to be between 2 up to 40 cases per 100,000 habitants in endemic areas, whereas in eastern France 152 per 100,000 cases were observed [2].

The transmission rate has increased in recent years and AE has gained significance as one of the worst non-tropic parasitosis particularly in Europe, Japan and China [2, 16]. Environmental factors like soil humidity influence the survival period of excreted eggs and create specific vegetation and thus probably the suitable habitat for hosts [2, 5]. Further, the population of infected definitive host has expanded (section 2.1). Amongst others, the role of raccoon dogs in AE transmission increases due to increasing immigration rates from eastern Asia and enhance the suitable host pool [2]. A direct correlation between the increase of infected definitive hosts and the increase of infected intermediate hosts was, until recently, not reported. A very recent publication by Peter Deplazes and co-workers found strong support that this is the case for AE in Switzerland [17]. Moreover, in the last years the risk of transmission to humans is likely to be increased due to the shift from sylvatic life cycles to domestic life cycles involving dogs, as it has been observed for regions in China and Alaska and a change to urban life cycle of red foxes in European areas [5-7, 18]. These changes lead to a higher density of infectious material and therefore, to higher transmission risks for humans.

2.3.2 Alveolar echinococcosis and its manifestation

In humans, the metacestode targets in most cases primarily the liver and can proliferate from single germinal cells to massive tissues, which is referred to as AE [13]. For untreated patients, the lethality rate of AE is 96% [15]. AE can persist for up to twenty years [14]. In the late infection, the metacestode can spread into the abdomen and other organs like spleen, brain, and bones. The early infection appears clinically asymptomatic without significantly affecting the host's quality of life and organ damage. This suggests immune modulatory properties of the parasite. Later on, the organs are impeded in their function through the infiltrative growth of *E. multilocularis*. This phase is accompanied by an exacerbated inflammatory response [19]. Abdominal pain, jaundice, hepatomegaly, sometimes fever and anaemia, weight loss, and pleural pain belong to the early symptoms and end in dysfunction of the affected organs resulting in the death of the host [8]. Interestingly, only approximately 10% of *E. multilocularis* expositions develop active AE [14]. Spontaneous calcification of the

lesions and cellular effector mechanism of the host defense suggested to cause early inactivation of the parasite in the remaining 90%. The granulomatous surrounding of the metacestode is mostly formed by macrophages, myofibroblasts and a high number of CD4+ T cells [20]. During the course of AE, the cytokine profile switches from a T_H1 pattern in the early stages to a T_H2 profile in the late stages. Hence, the established lesion is characterized by high levels of IL-4, IL-5, IL-6, IL-10 and INF- γ compared to the predominant high levels of IL-12, TNF- α , INF - γ early in infection [12, 19-22].

Chances of cure strongly depend on the time of diagnosis and adequate treatment. If AE is diagnosed within the first 10 years after infection, the survival rate ranges about 30%, within 15 years at 0% [8]. Imaging techniques for diagnose of AE are based on ultrasonography, computed tomography (CT) and magnetic resonance tomography (MRT). Especially with CT most of the lesions and calcifications can be detected [8, 23]. However, immunodiagnostic tests using a wide range of available antigens proved to be more effective than the imaging techniques for primary diagnosis [24-28]. The antigen Em2 isolated from the metacestode larval stage, for example, has been successfully used for detection of human and monkey AE via ELISA. Using a mixture of Em2 and E1p (also termed Em10; see section 2.4.1), the sensitivity of serodiagnosis was even further increased [23].

2.3.3 Treatment options and chemotherapy

Treatment options for AE are limited. Radical surgery of the parasite tissue has been recommended but has often proven difficult due to the metacestode's infiltrative growth. Liver transplantation has been used as an alternative therapeutic approach; however, the required immunosuppression may result in rapid growth of the remaining parasite material [14]. The surgery option should ideally be supported by life-long medication, but at least for a two-year minimum. Chemotherapeutic treatment is based on benzimidazole compounds such as mebendazole and albendazole [29, 30]. The efficiency of chemotherapy is difficult to evaluate due to the lack of methods to assess whether the parasite was killed. The success of treatment can be measured indirectly only via patients survival rates, reduced parasite proliferation or a lack of recurring lesions [31]. This requires continued surveillance of the clinical status with imaging tests over a long period. In Switzerland, this procedure cost an estimate of €350,000 per case [18]. Although benzimidazole derivates are effective in parasite killing *in vitro*, e.g. due to alterations on laminated and germinal layer, they are merely parasitostatic *in vivo* [32, 33]. The cellular targets of benzimidazoles are β -tubulins, which are essential components of the cytoskeleton [34]. However, due to the high level of similarity between host and parasite β -tubulins (approximately 94% on amino acid sequence level), benzimidazoles also have a high level of affinity to host tubulin, resulting in severe side effects and liver toxicity upon prolonged treatment (Fig. 2.4) [33, 35]. In the case of long-term treatment, proteinuria, hair loss, neurological deficit, gastrointestinal disorders, decreased numbers of leukocytes and thrombocytes, headache, fever, urticaria, and bone marrow toxicity were additionally stated as side effects [20]. For the antimycotic compound amphotericin-B, comparable effects on parasite growth could be shown *in vitro*, but for *in vivo* treatment, this drug is of limited use due to significant side effects [36, 37]. Nitazoxanide, a broad-range drug against intestinal bacterial and parasitical diseases, has recently been

shown to exhibit parasitocidal activity on *E. multilocularis* metacestode *in vitro* and in infected mice, in particular in combination with albendazol [33, 38]. Additionally, there are efforts to combine praziquantel and albendazole to obtain a synergistic effect for parasitocidal activity in the CE treatment. Joined application resulted in an increased number of patients with parasitic tissue compared to single medication [20]. Nevertheless, an alternative chemotherapy does not exist for patients who do not tolerate or do not respond to benzimidazole at the current time point.

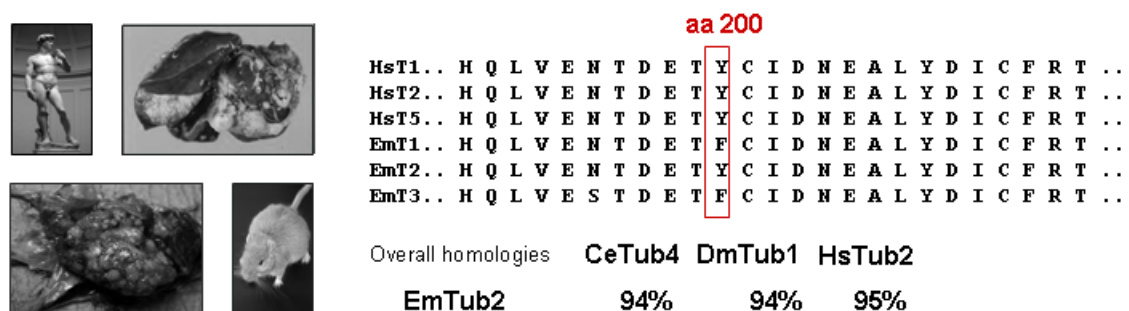


Fig. 2.4: Chemotherapy for AE- Benzimidazole derivatives target β -tubulins. Depicted is an amino acid sequence alignment of human and *Echinococcus* tubulins demonstrating high homology of the cellular benzimidazole targets [35]. Marked is amino acid residue 200, the major determinant of affinity of a given β -tubulin to benzimidazoles, which is typically Phe in certain invertebrate β -tubulins.

2.4 Signaling in developmental and proliferation processes

In mammals, the MAP kinase (MAPK) cascades are crucially involved in signal transduction mechanisms that control proliferation, development, and apoptosis. Four classical MAPK cascades have been described at least in humans. The MAPK modules are distinguished from each other by the activating stimulus and the particular nature of the activated MAPK, but share a consecutive three-step phosphorylation of intracellular kinases as the mutual signal transduction process (see Fig. 2.5): An upstream Ser/Thr kinase, the MAPK kinase kinase (MKKK), modifies its substrate kinase, the MAPK kinase (MKK), leading to its activation. The dual-specific Thr/Tyr MKK then activates a corresponding MAPK, another Ser/Thr kinase. The MAPK's phosphorylation occurs on the threonine and the tyrosine residues located in the highly conserved T-X-Y triplet within the activation loop [39].

A well-characterized mammalian MAPK cascade module is the Erk (extracellular signal-regulated kinase) 1/2- pathway, which regulates the cellular response to extracellular growth factors. The receptor tyrosine kinases (RTK) of insulin, EGF (epidermal growth factor), and FGF (fibroblast growth factor) signaling act as upstream sensors of this pathway (see Fig.2.5). The JNK/SAPK (c-Jun N-terminal kinase/ stress activated protein kinase) -pathway as well as the p38 MAPK pathway, on the other hand, are mainly involved in the stress response. Osmotic and oxidative alteration, ultraviolet radiation, heat shock, as well as

mechanical stress belong to the respective stimuli. In addition, transforming growth factor (TGF) β and other inflammatory signals (TNF (tumour necrosis factor) α , IL-1) are potential inducers of the p38 MAPK module. The fourth MAPK module leads to the activation of Erk5 (BigMAPK), also activated in response to stress and growth factor stimuli but not in response to inflammatory cytokines [39].

Together with the assembled core components, various regulator proteins affect the fine-tuning of the cascades. The specific cellular response is further dependent on the kinetics, the sublocalization of the kinases within the cells and the availability of substrates and scaffold proteins [40]. The identification of at least twenty MKKKs, seven MKKs and eleven MAPK in human cells indicates that MKKs are able to activate more than one MAPK and are activated by several MKKKs [41]. Nevertheless, the interactions of MKKs with their downstream kinases are specific since they recognize a tertiary structure of a specific MAPK instead of the linear sequence in which the T-X-Y motif is localized [41].

In the following passages, I will elaborate on several points of the aforementioned signal machinery, incipiently with RTK signaling and MAPK modules that are relevant for the present work. Then, I will continue with atypical MAPKs found in humans and some further aspects of signaling pathways.

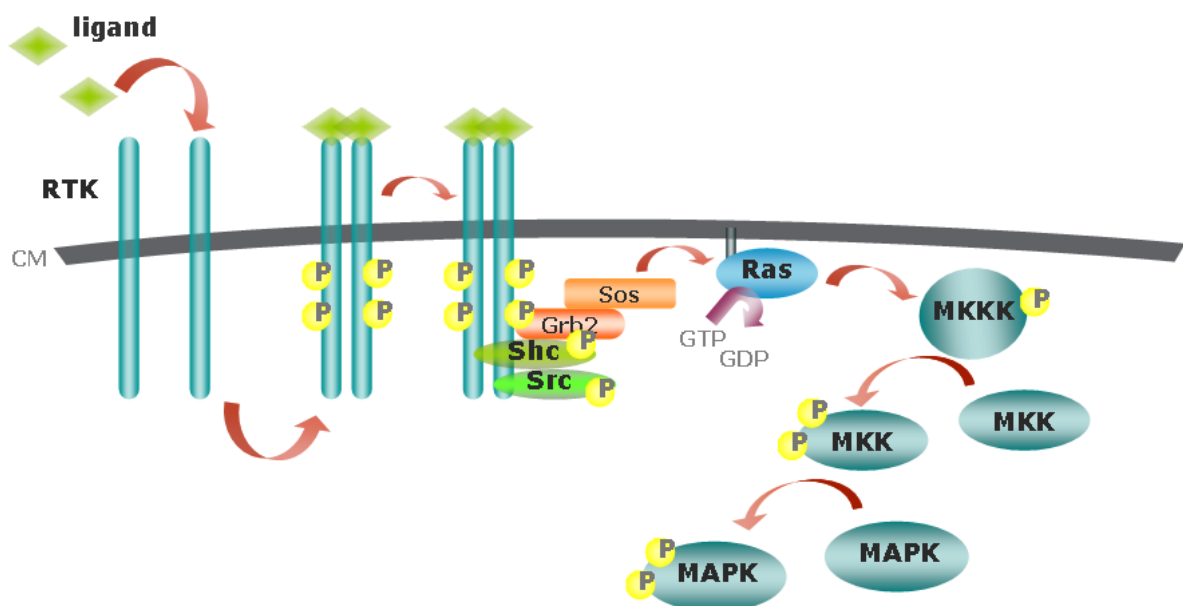


Fig. 2.5: RTK signaling and MAPK cascade activation. Upon binding of ligand such as EGF, the intrinsic kinase activity of the receptor tyrosine kinase (RTK) is activated leading to auto-phosphorylation of the kinase at critical tyrosine residues. That creates the docking sites for downstream effector like Shc, Src, Grb2 and Sos, which form a multiprotein complex at the intracellular domain of RTK. Activated Sos catalyzes the exchange of GDP to GTP of the membrane-associated Ras leading to its activation. In turn, GTP-Ras activates the upstream kinase of the MAPK cascade, namely MKKK, which phosphorylates MKK. Once activated, MKK activates the MAPK that on the one hand interacts in the cytosol with cytoskeleton-associated proteins and further kinases or it migrates into the nucleus enhancing specific gene transcription [42, 43].

2.4.1 Peptide growth factors and their receptors

In humans, four members comprise the epidermal growth factor receptor (EGFR) family (EGFR (ErbB1), ErbB2, ErbB3 and ErbB4) which sense at least thirteen ligands of the EGF family [43, 44].

The intracellular domain of the EGF RTKs is highly conserved and composed of a juxtamembrane domain involved in the binding of Src protein kinases (see below), followed by the tyrosine kinase domain and a weakly conserved C-terminal part. An exception of conservation is given for the kinase domain of ErbB3. Its intracellular domain lacks functional tyrosine residues. As consequence, ErbB3 acts only as regulatory receptor. The extracellular domain of the EGFRs displays less homology and so the RTKs show different affinities for the various ligands. The extracellular part contains an EGF-like domain, an immunoglobulin like-domain, heparine-binding and glycosylation sites. For example, EGFR preferably senses EGF, TGF (tumour growth factor) - α and amphiregulin stimuli. ErbB3 as heterodimer, however, displays preference towards neuregulin-1 and 2 [42, 43].

The binding of a ligand to a receptor induces, in addition to its activation, the migration from a caveolae component of the cell membrane into clathrin-coated pits where the associated receptors are internalized. The varying composition of receptor heterodimerization allows the stimulation of several different downstream signaling pathways [43].

The globular EGF peptide of 6.4 KDa represents the archetype of EGF-like proteins and was originally isolated from mouse submaxillary glands in 1962 [45]. EGF is a component of most human body fluids (plasma concentration 1 ng/ml) and is produced in a variety of tissues including kidney, brain, stomach, salivary glands. Its production is promoted by testosterone and suppressed by estrogen [46]. The EGF peptides from different phylogenetic species of vertebrates are well conserved and display over 70% identity. The biological activity of EGF depends on three intermolecular disulfide-bonds. Interference with these disulfide bonds has been shown to comprise proliferation and differentiation stimulation of various cell types. The closely related TGF- α is produced by various transformed cells and shows a similar spectrum of biological activity like EGF [47].

The peptide growth factors, which contain a single transmembrane domain (TM) exist as proform at the cellular surface. After cleavage of the extracellular domain representing the actual ligand by a disintegrin and metalloproteases, the ligand is capable to activate RTK in auto- or paracrine manner [43].

The activation of RTK is regulated by a spatiotemporal expression and the post-translational modification of the ligands and occurs frequently via a trans-activation process.

In principle, the growth factor stimulates the intrinsic tyrosine kinase activity of its corresponding receptor by the formation of 2:2 ligand-receptor-complex (depicted in Fig. 2.5). In this so called trans-activation mechanism, the receptors autophosphorylate specific Tyr residues, which increases their kinase activity. Once activated, adaptor proteins like Shc bind to the receptor and become tyrosine-phosphorylated by the receptor's kinase activity. Alternatively, other tyrosine kinases, for instance Src, are recruited to the activated receptors to mediate phosphorylation of downstream effector molecules. The phosphorylation of Shc, then, allows the association of the Grb2 adaptor protein and guanidine nucleotide exchange

factor (GEF) son of sevenless (Sos). The binding of Sos to the receptor complex results in the GDP to GTP exchange of Ras whereupon the Erk1/2 MAPK pathway is activated [47].

Fibroblast growth factor (FGF) signaling established among metazoans is involved in developmental processes as well. In humans, the FGF receptor family consists of four members FGFR1-4 in various splicing variants, which bind at least 22 growth factors of the FGF family [48]. The activation of members of the FGFR family occurs very similar to the mechanisms for EGFR activation. However, for the stable receptor-ligand-complex formation, heparin or heparin sulphate proteoglycans are required to increase binding affinity [48, 49].

Besides EGFs and FGFs, insulin and insulin-like growth factors (IGF) have been shown to stimulate the Erk1/2 MAPK cascade upon interaction with insulin receptors (IR). The ligand family consists, at least in humans, of nine IGFs, among them insulin, IGF-I and IGF-II and have been well characterized since the identification of insulin in 1921 by Banting and Best [50, 51]. Unlike insulin, which is produced by pancreatic β -cells to regulate sugar and fatty acid metabolism, IGF-I and -II are produced in various tissues and cell types. In addition to the classical receptors of the insulin/IGF receptor family (IR, IGF-IR1 and IGF-IR2), an insulin-receptor related receptor (IRR) was recently described, for which a corresponding ligand is, however, unknown as yet. IGF-I and IGF-II have nearly equal affinities to the ubiquitously expressed IGF receptors and can also activate IR [50].

2.4.2 The Erk1/2 MAPK module

The Erk1/2 MAPK module is activated by the small GTPase Ras in the GTP bound form upon ligand binding to RTK. Ras GTP mediates the localization of Raf MKKK (or other MKKKs) to the cytoplasmic membrane where Raf becomes activated by membrane-bound tyrosine kinases. Raf in turn activates MEK1 and MEK2, which then phosphorylate the Erk1 and Erk2 MAPKs. The activation of MEK1 requires the phosphorylation of Ser²¹⁸ and Ser²²² by Raf [52]. Erk1's double phosphorylation on the T-E-Y triplet leads to its dimerization and translocation into the nucleus, where it activates several transcription factors including Elk-1, c-Myc, STATs. Besides its involvement in gene regulation, Erk1 modifies cytoplasmic protein substrates on Ser/Thr residues within proline-directed motifs. Among the activated proteins are effectors involved in translation and cytoskeletal rearrangements, e.g. ribosomal S6 kinase and microtubule-associated proteins. Further, members of the MAPK module are phosphorylated by Erk1/2 suggesting a negative feedback mechanism.

In general, the activation of MEK1 and MEK2 by specific MKKKs depends on the environmental stimuli [39]. The MKKs of the Erk1/2 pathway in humans are MEK1 and MEK2, which share 80% amino acid sequence identity [53]. They display low homology (21% identity) in the MEK-specific sequence, which contains the recognition site for upstream kinase Raf [54]. In addition, they differ in their N-terminal region where both possess the Erk docking site but only MEK1 the nuclear exclusion sequence (NES). Since the NES determines the cytoplasmic localization of MEK1, it was supposed that MEK1 in its inactive state sequesters Erk1/2. Upon activation, MEK1 phosphorylates Erk1 and Erk2 and then dissociates. In turn, activated Erk1 and Erk2 translocate into the nucleus [39, 54, 55].

One way to achieve specificity of Erk and MEK might be the tissue specific expression patterns. Mouse MEK1 and MEK2 are differently expressed in the various tissues and it has been shown that *mek1* but not *mek2* null mice are embryonic lethal, indicating its important role during embryogenesis [54, 56].

Another way to determine the specific components of the MAPK module is accomplished by the varying set of scaffold proteins. In the case of the growth factor stimulated Erk1/2 pathway, KSR (kinase suppressor of Raf; isoforms KSR1 and 2) plays an important role through the formation of a high molecular weight complex with Raf, MEK1/2, ERK1/2, 14-3-3 and several chaperones. In the absence of growth factor stimuli, KSR forms a cytoplasmically located complex with MEK1/2, PP2A (protein phosphatase 2A), 14-3-3 and the Ras sensitive E3 ubiquitin ligase impedes mitogenic signal propagation (IMP). Upon stimulation, Ras activation leads to the degradation of IMP and its release from the complex. Simultaneously, KSR and Raf become dephosphorylated on residues involved in the 14-3-3/PP2A binding resulting in the translocation of the cleaved KSR- MEK1/2 complex to the plasma membrane. There, KSR-MEK1/2 assemble with Erk1/2 and Raf whereby the turn-in-turn phosphorylation subsequently proceeds [57].

The 14-3-3 proteins are evolutionary conserved and abundantly expressed in all cell types and are interaction partners of various components of the signaling pathways. Members of the 14-3-3 family very often regulate developmental processes by binding and alteration of the intracellular compartment of the target proteins thereby leading to their inactivation. Initially, 14-3-3 has been identified as the phospho-serine specific adaptor of Raf in the process described above. Further, 14-3-3 proteins interact amongst others with the cell-cycle regulating phosphatase Cdc25, members of the fork head transcription factor family and Bad, which prevents the cell entering apoptosis [58].

2.4.3 The p38 MAPK module

The Hog1 protein of budding yeast presents the archetype of p38 MAPKs, which is activated in response to physical stress [59]. The mammalian p38 MAPK family is composed of at least four isoforms, p38 MAPK α , β , γ and δ , which display around 60% identical amino acid residues [60]. p38 α and β are ubiquitously expressed, whereas isoform γ is mainly found in the skeletal muscle tissue and isoform δ in various tissues such as endocrine glands [61]. The mainly stress-activated p38 MAPK becomes phosphorylated on the dual-phosphorylation motif T-G-Y by MKK3, MKK4, and MKK6, which shows different preferences for the relevant isoforms. MKK6 preferentially activates p38 MAPK β , whereas p38 MAPK α is to the same degree the substrate of MKK3, 4 and 6 [62]. Substrates of p38 MAPK are MAPKAPK (MAPK activated protein kinases)-2 and -3, and the transcription factors ATF-2, AP-1, Max and Chop. Here, p38- β revealed a 20fold higher preference toward ATF-2 than the other isoforms tested in *in vitro* and *in vivo* experiments [63]. The varying preferences of the p38 isoforms for substrates and activator kinases suggest for each an individual task in the signaling transduction, which is not completely understood yet. The MKKs MEKK1-4, MLK 1-3 and TAK1 were described as upstream activator kinases, which are additionally involved in JNK MAPK pathway [39]. As mentioned above, stress-inducing agents and inflammatory cytokines are the predominant activation stimuli, however, p38 MAPK is weakly

sensitive towards growth factors in a Rac dependent manner. In other circumstances, the reduction of growth factor leads to p38 MAPK pathway activation inducing apoptosis [64]. Further, upon several stress stimuli, its activation results in Ser/Thr phosphorylation of the EGFR that is removed from the surface via endocytosis without its degradation. These functions of the p38 MAPK prevent cell survival under stress condition in two ways, the induction of apoptosis and through the removal of mitogenic receptors from the surface [64].

2.4.4 The atypical MAPKs

Apart from Erk1/2 MAPK, the characteristic of serum sensitivity is attributed to further MAPKs: Erk3 and Erk8. Together with Erk4 and Erk7, they belong to the atypical MAPKs due to alternative activation mechanisms that differ from the classical three-tier model. Upstream activator kinases for all three of them have not been identified yet [65]. Due to the relevance for the present work, the characteristics of Erk7 and Erk8 presented only. The Erk7 and Erk8 MAPKs are related MAPKs, which display an overall homology of 69% (on amino acid sequence level). They bear the canonical T-E-Y triplet of Erk-like MAPKs and possess a C-terminal extension, which has been shown to be important for their activity [66, 67]. Indeed, both Erk proteins contain two SH3 binding domains within their tails, which represent docking sites for Src non-receptor tyrosine kinases. This suggests the involvement of both Erk7 and Erk8 MAPK in Src-dependent signalling [65, 68]. *In vitro* studies have demonstrated that Erk7 and Erk8 are distinguishable in their activation and in their activity profile towards their substrates [66, 67]. However, despite structural and biochemical differences, it is uncertain if they represent paralogues since genome analyses rather suggested a classification as orthologues [66, 67, 69]. In spite of the remaining controversial discussion and distinct features, Erk7 and Erk8 are considered as distinct MAPKs in the present work.

2.4.5 Alternative pathways

Besides the MAPK cascade activation, additional pathways are activated in response to growth factor stimuli by RTK. Those are the lipid kinase phosphatidylinositol 3 kinase (PI3K), the STAT and the phospholipase C γ (PLC γ) pathway.

PLC γ is recruited to the cell membrane and becomes tyrosine phosphorylated by the activated RTK. Upon activation, PLC γ produces diacylglycerol (DAG) and inositol-(1,4,5)-P₃ (IP₃) by the hydrolysis of phosphatidylinositol-4,5-phosphate (PIP₂), which is followed by the Ca²⁺ release from the ER. Free Ca²⁺ ions and DAG act together in the activation of protein kinase C (PKC) which subsequently activates further effectors [64].

In the PI3K pathway, the p85 regulatory subunit of PI3K binds to the activated RTK leading to the activation of the p110 catalytic subunit of PI3K. Alternatively, PI3K is activated by Ras. Activated PI3K causes conformational alteration of IP₃, thereby unmasking binding sites for proteins containing phospholipid binding domains. As a consequence, PDK1 and PKB/Akt dock to the cytoplasmic membrane where Akt is phosphorylated by a heteromeric complex. Finally, activated Akt phosphorylation induces the apoptosis pathway.

The cytosolic STAT transcription factors are capable to dimerize upon direct activation by RTK. Subsequently, they are imported into the nucleus where they induce the expression of proliferation genes [64].

2.5 Host-parasite interplay during alveolar echinococcosis

2.5.1 Early molecular and biochemical approaches

In 1855, Rudolf Virchow described the clinical course of AE for the first time and *Echinococcus* sp. as causative agent of the disease [70]. Nevertheless, until the 1990s the biology of *E. multilocularis* was poorly characterized on the molecular level. By this time, investigations addressed mainly diagnostic probabilities and pathology. Screening of cDNA expression libraries with patient sera, some antigens such as Em2, EM10, EM13, Em16 and EM18 were identified and proved suitable for diagnosis [24, 25, 71, 72]. Amongst the antigens, EM10 was further analysed by functional studies [25, 73]. During this process, Em10 was identified as member of the ezrin-radixin-moesin (ERM) cytoskeleton associated protein family of *E. multilocularis* that interacts with PDZ-1 and was thereupon designated Elp (ezrin-radixin-moesin like protein) [74]. In general, the ERM proteins are involved in the cytoskeletal arrangement and in the signal transduction of Rho and PKB dependent developmental processes [75]. In 1999, the characterization of the *elp* gene locus was the first molecular study to shed light on organisation and expression of echinococcal genes [76]. A further significant work in the molecular characterization was the discovery of trans-spliced mRNA in cestodes by Brehm et al [77]. The conventional splicing process is defined as fusion of exons from a pre-mature mRNA, resulting in the excision of introns from the same RNA strand (cis splicing). In the case of trans-splicing, the exons from different transcripts are fused (Fig. 2.6). Usually, a mini-exon of a small nucleolar pre-mRNA, the so-called spliced leader (SL), is fused to the 5' end exon of a mRNA. In 1986, the process was initially described for *Trypanosoma brucei* by showing that all transcripts in this organism contained the same 5' end [78]. Later on, the mechanism was found in the nematode *C. elegans* where 60% of all transcripts were trans-spliced and four different SL exist [79, 80]. Among cestodes, trans-splicing was described firstly for *E. granulosus* and *E. multilocularis*, later for *T. solium* [77, 81]. The Echinococcus SL (36 nt) derives from a small non-poly-adenylated snRNA (104 nt) and carries a tri-methyl-guanosine cap. Although in trypanosomes and nematodes trans-splicing is clearly involved in resolving poly-cistronic transcripts into mono-cistronic units for translation, there are additional, as yet unknown mechanisms of gene regulation which require this specific mode of transcript processing. Likewise, since poly-cistronic transcripts have not yet been described in flatworms, the precise functions of flatworm SLs are presently unclear although for a few mRNAs it has been shown that the SL provides the start ATG for translation initiation [77, 81]. Since the mechanism does not occur in humans, SL-containing transcripts are essentially of parasite origin and can be employed for molecular techniques like differential display or SL cDNA libraries [81, 82].

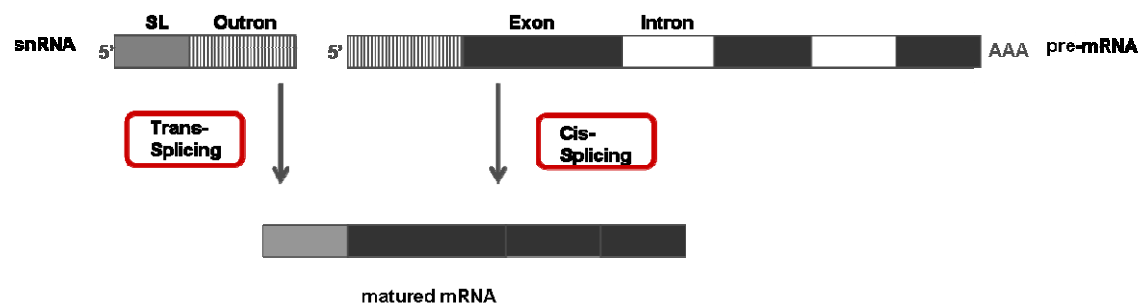


Fig. 2.6: Mechanism of trans-splicing. A mini-exon of a small nucleolar pre-mRNA (snRNA), the so-called spliced leader (SL), is fused to the 5' end exon of an mRNA.

2.5.2 *In vitro* cultivation of *E. multilocularis*

For the investigation of developmental processes in host-parasite interplay, it is important to reduce the complexity of the *in vivo* situation. The first *in vitro* cultivation of *E. multilocularis* metacystode larval stage was done in the presence of host tissue blocks or, later on, in the presence of defined hepatocyte cell lines [83, 84]. Secreted factors of feeder cells allow the metacystode to grow over months so that proliferation and differentiation could be observed *in vitro*. After starting the co-culture, the development of small vesicles of 1 to 2 mm in diameter takes up to two weeks while the development of brood capsules takes approximately two months. Refinement of the cultivation method was undertaken by excluding feeder cells. Here, metacystode vesicles were kept axenically under reducing conditions and a nitrogen atmosphere allowing studies on host-parasite interaction without indirect effects of host cells [85]. The differentiation to protoscoleces took place only in medium pre-conditioned with rat hepatocytes demonstrating the influence of secreted host factors of less than 15kDa on the parasite development [86]. Moreover, a culture system for *E. multilocularis* primary cell was recently established [13]. The primary cells were isolated from axenically cultivated vesicles and were incubated in the presence of feeder cells physically separated or alternatively with pre-conditioned medium under reducing conditions. Within a period of approximately five weeks, the primary cells generated new metacystode vesicles causing lesions as usual by subsequent injection into the peritoneum of mice [13, 86]. This method allows prospectively the genetic manipulation of *E. multilocularis* primary cells and in long-range, the regeneration of transgenic parasites. Taken together, the established cultivation systems of *E. multilocularis* allow the analysis of the host-parasite interplay and larval parasite development under laboratory conditions.

2.5.3 Genomic sequencing project

Important question in infectious diseases led to whole genome sequence projects by the Wellcome Trust Sanger Institute (Hinxton, Cambridge, UK). In cooperation with the groups of Klaus Brehm (Würzburg) and Cecilia Fernandez (Montevideo), the Sanger centre therefore

engaged in 2003 in a whole genome sequencing project for *E. multilocularis*, supported by extensive EST sequencing on both *E. multilocularis* and *E. granulosus* larval stages. Since this year, the genomic sequence as fourfold coverage is available under <http://www.sanger.ac.uk/projects/Echinococcus/>. Additional sequence information exists in the form of EST data from its relative, the dog tapeworm *E. granulosus* (<http://www.nematodes.org/NeglectedGenomes/Lopho/LophDB.php>) [82]. The access to genomic sequence data will considerably facilitate the work with *E. multilocularis* with respect to factors involved in the development of the parasite.

2.5.4 Evolutionary conserved signaling in *E. multilocularis*

Developmental processes in a metazoan organism require the exchange of information between cells. Hereby, a given cell does not only need knowledge about its location and function in the organism, but also needs the mechanisms to communicate with others to adjust to environmental conditions. The systems for cell-cell communication were established early in the evolution process of metazoans and can be found already in sponges, the most basal animals (see Fig.2.1) [87, 88]. Ions, cell metabolites, as well as hormones represent signals for cellular communication, among which the latter are suitable for the communication over long distances. Hormones are messengers produced in endocrine cells and exit their effect away from the production site by docking on their specific receptors. Amongst hormones, lipophilic steroids are capable to pass the cell membrane and to interact with their specific receptors and co-regulators in the cytoplasm or nucleus. In contrast, peptide hormones bind extracellularly to specific membrane-anchored receptors transducing the signal to inner components of the signal pathway. The mechanism of several evolutionarily conserved signaling pathways which are involved in development and growth are introduced in section 2.4

In recent years, several members of the respective *E. multilocularis* signaling pathways have been identified (Fig. 2.6). EmNHR1, EmNHR2, EmNHR3, EmSkip and EmGt198 have been characterized as factors of nuclear hormone signaling [89-91]. Belonging to peptide hormone pathways, the parasite's homologues of surface RTK of EGF, FGF as well as insulin pathways and four surface receptor serine/threonine kinases of the TGF- β family were identified [92-96]. For the transduction of external stimuli downstream of these surface receptors, the parasite's homologues of small GTP binding proteins, factors showing homology to MAPK cascade members as well as several Smad molecules have been shown to play an important role [97-100]. Since the signaling pathways essential for development and growth are conserved within the animal kingdom, the question arose to what extent they participate in the host-parasite interplay. Several influences of host cytokines on growth and differentiation of *in vitro* cultivated metacestode have been shown so far. Host EGF, for example, only slightly stimulates the growth of metacestode vesicles compared to the significant effect of host insulin. In contrast, host BMP-2 is able to direct differentiation process towards brood capsule formation rather than proliferation [85, 86, 93]. These findings suggest that host cytokines are not only essential for the parasite growth, but also might be involved in differentiation as well as in the establishment of larvae in the corresponding host. The investigation of these signaling pathways may lead to insights

concerning the question why protoscolecemes develop during the infection of the small rodent and less during the infection of humans.

To conclude, it is essential to examine the signaling pathways for the understanding of the host-parasite interplay since the survival of the worm depends not only on the protection against the host's immune defence, but also on the host derived growth factors.

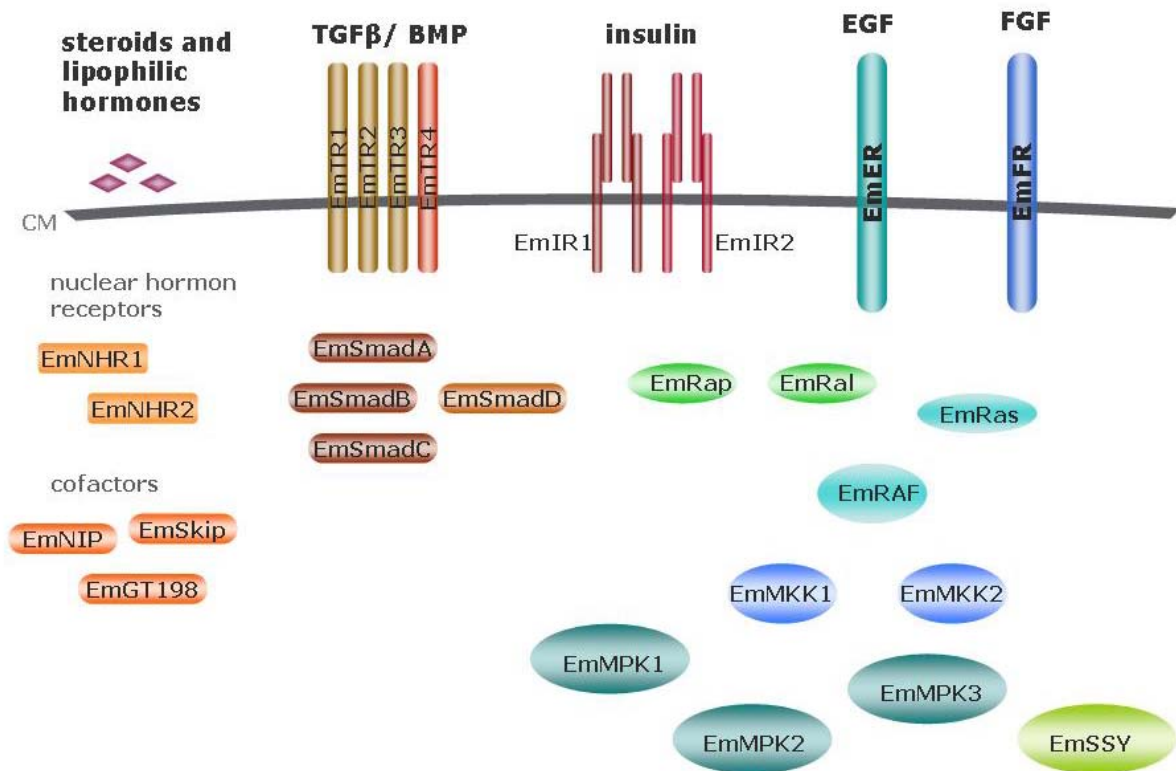


Fig. 2.7: Evolutionary conserved signaling in *E. multilocularis*. See section 2.5.4.

2.6 Aim of the project

The uptake of the *E. multilocularis* oncosphere larvae by humans causes the serious AE. The treatment of AE confine of surgery, if it could be applied, and of chemotherapy in any case. That means that in operable cases the application of pharmaceuticals should be continued for a minimum of two years and the relapse observed for ten years after surgery. For inoperable cases, a life-long chemotherapy is recommended. The chemotherapeutical option solely consists of the benzimidazole class, in particular albendazole and mebendazole. Severe side effects were reported as a result. Problematically, there are no alternatives for patients with an incompatibility for benzimidazoles.

Certainly, there are some efforts to enhance the efficacy of benzimidazole through simultaneous application of drugs approved against parasitic diseases such as praziquantel. Praziquantel was successfully used as drug of choice for schistosomiasis. However, evidences for development praziquantel resistance have emerged in the last decade [101]. In addition, studies on animals have shown that cases of resistance were mounted against benzimidazole by alteration of the target structure [20, 101].

The wealth of action with the available options for AE treatment is limited and the medication with benzimidazole derivates bears the aforementioned disadvantages, which implicates the pursuit of an innovative option. Reliable candidate target structures are parasite unique factors that are vital for its development. However, the current knowledge about such structures is insufficient since the research on helminths represents a neglected area, which is due to the fact that the impact of helminthic infections is insignificant in investing nations and the diseases affect primarily the developing world. The identification of such factors requires a large investment of cost and time, yet inhibitory agents are still not available at this point in time. The second group of suitable target candidates consists of parasite factors, which exist as counterpart in the host, but display a low level of homology combined with a significantly higher affinity towards the drug compound in comparison to host factors. Based on the differences between host and parasite signal transduction pathways a swift success through the access to enormous structural and functional data for human homologue can be expected. Moreover, inhibitory substances are available in a broad spectrum. Since several factors involved in the developmental and proliferation processes are conspicuous in tumour formation, amongst EGF receptor and members of MAPK cascade, activity inhibitory drugs for those, including even the data for the consequences for cell growth and pharmacokinetics, might be used with less additional cost and time. Miltefosine, for example, has been originally developed as anti-neoplastic agent, which exerts its effects as inhibitor of the PKB/Akt pathway, which is now employed with success for the treatment of leishmaniasis [102, 103].

Despite the fact that the signaling pathways are conserved among the animal kingdom, the most members of the *E. multilocularis* signal transduction display a lower level of homology to the respective host factor than the current target structure of the benzimidazole compounds. Therefore, the aim of this project was the characterization of signaling pathways involved in development and proliferation of the cestode. The identification of unique properties of the parasite signal transduction molecules, which distinguishes them from their human counterparts, will allow the development of novel anthelmintic therapies.

3. Results

3.1 EmMPK2 – the p38 MAPK orthologue of *E. multilocularis* as a possible target for the treatment of AE

3.1.1 Identification and characterization of *emmpk2*

After initial description of the Erk-like MAPK EmMPK1 by Spiliotis et al. (2006), a cDNA encoding a second *Echinococcus* MAPK has been identified in the course of a MD thesis by Rocio Caballero-Gamiz (unpublished). The respective protein was designated EmMPK2 (*E. multilocularis* MAPK 2), encoded by the gene *emmpk2*.

The trans-spliced cDNA was identified via degenerative PCR approach using oligonucleotides designed to bind the coding regions of the oligopeptides WSVGCI and WYRAPEIM, which are conserved within kinase domains of Ser/Thr kinases. The full-length cDNA of *emmpk2* was subsequently determined. It comprised 1371 bp (without polyA tail) including a 36 bp spliced leader sequence at the 5' end. A single ORF of 1104 bp was present which encoded a protein of 368 amino acids (a deduced molecular weight of 42.5 kDa; calculated by Compute pI/Mw; ExPasy [104]). EmMPK2 displays significant homology on amino acid sequence level to various p38 MAPK orthologues, e.g. human MAPK14, *D. melanogaster* MPK2, *C. elegans* PMK1 as well as yeast HOG1 (Fig. 3.1). Amino acid sequence identity values range from 38% to approximately 50% for yeast HOG1 and human p38 MAPKs, respectively. In the case of human p38 MAPKs, the highest homology could be found for isoform p38- α (HsMAPK14; 53% identity), followed by p38- β (51%), p38- γ (46%) and p38- δ (45%).

As indicated in Fig. 3.1, the *Echinococcus* protein contains all residues which are invariant in all known eukaryotic protein kinases [105]. In addition, a typical MAPK serine/ threonine kinase domain was predicted to be located between Tyr²⁵ and Phe³⁰⁹ by computer based SMART analysis [105, 106]. A hallmark of MAP kinases is the presence of a highly conserved T-X-Y motif close to the activation loop of the kinase domain in which both the Thr and the Tyr residues are phosphorylated by upstream MKKs. The typical consensus for this motif is T-G-Y in p38 MAPKs while Erk- and JNK/SAPK-like MAPKs harbor T-E-Y and T-P-Y motifs, respectively. EmMPK2 contained the T-G-Y motif which is typical for p38 MAPKs (Fig.3.2). Furthermore, the activation loop of EmMPK2 comprised 6 residues (Fig. 3.2) which is characteristic of p38 MAPKs while Erk- and JNK/SAPK-MAPKs typically contain activation loops of 12 or 8 residues, respectively [98].

Taken together, these structural features identified EmMPK2 as a member of the p38 subfamily of MAPKs. Interestingly, EmMPK2 showed several differences to known p38 MAPKs, which included amino acid exchanges at positions previously shown for yeast HOG1 and human p38 MAPK- α to be involved in the regulation of enzymatic activity [61, 107-109]. Furthermore, one of the conserved Asp residues in the so-called 'common docking site' is replaced by Asn in the case of EmMPK2. This site regulates the interaction of MAPKs with upstream MKKs and with phosphatases (Fig. 3.1)[110].

Analysis of the chromosomal *emmpk2* locus revealed that the ORF is contained within 10 exons, separated by 9 introns (Fig. 3.1), which all displayed canonical GT- and AG-motifs at

the splice-donor and -acceptor sites, respectively. Of these 9 introns, 7 shared conserved exon-intron boundaries with the human genes encoding p38 MAPKs while only 2 and 4 conserved boundaries were shared with introns of the human genes encoding Erk-like MAPKs and JNK/SAPKs, respectively. Besides the high degree of identity, this also indicates a close evolutionary relationship between *emmpk2* and mammalian p38 MAPK genes.

Using the cDNA sequence as query for genome data analysis, its chromosomal organization could be verified (Tab. 3.1). The *emmpk2* chromosomal locus localized to a contig of 21.211 bp and displayed a nucleotide sequence and exon-intron organization identical to that, which has been determined by PCR approach. As expected, the genomic locus contained a consensus splice acceptor site at the position where the SL was found in the cDNA (data not shown). Extensive BLAST analyses using the sequences of EmMPK2 and human p38 MAPK isoforms as queries did not reveal the presence of p38 MAPK encoding genes other than *emmpk2* in the *E. multilocularis* genome. However, a gene with high similarity to *emmpk2* was identified which encodes an unusual MAPK (EmSSY) and is presented in section 3.3.

Taken together, these data verified our analyses of the *emmpk2* cDNA and genomic locus and indicated that EmMPK2 is the only typical p38-like MAPK of the parasite.

Fig. 3.1: Amino acid sequence comparison between EmMPK2 and other p38 MAPKs. Shown are sequences of EmMPK2, human p38 MAPK- α (HsMAPK14; Q16539), *D. melanogaster* p38 MAPK (DmMK14A; O62618), *C. elegans* stress activated protein kinase PMK-1 (CePMK1; Q17446) and yeast HOG-1 (ScHOG1; P32485). The threshold for identical amino acid residues, which are highlighted in white on black background, is set to 60%. Similar residues are shaded in blue. Asterisks above the alignment mark residues which are highly conserved in eukaryotic protein kinases [106]. 'V's indicate intron positions on the encoding gene. Brackets above the lines highlight ATP-binding pocket, catalytic and activation loop as well as common docking (CD) site. 'P' marks Thr and Tyr residues of the conserved T-G-Y motif within the activation loop. Replacements of conserved residues within the CD site, which are assumed to be important for the interaction with regulator proteins are marked by 'U's [110]. 'M's above the alignment indicate mutation of residues which lead to constitutively activated forms of yeast HOG1 and HsMAPK14 [61, 107-109]. 'S' marked residues involved in stabilization of the L16 loop [109]. Black points indicate residues of human p38 MAPK- α , which are involved in the binding of pyridinyl-imidazole inhibitors [61].

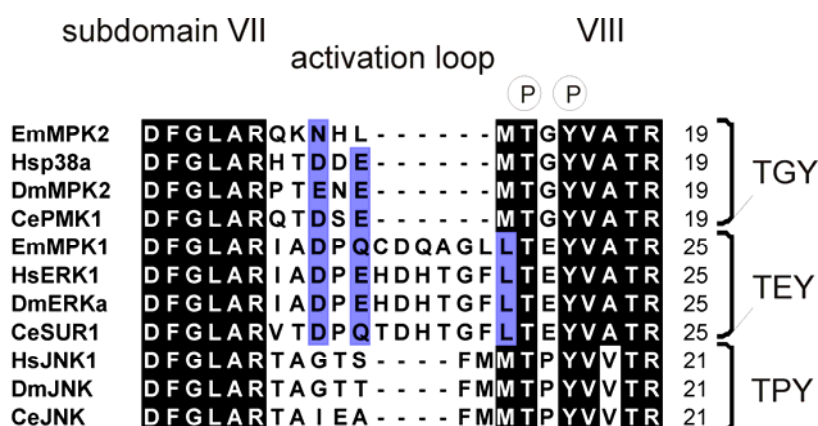


Fig. 3.2: Comparison of MAPK activation loops. Alignment of amino acid sequences of EmMPK2 and MAPKs from the p38, Erk and JNK/SAPK family of different phylogenetic origins. The activation loops are flanked by the highly conserved subdomains VII and VIII and contain the hallmark of MAPK, the dual-phosphorylation motif T-X-Y[105].

Contig No.		7471							
Exon/ Intron	No.	Start	End	Length	Sequence	AA	Corr. Ex/In in <i>hsp38a</i>	Corr. Ex/In in <i>hserk1</i>	Corr. Ex/In in <i>hsjnk1</i>
5' upstream		8017			...gcatttgaatccctcccagtc				
Exon	I	8039	8054	15	ATGCCCCGATGTAAATG				
Intron	1	8055	8201	146	gtaacgtggatcgccgagttgtgcatgctgcaactgtctcctgtgacctct accggatttctcttgcctgtatattaccacacactgacttccgaaccga tgcttggcgtaactcactactgtttcgtttctactttaag	Glu ⁵	-	-	+
Exon	II	8202	8299	97	AGCGACGGTTTGTCCCTGTTGAAATAAACAGCT ACGGTGGGATCTGCCGGACCGCTACACCCCGT TAATGTCGCCGGCCAGGGTAGCTTTGGAAC				
Intron	2	8300	8328	28	gtaaggatattttaaactcaaaaaatgattattaagtgtgacctccc aagcatgtgtccaatgcatgcattacag	Ser ⁴⁰	+	+	+
Exon	III	8329	8511	182	CTCCGCGTTGACAAGTACTTACAGAGAGAGGTG GCCATTAAGAAGTTGGATCGGCCTTTTCGAGAATG CAGAATCGCTAAGCGCACTTACCGTGAGTTGGCC ATTCTGCTCAAATGGATCATGAAAT				
Intron	3	8512	8586	74	gtgctgttcttctcctaccgtttttgctcactgagtaatggccactatt gttgcttcttgaag	Asn ⁸³	+	-	+
Exon	IV	8587	8649	62	GTTATTTGCCTCATCGATGCATTTACTCCGCAAAC CTCCTTGAGACTTTTGAAGACGTGTAC				
Intron	4	8650	10309	1659	gtatcatg...tctgttag	Val ¹⁰³	+	-	-
Exon	V	10310	10421	111	ATACCTTGTCACACCCCTGATGGATGCCGACCTG GGTGCTATTGTGGCTCAGCAGGTGCTCACTGAC GATCAGATCTGCTTCCCTCGCATACCAGATGCTGC GCGCGTGAAG				
Intron	5	10422	11329	907	gtaactg...tctgtagt	Lys ¹⁴⁰	+	-	-
Exon	VI	11330	11522	192	TACATGCATGGTGCCCATATAATCCATCGTGACC TGAAACCCTCCAACATCGGAGTAAACTCGGATGT GGAAGTGCCTATAATCGACTTCGGTTTGGCGCG GCAAAGAAATCACCTCATGACGGGCTACGTGGC CACTCGGTGGTACCGAGCGCCTGAAGTTATGCTT AATTGGATGCATTACAACGACTCAG				
Intron	6	11523	13543	2020	gtaggatt...cctcaag	Val ²⁰⁵	+	-	-
Exon	VII	13544	13695	151	TCGATGTGTGGTCAGTGGCGTGCATTTTGGTGG AACTGAAAACGCGCCAGCCCTCTCCGTGGGC TGAACCACATCGATCAGGTGAAGCAGATCATGAG CATCGTGGGCGCTCCGGACGAAGAATTGATGCA GAAAATACAGTAGCAGT				
Intron	7	13696	13770	74	gtaaggcttctccgctgtctccaccccgctttattgcttattgattgatt attgttctcccctcaatag	Ser ²⁵⁵	+	-	-
Exon	VIII	13771	13849	78	GCACGGGAATTTATTGAGAACTCAACTACACCA GCAAGAAGGATCTCAAGGATGCGTTTCCGTGGG CTTCGCCTGTTT				
Intron	8	13850	14702	852	gtgagtcg...gatgcttg	Leu ²⁸²	+	+	+
Exon	IX	14703	14852	149	TTCTGGATCCGGATCGGCGTCTGACAGCAGCAC AGGCTCTGGCACATCCATACTTCGCGGAATATCA CAACGAGAGTGATGAGCCTGTAGGAGAACCCT GGAAGACGATCTGATAGATTCCGACAACCTCACC ATGGAGGAGTGAAAG				
Intron	9	14853	14904	51	gtttggagttgatagcacatcccaatgactattgtcattgatcttg CAGAAGCTACATGGAATCTGCTGCAGAATTTAA	Glu ³⁴¹	+	-	+
Exon	X	14905	14993	88	GCCGAAGTTGACCTCCCTCCGACCGACAGACGC GTACTCGCCAATCAACGCGTGA				
3' down- stream		14994	15198	204	tgcttggcgccctccttgaccgctgttctgtctctgtgtgttaatt gtagcgctgtctgcaaatgacgctctctgttctctcactcactct cgttcttattcaagtcattcagtgacagttgctgctgcatatgaa agtgttctaatacgacaaatgcgaatagcattgattcat...				

Tab. 3.1: Gene structure of *emmpk2*. The gene *emmpk2* is localized of contig no.7471 of the first assembly. Eight exon/ intron boundaries could be found at corresponding positions in *hsp38 MAPK-α*, two exon/ intron boundaries in *hserk1* and four in *hsjnk1*. All exon/ intron boundaries display canonical GT...AG motifs.

3.1.2 Expression analysis of *emmpk2* in *Echinococcus* larval stages

The expression of *emmpk2* was analysed in larval stages metacestode and protoscolex before and after activation through pepsin/ low pH via semi-quantitative RT-PCR using RNA isolated from the corresponding stages as a template. The activation of protoscolex by the treatment with low pH and bile salts mimicks the transition of the larvae to the digestive system of the definitive host and leads to the evagination of the protoscolex. In a first step, the isolated RNAs were normalized for the expression of the housekeeping gene *elp* encoding the *Echinococcus* Ezrin-Radixin-Moesin (ERM) like protein Elp [73, 76]. As depicted in Fig.3.3 A, *emmpk2* is equally expressed in metacestode and in both protoscoleces preparations. In addition, the expression of *emmpk2* was compared between metacestode vesicles cultivated in the axenic system and vesicles cultivated in the presence of feeder cells. For this, the isolated RNA was reverse transcribed and the expression levels of the standard gene *elp* and *emmpk2* were addressed via multiplex PCR developed in this work. As presented in Fig. 3.3 B, *emmpk2* displays a constitutive expression level under both cultivation conditions.

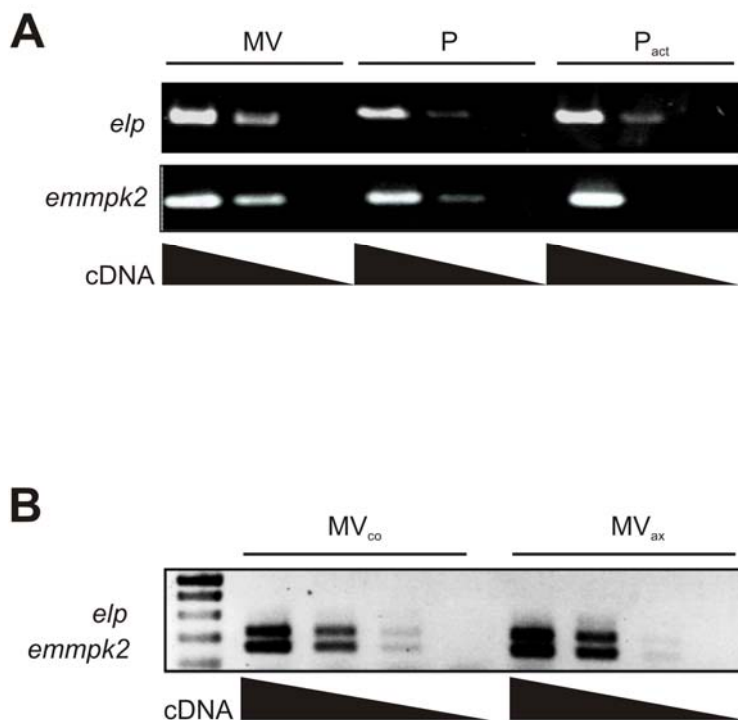


Fig. 3.3: Analysis of *emmpk2* expression in different larval stages of *E. multilocularis*.

(A) Total RNA was isolated from *in vitro* cultivated metacestode vesicles (MV) as well as from protoscoleces after cultivation in Mongolian jirds before (invaginated (P)) and after the *in vitro* activation (P_{act}) by low pH and bile salts. Different dilutions of cDNA were used in the semi-quantitative RT-PCR approach to analyze specifically the expression levels for *emmpk2* and the housekeeping gene *elp*. (B) Multiplex RT PCR analysis to compare the expression of *emmpk2* in metacestode vesicles of the co-culture (MV_{co}) and the axenic culture (MV_{ax}).

3.1.3 Expression and activity analyses of EmMPK2 in *Echinococcus* larval stages

3.1.3.1 Recombinantly expressed EmMPK2 - specific detection of the activated protein via antibodies raised against human p38 MAPK

For the detection of EmMPK2 in *Echinococcus* larval stages and for downstream analyses, suitable antibodies were needed. In the case of human p38 MAPK, an antibody specific for the phosphorylated form is commercially available, which recognizes the dual-phosphorylation motif pT-G-pY. To examine if this antibody also detects phosphorylated EmMPK2, EmMPK2 was recombinantly expressed in *E. coli* and purified under denaturing and native conditions using the pBAD expression system. Western blotting revealed that the phospho-specific antibody detected only the natively purified recombinant EmMPK2 appearing as band with an expected size of approximately 50kDa (Fig. 3.4 A). Since the suitability of this antibody had thus been proven, I used it to detect EmMPK2.

In lysates of echinococcal larvae, the antibody recognized a protein of approximately 47.5 kDa, which is in agreement with the deduced molecular weight of EmMPK2 (Fig.3.4 A). Nevertheless, the findings that this antibody detected several proteins in the crude lysate of metacystode vesicles raised the possibility that cross-reactivity with other MAPK might occur. Hence, supplementary approaches were carried out to clarify the specificity of the employed anti-phospho p38 MAPK antibody. For this, crude lysates of protoscoleces as well as recombinant EmMPK1 were subjected to Western blotting (Fig.3.4 B, C).

EmMPK1 has a deduced MW of 42 kDa (appearing as 46 kDa band) and might represent, due to its similarity with EmMPK2, one MAPK with which the phospho-p38 MAPK antibody might cross-react. Therefore, EmMPK1 was recombinantly expressed, fused to either GST (pGEX-3X vector) or to a hexahistidine tag and the V5-epitope (pBAD vector), and investigated using the anti-ERK and the anti-phospho-ERK antibodies (Fig.3.4 B). The result showed that EmMPK1 was correctly identified as fusion proteins in the expected sizes by the anti-ERK antibody. In contrast, EmMPK1 was not recognized by the phospho-specific ERK antibody confirming the previously presented data that EmMPK1 is not phosphorylated in its T-E-Y motif after recombinant expression [73, 76, 98]. However, the phospho-specific p38 antibody did not only detect recombinant EmMPK2 but also recombinant EmMPK1 of both expression systems, particularly in the pBAD system. Taken together, these findings suggest that the phospho-specific p38 antibody non-specifically also interacts with EmMPK1 and either recognizes the T-X-Y motif in its non-phosphorylated form or an epitope outside the T-X-Y motif. Nevertheless, despite non-specific interactions of the p38 antibody with EmMPK1 and several other proteins, the specific detection of EmMPK2 still was feasible as demonstrated by the following approach. I applied available p38 MAPK inhibitors to the *in vitro* cultivated metacystode vesicles and analyzed protein phosphorylation by Western blotting. Adding as little as 100 μ M ML3403 inhibitor abolished the detection of the 47.5 kDa protein in the lysates (Fig.3.4 C). Since EmMPK2 displays a pronounced autophosphorylation activity upon recombinant expression in *E. coli* (see above), these data indicate that the 47.5 kDa band indeed represents EmMPK2. This is also supported by the specificity of the ML3403 inhibitor towards EmMPK2, not EmMPK1 as outlined below. Additionally, regarding the calculated sizes of both MAP kinases with the corresponding

bands in Western blot experiments, the higher running band could represent EmMPK2. (Fig. 3.4 C).

Taken together, the human anti-phospho-p38 antibody clearly detected the 47.5 kDa band attributed to the parasite p38 MAPK orthologue EmMPK2.

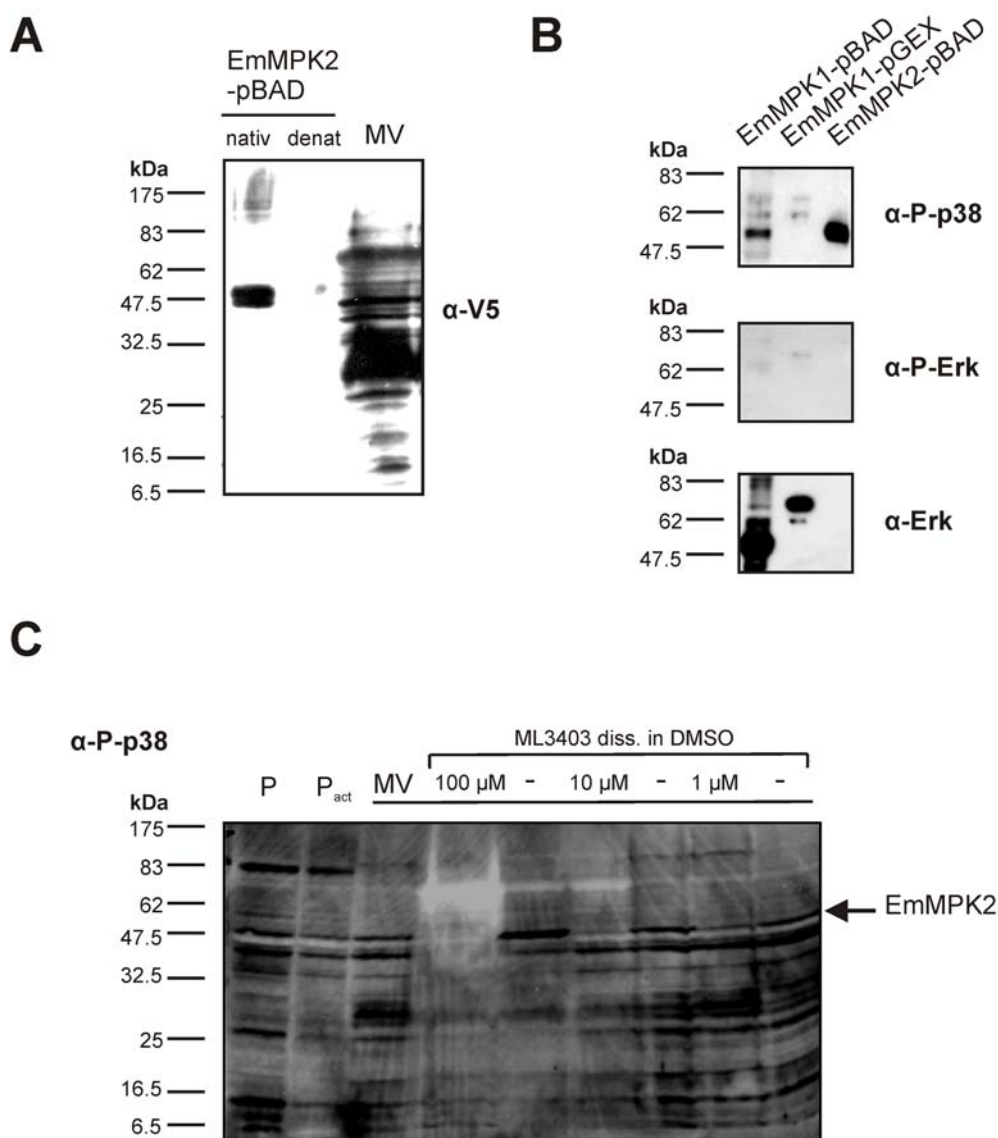


Fig. 3.4: Heterologue expression of EmMPK2 and its identification in *E. multilocularis* larvae with the cross-reacting human anti-active p38 antibody. Western blot analyses after sample separation via 12 % SDS-PAGE. **(A)** Detection of recombinant EmMPK2 after native and denatured protein purification (see also chapter 3.1.5) and analysis of EmMPK2 in *in vitro* cultured metacystode vesicles (MV) using the anti-phospho-p38 antibody. **(B)** Cross-reactivity of the anti-phospho p38 antibody analysed by comparison of recombinantly expressed MAP kinases of the parasite using the anti-Erk, the phospho-specific anti-phospho-Erk (recognizing the phosphorylated T-E-Y motif) and the phospho-specific anti-active p38 antibodies (produced against the phosphorylated T-G-Y motif). EmMPK1, the Erk orthologue was expressed in the bacterial expression vectors pBAD and pGEX-3x, EmMPK2 in the pBAD vector. **(C)** Analysis of lysates from protozoa before (P) and after activation (P_{act}) by low pH and bile salts and MV, which were cultivated without or with ML3403 (a p38 MAPK inhibitor) and the inhibitor solvent DMSO, respectively using the anti-phospho p38 antibody (see chapter 3.1.6).

3.1.3.2 Activity of EmMPK2

The expression of EmMPK2 was investigated in the different larval stages of *E. multilocularis* by Western blot analysis with the human anti-phospho-p38 antibody recognizing the dual-phosphorylated motif T-G-Y. Elp was used as loading control [73, 76]. As shown in Fig. 3.5, the western blot experiment confirmed the result of the RT-PCR that EmMPK2 is expressed and phosphorylated in the metacestode. It is also expressed and phosphorylated in activated, and to less degree in non-activated protoscolexes.

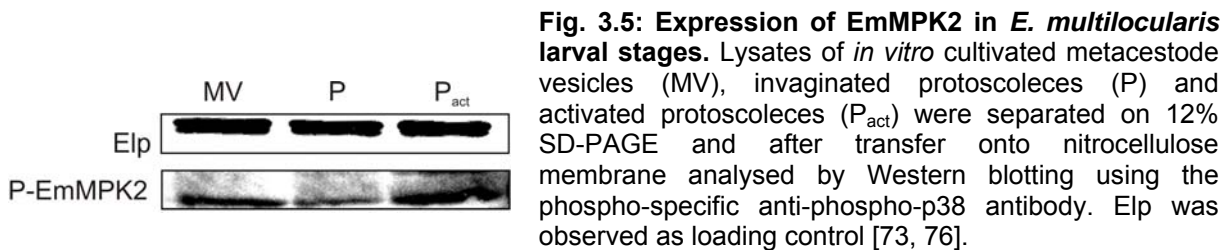


Fig. 3.5: Expression of EmMPK2 in *E. multilocularis* larval stages. Lysates of *in vitro* cultivated metacestode vesicles (MV), invaginated protoscolexes (P) and activated protoscolexes (P_{act}) were separated on 12% SD-PAGE and after transfer onto nitrocellulose membrane analysed by Western blotting using the phospho-specific anti-phospho-p38 antibody. Elp was observed as loading control [73, 76].

3.1.4 EmMPK2 activation in *in vitro* cultivated metacestode vesicles

Initial experiments to investigate the influence of exogenous stimuli on EmMPK2 activation revealed that the protein was always phosphorylated when the metacestode vesicles had been mechanically damaged prior to the application of sample buffer. Since p38-like MAPKs are known to be induced by stress conditions, these results could have been due to a similar function of EmMPK2 in *Echinococcus*. Therefore, in an alternative approach, intact metacestode vesicles were frozen in liquid nitrogen directly after isolation from culture and were then investigated through western blot analysis (Fig. 3.6 A). Indeed, after applying this procedure, phospho-EmMPK2 was no longer detectable, indicating that the protein is specifically activated upon physical disruption of metacestode vesicles and supporting the idea that EmMPK2 might serve as a stress-kinase in the parasite.

To verify the result that EmMPK2 is activated in response to mechanical disruption, metacestode vesicles were damaged by different methods. First, the vesicles were disrupted by resuspending with a pipette and the samples were prepared in the two ways, i.e. mechanical disruption before addition of sample buffer (A) or after the addition of sample buffer (B). Second, the vesicles were cut with a scalpel and third, the damage was performed by pricking the vesicles with a needle. Notably, EmMPK2 phosphorylation was detectable upon disruption only and independent of the order of working steps (Fig. 3.6 B). So the result indicated that the phosphorylation of EmMPK2 is induced by strong mechanical destruction of the vesicles. It needs to be mentioned that the phosphorylation induced by mechanical stress might be caused indirectly by osmotic changes due to the loss of hydatid fluid.

Based on this result, the subsequent investigation, which addressed the identification of activation or stress conditions for *E. multilocularis*, were performed on metacestode larvae pricked to remove the hydatid fluid.

Besides the mechanical stress, several oxidative stress situations, in which human p38 is activated, were tested on metacestode vesicles cultivated *in vitro*. DMSO, hydrogen peroxide

and paraquat were selected as oxidative stress inducers. However, neither of these stress conditions led to phosphorylation of EmMPK2.

In case of mammalian cells, it has been shown that p38 MAPK can be activated by TGF- β , BMP and insulin. Stimulatory effects of these factors on *E. multilocularis* could already be demonstrated [86, 93]. Thus, the potential influence of these host growth factors on EmMPK2 was addressed by incubation of metacestode vesicles in the presence of either host insulin, TGF- β , BMP or EGF. In addition, the presence of serum as well as the presence of feeder cells were tested as activation stimuli. However, in all experimental setups neither host factors nor serum had an effect on the EmMPK2 T-G-Y phosphorylation (data not shown). A possible explanation for failure to detect altered phosphorylation states of EmMPK2 could be normalization of samples for their total protein content via Western blotting for Elp. This could mean that changes in EmMPK2's amount in these otherwise normalized samples were overlooked. Several antibodies covering total amount of human p38 MAPK did not recognize EmMPK2 and therefore, Elp was observed only for protein content. Nevertheless, this seemed to be very unlikely explanation since a multitude of experiments was carried out. In neither case, an indication for altered amount of EmMPK2 was observed.

Taken together, the failure to stimulate phosphorylation of EmMPK2 suggests that the EmMPK2 signaling did not show resemblance to the activation of human p38 MAPK. Besides strong physical damaging of integer vesicles, no stimulus or stress situation could be identified leading to increased phosphorylation, i.e. activation of the p38 MAPK orthologue of *E. multilocularis* (Fig. 3.7).

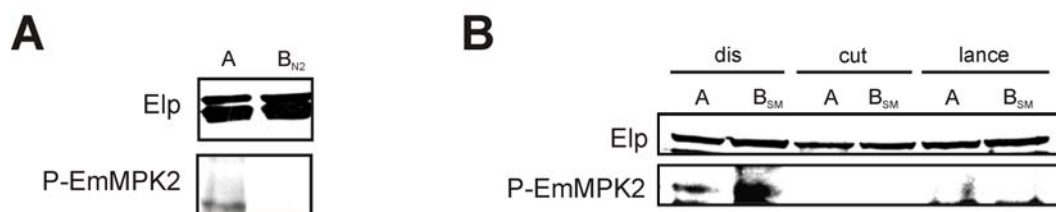


Fig. 3.6: Phosphorylation of EmMPK2 upon physical stress. Indicated are Western blot analyses of metacestode vesicle lysates, which were separated on 12% PAA detecting the phosphorylation on the activation motif T-G-Y of EmMPK2 by the anti-phospho-p38 antibody. Elp served as loading control. Vesicles were prepared for lysates in different ways: **(A)** Mechanical disruption before addition of sample buffer (A) or liquid nitrogen treatment before the addition of sample buffer (B_{N_2}).

(B) Addition of sample buffer before (A) or after (B_{SM}) damaging of vesicles. Damaging was performed by disruption with a pipette (dis), cutting with a scalpel (cut) and pricking with a needle (lance).

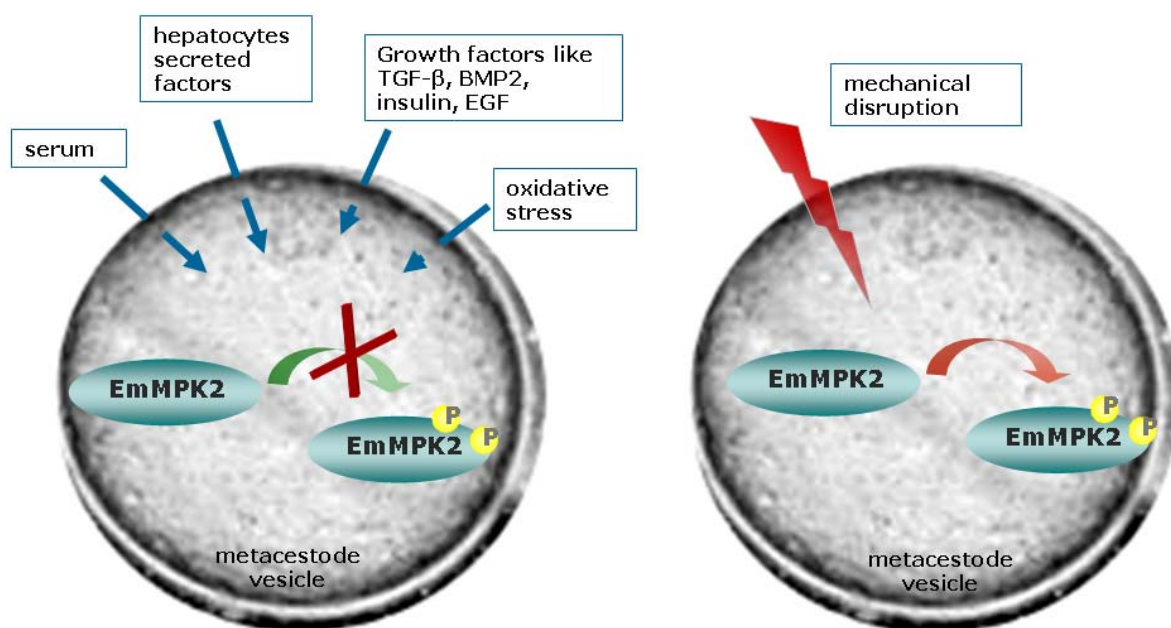


Fig. 3.7: Summary of environmental conditions tested on *in vitro* cultivated metacystode vesicles monitoring EmMPK2 phosphorylation.

3.1.5 EmMPK2 – an enzymatically active MAP kinase

3.1.5.1 TGY- phosphorylation of EmMPK2 after recombinant expression – differences to human p38 MAPK

Although sequence homology clearly identified EmMPK2 as a member of the MAPKs, no experimental data were available proving that it also exerts kinase activity. Toward this end, EmMPK2 was expressed as fusion protein with V5-epitope and 6xHis-tag in *E. coli* (see also 3.1.3). The purification was done either under denaturing or native conditions. Protein expression was performed via Western Blot analyses with anti-V5 antibody and detected EmMPK2 as fusion protein with the expected size of approximately 50 kDa as shown in Fig. 3.8 A. Further, I investigated whether EmMPK2 is enzymatically active after recombinant expression and subsequent purification. To this end, the anti-phospho-p38 antibody recognizing the dual-phosphorylated TGY motif of active p38 MAPK was used. The result showed that heterologously expressed EmMPK2 was both phosphorylated and active, only when purified under native conditions (Fig. 3.8 A). This was compared with the activity of host p38 MAPK- α expressed in the same way as EmMPK2. Using the anti-V5 antibody, the p38 MAPK- α fusion protein was detected with the expected size of approximately 48 kDa. When the activity of human p38 MAPK- α was analysed using the phospho-specific anti-p38 antibody, only a weak band was detected, meaning a lower activation level of the human kinase compared to EmMPK2. As negative control, lacZ was expressed.

3.1.5.2 *In vitro* activity of EmMPK2 and its inhibition

EmMPK2 kinase activity was tested through *in vitro* phosphorylation of the common kinase substrate myelin basic protein (MBP) in the presence of radioactively labelled γ -ATP. As shown in Fig. 3.9 A, EmMPK2 phosphorylated MBP. In contrast, human p38 did not exert detectable enzymatic activity.

Furthermore, the enzymatic activity of EmMPK2 could be blocked by incubation with commercial available ATP competitive p38 inhibitors SB202190 and ML3403 (Fig. 3.9 B) [111, 112]. In this assay, the kinase activity was reduced with increasing inhibitor concentration and ML3403 was more effective than SB202190.

Interestingly, in the assays using recombinant EmMPK2, an additionally 50 kDa band appeared. Since the recombinant *Echinococcus* protein has 50 kDa, this strongly suggested an auto-phosphorylation-reaction (Fig. 3.9 C). This auto-phosphorylation was also inhibited by the p38 inhibitors in the same manner as observed for MBP. In case of human p38 MAPK, no auto-phosphorylation was detected (Fig. 3.9 D).

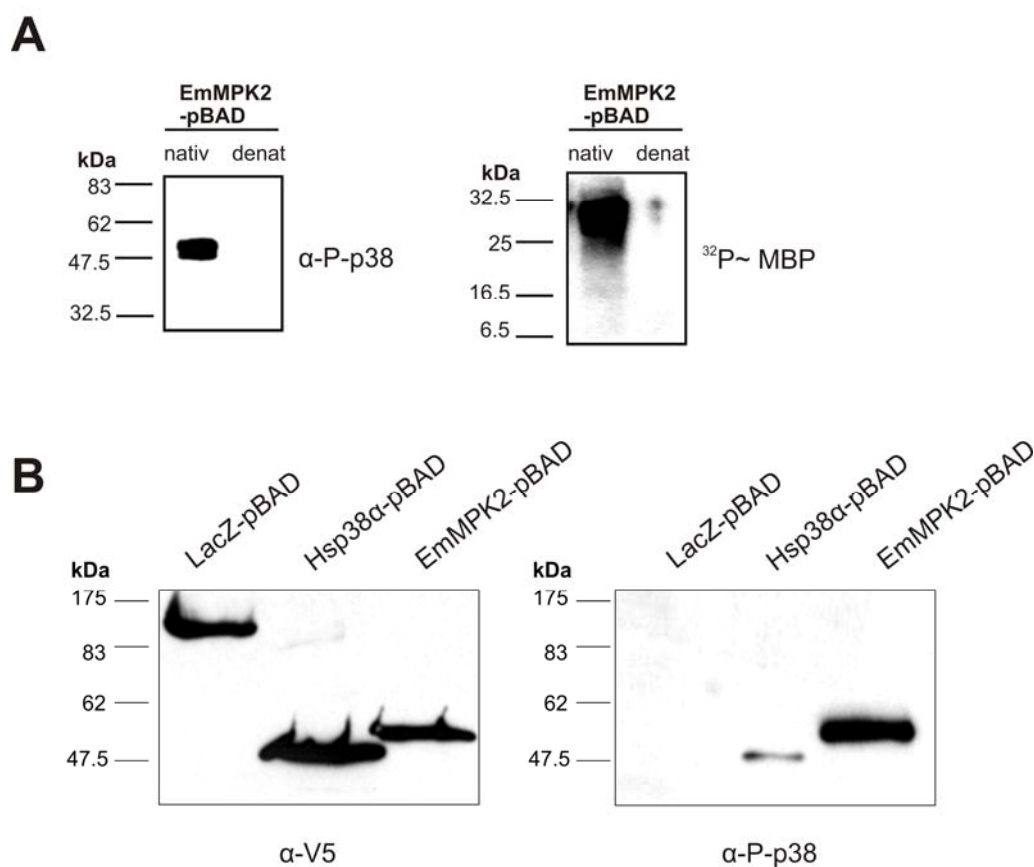


Fig. 3.8: EmMPK2 as active enzyme after recombinant expression and purification under native condition. Indicated are Western blot analyses after previous separation of recombinant proteins via 12% SDS-PAGE. (A) After heterologue expression of EmMPK2 as fusion protein in the bacterial expression vector pBAD and subsequent purification under native and denatured conditions the phosphorylation pattern of EmMPK2 was investigated using the anti-phospho-p38 antibody.

Additionally, the enzymatic activity of EmMPK2 from both preparations was observed by incorporation of radioactive labelled phosphate into the common kinase substrate myelin basic protein (MBP). The samples were separated on 15 % SDS-PAGE and the signal detected by exposing the blotted membrane on x-ray films. (B) Phosphorylation of EmMPK2 after recombinant expression and subsequent native preparation was compared to human MAP kinase p38 isoform α by unchanged experimental settings. LacZ was used as negative control. For Western blot detection, an anti-V5 antibody was used.

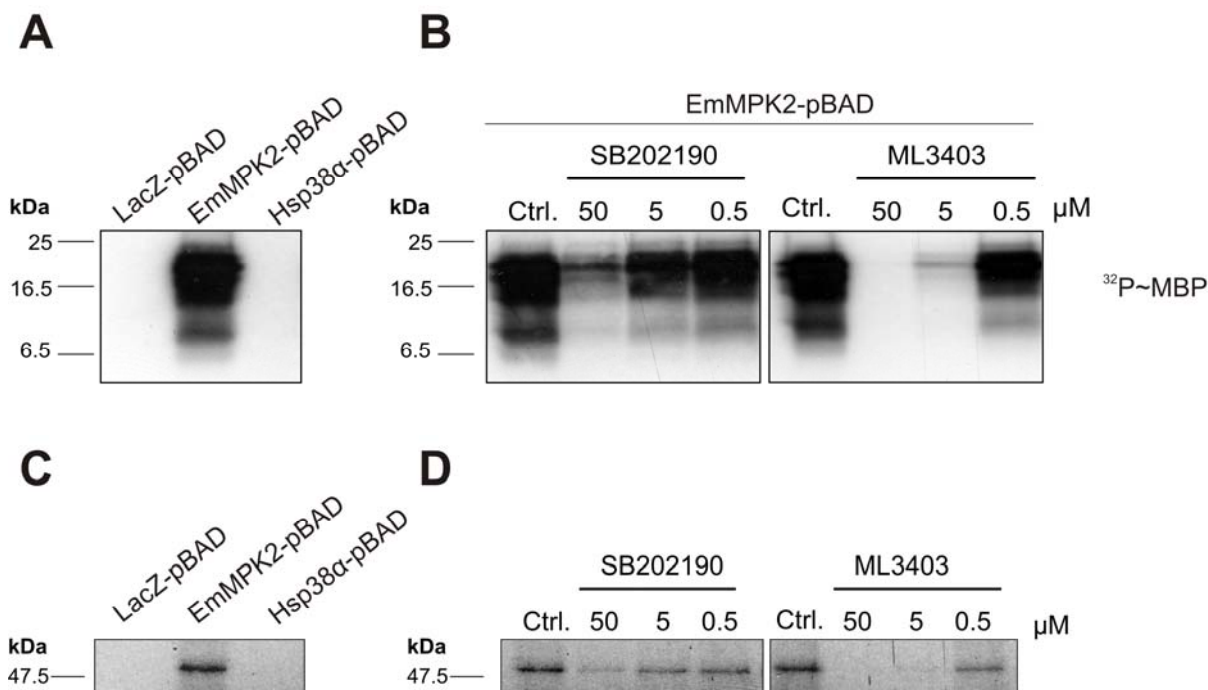


Fig. 3.9: *In vitro* kinase assay of EmMPK2 and its inhibition by human p38 inhibitor compounds. Enzymatic activity of echinococcal EmMPK2 and human p38- α was analysed detecting the incorporation of radioactive labelled γ - 32 P from ATP into myelin basic protein (MBP). As negative control LacZ in the pBAD expression vector was used. After expression in *E.coli*, the fusion proteins were affinity purified under native conditions and set in equal amounts in the kinase assay. The reactions were stopped by adding stop mix. The samples were separated on 15% SDS-PAGE and subsequently transferred on nitrocellulose membrane. X-ray films were exposed for 4 days. (A) Detection of radioactively phosphorylated isoforms of MBP by LacZ, EmMPK2 and Hsp38 α . (B) Inhibition of the substrate phosphorylation by incubation of EmMPK2 in the presence of two commercial available ATP competitive p38 inhibitors SB202190 and ML3403 in the indicated dilution. EmMPK2 was incubated with inhibitor dissolvent DMSO as control. (C) Detection of radioactive labelled kinases (D) Inhibition of autophosphorylation of EmMPK2 by SB202190 and ML3403.

3.1.6 Treatment of *in vitro* cultivated metacestode vesicles with pyridinyl imidazoles

3.1.6.1 Increased alkaline phosphatase activity as consequence of drug influence

The p38 inhibitor compound ML3403 was tested concerning influences on the growth of *in vitro* cultivated metacestode vesicles. In a first set of experiments, metacestode vesicles from hepatocytes co-culture were used and incubated in groups of five in 12well plates with normal culture medium containing 10% FCS. Incubation was performed for four days in the presence of the p38 inhibitor in the indicated dilution steps. Vesicles incubated in the presence of dissolvent DMSO served as controls.

As marker for vesicle viability, alkaline phosphatase (AP) activity in the culture supernatant was measured, using *p*-nitrophenyl phosphate as substrate according to the previously published protocol [113]. Figure 3.10 displays the absorbance of 405 nm over the time course representing free alkaline phosphatase activity. All values are normalized against rat hepatocytes incubating in culture. In the presence of ML3403, a significant increase of AP activity was measured at a concentration of 1 mM and a slight increase at 0.1 mM in comparison to DMSO treated vesicles.

After four days, sixty percent of the vesicles treated with 1 mM exhibited damage in the laminated and germinal layer and lost structural integrity as observed by light microscopy.

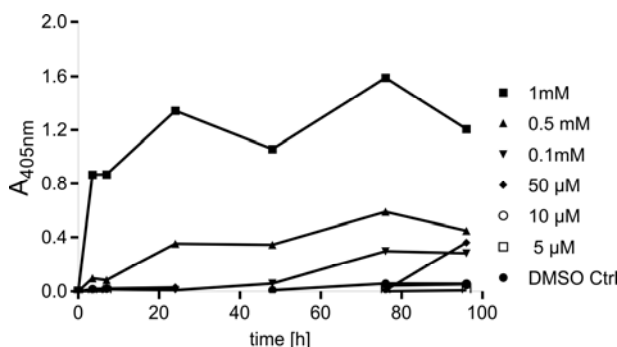


Fig. 3.10: Alkaline Phosphatase activity in the culture supernatant of *E. multilocularis* as indication of metacestode vesicle damage. p38 inhibitor ML3403 was tested in a time course experiment with *in vitro* cultured metacestode vesicles. Metacestode vesicles were incubated over 4 d in the presence of the compound in dilution steps of 5 µM up to 1mM and in the presence of dissolvent DMSO. At the indicated time points, the alkaline phosphatase activity was determined using *p*-nitrophenyl phosphate as substrate by measurement of absorbance at 405 nm.

3.1.6.2 Pyridinyl imidazoles specifically target EmMPK2

To investigate whether the pyridinyl imidazole compounds specifically targeted EmMPK2, the phosphorylation of EmMPK2 in drug treated metacestode vesicles was measured using the phospho-specific p38-antibody since, as outlined above, the phosphorylation of EmMPK2 mainly depends on autophosphorylation activity (Fig. 3.11). Additionally, the phosphorylation on the T-E-Y motif of EmMPK1, the Erk orthologue of *E. multilocularis* was assessed using the phospho-specific Erk-antibody [98]. The Elp protein and total EmMPK1 acted as

standards for protein content. As indicated in Fig.3.11, the dissolvent DMSO affected neither the activity of EmMPK2 nor the phosphorylation of EmMPK1; in contrast, the p38 inhibitor blocked specifically the phosphorylation on the T-G-Y motif of EmMPK2.

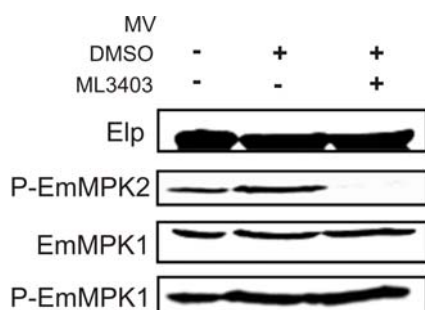


Fig. 3.11: The p38 inhibitor ML3403 targets EmMPK2, the p38 orthologue of the parasite.

One millilitre of axenically cultivated metacystode vesicles (MV) were incubated for 3.5 h with 10 μ M ML3403 or with the inhibitor dissolvent DMSO alone. Samples were separated on 12% PAA and analysed via Western blotting. EmMPK1 was detected by the anti-ERK antibody and the anti-phospho-ERK antibody, EmMPK2 by the anti-phospho-p38 antibody. Elp was used as loading control using the anti-Em10 antibody.

3.1.6.3 Inactivation of metacystode vesicles by pyridinyl imidazole compounds

The results from the *in vitro* MAPK assay revealed that the pyridinyl imidazole compounds ML3403 and SB202190 inhibit the enzymatic activity of EmMPK2. Hence, the influence of both cell-permeable drugs was investigated on *in vitro* cultivated metacystode larvae.

Metacystode vesicles which either derived from long-term axenic cultivation or from co-cultivation with feeder cells were incubated in groups of five in normal culture medium. After one day of incubation, vesicle integrity was assessed microscopically. ML3403 and SB202190 were then added in defined concentrations and the physical appearance of the vesicles was assessed daily. Structurally intact vesicles were defined as viable whereas vesicles that have lost turgor were defined as inactivated (for examples, see fig. 3.13).

As shown in Fig. 3.12, SB202190 and ML3404 significantly diminished vesicle survival in a concentration dependent manner. Approximately 50% of vesicles were killed by 5 μ M of SB202190 at day 4 (A, B), whereas for the same effect a lower concentration of 0.5 μ M ML3403 was sufficient (C, D). The survival on the last day of the experiment was analysed separately in the bar graphs E and F. The influence of 5 μ M of the two compounds was highly significant in comparison to the DMSO treated control. Furthermore, there was a significant difference in the ability of both drugs to inactivate metacystode vesicles, as evaluated by ANOVA and Tukey's multiple comparison test. The inhibitory concentrations (IC_{50}) of ML3403 and SB202190 were graphically determined by linear regression (Fig.3.12, G and H). For ML3403, IC_{50} values of 55 nM for vesicles originating from co-culture and 42 nM for vesicles from the axenic culture were obtained. Higher concentrations of 3.8 and 3.5 μ M, respectively, were calculated for SB202190 (Fig.3.12, I). Hence, although both drugs display different capacities to inactivate *E. multilocularis*, it was irrelevant whether the metacystode vesicles had previously been incubated in the presence of feeder cells or under axenic conditions.

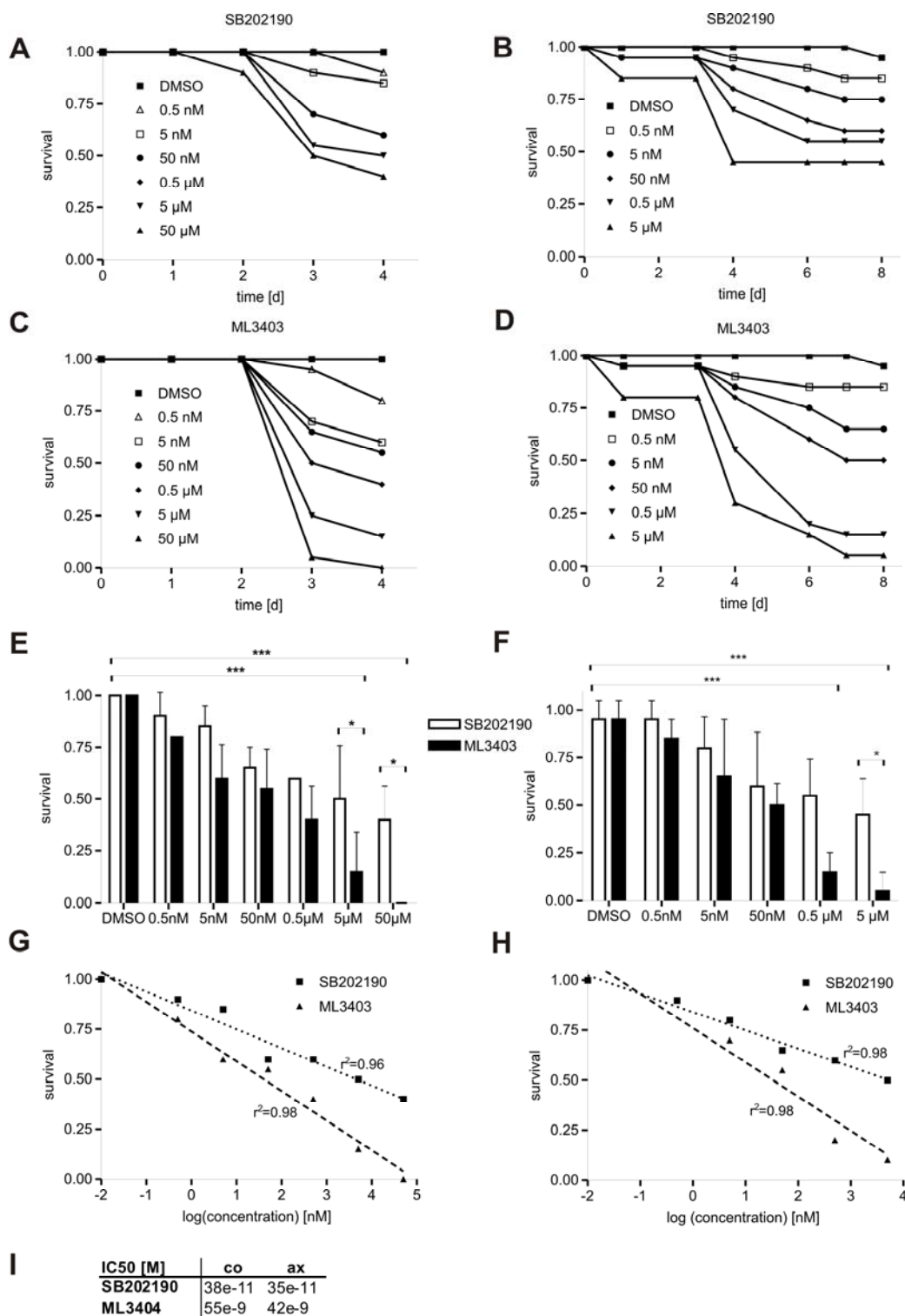


Fig. 3.12: Killing of *in vitro* cultivated metacestode vesicles upon treatment with the p38 inhibitors SB202190 and ML3403. Co-cultivated (A, C, E, G, I) and axenically cultivated (B, D, F, H, I) metacestode vesicles were transferred into culture medium including high serum concentration. One day later, the integrity of vesicles was assessed via LM and the time course experiment was started by adding inhibitor dissolvent DMSO or SB202190 (A, B) and ML3403 (C, D) in the indicated concentrations. The viability of the vesicles was monitored each day by light microscopy. At the end, the survival of metacestode vesicles was quantified and analysed separately in figure E and F. IC₅₀ values, indicating the concentration where 50% of the vesicles were killed, were determined via linear regression (G, H). Both r squared values indicate an extremely high significance of fitting. Accordingly, IC₅₀ of 3.8 μ M and 3.5 μ M, were calculated for SB202190; IC₅₀ of 55 nM and 42 nM for ML3403 (I).

3.1.7 Treatment of *Echinococcus* primary cells with pyridinyl imidazoles

Very recently, it has been reported that primary cell cultures from digested metacestode vesicles contain totipotent germinal cells (the cestode equivalent to planarian 'neoblasts') which are able to regenerate new vesicles when incubated *in vitro* [13]. Due to the fact that *in vitro* cultivated metacestode vesicles were inactivated by treatment with the compounds ML3403 and SB212090, the question arose whether a regeneration of new vesicles is possible after treatment. Axenically cultivated metacestode vesicles were incubated in DMEM containing 10% FCS, antibiotics and DMSO with or without ML3403 or SB202190. After 4 days, the time after which 90% or 50% of vesicles were destroyed by 5 μ M ML3403 or 5 μ M SB202190, respectively, *Echinococcus* primary cells were isolated and incubated in well- plates to assess the regeneration process for 4 weeks (Fig. 3.13). Primary cells from the DMSO treated control group formed cell aggregates with central cavities, indicating active regeneration. In contrast, primary cells from ML3403 treated vesicles remained single cells throughout the incubation. The result for vesicle regeneration originating from the SB202190 treated group was similar to ML3403 with the exception that several small aggregates were formed which did, however, not develop central cavities.

In a further experiment, primary cells were isolated from intact and untreated metacestode vesicles and then incubated in medium containing the inhibitory compounds. The time course of vesicles regeneration in the presence of DMSO without or with SB202190 or ML3403 is shown in fig. 3.14. After 7d, the formation of aggregates was similar in all groups. However, the morphology of drug treated cells was more granular as those of the control cells, an indication for decreased vitality. One week later, the number of DMSO treated primary cells had increased and the aggregates appeared cloudy indicating cavity formation. SB202190 treated cells formed slightly more aggregates than ML3403 treated cells but both cultures showed less and more amorphous cell clusters than the control.

In addition, the medium of the drug treated cells remained red in contrast to cells, which were incubated in the presence of DMSO, where the colour of culture medium containing pH indicator turned yellow after one week. This indicated the excretion of acid metabolism final products from the viable DMSO treated cells.

At day 28, all cell clusters of primary cells incubated in the presence of ML3403 were dissolved and the colour continued to be red. SB202190 treated primary cells showed small aggregates and spread diffuse in most instances on the well bottom. In the cavities of DMSO treated primary cells, on the other hand, small vesicles emerged.

After one week of cultivation, *emmpk2* expression was investigated using RT-PCR. As shown in Fig. 3.14 A, the *emmpk2* mRNA was clearly detectable in DMSO- and in ML3403-treated cultures. Furthermore, the 42 kDa protein band which reacted with the anti-phospho-p38 antibody was present in primary cultures (Fig. 3.14 B). Upon treatment with 5 μ M ML3403 for one week, phospho-EmMPK2 was no longer detectable (Fig. 3.14 B).

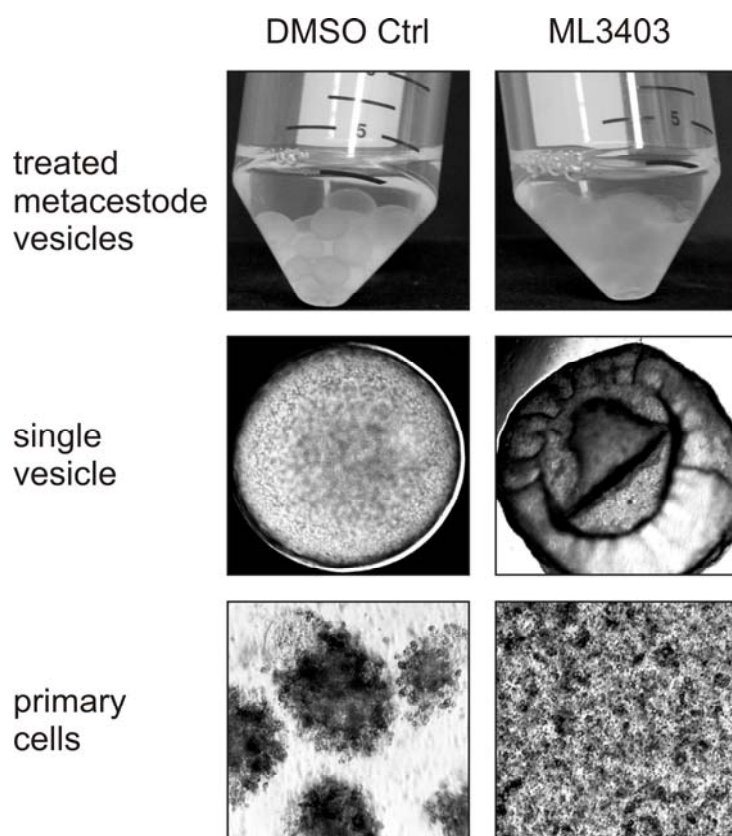


Fig. 3.13: Generation of metacestode vesicles out of *Echinococcus* primary cells in the presence of ML3403. Axenically cultivated vesicles were incubated in the presence of DMSO with or without 5 μ M p38 inhibitor ML3403 for 4 days, after which 90% of the vesicles were killed. Subsequent to isolation, primary cells from treated vesicles were seeded in 24 well plates. The formation of cell aggregates, central cavities and intact vesicles was only observed for primary cells that derived from DMSO-controls. No regeneration was observed for inhibitor-treated cultures.

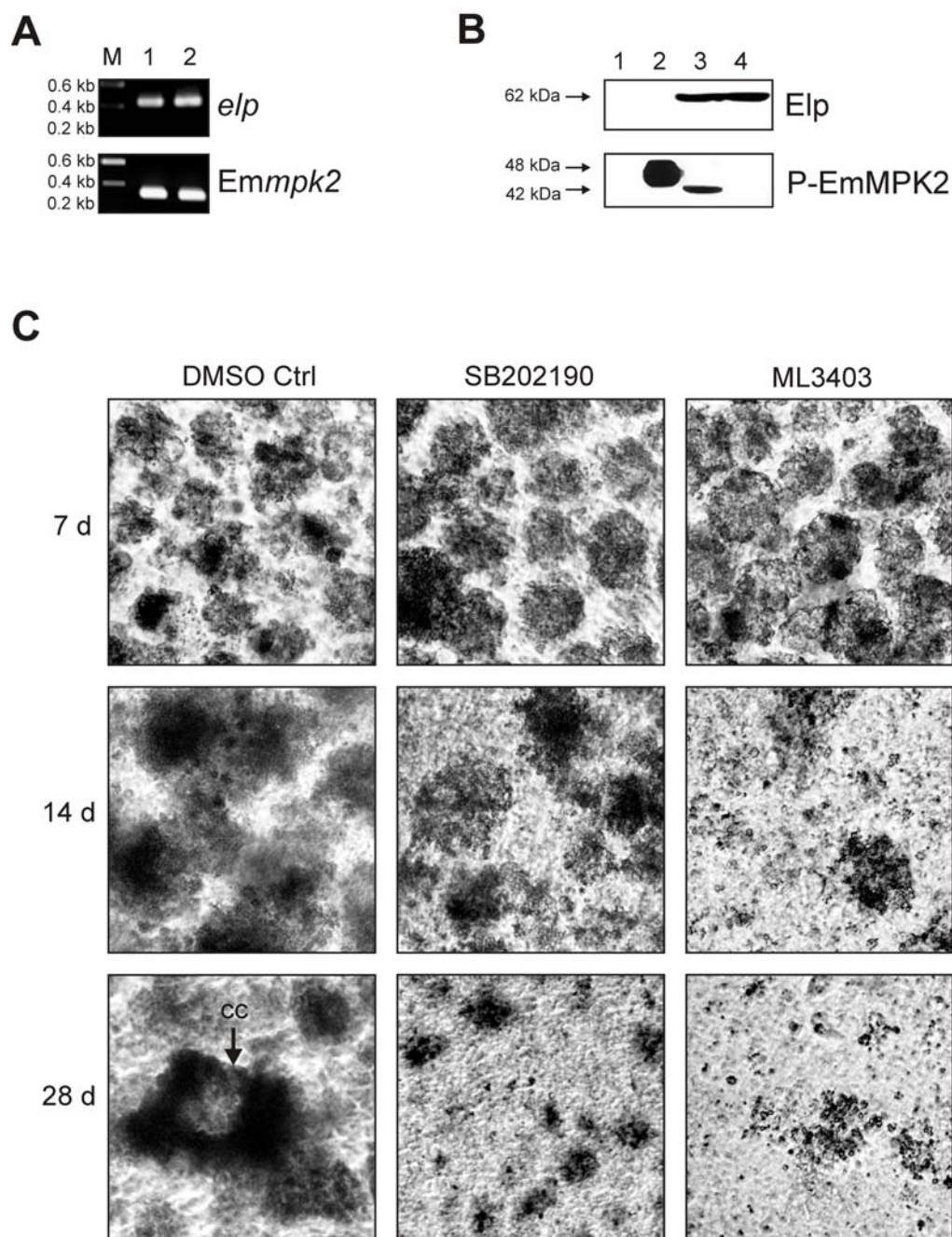


Fig. 3.14: Treatment of *Echinococcus multilocularis* primary cells with ML3403 and SB202190. Primary cells were isolated from axenically cultivated metacystode vesicles. Subsequent incubation occurred with pre-conditioned medium in 24well plates in the presence of inhibitor dissolvent DMSO with or without 5 μ M ML3403 and SB202190. After one week incubation, *emmpk2* and *elp* expression was analysed via RT PCR (**A**) in DMSO (lane 1) and ML3403 (lane 2) treated cells. At the same time point, EmMPK2 phosphorylation (**B**) was monitored in primary cells incubated in the presence of DMSO (3) and ML3403 (4). Recombinant LacZ (lane 1) and EmMPK2 (lane 2).served as controls (**C**).The pictures were taken after 7, 14 and 28 days of incubation time (CC = central cavity).

3.1.8 Treatment of *in vitro* cultivated protoscoleces with pyridinyl imidazoles

Addressing the survival capability of *E. multilocularis* larval stages in the presence of p38 MAPK inhibitors, protoscoleces of isolate J31 were cultivated *in vitro* under the influence of ML3403. The protoscoleces, derived from *in vivo* cultivated *E. multilocularis*, were treated with bile salts and pH2 after isolation to obtain evaginated larvae (thus also removing contaminating host cells). Aliquots of 100 μ l protoscoleces suspension in 1x PBS were incubated in 24 well plates with 1 ml DMEM containing high serum concentration and antibiotics per well. Control groups were larvae without and with DMSO. ML3403 was added to a final concentration of 10 μ M. At the beginning of the experiment, all protoscoleces appeared evaginated and were motile. Untreated and DMSO treated protoscoleces maintained this phenotype to the end of experiment; inhibitor-treated protoscoleces, on the other hand, displayed variable morphologies from lightly bloated to globular appearance (Fig. 3.15, A-E). In some cases a transparent blister could be observed on tail or head (Fig. 3.15, A, B). After two weeks, the majority of control larvae appeared globular. Rostellum and suckers were well-defined and the border of the body was clearly visible during three weeks of incubation. Protoscoleces, which were incubated in the presence of 10 μ M ML3403, condensed over time and presented an oval corpus, lacking a defined neck region. In addition, they were more granular and unable to move after two weeks. Bodylines did not appear well- defined and the tegument as well as single cells were detached.

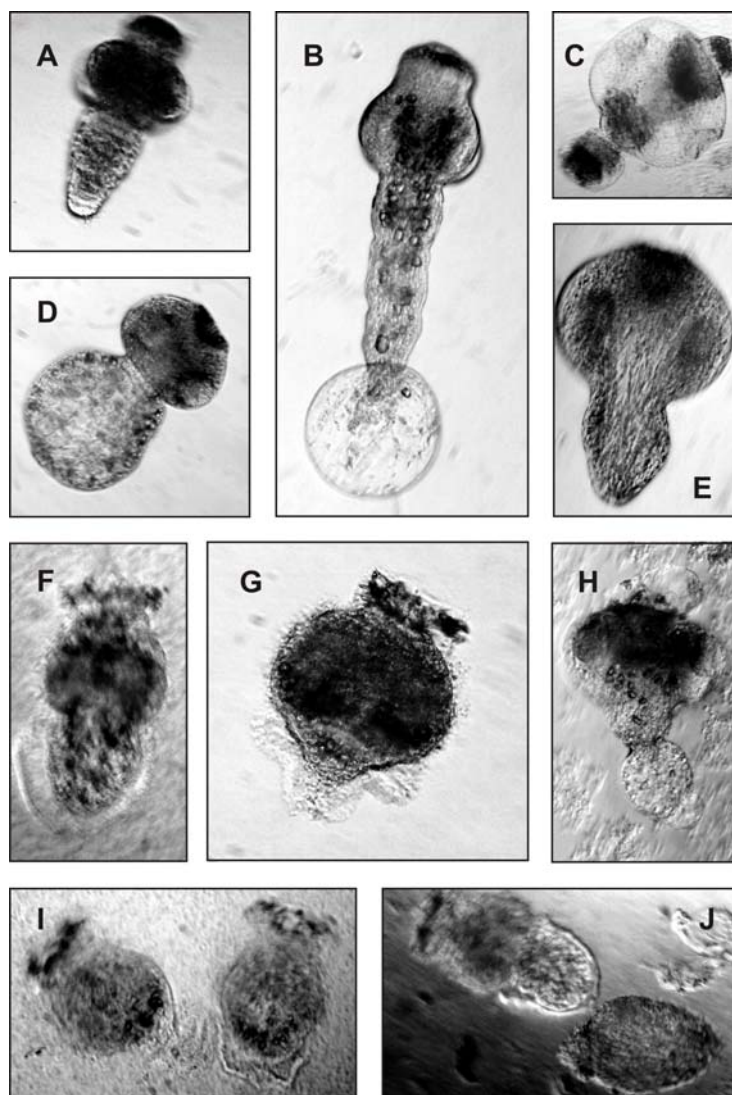


Fig. 3.15: Treatment of *in vitro* cultivated protoscoleces with ML3404. Jirds infected with *E. multilocularis* isolate J31 were sacrificed for protoscoleces recovery according to the standard procedure. Incubation with bile salts and low pH was performed successively for protoscolex activation and the elimination of host cells. For *in vitro* cultivation, 100 μ l of the obtained protoscolex suspension were transferred to 24 well plates with 1 ml DMEM including 10% FCS and antibiotics per well. 24 h later, ML3403 was added to a final concentration of 10 μ M, DMSO as control. During cultivation of three weeks, untreated protoscoleces appeared in variable morphology just like protoscoleces in the presence of DMSO (**A-E**). Most of protoscoleces presented the strobilar form with or without bubbles on head or tail (**A, B**) with high agility in the beginning and changed the morphology finally to the globular form (**C, D, E**). The body form with tegument and structures like rostellum and suckers were clearly defined throughout incubation. Drug treated protoscoleces appeared as indicated in **F-J**. Initially agile protoscoleces with well-defined structures showed a rounded off and contracted form with leaking-like blisters (coming off of the tegument) and were unable to move after two weeks. A neck structure was not identifiable anymore. The appearance was darker and more granular as in the DMSO control group.

3.1.9 Effects of pyridinyl imidazoles on mammalian cells

The influence of SB202190 and ML3403 on the viability of several host cell lines was investigated using inhibitor concentrations which effectively inactivated *in vitro* cultivated metacystode vesicles. For this, rat Reuber hepatoma cells (RH-), human brain-derived endothelial cells (HBMEC) and human embryonic kidney cells (HEK293) were incubated with concentration from 0.5 to 50 μ M of both drugs or DMSO. After 4 days, live-dead-staining of the mammalian cells was performed (Fig. 3.16). No significant effects on the viability were observed for either of these cell lines up to concentrations of 5 μ M. The only deleterious effect was detectable for ML3404 of 50 μ M on RH- cells. The result showed that both compounds SB202190 and ML3403 in concentrations of 0.5 to 50 μ M, which inactivated over 50% of the metacystode vesicles after 4 days, did not decrease the viability of the mammalian cells cultivated under comparable conditions.

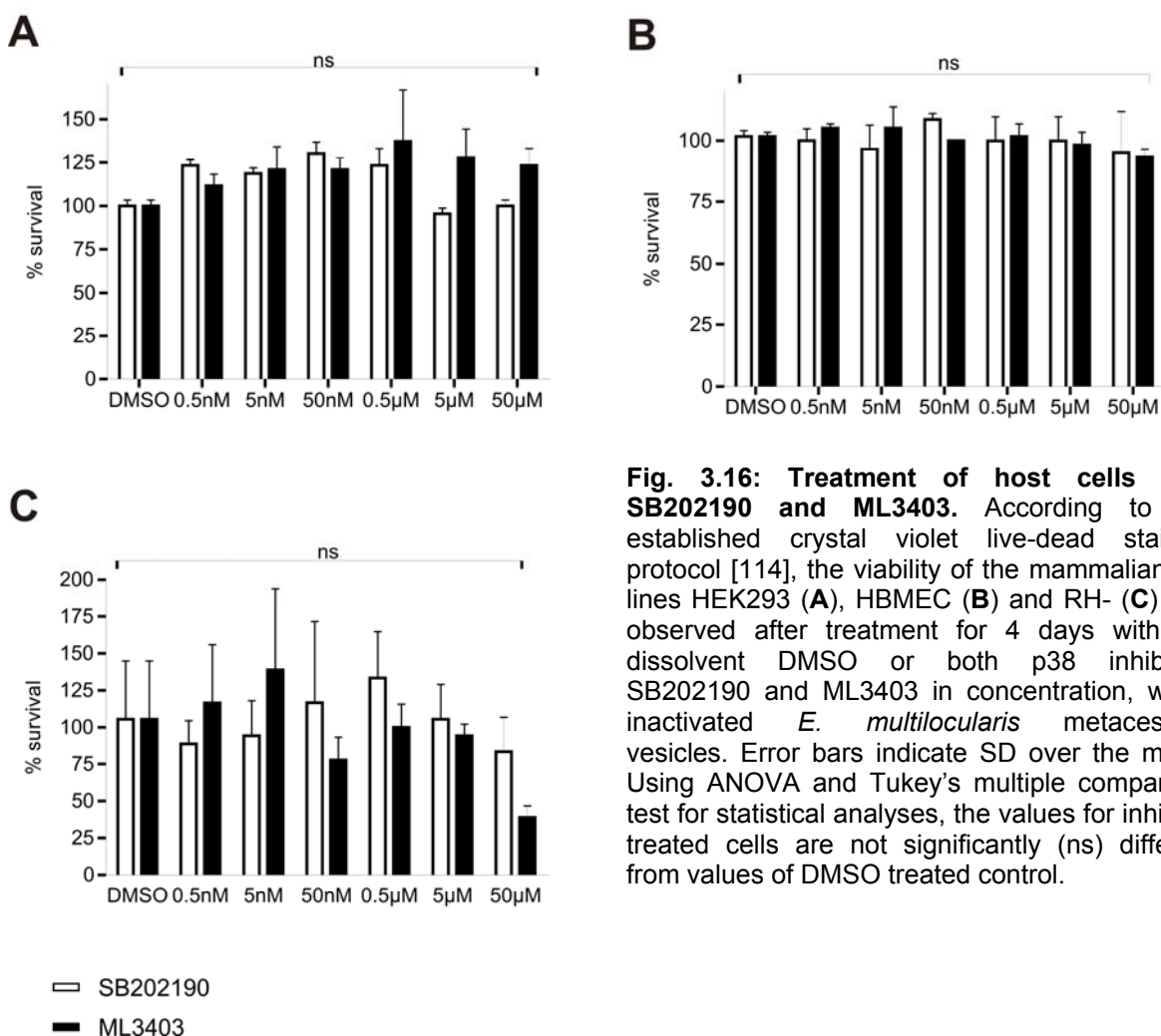


Fig. 3.16: Treatment of host cells with SB202190 and ML3403. According to the established crystal violet live-dead staining protocol [114], the viability of the mammalian cell lines HEK293 (A), HBMEC (B) and RH- (C) was observed after treatment for 4 days with the dissolvent DMSO or both p38 inhibitors SB202190 and ML3403 in concentration, which inactivated *E. multilocularis* metacystode vesicles. Error bars indicate SD over the mean. Using ANOVA and Tukey's multiple comparison test for statistical analyses, the values for inhibitor treated cells are not significantly (ns) different from values of DMSO treated control.

3.2 Treatment of the cestodes *E. granulosus* and *T. crassiceps* with pyridinyl imidazoles

In vitro cultivated metacestode larvae of *E. multilocularis* were killed by the compounds ML3403 and SB202190, which were originally designed to inactivate human p38 MAP kinases. In view of these results, the question arose whether the inhibitors show similar effects on other cestodes. In this regard, the p38 MAPK orthologues of *Taenia crassiceps* and *Echinococcus granulosus* were investigated as possible targets.

3.2.1 Partial characterization of the p38 MAPK homologue of *E. granulosus*

E. granulosus parasite material for inhibitor treatment is not readily available so that merely *in silico* analyses were performed to identify the EmMPK2 ortholog of *E. granulosus*. For this, the LophoDB database (<http://www.nematodes.org/NeglectedGenomes/Lopho/LophDB.php>) which contains numerous *E. granulosus* EST sequences obtained by Fernandez et al. (2002), was mined using the EmMPK2 activation loop sequence as a query.

A protein with significant homologies to EmMPK2 was encoded by EST EGC02047 and the respective protein was designated EgMPK2. The deposited EST sequence corresponded closely to the *emmpk2* cDNA sequence determined above with the exception that, probably due to alternative splicing, exon VIII was directly fused to exon X, thus completely removing the sequence information of exon IX (coding for amino acids 281 to 341). Due to this splicing event, a stop-codon is introduced directly after the exon VIII sequences, leading to a truncated protein which only encompasses amino acids 1 to 281. Whether this splicing mode is typical for *egmpk2* or whether, by chance, an mRNA containing a splicing error was sequenced, remains to be established. However, within the available parts of the cDNA, the deduced EgMPK2 amino acid sequence only differed in three positions from EmMPK2 (Fig. 3. 17), making it highly likely that both genes code for proteins that are to over 99% identical. Hence, if sensitivity to pyridinyl imidazoles solely bases on the structure of the p38 MAPK ortholog, it is highly likely that *E. granulosus* is also sensitive to this compound group.

3.2.2 The p38 MAPK homologue of *T. crassiceps*

3.2.2.1 Treatment of *in vitro* cultivated *T. crassiceps* larvae with p38 MAPK inhibitors

Since parasite material of *T. crassiceps* was available, metacestode larvae were treated *in vitro* with ML3403 and SB202190 in order to address the question whether *Taenia crassiceps* are sensitive to pyridinyl imidazoles. The experiments were performed under similar experimental settings as used for *E. multilocularis*. *T. crassiceps* cultivated in mice were isolated from the peritoneal cavity and transferred into the *in vitro* culture system. Initially, the cultivation conditions for *T. crassiceps* were optimized. Medium with or without 10 % FCS and antibiotics was tested and the larvae were incubated alone and in co-culture with rat hepatocytes. As indicated in Fig. 3.18, *T. crassiceps* showed better growth and maintenance in medium with high serum conditions and in the presence of host cells. The treatment of *T. crassiceps* larvae subsequently took place in medium with serum and antibiotics, but in the absence of feeder cells to avoid indirect effects. Interestingly, during 4

weeks treatment with pyridinyl imidazoles at concentrations which effectively inactivated *E. multilocularis* larvae, no significant effects on *T. crassiceps* were observed.

3.2.2.3 Identifying the p38 MAPK homologue from *T. crassiceps*

To investigate whether the failure to inactivate *T. crassiceps* larvae by pyridinyl imidazoles was due to differences in the structure of its p38 MAPK orthologue when compared to EmMPK2, biochemical and molecular studies were carried out.

In the first step, total RNA was isolated from *in vitro* cultivated metacestode larvae to produce first strand cDNA using Omniscript RT PCR kit. By a second PCR approach using the cDNA as template and oligonucleotids p38-kp-dw (5' GCT AAG CGC ACT TAC CGT GAG) and p38-lo-up (5' CGC CGA TCC GGA TCC AG) designed to amplify a partial sequence of *emmpk2*, an product of expected 693 bp length was obtained, cloned into the cloning vector pDrive (Qiagen) and sequenced. The DNA fragment coded for 231 AA of a protein with highest homologies to p38 MAPK family members. The deduced protein shows about 60% identical residues to human p38 MAPK- α and is depicted in 3.18. The protein was designated TcMPK2. The partial sequence of TcMPK2 exhibits 97% identity to EmMPK2 and contains the catalytic and the activation loop of Ser/Thr kinases as identified by SMART analyses. To complete the sequence, RACE experiments were performed but could not be finished in time.

The amino acid residues of the identified partial TcMPK2 sequence on positions known to be functionally important and involved in the interaction with pyridinyl imidazoles, did not differ from EmMPK2 [110]. The expression of the TcMPK2 on protein level was investigated via Western blot using the human anti-phospho-p38 antibody detecting the pT-G-pY motif within the conserved activation loop of p38 MAPK. As shown in fig. 3.19, a single signal of approximately 70 kDa was detected indicating that the p38 orthologue might be larger than EmMPK2. Without detailed sequence analysis of the TsMPK2 encoding cDNA, adequate conclusions about the molecular nature of the detected 70 kDa protein cannot be drawn. Since the antibody has been specifically designed to bind to phosphorylated T-P-Y motifs, it is, however, possible that TsMPK2 contains N- or C-terminal extensions which could affect the interaction with small molecule inhibitors. Future investigations are clearly necessary to address these points.

EgMPK2	MPDVNERQFVPVEINQLRWDLPD RYS P V N V A G Q S S F G T V S S A F D K Y L Q R E	50
EmMPK2	MPDVNERRFVPVEINQLRWDLPD RY T S V M V A G H G A Y G T V S S A F D K Y L Q R E	50
EgMPK2	V A I K K L D R P F E N A E F A K R T Y R E L A I L A Q M D H E N V I C L I D A F T P Q T S L E T F	100
EmMPK2	V A I K K L D R P F E N A E F A K R T Y R E L A I L A Q M D H E N V I C L I D A F T P Q T S L E T F	100
EgMPK2	E D V Y L V T P L M D A D L G A I V A Q Q V L T D D Q I C F L A Y Q M L R A L K Y M H G A H I I H R	150
EmMPK2	E D V Y L V T P L M D A D L G A I V A Q Q V L T D D Q I C F R A Y Q M L R A L K Y M H G A H I I H R	150
EgMPK2	D L K P S N I G V N S D V E L R I I D F G L A R Q K N H L M T G Y V A T R W Y R A P E V M L N W M H	200
EmMPK2	D L K P S N I G V N S D V E L R I I D F G L A R Q K N H L M T G Y V A T R W Y R A P E V M L N W M H	200
EgMPK2	Y N D S V D V W S V A C I L V E L K T R Q P L F R G L N H I D Q V K Q I M S I V G A P D E E L M Q K	250
EmMPK2	Y N D S V D V W S V A C I L V E L K T R Q P L F R G L N H I D Q V K Q I M S I V G A P D E E L M Q K	250
EgMPK2	I T S S S A R E F I E K L N Y T S K K D L K D A F P W A S P V - - - - -	281
EmMPK2	I T S S S A R E F I E K L N Y T S K K D L K D A F P W A S P V L L D L L S K M L V L D P D R R L T A	300
EgMPK2	- - - - -	281
EmMPK2	A Q A L A H P Y F A E Y H N E S G E P V G E P L E D D L I D S D N L T M E E W K E A T W N L L Q N F	350
EgMPK2	- - - - -	281
EmMPK2	K P K L T S L R P T D A Y S P I N A	368

Fig. 3.17: Amino acid sequence alignment of EmMPK2 with the homologue from *E. granulosus* (EgMPK2). The respective amino acid sequence of *E. granulosus* representing a partial sequence and is derived from the EST sequence with accession number EGC02047 from LophoDB database. Over the depicted area, the proteins share 98% identical residues.

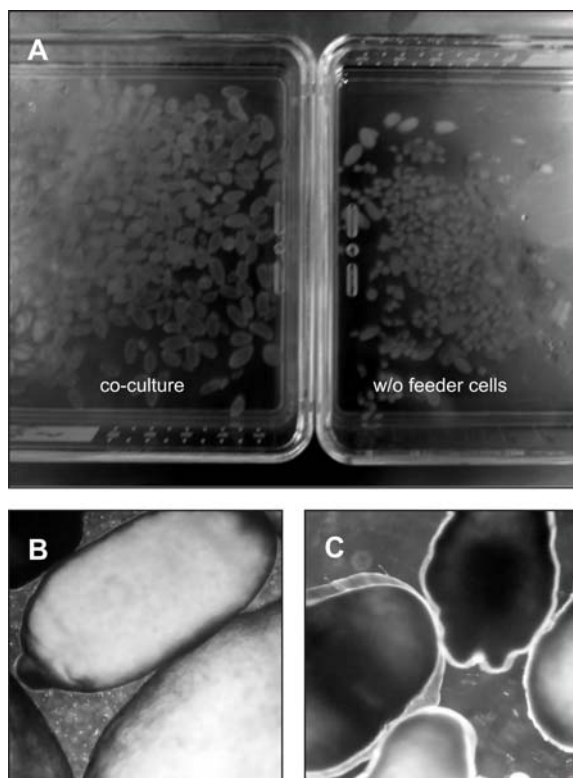


Fig. 3.18: Long-term *in vitro* cultivation of *Taenia crassiceps* larvae. Metacystode vesicles of *T. crassiceps* were cultured for four weeks in the presence (A, B) or absence (A, C) of rat hepatocytes in DMEM with 10%FCS and 1% penicillin/ streptomycin.

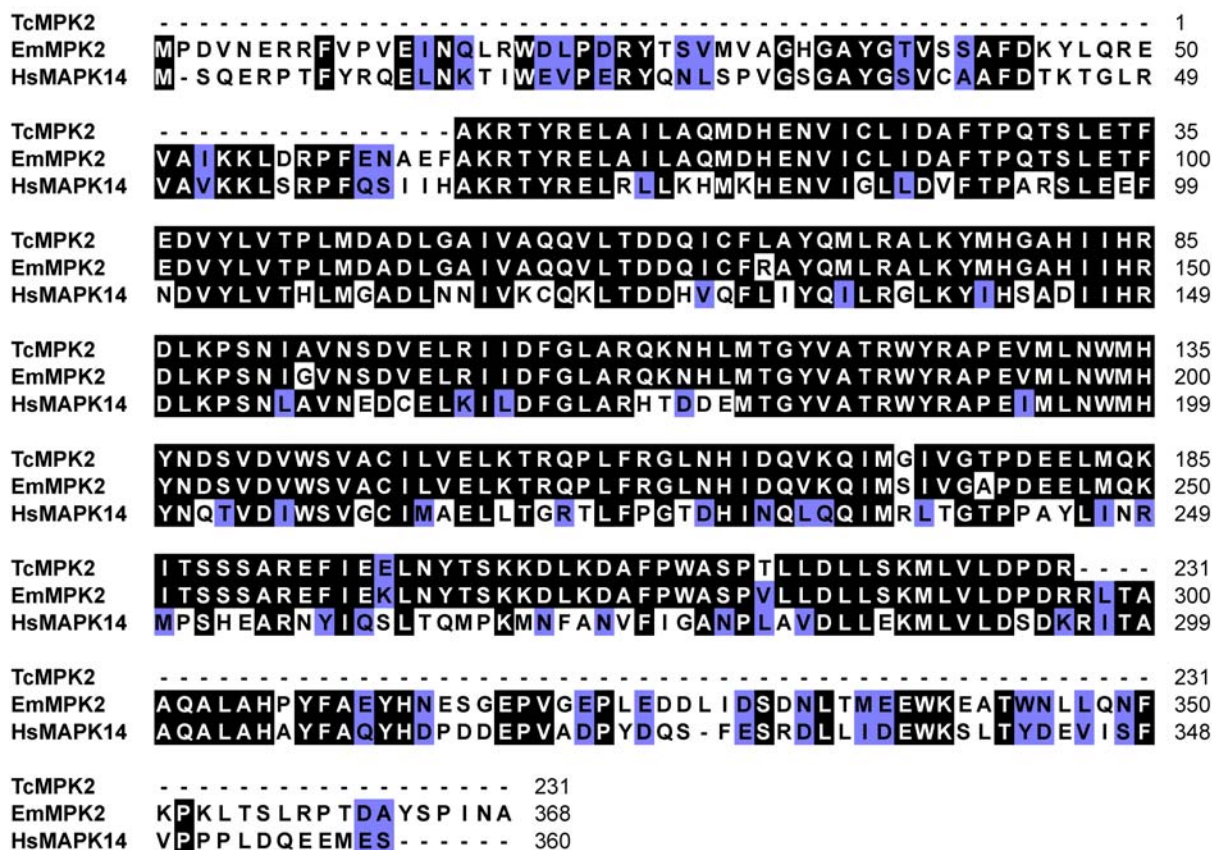


Fig. 3.19: Amino acid sequence alignment of p38 MAPK family members from the species *Taenia crassiceps* (TcMPK2; partial sequence), *E. multilocularis* (EmMPK2) and *H. sapiens* (HsMAPK14; Q16539). Identical amino acid residues are shaded in black, similar residues in blue.

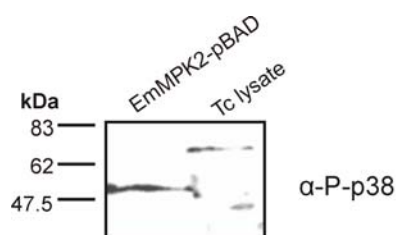


Fig. 3.20: Analysis of TcMPK2 expression. Lysate of *in vitro* cultivated *T. crassiceps* larvae were analysed for expression of a p38 MAPK like protein by immunoblotting using the anti-phospho-p38 antibody after sample separation on 12% acryl amid and transfer on nitrocellulose. Recombinantly expressed EmMPK2 served as positive control.

3.3 EmSSY- an unusual MAPK / a new type of MAPK?

Analyses of the *Echinococcus* genome sequences revealed that *emmpk2* encodes the only p38 like MAPK of the parasite with a typical T-G-Y motif as outlined in section 3.1.1. However, upstream of the *emmpk2* gene, a sequence was identified which displayed remarkable homology to *emmpk2*. In gene specific RT-PCR and RACE experiments, two different transcripts for this gene were identified (Fig.3.22). The respective sequences encoded proteins of 468 AA and 356 AA, respectively. The amino acid sequences were aligned with EmMPK2 and revealed 63% identical and 78% similar residues between the newly identified proteins and EmMPK2 (Fig. 3.21). By SMART analyses, a Ser/ Thr kinase domain amongst an ATP-binding pocket, a catalytic as well as an activation loop and a common docking site were identified (Fig.3.21) [106]. Hence, the unknown proteins were clearly identified as MAPKs. Interestingly, the activation loops did not feature any of the common dual-phosphorylation motifs, which would allow the classification of MAPK family members (see section 3.1.1). These proteins contained neither the T-E-Y (Erk-like), nor the T-P-Y (JNK/SAPK-like) nor the T-G-Y (p38-like) triplet. Instead, it revealed an unusual S-S-Y motif at the corresponding position within the otherwise conserved activation loop. Based on this unusual motif, the proteins were named *E. multilocularis* SSY MAPK, abbreviated EmSSY. Since there were two transcripts of the corresponding gene *emssy*, the resulting proteins were designated EmSSY-a and EmSSY-b (Fig. 3.21).

For computer based *emssy* gene analysis, the contig database was used again. It became obvious that *emssy* is composed of nine exons (I-IX; 43- 229 bp), which were interrupted by eight introns (1-8; 51-1801 bp) (Tab. 3.2). Seven of eight exon/ intron boundaries could be found at corresponding positions in *emmpk2* (see section 3.1.1). All exon/ intron boundaries display the canonical GT and AG motifs. The start codon for the longer *emssy-a* transcript is the first ATG highlighted in bold type in exon I. The length of this *emssy-a* transcript is due to an intron retention event at intron 1, leading to a 336 bp longer ORF. The ORF of the second transcriptional variant *emssy-b* started at the second ATG triplet within exon I and continued in exon II (Fig. 3.22, Tab. 3.2).

The expression of the splice variants was demonstrated by qualitative RT-PCR experiments with transcript specific oligonucleotides and cDNAs of the relevant larval stages as templates. The result was that *emssy-a* and *emssy-b* were transcribed in metacestode as well as resting and activated protoscolex (Fig. 3.23).

So far, these data did not allow the classification of EmSSY as a functional MAPK. Further investigation to characterize the function of EmSSY was not undertaken. An interesting topic would be to examine the enzymatic activity, which should be present according to the structural features, and the identification of interaction partners. Interestingly, extensive literature and database searches, revealed that proteins with considerable overall homology to p38 MAPKs but carrying a SSY motif have so far not been reported for any other organism. A protein with the highest similarity to S-S-Y triplet was identified from *C. elegans*. This protein contains a S-D-Y triplet and is classified as JNK MAPK (Kgb-2; O44182) for which the evidence exists only at transcriptional level and functional analyses are lacking.

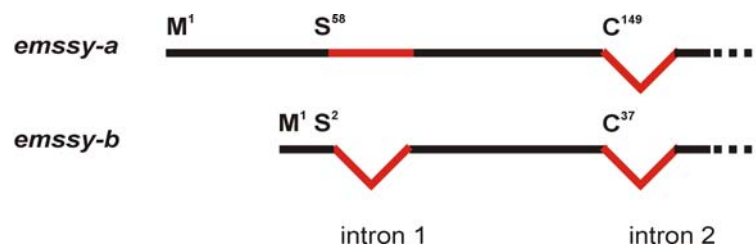


Fig. 3.22: The two transcriptional variants of *emssy*. Shown are the 5' ends of the both *emssy* transcripts which were identified by 5' RACE experiments. When the transcripts contained the extension at the 5' end, the reading frame was open to the interruption by intron 2 at the corresponding Cys¹⁴⁹ and encodes 468 AA (EmSSY-a). In the 5' region, ORF of *emssy-b* was interrupted by the additional intron 1 at the corresponding Ser² (see also Fig. 3. 21 and Tab. 3.2).

Contig No. 7471

Exon/ Intron	No.	Start	End	Length	Sequence	AA	Corr. Ex/In in <i>emmpk2</i>
5' upstream		420	529	109	...aacaatgtggctcaaaactgtagtcacgaagtgccattgcataagtaactcactctgtcccggccaac gataagctgtttgagctgccactctgtatgct		
Exon I	I	530	573	43	ATG CTTTTGCTTAATGTGCACAAGTTTGTACGAATGCAGCGTGGTCTTTT CGCCGTGATTTTGAAAATGGACTAGCAATTTTACTTGGCTTTGTATTGTG GCTTTCGTTTCAGTCAAATGTGTATATGACTTGTGCGCTGTGCCTGCGTTTT AGCTTACTAATTAGTATGCTTG		
Intron 1	1	574	839	265	gtacgttaaa...tctcacgcag	Ser58	+
Exon II	II	840	937	97	AGCGCAACTTCGTTTCCGTCGAATTTAATGGGCTTTGCTGGACCCTCCCT GATCGTTATTCTGACCTCATGTCAGTCGGAAGTGGGGCCTTTGGGGTC		
Intron 2	2	938	1014	76	gtatgggtgag...ttatftcag	Cys149	+
Exon III	III	1015	1139	124	CTCTGCAAAGGACAACATTTTGCAGCGCATGGTGGCTATAAAACATATTG CTAAACCATTCGACACACTCGAAGATGCCAAACGTAATTATCGTGAGTTG GCTATCATGGCGCATATGGATCATGAGAAC		
Intron 3	3	1140	2941	1801	gtgagttccg...ttacaaaag	Asn193	+
Exon IV	IV	2942	3000	58	GTCGTAECTCTGGTGGACGCATTTACTCCACAACAGCATTGGAAAGTTT CAACGAGAT		
Intron 4	4	3001	3097	96	gtaagtacca...ttcgctttag	Ile212	+
Exon V	V	3098	3209	111	TTTTTTTGTAATGCCTCTGATGGCAGGTGATTTGGCGGAGGTTTTAAAGT ATCAAGTCTCGATGACGACCAAATAACCTTCTGGTGTACCAAATTCCTC GAGCTCTCAAG		
Intron 5	5	3210	4360	1150	gttttttt...aattctccag	Lys249	+
Exon VI	VI	4361	4553	192	TACATGCATGGCGCGAACATTATTCATCGAGATCTGAAGCCCAAGAACAT AGCTGTGGATGAGGACTGCAATCTACGAATCCTGGACTTGGATTGGCTC GTCGGTGGACGAGAATATGTCAGTTATGTGGTAACACGATGGTATCGA GCACCTGAACCTATCGCAAATTGGATAAATACAACGACACAG		
Intron 6	6	4554	4605	51	gtgggtgtt...tttttccag	Thr314	+
Exon VII	VII	4606	4757	151	TTGACGTCTGGTCGGTGGCATGTATTCTGGTAGAGATGAAGATTTCGCAGA CCCCTATTCCGTGGTATAATCCCATAACAACCTTGGAGAAATTCCTGCT GTGGTTGGCCC GCCAGATGAAGGATTTTCGACAGAAGATTAGTAGCGATA GT		
Intron 7	7	4758	4868	110	gtaagtggct...tctttttag	Ser365	+
Exon VIII	VIII	4869	4948	79	GCTAGGGCATTTCATTAAGACCCATAACCTCCCACCAAGACGTGATCTTAA GGAGTCTTTCGTTGGGCATCAGACGTGT		
Intron 8	8	4949	5163	214	gtaagtttagc...ctagtgttag	Asp389	-
Exon IX	IX	5164	5393	229	ATCTCCTCTCCAAGATGCTTGTCTTGTATCCGGACCGTTCGATTGAGGGCA TCAGAAGCCTTGGCAGATCCATTCTTTGCTGAATACCACGATGCAAATGA TGAACAGGAGGGCACACCGTTGGAGGATGAACCTATTTCATCCAACTTCT TGACCATTGATCAGTGGAAAGGTAACGATTACTTCTAGAACACCTCATG GTAATTGCTGCCGATGGGTGTCGTATGTAG		
3' downstream		5394	5550	156	gttggcactactagaggggcaatgccccgattacgggcagaatgcatgattggagtgacaaatcgtac cacacctaccctaatttcgtattgacacggattcttagatcaatgaggcctgacaaaaccccgacag cgtagccccctgag....		

Tab. 3.2: Genomic characterization of *emssy*. The gene *emssy* is localized upstream of the *emmpk2* gene and is composed of nine exons (I-IX; 43- 229 bp) and eight introns (1-8; 51-1801 bp). Seven of eight exon/ intron boundaries could be found at corresponding positions in *emmpk2* (see section 3.1.1). All exon/ intron boundaries display canonical GT...AG motifs. Two different transcripts for *emssy* were identified. The start codon for *emssy-a* is the first ATG highlighted in bold type in exon I. In this transcript, intron 1 was not spliced out leading to a 336 bp longer ORF. The ORF of the second transcriptional variant *emssy-b* started at the second ATG triplet within exon I and continued in exon II.

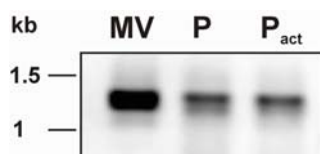


Fig. 3.23: Expression of *emssy* in the larvae metacestode (MV), protoscolex before (P) and after activation (P_{act}) by low pH and bile salts. RT-PCR analysis was conducted with cDNAs of the indicated larval stages as templates and *emssy* gene specific oligonucleotides. The amplicons of expected 1407 bp represented the complete ORF of *emssy-a*.

3.4 Effects of miltefosine and perifosine on *in vitro* cultivated parasite material

3.4.1 *In vitro* treatment of *E. multilocularis* metacestode vesicles

Miltefosine and perifosine, originally developed as antineoplastic drugs, are anti-protozoal compounds which target the PIP3K/ AKT pathway as well as SAPK/JNK and Erk MAPK pathways [102, 103, 115, 116]. In particular, miltefosine was shown to be effective against *Leishmania* and *Trypanosoma* [117, 118]. The influence of both cytostatic drugs on *Echinococcus* growth was investigated. Co-cultured metacestode vesicles were separated from host cells and settled in groups of five into medium containing 10% FCS and antibiotics in 24 well multiplates. Treatment with miltefosine (D-18506, Zentaris) and perifosine (D-21266, Zentaris) took place over two weeks in concentrations from 25 nM to 250 μ M in 10fold dilution steps. Light microscopical observation and the determination of AP activity in the supernatant were done daily to assess the integrity of vesicles. As illustrated in Fig. 3.24, the untreated control vesicles and vesicles incubated in the presence of less than 250 μ M of either drug were not affected and remained intact till end of the experiment. High dosages of D-18606 and D-21266 led to damaging effects on laminated layer after 5 days, but neither of the supernatants showed a detrimental increase in AP activity.

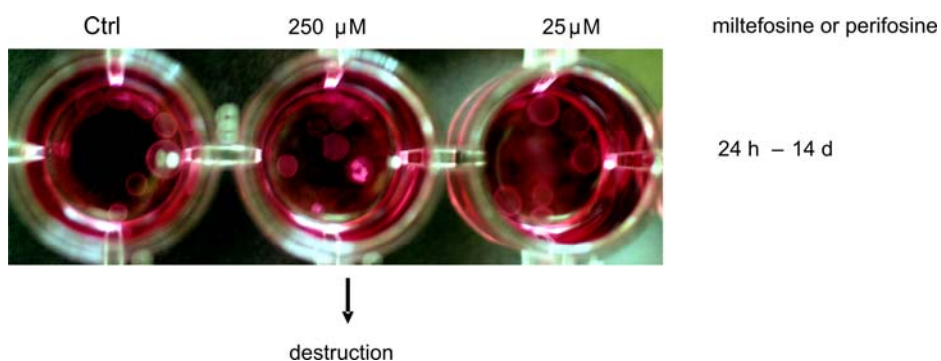


Fig. 3.24: Treatment of *in vitro* cultivated metacestode vesicles with miltefosine and perifosine. Metacestode vesicles were cultured in groups of five in 24 well plates in the presence or absence of drug compounds miltefosine (D-18506, Zentaris) or perifosine (D-21266, Zentaris) dissolved in sterile water in various concentrations for 14 d. Vesicle viability was controlled daily via LM. A destruction of metacestode vesicles was visible only by treatment with high dosages for both drugs. In addition, AP activity in the supernatant of treated vesicles was measured as marker for destruction, but no increase of AP activity was detectable over the whole time course.

3.4.2 *In vitro* treatment of *E. multilocularis* primary cells

Simultaneously to the incubation of the metacestode vesicles, *E. multilocularis* primary cells were treated with miltefosine (D-18506) and perifosine (D-21266). Metacestode vesicles grown for four weeks in the axenic culture system after breeding for four weeks in the presence of hepatocytes were utilized for the isolation of primary cells. After isolation, the cells were seeded with pre-conditioned A4 medium and the supplements β -MEtOH, BAT and L-cysteine in 24 well multiplates. D-18506 and D-21266 were dissolved in sterile water and added to a final concentration of 50 μ M, untreated primary cells were used as control. Shown in Fig. 3.25 is the course of vesicle formation after 7, 14, and 28 days. After one week, primary cells aggregated to clumps in which cavities formed in the following week. Further two weeks later, small vesicles appeared. These progression steps of cyst formation could not be observed for primary cells incubated in the presence of the drug compounds. Treated primary cells remained spreaded on the well bottom and appeared granular as indication for low vitality after seven days. The effects of both drugs were similar. Western blot analyses of treated primary cell lysates did not show influences on EmMPK1 and EmMPK2 phosphorylation (data not shown).

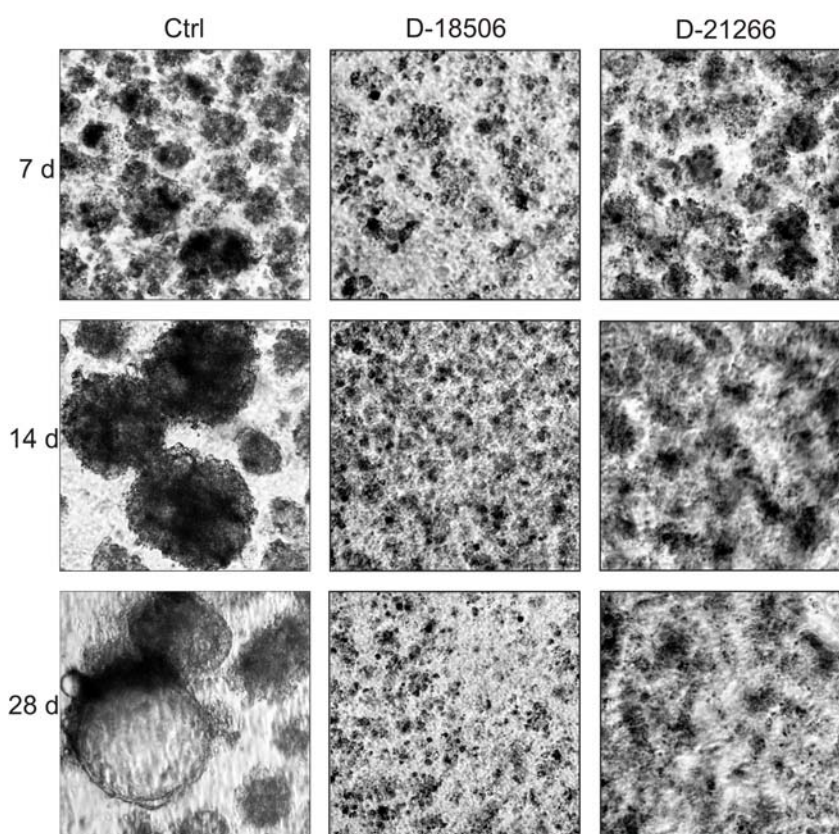


Fig. 3.25: Treatment of *Echinococcus multilocularis* primary cells with the compounds miltefosine (D-18506, Zentaris) and perifosine (D-21266, Zentaris). Primary cells were isolated from axenically cultivated metacestode vesicles and subsequently incubated with pre-conditioned medium in 24well plates in the presence of D-18506 or D-21266. The pictures were taken after 7, 14 and 28 days of incubation.

3.5 EmMCK2 - a factor of the *E. multilocularis* MAP kinase cascade

Although the initially identified *E. multilocularis* MKK (EmMCK1) has been shown to interact with EmRAF in yeast two hybrid binding studies, it did not interact with EmMPK1 [86]. This suggested that EmMCK1 does not represent the upstream kinase of EmMPK1 in the *E. multilocularis* MAPK cascade. Hence, one aim of this work was the identification of a so far unidentified *Echinococcus* MKK which could form the link between EmRaf and EmMPK1.

3.5.1 Classification of EmMCK2 as MAPK kinase on the basis of structural features

A cDNA fragment of 300 bp was amplified via degenerative PCR using oligonucleotides against regions encoding highly conserved residues of MKKs (IVGFYGF and CDFGVSG). Sequence analysis revealed the amplicon as part of a full-length transcript with homology to MKK1/2 kinases. The transcript was completed via 5'RACE and 3'RACE experiments and the corresponding gene designated *emmck2* for *E. multilocularis* map kinase kinase 2. The contained ORF of *emmck2* cDNA comprises 1614 bp (excluding the polyA tail) and codes for a 250 AA protein (57.2 kDa) (Fig. 3.26). For the *emmck2* transcript a spliced leader sequence on the 5'end could not be identified. In addition, all characterized transcripts showed the same ORF sequence indicating the absence of splice variants.

The translated ORF displayed all conserved residues for eukaryotic protein kinases at the corresponding positions. Further, *in silico* analyses using the SMART tool identified a catalytic Ser/ Thr protein kinase domain as well as the hydrophobic ATP-binding clamp with the consensus motif GxGxxGxV (x for any amino acid residue) [106]. The catalytic loop with the motif HRDVKxxN with Asp as proton-acceptor and the conserved Glu and Lys involved in the ATP-binding is identical in all displayed MKKs. The 'DFG' triplet marks the beginning of the activation loop which ends with the 'APE' triplet. The residues in-between are highly conserved among MKK protein family members and are important for substrate recognition. Notably, on structural level, EmMCK1 shows higher homologies to mammalian MKK3/6 whereas EmMCK2 is more similar to mammalian MKK1/2 [58]. At the C-terminus, EmMCK1 and EmMCK2 share the Hxah consensus motif of serine protein kinases, where 'a' represents an aromatic and 'h' a hydrophobic amino acid residue [105]. EmMCK2, however, displayed the highest homology to the MAPK kinases 1/2 with 50% identity and 67% similarity, respectively. Ser residues for phosphorylation and MKK activation by upstream MKKs such as Raf were also present (Ser²¹⁸ and Ser²²²; Fig. 3.26) and displayed a sequence context with considerable homology to mammalian MKKs [119]. Computer analyses using the freely available ELM tool (<http://elm.eu.org/>) identified the N-terminal oligopeptide 'HTSTSS' as putative binding domain for 14-3-3 proteins in EmMCK2, such a domain was present in EmMCK1 [120]. The same software tool identified the motif 'RRSSIRF' as docking motif for MAPKs. The classic consensus sequence for a Kinase interaction motif (KIM) is (R/K)xxxhxx and is usually located close to the N-terminus [58]. Two putative KIMs were present in EmMCK1 next to the N-Terminus. EmMCK2, on the other hand, carried the predicted MAPK interaction motif close to the C-terminus.

Since comprehensive information on the *E. multilocularis* genome sequence is available, genomic analyses for the chromosomal *emmck2* locus were performed *in silico*. The

genomic locus of *emmkk2* was present on contig 803 and 804 of the first assembly and comprised six exons (47-526 bp). The ORF was interrupted by five introns (145-2342 bp) (Fig. 3.26 and Tab. 3.3). Conserved exon/ intron boundaries in the genomic loci of *emmkk2* and the human homologues were not observed with two exceptions. On position Gly²⁴⁶ (Gly¹⁴⁶, respectively) and position Pro³⁴⁶ (Ser²⁴⁶) of the coding sequences of *emmkk2* and *hsmkk1*, introns are present. Furthermore, the exon/ intron boundaries of the *Echinococcus* genes *emmkk1* and *emkk2* do not match. In general, these findings reflect the situation in homologous *mkk* gene families where the positions of exon/ intron boundaries are usually not conserved. All introns *in emmkk2* appear with the canonical GT at splice-donor and AG at splice acceptor sites.


```

1      ACTCTGGGATTGGTGTGCAAAGATCGGCGCCGCGACTACCAGCTGAAGACTGAAATGTCGGGTCTGACGGACAGCACGCC 80
      V A G G G S S G D H L E T G V D P S R P P T G P Q S
81     GGTAGCAGGAGGCGGCAGTAGCGGGGATCACCTGGAGACCGGTGTGGACCCATCGAGACCGCCTACGGGGCCGAGTCCC 160
      Q A S G L R F A G K R Q V T I Q N L D L T P L R L D D
161    AGGCCTCAGGATTACGATTTCGAGGCAAACGGCAGGTGACTATCCAGAACCCTGACCTACCCCCCTACGACTGGACGAT 240
      P P S H H T S T S S N T N T N P S S K P T R V R L P P
241    CCCCCCTCCCATCATACCTCCACCTCTTCCAACACCAACTAACCCCTCGTGAAGCTACTCGCGTCCGCTCCCACC 320
      L T S I G A A E A S T D N F S V L R H D R S G A N K
321    GCTCACCAGCATCGGCGCTGCTGAAGCCTCCACCGACAACCTCTCCGTCCTTCGACATGATCGCAGCGGGGCCAACAAAC 400
      P N D R M S T G P V D L A A A Q R Q L D D Q Q L D D S
401    CTAATGATCGCATGAGCACTGGACCTGTTGATCTCGTGCTCAACGCCAACTCGATGATCAGCAATTGGATGACAGC 480
      Q R E R I E E F L R Y K K D I H E L H P E D F T K I S
481    CAGCGAGAGCGCATTGAGGAATTTCTGCGTTACAAGAAGGACATCCATGAGTGCACCCGGAAGACTTTACTAAGATCTC 560
      E L G S G N W G V V S R V R Y N R T N I I M A K K T
561    CGAGCTGGGCTCAGGCAATTGGGGTGTGGTTAGTCTGTACGCTACAACCGGACTAACATCATAATGGCCAAGAAGACCA 640
      I R L D I K H E V G T Q I L R E L E I L H D C A S P Y
641    TTCGGTTGGACATTAAGCATGAAGTAGGTACGCAAATACTCCGAGAAGTTGAGATTCACACGATTGCGCATCGCCTTAC 720
      I I G F Y G A F L A D G T I N I C H E Y M D G G S L G
721    ATTATCGGGTTCTATGGTGCATTCCTGGCTGATGGGACCATCAACATATGCCATGAGTATATGGATGGGGGAAGTTTGGG 800
      H V L K H A G R M P E P I V S R I L Y A V L C G L E
801    ACATGTGCTGAAGCACGCCGGTCGAATGCCCGAGCCAATTGTGTCCCGCATTCTATATGCCGTTCTTTGTGGCCTTGAAT 880
      Y L R K Q L S M I H R D V K P S N I L M R R N G E I K
881    ATCTACGCAAACAGCTCAGCATGATTCACAGGGATGTGAAGCCGTCGAACATTCTGATGCGTCGAAATGGTGAGATCAAG 960
      L C D F G A S G K L I D S V A H S F V G S R S Y M A P
961    CTGTGCGATTTTGGAGCGAGCGCAAGTTGATCGACTCGGTGGCGCACTCCTTTGTAGGCTCACGGTCTATATGGCGCC 1040
      E R I S G Q S Y N T S S D V W S L G L T L I E L A T
1041   AGAGCGCATTCTGGTCAGTCTCAACACATCCTCGGATGTGTGGAGCCTCGGATTGACTCTCATAGAACTAGCCACTG 1120
      G R Y P I P A I E N E T Q Y Y T G F S N D R Q T N L K
1121   GTCGCTATCCTATCCCCGCTATTGAGAACGAAACCAATACTATACCGGATTTTCTAATGATCGGCAGACCAACCTGAAG 1200
      E H I A A A R E G R K L P P V T T L E Q A P L S I F E
1201   GAACATATTGCTGCTGCTCGGGAGGGACGAAAACCTCCGCCCCGTAACGACACTGGAACAGGCACCATTGTCTATTTTCGA 1280
      L L V L I V E Q P L P R L P R T C F S D D F I D L V
1281   GTTGTGGTGTCTATTGTGGAGCAGCCGCTGCCCCGCTGCCACGAACATGCTTCAGTGACGATTTTCATAGACCTCGTAG 1360
      A S C L R T E S V E R P S L E V L Q N H A F V A T V A
1361   CTTCTGCCTACGCACAGAGCGTAGAGCGACCGTGCCTGGAGGTGCTTCAAACCACGCCTTTGTGCGCCACGGTGGCG 1440
      G L V P A G A N R R S S I R F R D F P T A A T A R N A
1441   GGTCTGGTACCCGCGGAGCGAATCGACGCAGCAGCATTGATTCCGCGATTCCCCACCGCTGCTACTGCTCGTAATGC 1520
      P C G S Q D T N V D L N M D D I A F Y L S H I L P P
1521   ACCTTGCGGCTCTCAAGATACTAATGTCGATTGAATATGGACGATATCGCCTTCTACCTCTCTCACATCTTACCACCTC 1600
      H D G I G *
1601   ATGATGGCATCGGCTAGACTCCTTGGGGTCCACCATCCACTAATGCTGGTGACGATAGTGATTAACCTCCCCTTTTAT 1680
1681   TCTCTAACACTACTCTCTCCACCTCTGATGTTGTATTGCTACTGTAGTTTGCCTGTGACTACTTCTATTTCTATTTT 1760
1761   TCAGTGAGTAAAAAAAAAAAAAAAAAAAAAAAAAAAAAAAAAAAAAAAAA

```

Fig. 3.26: cDNA of *emmkk2* with deduced amino acid sequence. The two possible ATG start codons are highlighted in red. The stop codon is marked by asterisks and the putative polyadenylation signal sequence (ATTA AAA) is accentuated by the line above the sequence. The position of introns in the genomic sequence is indicated by arrows. The Ser/ Thr kinase domain (in blue letters) was identified between Ser¹⁵⁷ and Val⁴⁵⁷ by SMART, the putative 14-3-3 protein interacting motif 'HTSTSS' (green) and the MAPK interacting motif 'RRSSIRF' (green) by the ELM software tool.

```

EmMKK2  M SGLT DSTP VAGGSS GDHL ET GVDPS RPPT GPQS QASGL RFAGKRQVT I QNLDLT PLRL 60
DmSOR1  M -----SKNKLNLVLPVNT EATVAAATV 24
HsMEK1  M -----PKKKP-----TPIQL 11
EmMKK1  M -----SAVR 5
DmMKK3  M -----SKRH 5
HsMKK6  M -----SQSKGK 7

EmMKK2  DDP PSHHTSTSSNTNTNPSSKPTRVRLPPLTS I GAAEASTDNF SVLRHDRSGANKPNDRM 120
DmSOR1  APT PPFKTPSGTDHS -----LL 42
HsMEK1  NPAPDGS AVNGTSS -----25
EmMKK1  RPLP-LNLGETRRIPG-----20
DmMKK3  RLTP-FTIAKE-----15
HsMKK6  KRN PGLKIPKEAFEQ-----22

EmMKK2  STGPVDLAAQRQL DDQQL DDSQRER I EEF LRYK KDI H E L H P E D F T K I S E L G S G N W G V V S 180
DmSOR1  GKPKTS I DAL T E T L E G L D M G D T E R K R I K M F L S Q K E K I G E L S D E D L E K L G E L G S G N G G V V M 102
HsMEK1  --AETNL EALQKKL EEL E L D E Q Q R E -- A F L T Q K Q V G E L K D D D F E K I S E L G A G N G G V V F 80
EmMKK1  -----V I L P V E I G P S T Q L S N R T D V I I N G Q K V T I D A R D L E V K E E L G R G E Y A R V H 68
DmMKK3  -----P E A A I V P P R N L D S R A T I Q I G D R T F D I D A D S L E K I C D L G R G A Y G I V D 61
HsMKK6  -----P Q T S S T P P R D L D S K A C I S I G N Q N F E V K A D D L E P I M E L G R G A Y G V V E 68

EmMKK2  R V R Y N R T N I I M A K K T I R L D I K H E V G T Q I L R E L E I - L H D C A S P Y I I G F Y G A F L A D G T I N I C 239
DmSOR1  K V R H T H T H L I M A R K L I H L E V K P A I K K Q I L R E L K V - L H E C N F P I I V G F Y G A F Y S D G E I S I C 161
HsMEK1  K V S H K P S G L V M A R K L I H L E I K P A I R N Q I R E L Q V - L H E C N S P Y I V G F Y G A F Y S D G E I S I C 139
EmMKK1  R M Y H A P S K C E F A V K R L P F E V E T S D R S R I L N D W N V S M R T S T C P Y A V L S Y G A L S V G C E F W V V 128
DmMKK3  K M R H K Q T D T V L A V K R I P M T V N I R E Q H R L V M D L D I S M R S S D C P Y T V H F Y G A M Y R E G D V W I C 121
HsMKK6  K M R H V P S G Q I M A V K R I R A T V N S Q E Q K R L L M D L D I S M R T V D C P F T V T F Y G A L F R E G D V W I C 128

EmMKK2  H E Y M D G - - - G S L G H V L K H A G R M P E P I V S R I L Y A V L C G L E Y L R K Q L S M I H R D V K P S N I L M R 296
DmSOR1  M E Y M D G - - - G S L D L I L K R A G R I P E S I L G R I T L A V L K G L S Y L R D N H A I H R D V K P S N I L V N 218
HsMEK1  M E H M D G - - - G S L D Q V L K K A G R I P E Q I L G K V S I A V I K G L T Y L R E K H K I M H R D V K P S N I L V N 196
EmMKK1  M E L M D D S L D K F L Q K V Y A Q G K I I P E N L L A Y V A F C V V T A L E Y L R K D L V T M H R D V K P S N I L I D 188
DmMKK3  M E V M S T S L D K F Y P K V F L H D L R M E E S V L G K I A M S V S A L H Y L H A Q L K V I H R D V K P S N I L I N 181
HsMKK6  M E L M D T S L D K F Y K Q V I D K G Q T I P E D I L G K I A V S I V K A L E H L H S K L S V I H R D V K P S N V L I N 188

EmMKK2  R N G E I K L C D F G A S G K L I D S V A H S F V G S R S - Y M A P E R I S G Q S - - - - Y N T S D V S W S L G L T L 350
DmSOR1  S S G E I K I C D F G V S G Q L I D S M A N S F V G T R S - Y M S P E R L Q G T H - - - - Y S V Q S D I W S L G L S L 272
HsMEK1  S R G E I K L C D F G V S G Q L I D S M A N S F V G T R S - Y M S P E R L Q G T H - - - - Y S V Q S D I W S M - L S L 249
EmMKK1  R A G H V K V C D Y G V S G E L K N S M A Q S N T G T C R - Y M A P E R I D P S R S A G G G F R I Q A D V W S L G L T L 247
DmMKK3  R A G Q V K I C D F G I S G Y L V D S I A K T I D A G C K P Y M A P E R I D P Q G N P A Q - Y D I R S D V W S L G I G M 240
HsMKK6  A L G Q V K M C D F G I S G Y L V D S V A K T I D A G C K P Y M A P E R I N P E L N Q K G - Y S V K S D I W S L G I T M 247

EmMKK2  I E L A T G R Y P I P A I E N E T Q Y Y T G F S N D R Q T N L K E H I A A A R E G R K L P P V T T L E Q A P L S I F E L 410
DmSOR1  V E M A I G M Y P I P P P N T A T L E S I F - - - - A D N A E E S G Q P - - - - - T D E P R A M A I F E L 316
HsMEK1  V E M A V G R Y P I P P P D A K E L E L M F G C Q V E G D A A E T P P R P R T P G R P L S S Y G M D S R P P M A I F E L 309
EmMKK1  L E L A T G K H P Y E S - - - - - F V N Q F E L 266
DmMKK3  I E M A T G R Y P Y D N - - - - - W R T P F E Q 259
HsMKK6  I E L A I L R F P Y D S - - - - - W G T P F Q Q 266

EmMKK2  L V L I V E Q P L P R L P R T C - F S D D F I D L V A S C L R T E S V E R P S L E V L Q N H A F V A T V A G L V P A G A 469
DmSOR1  L D Y I V N E P P P K L E H K I - F S T E F K D F V D I C L K K Q P D E R A D L K T L L S H P W I R K A E - - - - - 368
HsMEK1  L D Y I V N E P P P K L P S G V - F S L E F Q D F V N K C L I K N P A E R A D L K Q L M V H A F I K R S D - - - - - 361
EmMKK1  L K H V V H E A P P N V P E S V P Y S Q D F R D I V S Q C L V K E E S A R A N Y L R L L D S P F L R S V C V E R - - - - 322
DmMKK3  L R Q V V E D S P P R L P E G T - F S P E F E D F I A V C L Q K E Y M A R P N Y E Q L K H S F I - - - V E H L Q - - - - 312
HsMKK6  L K Q V V E E P S P Q L P A D K - F S A E F V D F T S Q C L K K N S K E R P T Y P E L M Q H P F F - - T L H E S - - - - 319

EmMKK2  N R R S S I R F R D F P T A A T A R N A P C G S Q D T N V D L N M D D I A F Y L S H I L P P H D G I G 520
DmSOR1  - - L E E V D I S G W V C K T M D L P - P S T P K - R N T S P N - - - - - 396
HsMEK1  - - A E E V D F A G W L C S T I G L N Q P S T P T - H A A G V - - - - - 389
EmMKK1  - - - D A P L M A Q F V S S I L D H Q - - - - - 338
DmMKK3  - - - R N T D I S E F V A R I L D L P D A Q P A Q - - - - - 334
HsMKK6  - - - K G T D V A S F V K L I L G D - - - - - 334

```

homology to	EmMKK1	EmMKK2
DmMKK3	43% / 63%	36% / 53%
HsMKK6	42% / 62%	35% / 52%
DmSOR	36% / 53%	50% / 67%
HsMKK1	35% / 51%	50% / 67%

identities/ similarities

Fig. 3.27: Amino acid sequence alignment of EmMKK2 and EmMKK1 with MAP kinase kinases from humans (HsMKK6; P52564 and HsMEK1; Q02750) and *D. melanogaster* (DmMKK3; O62602 and DmSOR1; Q24324). Shading with a threshold set for 60% indicates similar residues (blue) and identical residues (black). Homologies of aligned proteins to both *Echinococcus* MAPK kinases are listed below the alignment (% identities/ % similarities). Highly conserved residues among all eukaryotic protein kinases are marked by asterisks above the sequences [105]. The conserved motifs of protein kinases Gly-x-Gly-x-x-Gly-x-Val at the N- terminus and His-Arg-Asp-Leu/Val-Lys-x-x-Asn known as the catalytic loop are marked. In subdomain VII, the conserved 'DFG' triplet is marked as start for the activation loop (line above), which ends with the conserved 'APE' triplet in subdomain VIII [105]. At the C-terminus, the consensus sequence for protein serine kinases His-x-a-h is highlighted, whereas 'a' indicates any aromatic and 'h' any hydrophobic residue [105]. Conserved serine residues predicted to be phosphorylated by upstream kinases are highlighted with an encircled 'P'.

Contig No.	Exon/Intron	No.	Start	End	Length	Sequence	AA
803	5' upstream sequence		6500	6604	104	...gtcaaaagtaagattgacatttctgagcaactttctgcagttcatgcataattgttctaactcagctct acatgatgatacgaatgctccagttttcaagcgcc	
	Exon	I	6605	6652	47	ACTCTGGGATTGGTGTGCAAAGATCGGCGCCGCGACTACCAGCT GAAG	
	Intron	1	6653	8995	2342	gtgaggtatt...tcgctgtag ACTGAAATGTCGGGTCTGACGGACAGCACGCCGGTAGCAGGAGG CGGCAGTAGCGGGGATCACCTGGAGACGGGTGTGGACCCATCG AGACCGCTACGGGGCGCAGTCCCAGGCCTCAGGATTACGATT CGCAGGCAAAACGGCAGGTACTATCCAGAACCTTGACCTCACCC	
	Exon	II	8996	9389	393	CCCTACGACTGGACGATCCCCCTTCCCATCATACTCCACCTCTT CCAACACCAACTAACCCTCGTCAAGCCTACTCGCGTCCGCC TCCCACCGCTCACCAGCATCGGCGCTGCTGAAGCCTCCACCGAC AACTTCTCCGTCTTCGACATGATCGACGCGGGGCAACAACCT AATGATCGCATGAGCACTGGACCTGTTGATCTCGTGCTGCG	
	Intron	2	9390	9535	145	gtaaattcc...acatttttag TCAACGCCAACCTCGATGATCAGCAATTGGATGACAGCCAGCGAGA GCGCATTGAGGAATTTCTGCGTTACAAGAAGGACATCCATGAGTT GCACCCGGAAGACTTTACTAAGATCTCCGAGCTGGGCTCAGGCA ATTGGGGTGTGTTAGTCTGTACGCTACAACCGGACTAACATCA TAATGGCCAAGAAGACCATTTCGGTTGGACATTAAGCATGAAGTAG GTACGCCAAATACTCCGAGAATTGAG	Ala130
	Exon	III	9536	9784	248	TCAACGCCAACCTCGATGATCAGCAATTGGATGACAGCCAGCGAGA GCGCATTGAGGAATTTCTGCGTTACAAGAAGGACATCCATGAGTT GCACCCGGAAGACTTTACTAAGATCTCCGAGCTGGGCTCAGGCA ATTGGGGTGTGTTAGTCTGTACGCTACAACCGGACTAACATCA TAATGGCCAAGAAGACCATTTCGGTTGGACATTAAGCATGAAGTAG GTACGCCAAATACTCCGAGAATTGAG	
	Intron	3	9785	10973	1188	gtgggtcacc...tccacccccag TCAACGCCAACCTCGATGATCAGCAATTGGATGACAGCCAGCGAGA GCGCATTGAGGAATTTCTGCGTTACAAGAAGGACATCCATGAGTT GCACCCGGAAGACTTTACTAAGATCTCCGAGCTGGGCTCAGGCA ATTGGGGTGTGTTAGTCTGTACGCTACAACCGGACTAACATCA TAATGGCCAAGAAGACCATTTCGGTTGGACATTAAGCATGAAGTAG GTACGCCAAATACTCCGAGAATTGAG	Ile214
	Exon	IV	10974	11191	217	TCAACGCCAACCTCGATGATCAGCAATTGGATGACAGCCAGCGAGA GCGCATTGAGGAATTTCTGCGTTACAAGAAGGACATCCATGAGTT GCACCCGGAAGACTTTACTAAGATCTCCGAGCTGGGCTCAGGCA ATTGGGGTGTGTTAGTCTGTACGCTACAACCGGACTAACATCA TAATGGCCAAGAAGACCATTTCGGTTGGACATTAAGCATGAAGTAG GTACGCCAAATACTCCGAGAATTGAG	
	Intron	4	11192	11372	180	gtgggtcacc...tcggttttag TCAACGCCAACCTCGATGATCAGCAATTGGATGACAGCCAGCGAGA GCGCATTGAGGAATTTCTGCGTTACAAGAAGGACATCCATGAGTT GCACCCGGAAGACTTTACTAAGATCTCCGAGCTGGGCTCAGGCA ATTGGGGTGTGTTAGTCTGTACGCTACAACCGGACTAACATCA TAATGGCCAAGAAGACCATTTCGGTTGGACATTAAGCATGAAGTAG GTACGCCAAATACTCCGAGAATTGAG	Arg286
	Exon	V	11373	11701	328	TCAACGCCAACCTCGATGATCAGCAATTGGATGACAGCCAGCGAGA GCGCATTGAGGAATTTCTGCGTTACAAGAAGGACATCCATGAGTT GCACCCGGAAGACTTTACTAAGATCTCCGAGCTGGGCTCAGGCA ATTGGGGTGTGTTAGTCTGTACGCTACAACCGGACTAACATCA TAATGGCCAAGAAGACCATTTCGGTTGGACATTAAGCATGAAGTAG GTACGCCAAATACTCCGAGAATTGAG	
803-804	Intron	5	11702	1563	?	gtgagtttac...cctcttcaag CCCGTAACGACACTGGAACAGGCACCATTGTCTATTTTCGAGTTG TTGGTGTTATTGTGGAGCAGCCGCTGCCCGCCTGCCACGAAC ATGCTTCAGTGACGATTTTCATAGACCTCGTAGCTTCTTGCTACG CACAGAGAGCGTAGAGCGACCGTCCGCTGGAGGTGCTTCAAAGC ACGCCTTTGTCCGACGGTGGCGGGTCTGGTACCCGCGGAGC GAATCGACGCAGCAGCATTTCGATTCCGCGATTTCACCACCGCTG CTACTGCTCGTAATGCACCTTCCGCGCTCTCAAGATACTAATGTCC ATTTGAATATGGACGATATCGCCTTCTACCTCTCTCACATCTTACC ACCTCATGATGGCATCGGCTAGACTCCTTGGGGTCCACCACAC TAATGCTGGTGACGATAGTGATTAACCTCCCTTTTATTCTCTA ACACTACTCTCTCCACCTCTGATGTTGTATTGCTACTGTAGTTT GCCTGTGACTACTTCTATTTTCTATTTTTCAGTGT tacgctatcctctatgctttgagcagctaaagacggtagtagtactgtatctgtgtagctattaatga ggaaaa...	Pro396
804	Exon	VI	1564	2090	526	CCCGTAACGACACTGGAACAGGCACCATTGTCTATTTTCGAGTTG TTGGTGTTATTGTGGAGCAGCCGCTGCCCGCCTGCCACGAAC ATGCTTCAGTGACGATTTTCATAGACCTCGTAGCTTCTTGCTACG CACAGAGAGCGTAGAGCGACCGTCCGCTGGAGGTGCTTCAAAGC ACGCCTTTGTCCGACGGTGGCGGGTCTGGTACCCGCGGAGC GAATCGACGCAGCAGCATTTCGATTCCGCGATTTCACCACCGCTG CTACTGCTCGTAATGCACCTTCCGCGCTCTCAAGATACTAATGTCC ATTTGAATATGGACGATATCGCCTTCTACCTCTCTCACATCTTACC ACCTCATGATGGCATCGGCTAGACTCCTTGGGGTCCACCACAC TAATGCTGGTGACGATAGTGATTAACCTCCCTTTTATTCTCTA ACACTACTCTCTCCACCTCTGATGTTGTATTGCTACTGTAGTTT GCCTGTGACTACTTCTATTTTCTATTTTTCAGTGT tacgctatcctctatgctttgagcagctaaagacggtagtagtactgtatctgtgtagctattaatga ggaaaa...	
	3' downstream sequence		2091	2195	104	ggaaaa...	

Tab. 3.3 : Genomic structure of *emmkk2*. The *emmkk2* gene codes on two contigs (no. 803 and 804 of the first assembly) and comprised six exons (I-VI; 47-526 bp). The encoded ORF is interrupted by five introns at corresponding triplets coding for indicated AA. All exon/ intron boundaries carry the GT at the splice acceptor and the AG motif at the splice donor site.

3.5.2 Expression of *emmkk2* in *E. multilocularis* larvae

RT PCR was performed to investigate *emmkk2* expression in *E. multilocularis* larval stages which are involved in the infection of the intermediate host. Specific transcripts were detected in metacystode as well as in protoscoleces before and after activation by low pH and bile salts mimicking the passage through the digestion tract of the final host. Additionally, it was analysed whether *emmkk1* and *emmkk2* are co-expressed. The expression of both genes relative to the expression of the housekeeping gene *elp* was investigated using a semi-quantitative PCR approach [73, 76, 77]. Furthermore, expression of one putative interaction partner, a previously identified 14-3-3 orthologue of *E. multilocularis*, was assessed (see also section 3.5.3). As indicated in Fig.3.28, *emmkk1* was considerably less expressed in metacystode vesicles and in protoscoleces upon activation than *emmkk2*. Moreover, *emmkk2* showed an increased expression in both protoscolex preparations. *Em14-3-3* expression was detected in metacystode and resting protoscoleces whereas no expression was observed for activated protoscoleces (Fig. 3.28). This confirmed a result previously obtained by Siles Lucas et al. [121].

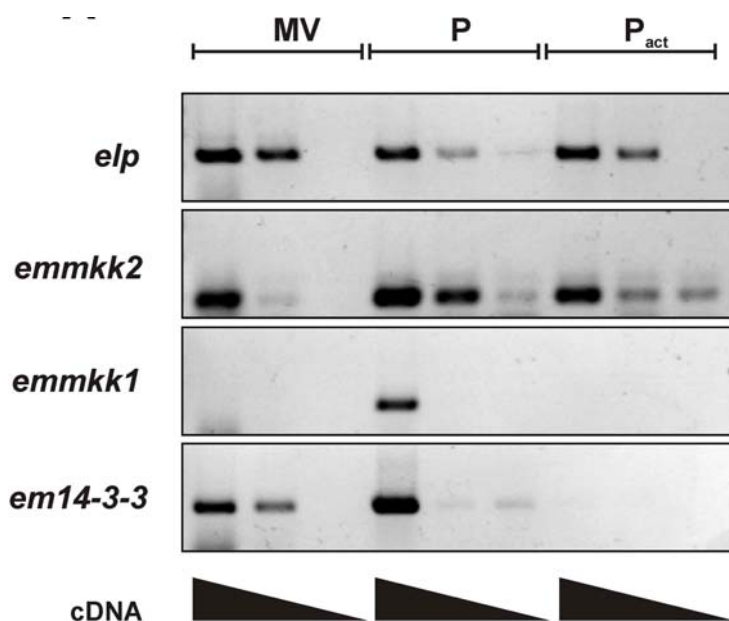


Fig. 3.28: Expression of *emmkk2* in *E. multilocularis* larvae. Indicated are semi-quantitative RT-PCR analyses of *Echinococcus* gene expression in *in vitro* cultivated metacystode vesicles (MV) and protoscoleces in non-activated form (P) and after activation with low pH/pepsin and bile salts (P_{act}). cDNAs of corresponding larval stages were used as template in a serial of 10-fold dilution steps (indicated by triangles) for PCR setups specific for the housekeeping gene *elp* as internal standard [73, 76, 77], *emmkk2*, *emmkk1* and *em14-3-3*.

3.5.3 Interaction studies between EmMKK2 and potential members of the *E. multilocularis* MAPK cascade

Based on the homology of EmMKK2 to MAPK cascade members, interaction for several *E. multilocularis* factors was carried out using yeast two hybrid. Fusion constructs for EmMPK1, EmMPK2, EmMKK1, EmMKK2, EmRAF and Em14-3-3 with the GAL4 DNA-binding domain or the GAL4 trans-activation domain were co-transfected into yeast strain AH109 [98, 121, 122]. For protein-protein interaction under high stringency conditions, double transfectants were selected on leucin-tryptophan-histidin-adenin-deficient medium (Fig. 3.29 A). Individual yeast colonies were picked and plated repeatedly on quad minus medium for 48 h to eliminate false positive clones. In these experiments, EmMKK2 and EmMPK1, the Erk orthologue of the parasite, strongly interacted. In addition, EmRAF representing the putative upstream kinase of *E. multilocularis* MKKs interacted with EmMKK2. In line with the above structural data showing that EmMKK2 contained a consensus motif for interactions with 14-3-3 proteins (see section 3.5.1), EmMKK2, but not EmMKK1 interacted with Em14-3-3 in the yeast two hybrid. The interaction of EmMKK1 with EmRAF as well as the absence of interaction with EmMPK1 confirmed the results of Y2H analysis conducted by Spiliotis [98]. No homo-dimerization was observed for all factors analyzed. In addition, none of the *Echinococcus* MKK interacted with the p38 orthologue EmMPK2. This result was interesting in so far as that human MKK3/6 homologues interact with p38 MAPK isoform α to which EmMKK1 displays highest homologies.

To verify the interaction between EmMKK2 and EmMPK1, co-immunoprecipitation with ectopically expressed and purified fusion proteins was performed. EmMKK2 fused to a V5 epitope and thioredoxin tag was immobilized via anti-thioredoxin antibody on agarose G beads and incubated with EmMPK1 GST fusion protein. The interaction of EmMPK1 and EmMKK2 was detected with both the anti-GST-antibody and anti-Erk antibody via Western blot (Fig. 3.29 B). No signal was detected using the anti-phospho-Erk antibody indicating, as expected, that the interaction between EmMKK2 and EmMPK1 is independent of EmMPK1 phosphorylation at the TEY motif.

In conclusion, these interaction analyses identified EmMKK2, the parasite MKK1 homologue, as a component of the *Echinococcus* MAPK cascade. In this cascade, EmMKK2 acts as transducer between the upstream factor EmRAF and the downstream factor EmMPK1. For EmMPK2, no activating kinase could be identified by this approach.

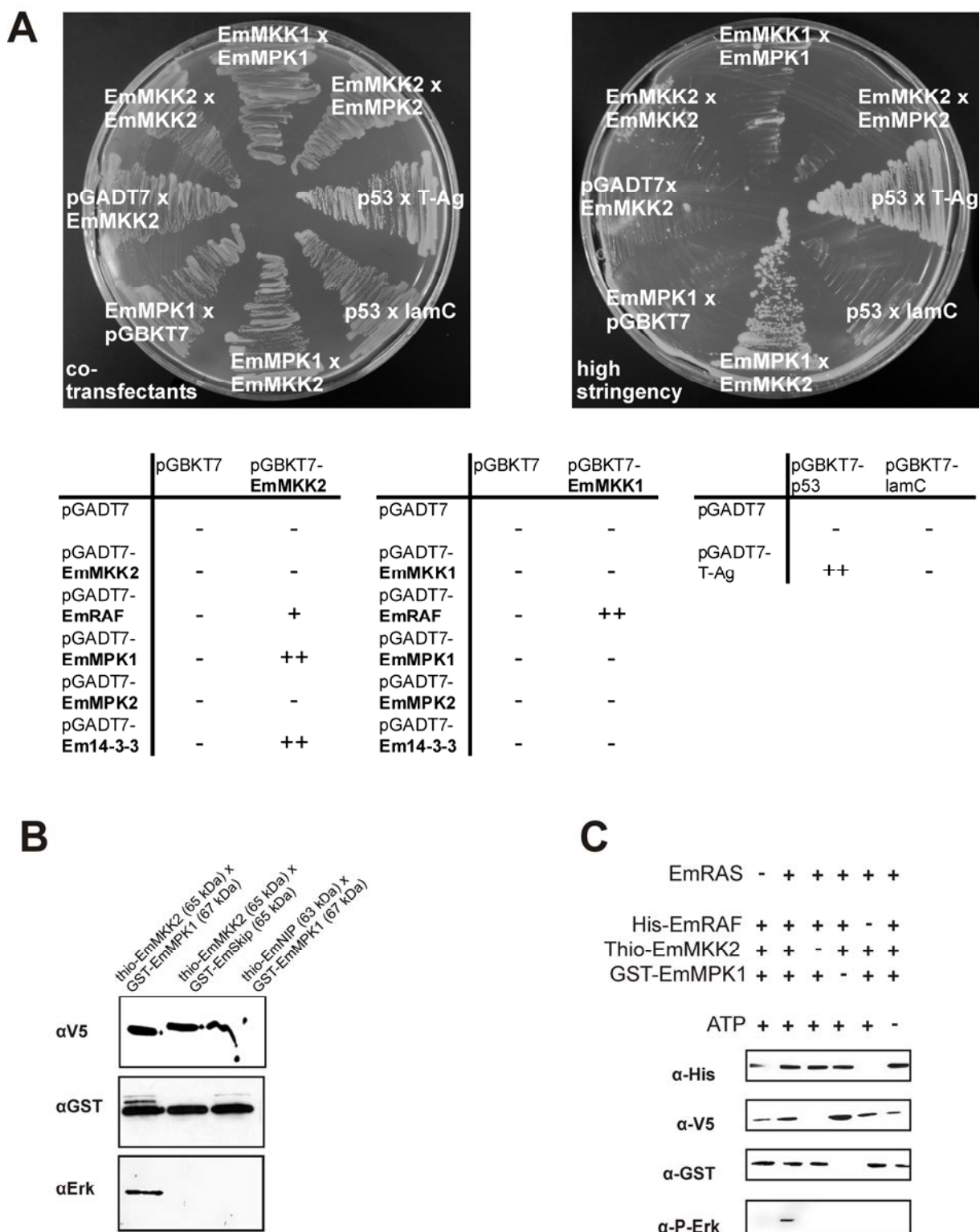


Fig. 3.29: Interaction analyses of MAPK cascade members from *E. multilocularis*. (A) Listed are results of yeast two hybrid protein-protein interaction assays under high stringency conditions of experiments with fusion constructs for EmMKK1, EmMKK2, EmRaf, EmMPK1, EmMPK2 and Em-14-3-3 with activation domain (pGADT7) or DNA-binding domain (pGBKT7) of yeast transcription factor Gal4. Co-transfected yeast cells of the strain AH109 were selected on leucine and tryptophan deficient agar plates. The correct expression of fusion proteins was analysed by Western blot (data not shown). Selection for interaction took place under high stringency on quad drop out medium. As controls, the expression plasmids of the large T- antigen of virus SV40 as pGADT7 construct with tumour suppressor p53 in pGBKT7 (positive control) and T-Antigen with lamin C in pGBKT7 (negative control) were co-transfected. Moderate growth is indicated by one '+', good growth by '++'. No growth by '-'. (B) Western blot analysis of MAPK cascade members. Lanes are labeled with thio-EmMKK2 (65 kDa) x GST-EmMPK1 (67 kDa), thio-EmMKK2 (65 kDa) x GST-EmSKIP (65 kDa), and thio-EmMPP (63 kDa) x GST-EmMPPK1 (67 kDa). Blots are shown for alphaV5, alphaGST, and alphaErk. (C) Western blot analysis of MAPK cascade members. Lanes are labeled with EmRAS (-, +, +, +, +, +), His-EmRAF (+, +, +, +, -, +), Thio-EmMKK2 (+, +, -, +, +, +), GST-EmMPK1 (+, +, +, -, +, +), and ATP (+, +, +, +, +, -). Blots are shown for alpha-His, alpha-V5, alpha-GST, and alpha-P-Erk.

(B) Co-immunoprecipitation of EmMPK1 with EmMKK2. After heterologous expression in *E. coli* and subsequent purification of EmMPK1 as GST fusion protein and EmMKK2 as fusion protein with V5 epitope and thioredoxin tag, EmMKK2 was bound by anti-thioredoxin antibody to agarose G beads. Subsequent to repeated washing steps, GST-EmMPK1 was added. After washing again, the beads were transferred into 2x stop mix and boiled for five minutes. The samples were spun down and the supernatant separated on 12% polyacrylamid gel. Precipitated proteins were analysed via Western blot experiments using the anti-V5 antibody, the anti-GST antibody and the anti-Erk1/2 antibody as indicated. As negative controls, EmSkip was used as GST fusion protein and EmNIP as fusion with V5 epitope and thioredoxin tag [89, 91]. (C) *In vitro* activity assay of the MAPK cascade. EmRas activated or non-activated EmRaf as His-tagged protein were incubated together with EmMKK2 as V5 fusion protein and GST-EmMPK1 with or without ATP [98, 123]. The protein content of the samples were separated by PAGE and examined by Western blotting using the indicated antibodies directed against the tags as well as the dual-phosphorylation motif pT-E-pY of Erk-like MAPKs.

3.5.4 *In vitro* activity of the parasite MAPK cascade

Due to the results from the interaction analyses it was investigated whether EmRAF, EmMKK2 and EmMPK1 constitute a functional MAPK cascade. EmRas carrying an activating mutation was co-expressed with EmRaf in insect cells to obtain the parasite MKKK in an activated form (EmRaf*). Following purification, EmRAF* was incubated with EmMKK2 and EmMPK1, each separately expressed in *E. coli* and purified, to perform an *in vitro* activity assay. Phosphorylation of EmMPK1 was then measured via Western blot using the anti-phospho-Erk antibody. To ensure the specificity of this *in vitro* assay, I omitted either one component including ATP in the reaction. As indicated in Fig 3.29 C, EmMPK1 was phosphorylated only in the presence of ATP and the complete protein contingent. This indicated that EmRas activated EmRAF, which in turn lead to the phosphorylation of EmMKK2 subsequently leading to the activation of EmMPK1. Thus, the Erk-like MAPK module in *Echinococcus* is formed by EmRAF, EmMKK2 and EmMPK1.

3.6 Analysing and targeting the EGF signaling pathway of *E. multilocularis*

3.6.1 Phosphorylation of Elp in response to host EGF and the effects of inhibitors

Members of the ERM protein family are involved in the regulation of cell morphology via acting as molecular linkers between the actin cytoskeleton and the cytoplasmic membrane. This involves phosphorylation of ERM proteins at a conserved C-terminal motif in growth factor (e.g. EGF) dependent ways [124-126]. To investigate whether a similar mechanism is acting on the *E. multilocularis* ERM orthologue Elp, experiments concerning Elp phosphorylation in intact metacystode vesicles upon exogenous stimulation through host EGF were carried out. As shown in Fig. 3.30., phosphorylation of Elp is no longer detectable once metacystode vesicles from co-culture were incubated for 4 days in the absence of host serum and feeder cells (i.e. 'serum starving' conditions). However, when during serum starvation host EGF (100 nM) is present, Elp phosphorylation is as intense as in vesicles from co-culture. This suggests that the ERM orthologue of the parasite is regulated via

phosphorylation through a so far unidentified kinase in an EGF dependent signaling cascade. Concerning the question, which molecules could be involved, metacestode larvae were treated with PP2 as inhibitor of Src kinases and leflunamide as anti-proliferative agent and broad-range inhibitor of tyrosine kinases [127, 128]. After 2 hours, metacestode vesicles were harvested and examined for Elp phosphorylation. As depicted in Fig. 3.30 B, the phosphorylation of Elp was completely blocked upon treatment with PP2. In the case of leflunamide, Elp phosphorylation was still detectable, albeit at lower level compared to the DMSO control. In addition, the influence of both inhibitors on EmMPK1 phosphorylation was analysed. For both inhibitors, the phosphorylation of EmMPK1 was minimally diminished compared to the control (Fig. 3.31 B).

In summary, these results indicated that exogenous serum derived factors, among them host EGF, stimulated Elp phosphorylation. On the assumption that PP2 and leflunamide were able to target the same classes of worm kinases like in mammalian cells, tyrosine kinases, in particular members of the Src family could be responsible in the growth factor activation of Elp. Furthermore, no significant effects of PP2 and leflunamide on Erk1/2 like MAPK signaling were observed.

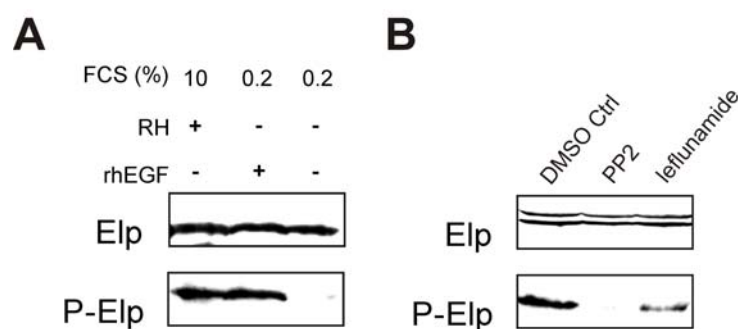


Fig. 3.30: Growth factors cause Elp phosphorylation. Indicated are Western blot analyses of metacestode lysates in turn of PAGE. Whole amount Elp was detected with the anti-EM10 antibody and as phosphorylated protein with the anti-phospho-ERM antibody. (A) Before co-cultivated metacestode vesicles in rich medium were subsequently incubated under low serum condition in the presence or absence of 100 nM EGF. (B) The larval material was kept rich medium supplemented with 200 μ M PP2, 300 μ M leflunamide or with the inhibitor dissolvent alone.

3.6.2 Activation of EmMPK1 in response to host EGF

The influence of host serum or the integrity of metacestode vesicles on EmMPK1 activation has been examined by Spiliotis et al. [98]. The results demonstrated a positive effect of mammalian serum on the phosphorylation of EmMPK1. A potent inducer of the MAP kinase cascade and, thus, of ERK phosphorylation in mammalian cells is EGF via binding to the EGF receptor [129]. Since EGF is present in mammalian serum [130], the question arose whether the phosphorylation state of EmMPK1 in metacestode vesicles can be altered in response to exogenous host EGF (Fig. 3.31). Physically intact metacestode vesicles from *in*

vitro culture were initially incubated for 4 days in medium containing 0.2 % FCS in the presence or absence of 100 nM human EGF. After the incubation, phosphorylation of EmMPK1 was undetectable in the absence of EGF and detectable in the presence of EGF (Fig. 3.31 A). Second, the metacestode vesicles were kept for 4 d in low serum concentrations and subsequently stimulated for 30 min with EGF (Fig. 3.31 B). Phosphorylation of EmMPK1 could be reconstituted by adding host EGF as well as serum to a final concentration of 10%. These findings reflected the starting situation of phosphorylated EmMPK1 in axenically cultivated and growing metacestode vesicles. These experiments indicated that intact *E. multilocularis* metacestode vesicles are responsive to exogenous host EGF and that the stimulation triggers the parasite's MAPK cascade as shown by increased phosphorylation of the parasite's ERK-like kinase.

An important question concerns the *in vivo* relevance of the EGF effect on the *Echinococcus* MAP kinase cascade. *E. multilocularis* could, indeed, come into close contact with host EGF during an infection since this cytokine is produced by a wide variety of host cells [44, 131, 132]. In the liver, EGF is mainly produced during regeneration after hepatectomy or in response to chemical injury [131, 133]. A possible scenario is that hepatocytes are injured either directly by the parasite or indirectly through the host immune response around the metacestode, upon which the liver tissue responds with regeneration and the release of EGF. Therefore, the question arose whether the feeder cells in the co-culture system synthesize EGF. The expression of EGF has been validated by a PCR approach with gene specific primer and RH- cDNA as template (data not shown).

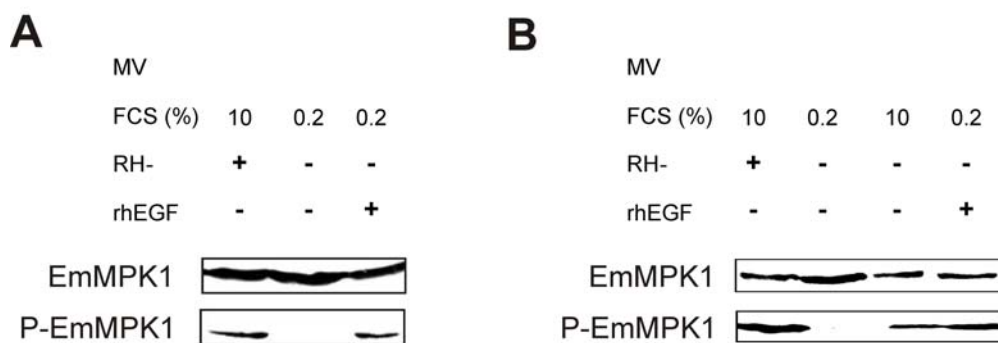


Fig. 3.31: Phosphorylation of EmMPK1 in response to host EGF. Depicted are Western blot experiments of vesicle lysates using the anti-Erk1/2 and the anti-phospho-Erk antibodies detecting overall EmMPK1 and phosphorylated EmMPK1, respectively after separation on 12% acrylamid. **(A)** Intact metacestode vesicles (MV) (axenically cultivated) were kept in medium pre-conditioned with hepatocytes (RH-) containing 10% FCS (lane 1), 0.2% FCS (lane 2) or 0.2% FCS and 100 nM host EGF for 4 d. **(B)** MVs had been incubated for 4 d in medium with 0.2% FCS (lane 2) and were then placed placed for 30 min into medium containing 10% FCS (lane 3) or 0.2% FCS/ 100 nM EGF (lane 4). Lane 1 shows MVs before incubation in 0.2% FCS.

3.6.3 Enhanced proliferation of *E. multilocularis* in response to host EGF

In addition to the activation of the MAP kinase cascade in cultivated metacestode larvae, host EGF was tested as putative inducer of parasite proliferation. The mitotic activity of the metacestode was determined upon EGF stimulation through detection of incorporated 5-bromo-2-deoxyuridine (BrdU) into newly synthesized DNA [134]. Axenically cultivated vesicles were transferred into normal culture medium containing 10% or 0.2% FCS. After 4 days, the metacestode vesicles were stimulated for 3 h with 50 and 100 nM of either human EGF or TGF- α . At the same time, the medium was supplemented with BrdU to a final concentration of 1 mM. Following isolation, the genomic DNA (0.1, 0.5 and 1 μ g) was blotted onto nitrocellulose. DAPI staining was performed to confirm that equivalent amounts of DNA have been applied to the blot. Subsequently, *de novo* DNA synthesis was measured by immuno-staining using the anti-BrdU antibody. Co-isolated RNA has been removed to avoid cross-reactivity of the antibody to endogenous uridine.

As shown in Fig. 3.32, significantly more BrdU was incorporated by the parasite in the presence of 50 nM EGF for both low and high serum conditions. Interestingly, a concentration of 100 nM EGF still led to increased BrdU incorporation but to a lesser extent than in the case of 50 nM EGF. In the case of TGF- α , significant stimulation was also observed, but only for a concentration of 50 nM.

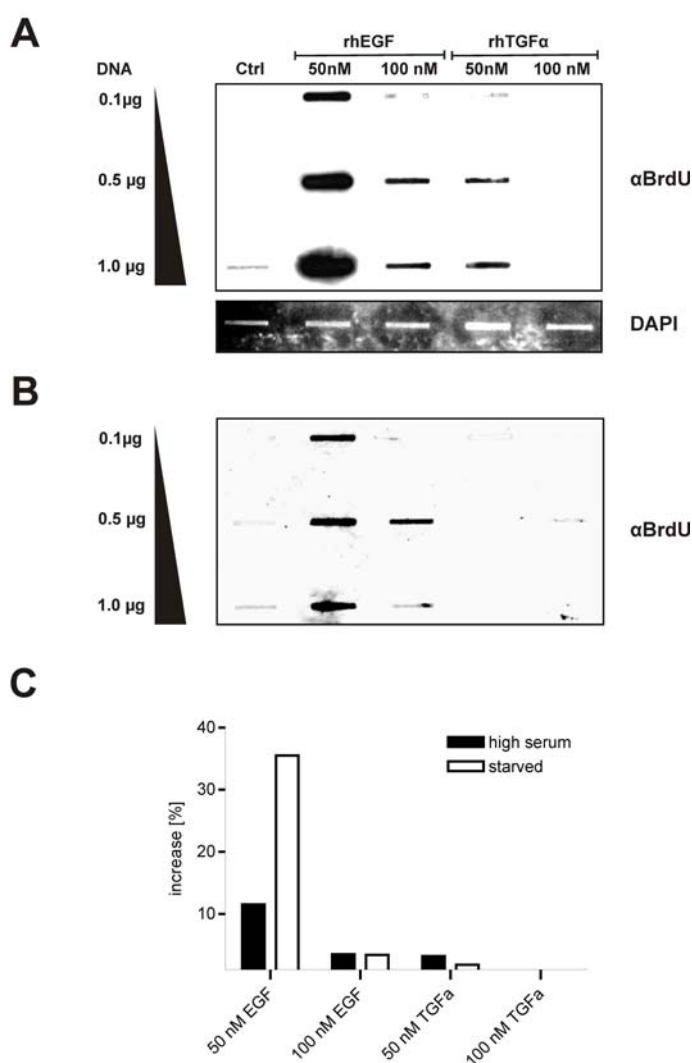


Fig. 3.32: Mitotic effects on metacestode larvae upon stimulation with host growth factors.

In vitro cultivated metacestode vesicles were incubated in the presence of BrdU under low (**A**) and high (**B**) serum conditions and subsequently stimulated with the indicated concentration of host EGF and TGF- α . The genomic DNA of metacestode vesicles was slot-blotted following isolation onto nitrocellulose and the incorporation of BrdU into the newly synthesized DNA was detected by immunostaining using the anti-BrdU antibody. The transferred DNA content was confirmed with DAPI staining. (**C**) Quantification of the proliferation increase in stimulated metacestode vesicles. The intensity of the bands were quantified and the values normalized against non-stimulated control using NIH ImageJ software.

3.7 *In vitro* treatment of metacestodes with tyrosine kinase and MAPK cascade inhibitors

To test whether small molecule compounds originally designed to inhibit human MAPK cascade factors might also affect the respective parasite orthologs and thus inhibit *E. multilocularis* growth and development, *in vitro* inhibition studies were carried out. Due to the limitations of co-culture models (indirect effects of drugs on mammalian feeder cells), axenically cultivated vesicles were used for these experiments.

First, BAY439006 (RAF inhibitor) as well as M-INH and PD184352 (MEK inhibitors) were tested for inhibition of EmMPK1 phosphorylation [135, 136]. As indicated in Fig. 3.33, all three compounds blocked EmMPK1 phosphorylation when the vesicles were kept for 2 h in DMEM 10 % FCS in the presence of 100 μ M of each drug. Long-term cultivation for 4 weeks (exchange of medium including inhibitors was performed 4 d), however, did neither result in damage of vesicles nor to an increase of alkaline phosphatase activity in the supernatant of cultivated vesicles. Second, metacestode vesicles were treated with PD168393 and PD173074, directed against members of the EGF- and FGF-receptor families, respectively, in concentrations between 1 nM up to 50 μ M (final concentration) [94, 95, 137-139]. Since activity assays for EmER and EmFR are not yet established, EmMPK1 phosphorylation was used as read out. However, under these conditions no effects were observed on EmMPK1 phosphorylation (short term incubation), not on vesicle viability or AP activities in the supernatant (4 weeks incubation).

Finally, although the Src kinase inhibitors PP2 and leflunamide clearly inhibited EIp phosphorylation in response to EGF (see above), these drugs did not affect EmMPK1 phosphorylation (Fig. 3.33) nor did they exert effects on vesicle viability during long-term cultivation (each 50 nM- 500 μ M final concentration).

In summary, the activation of the *E. multilocularis* Erk-like MAPK cascade could be blocked by adding inhibitors originally designed against mammalian Raf and MEK factors to metacestode vesicles. Albeit these inhibitors lead to a decreased EmMPK1 activity as confirmed by Western blotting, a negative effect on parasite survival could not be detected.

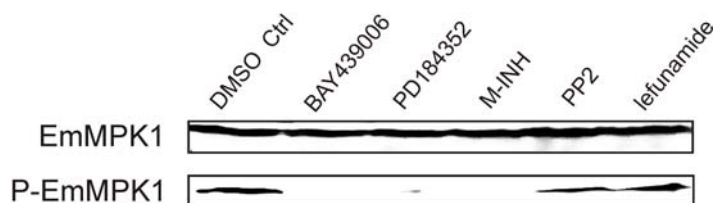


Fig. 3.33: Inhibition of the parasite MAPK cascade in the *in vitro* cultivated metacestode larvae. Depicted are Western blot experiments of vesicle lysates using the anti-Erk1/2 and the anti-phospho-Erk antibodies detecting overall EmMPK1 and phosphorylated EmMPK1, respectively after separation on 12% acrylamid. Axenically cultivated metacestode vesicles were kept for 2 h in rich medium supplemented with DMSO and with or without RAF inhibitor BAY439006, MEK inhibitors PD184352 and M-INH (100 μ M each), 200 μ M PP2 or 300 μ M leflunamide.

3.8 Influence of various host growth factors on vesicle regeneration

An *in vitro* system for long-term *E. multilocularis* primary cell cultivation has recently been introduced [13]. In this system, *Echinococcus* cells which derived from metacestode vesicles fully regenerated viable and intact vesicles in the presence of host feeder cells or hepatocyte-conditioned medium, indicating an important role of secreted host factors on parasite regeneration [84, 85]. In the present work, experiments were carried out to test whether host insulin, EGF and/or FGF could play a role in parasite regeneration. *E. multilocularis* primary cells were isolated according to a previously established protocol [13] and kept in the presence of medium containing 1% FCS with or without growth factors. As shown in Fig 3.34 B, primary cells kept for 21 days in 1% FCS proliferated and formed cell aggregates with central cavities, indicating parasite regeneration [13]. In the presence of 1 nM host insulin, a significant effect on vesicle regeneration was observed which occurred faster and involved the formation of larger cell aggregates (Fig. 3.34 C). In addition, central cavities within cell aggregates were significantly larger than in cultures without additional host insulin. Upon co-incubation with host EGF (50 nM) as well as acidic or basic FGF (both at 1 nM), aggregate size and central cavity diameters were similar to controls (Fig. 3.34 D, E, F). It appeared, however, that more aggregates were formed under the influence of these host factors.

Since EGF, FGF and particularly insulin apparently had an influence on vesicle regeneration, respective signaling pathways were further investigated. *Echinococcus* cells were incubated for long-term in the presence of drug compounds known to inhibit the putative RTKs of the respective cytokine signaling pathways in human cells. Among these was the cell permeable pyridopyrimidine compound PD173074 which reversibly blocks (in nM range) the activities of FGF and VEGF receptor *in vitro* by ATP competitive binding. When added in higher concentrations (μ M range), this substance also inhibits members of the insulin and EGF receptor families [137, 138]. The quinazoline derivate PD168393, on the other hand, operates as cell permeable, irreversible and selective inhibitor of EGFR by binding to the intracellular catalytic domain [139]. Both compounds were selected on the basis of homology comparison of the two parasite kinases EmFR and EmER to human RTKs. Both EmFR and EmER displayed in their catalytic domains residues which were putatively involved in drug binding. For example, Cyt⁷⁷³ in the ATP binding pocket in EGFR is present in EmER as residue Cyt¹⁰⁸⁴ and therefore a putative interacting residue for PD168393 [139]. For the experiment, freshly isolated *Echinococcus* primary cells were cultivated in pre-conditioned medium supplemented with PD173074 and PD168393 each at 50 μ M final concentration and the assembly of aggregates was monitored for 4 weeks. However, an effect on primary cell regeneration could not be measured for PD173074 and PD168393 despite the homology in the respective target structures. Like the DMSO treated control group, the primary cells formed aggregates, central cavities and new vesicles in the presence of PD173074 and PD168393. Furthermore, after 3, 12, and 24 h treatment, phosphorylation of EmMPK1 remained unchanged (data not shown).

Treatment of primary cells with the cell permeable insulin receptor tyrosine kinase inhibitor HNMPA-(AM)₃, however, clearly affected regeneration. On *in vitro* cultivated human cell lines, the ATP non-competitive HNMPA-(AM)₃ revealed inhibitory capacity on Tyr kinases

over Ser kinases and was proved to block the auto-phosphorylation on Ser¹³⁰⁵/Ser¹³⁰⁶ of human InsR [140, 141]. Inhibitory activity against PKC and PKA was not reported, however, the blocking of insulin-stimulated glucose oxidation [141]. In *Echinococcus* primary culture, the presence of 25 μ M HNMPA-(AM)₃ for three weeks prevented regeneration of vesicles (Fig. 3.35 A). The cells remained as single cells and occasionally only small clusters of cells were formed. Primary cells which were cultivated in rich medium containing the inhibitor dissolvent DMSO, were capable of forming cell aggregates and central cavities within three weeks. The cultivation under same conditions with addition of insulin resulted in the above described large agglomeration of aggregates and in large size vesicles. The combined treatment of HNMPA-(AM)₃ and insulin led to an improved cell clustering than in the presence of the inhibitor alone, but the cells never reached the level of aggregation than in the absence of inhibitor (Fig. 3.35 A).

Since it has been demonstrated that insulin stimulated EmMPK1 phosphorylation could be inhibited in the presence of HNMPA-(AM)₃ in *in vitro* cultivated metacestode larvae [93], the status of EmMPK1 phosphorylation was examined in *Echinococcus* primary cells. Freshly isolated primary cells were kept in rich medium as well as under serum starvation conditions and treated with 0.5 μ l/ml or 2 μ l/ml insulin (final concentration 1 nM and 4 nM, respectively) 1 nM) and/or 25 μ M HNMPA-(AM)₃ for 20 and 40 minutes as well as 4, 8 and 24 h. The samples were subsequently prepared for Western blot experiments detecting total EmMPK1 and pT-E-pY phosphorylated EmMPK1. For none of the examined experimental condition, an alteration of EmMPK1 phosphorylation was detectable as exemplary shown in 3.35 B. Moreover, the presence of insulin did not result in an increased phosphorylation under serum starving condition as has been reported for metacestode vesicles. The treatment of primary cells with the tyrosine kinase inhibitor HNMPA-(AM)₃ did not affect EmMPK1 phosphorylation as depicted in 3.35 B. Interestingly, by examining treated primary cells in Western blot analyses using the anti-Erk 1/2 antibody, an additional band representing a so far unknown protein of estimated 120kDa consistently appeared. This signal disappeared when primary cells were cultivated with HNMPA-(AM)₃ under serum starving condition as shown in Fig. 3.35 B. In addition to this, a protein of approximately 70 kDa (question mark in Fig. 3.36 B) was detected by the anti-phospho-Erk antibody (but not by the anti-Erk antibody) exclusively under high serum conditions. This protein was further investigated as outlined in section 3.9. Although the 120 kDa protein which interacted with both antibodies could represent an as yet uncharacterized 'big MAPK' (such as Erk5) orthologue in the parasite, no indications for such a kinase was obtained by screening genomic contigs. Hence, the molecular nature of this cross-reacting protein is presently unknown.

As demonstrated in this section, treatment of *Echinococcus* primary cells with host cytokines affected the developmental process in various manners. The presence of host EGF in primary culture led to smaller cell aggregates which, however, occurred in higher number, indicating that EGF enhanced the proliferation of primary cells. I observed a comparable outcome by treatment with acidic and basic FGF. Remarkable was the influence of insulin, which resulted in the strongest stimulation of vesicle regeneration. In fact, in the presence of insulin, primary cells aggregated to large size, which were mainly associated with each other and resulted in large size vesicles. The attempts to prevent the assembly of *Echinococcus* primary cells by targeting the respective signal receptors were not successful

with one exception, the treatment with the insulin tyrosine kinase inhibitor. In the case of EGF- and FGF-receptor inhibitors, this might be due to diminished affinities of the drugs to EmER and EmFR. Concerning the influences on protein level, neither the host cytokines nor the corresponding inhibitors of the signal pathways led to alterations of EmMPK1 phosphorylation.

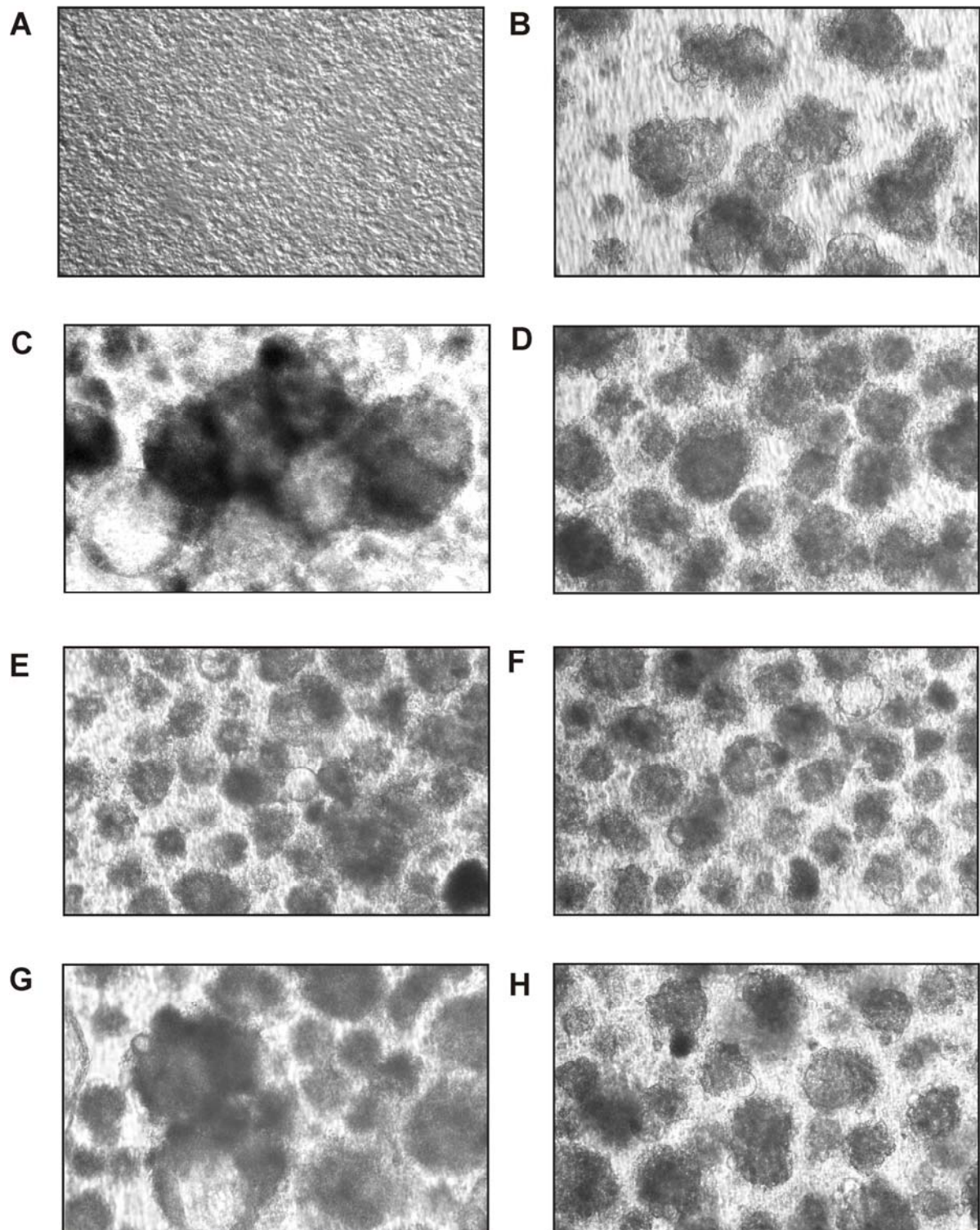


Fig. 3.34: Influence of selected host growth factors on *Echinococcus* primary cell cultures. Primary cells were cultivated in medium containing 1% FCS (directly after isolation (A)) and cultivated for 21 d in the absence (B) or presence of additional growth factors (C-H). The medium supplemented with the growth factor was refreshed every fourth day. Shown are primary cells cultivated in the presence of 1 nM host insulin (C), 50 nM EGF (D), 1 nM aFGF (E), 1 nM bFGF (F), insulin together with EGF (G) and EGF together with acidic and basic FGF (H) at day 21.

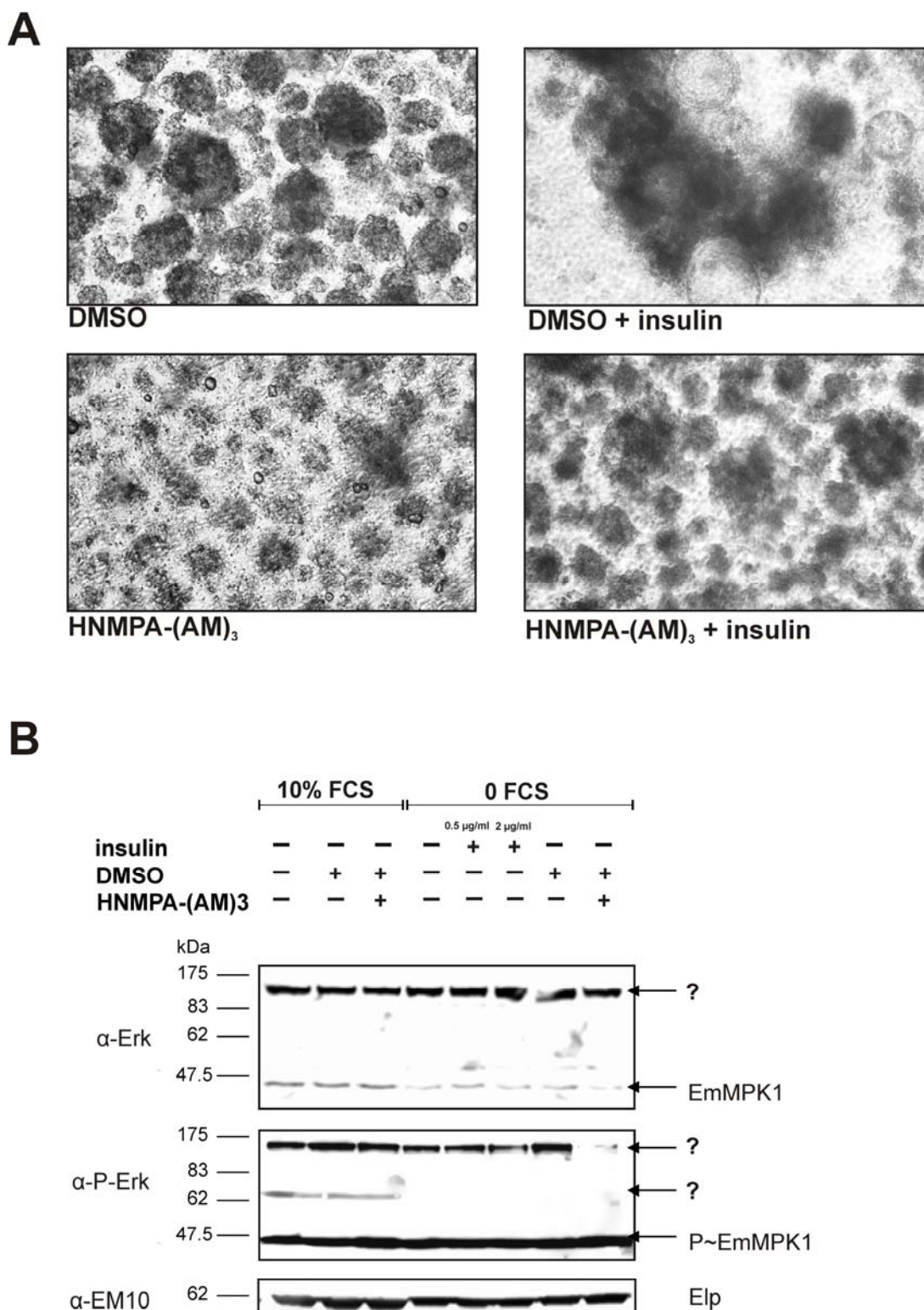


Fig. 3.35: Treatment of *Echinococcus* primary cells. (A) Freshly isolated primary cells were incubated in rich medium supplemented with DMSO, DMSO and insulin, HNMPA-(AM)₃ as putative inhibitor of the *Echinococcus* insulin receptors or HNMPA-(AM)₃ combined with insulin. Shown are primary cells after three weeks with the designated treatment. (B) After 3 h treatment, which was carried out as indicated on top, primary cells were processed for Western blot approach. Detection was performed with the anti-Erk1/2, anti-phospho-Erk and the anti-Em10 antibodies as indicated to the left.

3.9 EmMPK3 – a serum sensitive MAPK

As already mentioned, stimulation of *Echinococcus* primary cells with host cytokines or serum did not affect the phosphorylation of EmMPK1 on the T-E-Y motif which is contrary to the situation in intact metacestode vesicles (chapters 3.6 and 3.8). By Western blot analyses on primary cells, however, an additional protein of approximately 70 kDa was detected with the anti-pT-E-pY antibody when the cells were kept under high serum conditions. The appearance of the respective protein in response to serum stimulation was verified in an additional experiment. Primary cells were stimulated by adding 10% serum to culture medium for 3 h following isolation and incubation in the absence of serum for one day. As depicted in Fig. 3.36, a clear signal representing a protein of ca. 70 kDa was detected upon stimulation with serum. The protein was recognized by the phospho-specific antibody for Erk MAPK, which is directed against the pT-E-pY motif. *In silico* analyses of the *Echinococcus* genome were performed using the BLAST tool with the activation loop of EmMPK1 and the human Erk MAPK as queries. Only two factors containing the T-E-Y motif were identified. One was the already characterized Erk-like kinase EmMPK1. The second factor was a recently described kinase, EmMPK3, which displayed highest homologies to Erk7/Erk8 family members [97].

By repeating TBLASTN analysis with the EmMPK3 sequence against the genome data base, the protein sequence of 625 AA was confirmed and yielded a calculated MW of 69 kDa. No further factors with T-E-Y triplet in the context of a Ser/Thr kinase activation loop were recorded. Hence, the protein of around 70 kDa detected with the anti-pT-E-pY antibody upon serum stimulation could indeed be EmMPK3. It was not to be expected that EmMPK3 was detected with the anti-Erk1/2 antibody since EmMPK3 does not contain the oligopeptid (PFTFDMEELDDLPERLKE LIFQETARFQGAPEAP) against which the antibody is directed.

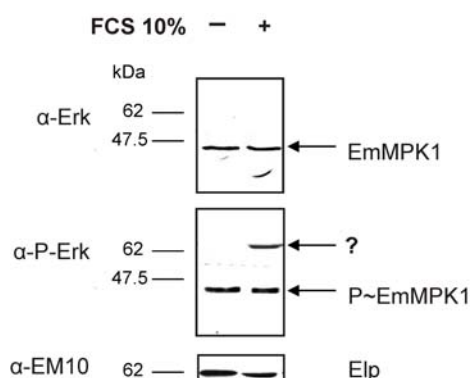


Fig. 3.36: Stimulation of *Echinococcus* primary cells with serum. Freshly isolated primary cells were incubated in medium without serum for 24 h and afterwards stimulated with 10% FCS for 3 h. A Western blot analysis of these cells was realized after sample separation on acrylamid gel using the anti-Erk1/2, anti-phospho-Erk and the anti-Em10 antibodies as indicated to the left.

Besides structural analyses, functional analyses on EmMPK3 were performed in this work. First, I examined the interaction of EmMPK3 with the two MKKs of *Echinococcus*. After cloning of the EmMPK3 ORF into yeast expression vector pGBKT7 to obtain translational fusion products with the DNA-binding domain of the Gal4 transcription factor, co-transfections of yeast strain AH109 were carried out together with pGADT7 plasmids coding

for EmMKK1 and EmMKK2 fusion proteins as listed in Tab. 3.4. Co-transfected clones were incubated on agar plates to identify protein-protein-interaction under low and high stringency condition. Under neither condition, an interaction of EmMPK3 was detected with EmMKK1 or with EmMKK2 (Tab. 3.4).

Second, EmMPK3 was ectopically expressed as fusion protein with V5 and hexahistidin tag and subsequently purified under native condition to investigate enzymatic activity *in vitro*. For this purpose, EmMPK3 was incubated in the presence of radioactively labelled ATP and the common kinase substrate myelin basic protein (MBP). As displayed in Fig. 3.37, the recombinantly expressed EmMPK3 possessed enzymatic activity as determined by incorporation of γ - ^{32}P into MBP. The phosphorylation status of EmMPK3 after expression in *E.coli* was further investigated in Western blot experiments. Here, EmMPK3 was detected with the anti-V5 antibody at the expected size of 75kDa. Moreover, recombinant EmMPK3 was recognized by the human anti-phospho-Erk antibody (Fig. 3.37) indicating the phosphorylation on T-E-Y.

	pGBKT7	pGBKT7- EmMPK3		pGBKT7- p53	pGBKT7- lamC
pGADT7	-	-	pGADT7	-	-
pGADT7- EmMKK1	-	-	pGADT7- T-Ag	++	-
pGADT7- EmMKK2	-	-			

Tab. 3.4: Protein-protein interaction analysis of EmMPK3 with MKKs of the parasite. Tabulated are yeast two hybrid results for high stringent interaction with generated fusion constructs of EmMKK1, EmMKK2 and EmMPK3 with the activation domain (pGADT7) or the DNA-binding domain (pGBKT7) of yeast transcription factor Gal4. Co-transfected yeast cells of the strain AH109 are selected on leucine and tryptophan deficient agar plates. Correct expression of the fusion proteins was analysed by Western blotting (data not shown). As controls, expression plasmids of the large T- antigen of SV40 as pGADT7 construct with tumour suppressor p53 in pGBKT7 (positive control) and the T-Antigen with lamin C in pGBKT7 (negative control) were co-transfected. Moderate growth is indicated by one '+', good growth by '++'. No growth by '-'.

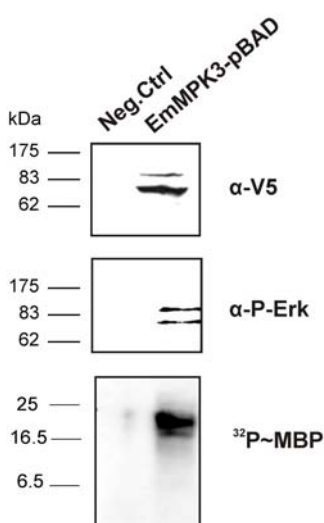


Fig. 3.37: Heterologous expression and *in vitro* activity of EmMPK3. Ectopically expressed and purified EmMPK3 as fusion protein with V5 epitop and hexahistidine tag was separated by PAGE. Western blot detection was performed with antibodies against the V5-epitope (top) and the pT-E-pY motif of Erk MAPKs (middle). The MPK3 activity assay was performed as done for EmMPK2 (section 3.1). Incorporation of ^{32}P into the common MAPK substrate myeline basic protein (MBP) is shown below. Marker sizes are indicated beside the blots.

3.10 Activity assay for EmER, the EGF receptor of *E. multilocularis* - Preliminary data

Several effects of human EGF on the parasite's signaling pathways were observed so far (see section 3.6). Despite the structural characterization of *E. multilocularis* EGF receptor homologue EmER, it is, however, not yet clear whether EmER indeed functions as a direct sensor of host EGF [95]. Because of this, the signaling pathway triggered upon activation of EmER and its potential role as a receptor for host ligands were analyzed. Towards this end, I produced expression constructs for wildtype EmER and chimeras with both the amino and the carboxyl terminal part of human EGF receptor ErbB-3 (P21860) and ErbB-1 (EGFR; P00533). In human cell lines HEK293 and BA/F3 expressing the constructs, it should be possible to measure the EmER activity as phosphorylation of the downstream Erk MAPK or as tyrosine phosphorylation of the receptor itself upon EGF stimulation. In particular, the BA/F3 cell line should be suitable for these analyses due to the absence of endogenous EGF receptor. HEK293 expression of the constructs were first investigated in Western blot analysis using antibodies recognizing the fused myc and HA tag of expression vector pSecHygro A. Unfortunately, no expression of wildtypes EmER or the ErbB1 and ErbB3 chimera was observed.

However, constructs were employed in an activity assay using *Xenopus* oocytes for expression in cooperation with C. Dissous (Institute Pasteur, Lille). *Xenopus* oocytes have been established as a suitable model for investigating receptor tyrosine kinase activation and transduction cascades. They are physiologically arrested at the G2-M transition of the first meiotic prophase. This blockade can be abolished upon activation of receptor tyrosine kinase-dependent pathways. The activation of Ras triggers the MAPK cascade and leads to phosphorylation of the MAP kinase, which is necessary and sufficient to induce meiosis as indicated by oocyte germinal vesicle breakdown [142, 143]. Fourteen *Xenopus* oocytes each were transfected with translational expression constructs for full-length EmER as well as chimera of the N-terminal half of EmER and the C-terminal half of ErbB3 (including the transmembrane domain) and were subsequently stimulated with human EGF. Human EGFR and *S. mansoni* EGF receptor SER served as controls [142]. A vesicle breakdown was observed only in eight of fourteen oocytes (57%) expressing EmER (Tab. 3.5). An explanation for this result might be that the transduction machinery of the *Xenopus* oocytes does not fully interact with the *Echinococcus* receptor. A vesicle breakdown did not occur in the set ups with the chimera. This result was expected, since ErbB3 lacks a functional kinase domain [43]. Since ErbB3 homodimers are neither capable to activate the MAPK pathway nor to sense EGF and the heterodimers of ErbB3 and one of the other EGF receptor homologues (EGFR, ErbB2 or ErbB4) are only activated by neuregulins, constructs for ErbB3 expression represent suitable negative controls.

	EGFR	EmER	N-EmER/ C-ErbB3	SER
vesicle breakdowns	11/14	8/ 14	0/ 14	13/ 14

Tab. 3.5: EmER activity in *Xenopus* oocytes. Vesicle breakdowns were measured as indication for receptor activity after ectopic expression of EmER (full length) and chimera of N-terminal extracellular domain of EmER and C-terminal part of ErbB3 upon stimulation with human EGF.

4. Discussion

For metazoan organisms, cell-cell-communication is imperative to organize a broad range of developmental processes. Commonly involved are lipophilic or water-soluble hormones activating the signal receiver, i.e. intracellular or trans-membrane receptors, which activate intracellular signaling networks to convert the extracellular signals into an appropriate cellular response. This principle developed very early in the evolution of the animal kingdom and is therefore present in *E. multilocularis* and its hosts. Due to conservation of several families of growth factors and hormones as well as their cognate receptors, hormonal crosstalk between parasite and its host might represent a system through which parasite development is regulated depending on the status of the host. Despite the high degree of homology in invertebrate and vertebrate signaling systems, cestodes and mammals developed independently long enough so that several differences in their signalling cascades have accumulated. These differences could be exploited for the development of novel anthelmintic drugs.

In the present work, I investigated peptide growth factor signaling pathways which are likely involved in proliferation and differentiation processes of the parasite. This assumption is based on preliminary data showing that Erk1/2 like MAPK cascade regulates the growth of *E. multilocularis* but mostly on the findings that mutations in homologous mammalian pathways often lead to the formation of cancer [41, 98].

Hence, a wealth of data, particularly concerning the biochemistry of the factors involved and on small molecules to inhibit their activities is already available. Employing inhibitors of serine/ threonine and tyrosine kinases, I examined the role of respective kinases in the development of *Echinococcus*. In a second step, structural and functional differences between human and its echinococcal homologue were worked out.

Targeting EmMPK2- the p38 orthologue of *E. multilocularis*

Among the analysed *Echinococcus* factors, I suggest EmMPK2, the p38 orthologue, as the most promising target for AE treatment. Several lines of evidence clearly indicate that EmMPK2 is a functionally active member of the p38 MAPK subfamily. EmMPK2 displays clear homologies to p38 MAPKs from phylogenetically different organisms and contains a T-G-Y motif in the activation loop which is a the hallmark of this subclass of MAPKs. The exon-intron structure of the encoding gene, *emmpk2*, is highly similar to that of mammalian p38 MAPK genes and differs from genes encoding Erk- or JNK/SAPK-like proteins. EmMPK2 is capable of auto-phosphorylation at the dual-phosphorylation T-G-Y motif that is recognized by an antibody originally raised against human p38 MAPK. Recombinantly expressed, purified EmMPK2 phosphorylated MBP, a common substrate of MAPKs. The enzymatic activity of EmMPK2 could be blocked by pyridinyl imidazoles specifically designed to inhibit human p38 MAPKs. Genomic analyses further indicate that EmMPK2 is the only member of the p38 MAPK family in *E. multilocularis*. Due to the important role of p38 MAPKs in cellular signaling of animal cells, the constitutive expression of *emmpk2* is not surprising, at least in the larval stages that are involved in the infection of the intermediate host (including primary cells, which give rise to metacystode vesicles). Compared to metacystode vesicles and

activated protoscoleces, a somewhat lower level of phosphorylated EmMPK2 was detected in resting protoscoleces. As will be discussed below, one of the functions of EmMPK2 could be, like in the case of other p38 MAPKs, the induction of stress responses. The lower levels of phospho-EmMPK2 in resting protoscoleces might therefore be due to the fact that this stage is located within metacystode vesicles and thus relatively well protected from the host's immune response (having the metacystode's germinal and laminated layers as first lines of defense). On the molecular level, it remains to be established whether the lower phospho-EmMPK2 levels in resting protoscoleces are due to diminished translation of the protein, to differences in the activity of upstream regulators, or to lower auto-phosphorylation activity. However, based on the robust auto-phosphorylation activity of EmMPK2 after ectopic expression and the fact that an interaction with the only two upstream MAPK kinases could not be identified (see below), translational effects are most likely involved. As an alternative, corresponding dual-specific phosphatases, which are present in the parasite's genome, could have elevated activities in the resting protoscolex.

One of the most important findings of this study is that EmMPK2 displays a significantly higher basal activity (towards MBP and towards itself as a substrate) than p38 MAPK orthologues from humans. Although I have only tested the physiologically most important human isoform p38- α , no other isoform (β , γ , or δ) has been reported to display a basal activity higher than that of p38- α [61, 144]. The molecular basis of the high basal activity of EmMPK2 is unknown at present. Overall, the protein displays significant homologies to human p38 MAPKs but also contains many amino acid exchanges which could affect folding and thus basal activity, the interaction with upstream regulators and the responsiveness to extracellular signals. Interestingly, when screening the yeast p38 MAPK orthologue HOG1 for activating mutations, Bell et al. and Diskin et al. identified several hyperactive forms that carried exchanges within domains that are important in forming the interface for p38 MAPK dimerization [107, 109, 145]. When introduced into human p38 MAPKs, exchanges in three of these residues (D¹⁷⁶A, Y³²³S, Y³²³L, F³²⁷L, F³²⁷S in p38- α) also led to constitutively hyperactive forms [61]. In EmMPK2, the residues at corresponding positions are N¹⁷⁷ (instead of D), L³²⁴ (instead of Y) and L³²⁸ (instead of F) (Fig. 3.1). In EmMPK2, two of these three residues are similarly exchanged at positions 324 (L instead of Y) and 328 (L instead of F). Although EmMPK2 carries N at position 177 (instead of D) which differs from the corresponding exchange in hyperactive mutants (D176A), an involvement of this residue in EmMPK2 hyperactivity is nevertheless possible. Hence, it appears that mutations which have to be introduced into yeast and mammalian p38 MAPKs to yield constitutively hyperactive forms, are already present in the wild-type form of EmMPK2.

Questions concerning the cellular function of EmMPK2 and its participation in signaling pathways in *E. multilocularis* cannot be conclusively answered at present. At least on the basis of the inhibitor studies (see below), an important role of the kinase in parasite viability is apparent. When investigating the influence of different stress conditions (e.g. hydrogen peroxide, paraquat or DMSO as producers of reactive oxygen intermediates) on EmMPK2 activity, only a slight increase in phosphorylation upon physical disruption of metacystode vesicles was observed. This could indicate a role in osmotic stress regulation but surely requires further investigation. Likewise unclear is whether EmMPK2 is regulated in a similar fashion as p38 MAPKs in other organisms.

Up to now, three different ways of p38 MAPK activation have been reported of which two are unlikely to occur in *E. multilocularis*. These are the activation through phosphorylation at a non-canonical activating residue, Y³²³ in p38- α , which occurs in mammalian T cells upon activation of the T cell antigen receptor (TCR) and the TGF- β -dependent activation involving direct interaction between p38- α and TAB1 (Transforming growth factor- β -activated protein 1 (TAK1)-binding protein) [146]. Since EmMPK2 carries a leucine at the respective position (L³²⁴) and flanking residues which do not match the sequence stretch in the human counterpart, a regulatory mechanism through a TAB-1 homologue is virtually unlikely. Furthermore, genes coding for TAB-1 or TCR homologues are not present in the parasite's genome. The best studied pathway for p38 MAPK activation is dual phosphorylation at the T-G-Y motif by upstream MKKs [146]. For these interactions, however, the conserved aspartates of the common docking domain are highly important and at least one of these residues is replaced by Asn in EmMPK2 (Fig.3.1) [110]. A similar exchange in the *Drosophila* MAPK, Rolled, renders the insect enzyme constitutively active and severely weakens the interaction with regulators such as MKKs or phosphatases [145]. Since the two different members of the MKK family in *E. multilocularis* EmMKK1 and EmMKK2 did not interact with EmMPK2 in yeast two-hybrid and in activity assays, it is indeed possible that EmMPK2 is only under very limited control by upstream regulatory pathways. This is further supported by analyses in which effects of growth factors such as EGF, insulin, TGF- β or bone morphogenetic protein on the EmMPK2 phosphorylation state, when added exogenously to metacestode vesicles, were never observed although, under similar conditions, the Erk-like MAPK EmMPK1 is clearly activated, at least by EGF-treatment (discussed below).

Taken together, all structural and functional data suggest that the accumulation of activating mutations, particularly the leucine residues and the alteration of the common docking domain, rendered EmMPK2 a constitutively active MAPK. Hence, EmMPK2 may be regulated by alternative mechanisms, but its activation at least seems not to be under direct control by upstream MKKs.

Therefore, EmMPK2 phosphorylation at the conserved T-G-Y motif should solely depend on EmMPK2 auto-phosphorylation activity. This is supported by the data in which the treatment of metacestode vesicles or primary cells with p38 MAPK inhibitors led to complete dephosphorylation of EmMPK2. In this context, it still remains to be established whether EmMPK2 auto-activity leads to dual-phosphorylation of both T¹⁸¹ and Y¹⁸³, as has been reported for TCR-activated p38- α or only to the phosphorylation of T¹⁸¹, as observed for hyperactive L16-loop mutants of HOG-1 and human p38 MAPKs [109, 147]. In principle, the data support both scenarios since antibodies against the dual-phosphorylated pT-G-pY motif of p38 MAPKs very frequently also recognize mono-phosphorylated pT-G-Y and a similar situation cannot be excluded for my experiments with EmMPK2 [109]. For the model of EmMPK2 being a constitutively hyperactive p38 MAPK, on the other hand, this distinction seems not to be critical since it has already been firmly established that threonine-, but not tyrosine-phosphorylation within the T-G-Y motif is necessary for obtaining hyperactive forms of the enzyme [109].

The biochemical analyses showed that EmMPK2 can be effectively inhibited by the p38 MAPK inhibitors SB202190 and, in particular, by ML3403. Both substances are cell-permeable pyridinyl imidazole compounds that act on p38 MAPKs in an ATP-competitive

manner [112, 148]. While SB202190 belongs to the first generation of pyridinyl imidazole inhibitors, which exhibit severe liver toxicity through interference with hepatic cytochrome P450 enzymes, the toxic side effects have been minimized in second generation inhibitors such as ML3403 [148]. In studies on the widely used model compound SB203580, it has previously been shown that two residues in the ATP-binding pocket of target kinases, M¹⁰⁹ and K⁵³ of p38- α , are in direct contact with pyridinyl imidazoles and contribute decisively to inhibition [144, 149]. In EmMPK2, these two residues are invariably present (M¹¹⁰ and K⁵⁴). Furthermore, it is known that target specificity is mainly conferred through one single residue, T¹⁰⁶ in p38- α [144]. Mutation of this residue in p38- α renders the enzyme insensitive to pyridinyl imidazole inhibitors while introduction of the residue into Erk- or JNK/SAPK-like MAPKs leads to sensitivity towards this class of compounds [144, 150]. In EmMPK2, this residue is present at the corresponding position (T¹⁰⁷) which, together with the presence of M¹¹⁰ and K⁵⁴, explains the sensitivity of EmMPK2 towards pyridinyl imidazoles. In EmMPK1, on the other hand, T¹⁰⁷ is replaced by D¹⁰², which is in concordance with the presented data showing that the Erk-like MAPK of the parasite is not affected by p38 inhibitor treatment [98]. Apart from the three residues mentioned above, structural studies by Gum et al. revealed ten additional residues that are involved in p38- α inhibition through SB203580, the exchanges of which either lead to higher or lower affinity between enzyme and drug [149]. Four of these are different between EmMPK2 and human p38- α (Fig. 3.1). Different pyridinyl imidazole compounds display a wide variety of activities towards the four human p38 MAPK isoforms (SB203580 strongly inhibits isoforms p38- α and β , but not γ and δ), depending on amino acid residue exchanges in critical position. Considering that, it should be possible to obtain, by chemical modification of ML3403, compounds that display high activity against EmMPK2 while being only weakly active on human p38 MAPKs [144]. Based on the EmMPK2 activity assay established in this work, screening assays can be realized in which different pyridinyl imidazoles are tested for high affinity towards EmMPK2 while exerting diminished inhibitory activity towards human p38 isoforms.

Both p38 MAPK inhibitors tested in this study, but particularly ML3403, proved to be effective in inactivating *in vitro* cultured larvae, metacystode vesicles and evaginated protoscoleces. Due to difficulties in handling protoscoleces *in vitro*, the effect of ML3403 on this larval stage could not be readily quantified. Nevertheless, I could record toxic effects on these larvae in response to ML3403, which were clearly inactivated after two weeks. The metacystode representing the larval stage which is mainly to be addressed during AE treatment, was much more sensitive towards the inhibitors. Here, after 4 days of ML3403 treatment at concentrations of 0.5 to 5 μ M, which showed no effects on cultured mammalian cells that express p38- α , more than 50% of metacystode vesicles lost structural integrity and displayed no further capacity to regenerate novel vesicles. It was unexpected that much higher doses of the drug had to be given to see effects in the alkaline phosphatase (AP) assay since, in former studies using benzimidazoles or nitazoxanide as drugs, this method proved to be very sensitive [33, 113]. However, at least in mammalian cells it is well established that AP expression is controlled through the p38 MAPK pathway and a similar scenario cannot be ruled out in *E. multilocularis* [151, 152]. Consequently, ML3403 treatment and the inhibition of EmMPK2 could have led to decreased overall levels of the enzyme in metacystode

vesicles so that significant activities in the supernatant were only detectable after killing of many parasite cells in the presence of 1 mM of the drug.

As yet it is not clear whether the elevated sensitivity of *E. multilocularis* towards ML3403, when compared to cultured mammalian cells, is due to better binding of the drug to EmMPK2 than to mammalian p38 MAPKs. Once comparable activity assays are available, this topic has to be analysed. However, I would assume that the difference lays in the basal activity of EmMPK2 and mammalian p38 MAPKs, which renders the parasite more sensitive. While the mammalian isoforms are only activated under certain stress conditions or in response to specific cytokines, the parasite's cell physiology seems to be highly adapted to constitutive p38 MAPK activity, which could result in high sensitivity if parts of this activity are knocked down by specific drugs. If EmMPK2 is also constitutively activated during *in vivo* infections, which must be assumed, ML3403 could already be an effective drug for AE treatment. At least in *Toxoplasma gondii* infected mice, curative, long-term treatment with second generation p38 MAPK inhibitors did not show detrimental effects on host viability or immune responses [153]. Furthermore, orally administered doses of ML3403 that led to plasma concentrations of the drug in the range between 0.5 and 5 μ M were well tolerated by the animals [112]. In future studies it should therefore be worthwhile to investigate the effects of ML3403 on parasite larvae during infections of laboratory hosts.

It also appears interesting to extend the pyridinyl imidazole studies on other cestodes. This will not only reveal their potential lethal influence on these parasites, but also be useful to understand the general function of p38 MAPK orthologues in helminths other than *E. multilocularis*. It would be interesting to study the influence of ML3403 on *E. granulosus* larvae from which the target structure appears with subtle change, but the proliferation of the lesions during infection clearly differ (exogenous versus endogenous budding, see section 2). For these experiments, microcyts cultivated *in vitro* could be used to investigate if pyridinyl imidazole also inactivate *E. granulosus* larvae. In addition, the effects of ML3403 on recombinant EgMPK2 could be analysed and activity assays for EgMPK2 could be established as done for EmMPK2. The question why SB202190 and ML3403 did not affect the integrity of metacestode larvae of *T. crassiceps* remains unanswered yet. One reason might be structural differences in the p38 MAPK orthologues of *E. multilocularis* and *T. crassiceps* as indicated by different protein sizes and certain differences in the primary structure. It is unlikely, however, that morphological differences between the metacestodes of *E. multilocularis* and *T. crassiceps* are responsible for the different sensibility to pyridinyl imidazoles. Due to the absence of a laminated layer in *T. crassiceps*, drug accessibility should even be better than in the case of *E. multilocularis*.

Several structural and functional data of this work clearly show that EmMPK2 is specifically inhibited by pyridinyl imidazoles. It can, however, not be excluded that the second *Echinococcus* kinase with structural homologies to p38 MAPK, EmSSY, is also affected by this class of compounds. EmSSY shares 63% identity with EmMPK2 and was clearly identified as Ser/Thr kinase of the MAPK family based on the presence of ATP-binding domain, catalytic and activation loop and CD site (Fig.3.21). Contrary to all other known members of the MAPK family, however, EmSSY contained an S-S-Y motif in the activation loop instead of the typical T-X-Y. Expression analysis revealed that the encoding gene, directly located upstream of the *emmpk2* locus, is expressed in form of two transcripts in the

echinococcal larval stages resulting in two proteins of 486 and 356 AA (named EmSSY-a and EmSSY-b varying in the N-terminal region). Due to the presence of introns at positions which correspond to the introns of the *emmpk2* gene and the location upstream of *emmpk2*, *emssy* might have been created by gene duplication of the *emmpk2* locus. Since the expression of *emssy* was clearly demonstrated, it can be excluded that *emssy* represents a pseudogene. It would therefore be of general interest to analyze the function of EmSSY. If EmSSY-a and b are functional MAPKs, the question arises how they are regulated and which are their downstream targets. On the one hand, the EmSSY isoforms both contain a conserved common docking domain which mediates interaction with regulatory factors such as MKKs and phosphatases. It is not known, on the other hand, whether a S-S-Y motif (instead of T-G-Y) is recognized by MKKs and corresponding phosphatases. Hence, from the biochemical point of view, the EmSSY isoforms would be of considerable interest. Likewise interesting would be whether EmSSY is a constitutive hyperactive form like EmMPK2. Two of the corresponding residues turning the human MAPK into hyperactive mutants upon exchange are naturally present in EmSSY (L⁴³³, L⁴³⁷). Thus, EmSSY might be a constitutive p38-like MAPK. It remains uncertain, if EmSSY and EmMPK2 have similar functions or even overlapping functions. Nevertheless, the question arises whether the pyridinyl imidazole compounds could inhibit EmSSY. Concerning this, seven of the residues which contribute to pyridinyl imidazole binding in mammalian are invariably present in EmSSY [149]. These are even more corresponding residues as in the case of EmMPK2, which has been proven to be sensitive towards the p38 inhibitors. Thus, EmSSY might be sensitive towards the p38 inhibitors, too.

Targeting growth factor signaling pathways of *E. multilocularis*

In humans, key players in tumour formation are the Ser/Thr kinases of the Erk1/2 MAPK cascade, which is activated in response to growth factors like EGF [129]. Since the *E. multilocularis* metacestode expresses a member of the EGF receptor family, EmER, and since EGF is present in serum which is necessary to support parasite growth, the question arises whether exogenous EGF could stimulate the parasite's Erk-like MAPK cascade through EmER [95, 98]. In this work, several results were presented which support this hypothesis.

First, EGF stimulated the phosphorylation of the echinococcal ERM homologue EIp in intact metacestode vesicles *in vitro*. ERM proteins act as regulatory link between the actin cytoskeleton and the plasma membrane. While their C-terminal domain (C-ERMAD) directly binds to filamentous actin, the N-terminal domain (N-ERMAD) either directly or indirectly interacts with membrane-associated receptors. They are involved in several processes like microvilli formation, membrane trafficking and ruffling, cell-adhesion and cell-motility and occur in an inactive and active form [75]. In the inactive state, which is found in the cytosol, the intramolecular interaction of C- and N-ERMAD prevent the interaction with binding partners and thereby the translocation to the plasma membrane. One mechanism to regulate the interaction of ERM proteins is the conformational change upon PIP₂ binding to N-ERMAD and the subsequent phosphorylation of a crucial threonine residue within the C-ERMAD by Rho, Cdc42, and, presumably, also Rho kinases [154, 155]. Activated ERM proteins are

further capable to bind GEFs that in turn activate Rho. Taken together, ERM proteins are competent to indirectly activate Rho family members by interaction with positive and negative regulators [75].

Previous investigations by Hubert et al. (1999) already demonstrated that Elp fulfills similar cellular functions in *E. multilocularis* as the members of the ERM family in mammals. In the present study, it was clearly shown that Elp is phosphorylated at a conserved C-terminal Thr residue (Thr⁵⁴⁰, see supplements Fig. 6.1) upon incubation of metacestode vesicles with host EGF. This indicates that the parasite ERM factor might also be regulated in a similar way as the mammalian orthologs [75, 156]. Like in the case of mammalian ERMs, this might be mediated by parasite orthologs of Cdc42, Rho, and PKC, for which genetic information is present in the genome [125, 155, 157]. On the other hand, several modifications such as the EGF dependent phosphorylation of Tyr¹⁴⁵ and Tyr³⁵³ in ezrin, which is involved in the induction of morphological changes and cell survival, seem to be absent in Elp since the respective Tyr residues are not present.

Since the activation of Elp was clearly suppressed upon vesicle treatment with PP2 and the less stringent inhibitor leflunamide, tyrosine kinases, particularly of the Src kinase family seem to be involved in the activation mechanism. An Src-dependent phosphorylation of ezrin in response to EGF receptor activation has been already reported in human cells [158, 159]. However, this activation occurred at a tyrosine residue (Tyr¹⁴⁵) which is not conserved in Elp. Hence, it is rather likely that parasite Src kinases activate cellular mechanisms which result in Elp phosphorylation at the conserved C-terminal Thr residue. A possible candidate for this type of regulation would be PKC, which is expressed by the parasite. In mammals, PKC is known to be regulated through Src kinases [160]. Furthermore, PKC is known to phosphorylate ERM family members at the conserved Thr residue in the actin binding domain [157]. To clarify the situation, it would be worthwhile in future studies to also test the effects of PKC inhibitors on *Echinococcus* EGF signaling. The MAPK cascade of the parasite did not seem to be effected by PP2 and leflunamide as demonstrated by phospho-EmMPK1 staining. These findings are in line with data on the ERM activation upon EGF stimulation in human cells [161, 162].

Despite the fact that Elp phosphorylation was clearly suppressed upon treatment with PP2 and leflunamide, long-term incubation of metacestode vesicles in the presence of these compounds did not result in vesicle inactivation. However, Src kinases do not appear as promising target candidates to kill the parasite.

Second, it could be shown that DNA *de novo* synthesis is clearly increased upon stimulation of metacestode larvae with host EGF and TGF- α . Mitogenic effects of EGF and TGF- α have been frequently reported for normal and cancer cells [42, 163]. Since EGF and TGF- α are produced by a variety of host cells including hepatocytes, in particular during regeneration of liver tissue, it can be assumed that the metacestode is exposed to host EGF and TGF- α during an infection *in vivo* [44, 131-133, 163]. It is further conceivable that the infiltrative growth of the larvae into the surrounding host tissue triggers the host immune response inducing liver injury upon which the production of EGF is upregulated. The proliferative effects of EGF and TGF- α on metacestode cells were more apparent when the cysts were kept under starvation conditions. This might be explained through the presence of cytokines

in serum. In addition, EGF was a stronger inducer than TGF- α . The findings implicate that EmER might be a receptor with the higher affinity for EGF than for TGF- α . Similar effects have been reported for EGF signaling in hepatocytes [163]. Furthermore, it is noteworthy that, at least *in vitro*, lower EGF concentrations exerted a stronger effect on *Echinococcus* proliferation than higher cytokine concentration.

Like in the case of mammalian EGFR, this could be due to the presence of different high- and low-affinity binding sites for EGF in EmER [164]. In several human cell systems it has previously been demonstrated that proliferation and apoptosis are differentially regulated in a concentration and time-dependent manner through differential binding of EGF to different sites in EGFR [165]. Since only two concentrations and one time point were investigated for proliferative effects, it would be interesting to extend the experimental settings studying the impact on the proliferation capacity and the involvement of pro-apoptotic pathways. Further, the metacestode vesicle is built up of various cell types, which probably respond in distinct ways to EGF dependent stimulation.

The results of the proliferation studies conclusively indicate that intact metacestode vesicles respond with an increased proliferation rate to stimulation with host EGF and TGF- α . The DNA *de novo* synthesis in response to growth factors could be a downstream effect of, at least, three different pathways, the parasite equivalent of the Erk1/2 MAPK module, the PKB/Akt and the PI3K pathway. A role of the latter two cannot be excluded, but the Erk1/2 like MAPK pathway is definitively involved and is discussed in the following.

In this work, it could be shown that EmMPK1 is activated in response to host EGF. For the mammalian homologue, two mechanisms of activation are known. In one of these, RTKs transduce the extracellular signal to Erk1/2 via Ras, while the second occurs via G-protein coupled receptors, which activate Raf directly and independently of Ras. Albeit it could not be clearly shown that EmER represents the molecule sensing exogenous EGF, the data presented in this work strongly support that EmER triggers a signaling cascade which induces the phosphorylation and activation of EmMPK1. Prior to the present study, only EmRAF and EmMPK1 had been identified as putative components of the echinococcal MAPK cascade. The previously identified Ser/Thr kinase homologue EmMKK1 did not represent the MKK which links EmRaf to EmMPK1 [86, 98, 122]. Its homology to MKK3/6 family members rather indicates an involvement in JNK/SAPK-like MAPK signaling. With the identification and characterization of EmMKK2 in this work, the missing component of the Erk-like MAPK cascade could be found, which is supported by several structural and functional data. EmMKK2 possesses a Ser/Thr kinase domain between S¹⁵⁷ and V⁴⁵⁷ displaying clear homology to other members of the MKK family. In detail, the primary structure within the activation loop shares most of the amino acid residues with MKK1/2 homologues from different phylogenetic origins. Most critically, with S³¹⁵ and S³¹⁹, two Ser residues are conserved which are homologous to S²¹⁸ and S²²² in mammalian MEK1/2 and modified by the upstream activator Raf. Furthermore, EmMKK2 contains an extension (A³⁶² - A⁴⁰³) that corresponds to the proline-rich insertion (P²⁶⁵ - P³⁰²) of human MEK1 and MEK2. EmMKK2 contains a MAPK interaction motif and a 'HTSTSS' motif allowing the interaction with 14-3-3 proteins. On expression level, it could be shown that *emmkk2* is transcribed but in contrast to the situation in humans, most probably only as a single splice variant. The identification of transcripts of *emmkk2* and its potential upstream and downstream interaction

partner *emraf* and *emmpk1*, in metacestodes as well as non-activated and activated protoscolexes provided the first support that the encoded proteins could be part of a single MAPK module. Clear evidence for this was further provided by the *in vitro* interaction and activity assays.

Furthermore, EmMKK2 binds Em14-3-3 *in vitro*. 14-3-3 proteins are scaffolds for the Erk 1/2 MAPK pathway, but 14-3-3 proteins interact usually with the upstream signaling pathway on the level of Raf [58, 166]. The interaction of a MEK and a 14-3-3 protein has not been reported yet. The expression analysis indicates a decreased level of expression of *em14-3-3* during the developmental transition from metacestode to activated protoscolex confirming the result of Siles-Lucas et al. who reported the stage-specific expression of Em14-3-3 [121]. During the analyses of Spiliotis, neither an interaction of EmMKK1 with EmRaf nor of EmRaf with 14-3-3 could be detected although in both cases the structural requirements were met [86]. In addition, EmMKK1 lacks a 14-3-3 interaction motif. Quite interestingly, EmMKK2, which possess this motif, interacted with Em14-3-3 (this work). This unusual interaction needs to be further analyzed. Nevertheless, together with the failure to identify an interaction between EmRaf and Em14-3-3, this might indicate a different scaffolding mechanism in the parasite's signaling cascade.

As outlined in section 3.5.1, the ELM software tool predicted the heptapeptide 'RRSSIRF' in the C-terminal part of EmMKK2 as potential MAPK interaction motif (KIM) [120]. However, such a C-terminal location of the motif which mediates binding to MAPKs would be very unusual since KIMs have mostly been reported to be N-terminally located [58, 110, 167-169]. With regard to the amino-acid alignment of the MEK homologues, I like to suggest the $K^{45}RQVTIQNLD_{55}$ sequence close to the N-terminus as actual MAPK docking motif of EmMKK2.

Several functional studies concerning human MEK1 have shown that the replacement of S²¹⁸ and S²²² with phospho-mimetic residues (D²¹⁸, D²¹⁸D²²², E²¹⁸E²¹⁸) results in constitutively active mutants [170-172]. Interesting experiments would be to use constitutive active EmMKK2 mutants to analyse the growth behaviour of the *E. multilocularis* upon transfection of primary cells.

Members of the MEK1/2 family contain a unique, proline-rich insert C-terminal to the kinase domain which is important for the regulation of these kinases through Raf-independent mechanisms. This insert contains several conserved phosphorylation sites and the two threonine residues within the proline-rich insertion (Thr²⁸⁶, Thr²⁹² and Thr³⁸⁶) in human MEK1 that are targeted by MAPKs, CDC42 and proline-directed kinases. In most cases, phosphorylation at these sites is inhibitory and results in a dissociation of formed MEK-Raf-Ras complexes [173]. While this insert is clearly present in EmMKK2 (F⁴²⁷-A⁴⁸⁶), it is absent in EmMKK1, which further supports the notion that EmMKK2 acts within the Erk-like MAPK cascade of *E. multilocularis*. Interestingly, although the conserved threonine residues are also invariably present in EmMKK2, the insert region in the *Echinococcus* proteins contains very few proline residues. It is therefore likely that EmMKK2 is also regulated by *Echinococcus* kinases different from EmRaf, although the precise regulatory mechanisms require further biochemical analyses.

Another point in which human and parasite MKK1 homologues apparently do not correspond is the NES. By ELM and SMART analysis, a NES has not been identified in EmMKK2, which

is present in human MKK1 but not in human MKK2. The NES is necessary for the cytosolic localization of MKK1 that keep Erk1/2 in the cytosol until its activation and subsequent translocation into the nucleus [55]. Since one of the functions of human MKK1 is the regulation of the MAPK cascade, the regulation of the echinococcal MAPK cascade comprising EmRaf, EmMKK2 and EmMPK1 is one of the topics to be analyzed in the future.

The identified stimulatory effect of host EGF, acting via the conserved MAPK module, let to the analyses whether this cascade could be a promising target for the development of anti-*Echinococcus* drugs. As demonstrated, the activation of EmMPK1 could be blocked upon treatment of *in vitro* cultured cysts with BAY43-9006 and PD184352, two known anti-tumourgenic compounds, and M-INH. All three drugs were able to inhibit the EmMPK1 activation more or less to the same extent.

The bisarylurea compound, BAY439006, is a multi-kinase inhibitor and blocks the activity of Raf-1, B-Raf, and the vascular endothelial growth factor receptors in various cell lines and in animal models. In spite of its application in various studies, the blocking mechanism is still not understood. Nevertheless, the anti-cancer activity of BAY439006 has been attributed to both the inhibition of tumour cell proliferation and angiogenesis, particularly in cancer types which involve Ras/Raf mutants or overexpression of RTK leading to enhanced Erk1/2 MAPK module activation [135, 174]. Although the exact target in the parasite's signaling pathway has not been determined, the inhibitory effect of BAY439006 on the activity of EmMPK1 could clearly be demonstrated.

The MEK inhibitor compound M-INH also interferes with the human MAPK cascade. The assumption that M-INH targets EmMKK2 as the echinococcal homolog of MEK1 might explain the absent EmMPK1 phosphorylation upon the treatment of metacestodes *in vitro*. Further inhibitory effects on EmMPK1 phosphorylation could be demonstrated by applying PD184352. The non-ATP competitive PD184352 has been characterized as a highly selective inhibitor of human MEK1 in several studies and is the first MEK-targeted compound which entered clinical trials [175]. Using yeast genetic screens of randomized human MEK mutants, six residues have been identified the exchange of which resulted in a reduced sensitivity for PD184352. Only one MEK1 mutant (L115P) was fully insensitive. Four of the respective residues have been localized to a cluster in MEK1 limited between S⁹⁰ and D¹³⁶ while two residues (F⁵³, E²⁰³) were localized outside of this cluster. Together, these residues form a binding clamp for the MEK-inhibitor that is distinct from the ATP-binding pocket [176]. All six residues (F⁵³, I¹⁰³, L¹¹⁵, H¹¹⁹, G¹²⁸, E²⁰³) are invariantly present in EmMKK2 at the corresponding positions (F¹⁵⁰, I²⁰⁰, L²¹², H²¹⁶, G²²⁵, E³⁰⁰). In the region of the inhibitor binding clamp, EmMKK2 shares much more homology with human MEK1 than EmMKK1. Furthermore, none of above mentioned residues which are important for drug binding is conserved in EmMKK1. Thus, it can be assumed that PD184352 selectively inhibits EmMKK2, not EmMKK1. These findings support previous results that EmMKK2 is the upstream kinase of EmMPK1. Further, recent analysis revealed that MEK1, MEK2 and MEK5 (which displays homology to MEK1/2) can be affected by PD184352, but none of the other MEK family members, underlining the selectivity of this compound [175, 176]. Since the genomic screening of the *Echinococcus* database did not identify a third gene coding for a MKK homologue, it seems very likely that this compound solely inhibits EmMKK2.

It is noteworthy that none of the MAPK cascade inhibitors affected the structural integrity of vesicles during long-term treatment. Since the presence of the compounds resulted in the inhibition of EmMPK1 activity, one may conclude that the Erk1/2-like pathway of the parasite is not essential to preserve the vesicle integrity or parasite survival. However, the results reveal the involvement of EmMPK1 in the regulation of the parasite's growth after the stimulation with growth factors.

Data obtained in this work indicates that the *E. multilocularis* MAPK cascade might fulfill different roles in established metacestode vesicles when compared to regenerating primary cells. On the one hand, host-derived insulin, EGF and FGF had a clear effect on the vesicle regeneration process; insulin induced the formation of massive cell aggregates with larger central cavities while EGF and FGF led to the formation of a higher number of smaller aggregates. The addition of insulin, EGF and FGF to regenerating primary cells did, however, not lead to an increased phosphorylation of EmMPK1. This is in clear contrast to the effects of exogenous EGF, FGF and, to a somewhat lower extent, insulin on established metacestode vesicles in which EmMPK1 phosphorylation was induced [93, 94, 98]. Thus, the *E. multilocularis* MAPK cascade might only be functioning downstream of the respective RTKs in established metacestode vesicles while other pathways (e.g. the PIP3K/AKT) might be mediating the host-cytokine effects in primary cells.

A potential role of the PIP3K/ AKT pathway in primary cells is supported by the data of the miltefosine/ perifosine experiments. Miltefosine and perifosine target the respective pathway in human cells. In particular, they accumulate in cell membranes and interfere with lipid associated signal transduction pathways such as the PIP3K/AKT survival pathway and the SAPK/JNK pathway [116]. In this work, neither compound affected the viability of intact vesicles, but primary cells did not regenerate into vesicles in the presence of these drugs. The findings for miltefosine being ineffective to inactivate the metacestode confirmed previously published results [177]. Since it could be shown that the derivative perifosine is equally ineffective to inactivate the vesicles, both alkylphospholipid derivatives appear unsuitable for the development of a chemotherapeutic drug against established metacestode lesions. Both compounds, however, might be useful to interfere in the formation of metastases since the inhibitory effect on regenerating primary cell, i.e. germinal cells, could be demonstrated. Furthermore, miltefosine and perifosine could be used to investigate mechanisms of PIP3K/ AKT signaling in *E. multilocularis*. In mammalian cells, the PIP3K/ AKT pathway is responsible for an enhanced glucose uptake and survival signals upon insulin stimulation. An involvement of this pathway in the echinococcal primary cells may explain the enlarged and faster vesicle generation in the presence of insulin.

Taken together, the presented data strongly suggest that the Erk1/2-like MAPK pathway promotes metacestode growth, but not survival. In primary or germinal cells, the pathway promoting growth seems to be the PIP3K/AKT-like pathway. Regarding the infectious process, the data may indicate that insulin via activation the PIP3K/AKT-like pathway is important in the early phase of metacestode establishment while EGF-dependent induction of the Erk1/2-like MAPK pathway is involved in metacestode proliferation at a later time point of infection.

EmMPK3 – an atypical MAPK of *E. multilocularis*

Another difference in the signaling mechanisms of established vesicles and regenerating primary cells involves a third MAPK, named EmMPK3.

Several lines of evidence presented in this work indicate that EmMPK3 is the parasite's Erk7/8 homologue. First, EmMPK3 shares significant sequence homology with the atypical human MAPK Erk8. EmMPK3 contains a Ser/Thr kinase domain with a conserved T-E-Y motif as part of the activation loop. As in the case of atypical kinases Erk7 and Erk8, EmMPK3 possesses a C-terminal extension and at least five putative SH3 binding boxes (PxxP). Second, EmMPK3 did not interact with the parasite's MKKs *in vitro*. Third, upon ectopic expression and subsequent purification, EmMPK3 was auto-activated as indicated by the phosphorylation at the threonine and tyrosine of the T-E-Y triplet. Moreover, the recombinant protein phosphorylated MBP, a typical MAPK substrate directly implying enzymatic activity.

The identified features of EmMPK3, however, do not yet allow its classification as Erk7 or Erk8 MAPK homologue (see section 2.4.4) since EmMPK3 shares features of both. Rat Erk7 and human Erk8 MAPKs share approximately 69% overall identity (82% within the kinase domain) and both contain an extended C-terminal domain with two SH3 binding boxes. Erk7 possesses a putative NLS (PARKRGP) in its C-terminal tail and indeed localized to the nucleus upon overexpression [66, 178]. Contrary to Erk1/2, Erk7 is localized to the nucleus independently of its activation state [66]. An NLS could not be indeed identified for EmMPK3, but several stretches with similar amino acid residues are present in the C-terminal tail. One of those might serve as NLS for EmMPK3 and be responsible for a putative nucleolar localization of EmMPK3. Ectopically expressed Erk7 is constitutively active towards various substrates and phosphorylated on T-E-Y presumably due an auto-activation mechanism as has been revealed in studies using a dominant negative K43R mutant [66]. Furthermore, it has been reported that typical activators of Erk1/2, e.g. serum, EGF and okadaic acid, did not affect the Erk7 activity. This is in accordance with the role of Erk1/2 in cell proliferation and Erk7 as a negative regulator of cell growth. Due to the presence of tyrosine-phosphorylation sites in the C-terminal tail of Erk7, it has been assumed that Src kinases are involved in the regulation of its activity. Further studies have shown that Erk7 activity is mainly regulated in a MKK independent manner through modification of the C-terminal extension and that its conserved T-E-Y motif is exclusively subject to auto-phosphorylation [66, 68]. MKK-independent activation has been described for Erk8 [67]. Erk8, however, exerted a lower level of basal kinase activity than Erk7 and appeared to be sensitive to serum. Its activation has been shown to be associated with Src-kinase activity [67]. Considering the presented features of EmMPK3, it is apparent that the *Echinococcus* kinase displays biochemical properties of both Erk7 and Erk8. EmMPK3 shares with Erk7 the elevated basal activity. This should be further verified involving mutation studies with the replacement of K43 by arginine and truncated C-terminal versions of EmMPK3. Furthermore, EmMPK3 seems not to be controlled by upstream MKK since it did not interact with EmMKKs in yeast two hybrid analyses. In cell culture experiments, EmMPK3 was clearly phosphorylated in response to serum. This activation of EmMPK3 upon stimulation with serum occurred only in primary cells but not in metacystode vesicles. Like Erk7, EmMPK3 was

insensitive to EGF, FGFs and insulin but like Erk8 sensitive to serum. Hence, serum factor (or serum factors) other than EGF, FGFs or insulin must be responsible for the phosphorylation of EmMPK3. The responsible factor for Erk8 activation has not been reported yet. It would therefore be worthwhile to study EmMPK3 activation using serum fractions for the stimulation of primary cells.

In conclusion, the data presented clearly showed that EmMPK3 belongs to the 'atypical' (Erk7/8) MAPK family and that its phosphorylation is induced in *Echinococcus* primary (germinal) cells in a host-serum responsive manner. Due to the important role of host-factor induced germinal cell activation in the pathogenesis of alveolar echinococcosis, further studies on regulatory mechanisms which involve EmMPK3 are surely worthwhile.

5. Material and methods

5.1 Material

Equipment

Agitation Incubators G25	New Brunswick Scientific, Edison, NJ, USA
Blotting Tanks: Mini Trans-Blot cell (7.5 x 10 cm blotting area)	BioRad, Munich
Cooling Centrifuge RC-5B	Heraeus, Hanau
DNA – Gel Electrophoresis Chamber	BioRad, Munich
Gel-Documentation System MidiDOC	Herolab, Wiesloch
Heating Block, DB-3	Techne, Cambridge, UK
Incubators	Heraeus, Hanau
Overhead Agitation Wheel	Renner GmbH, Dannstadt
Power Supplies Power Pack P25 und P24	Biometra, Göttingen
Protein Separation Chambers: Mini-Protean	BioRad, Munich
Sequencing Apparatus, ABI Prism™ Sequencer 377	Perkin Elmer, Weiterstadt
Spectrophotometer NanoDrop™ 1000	Thermo Scientific, Wilmington, USA
Spectrophotometer GeneQuant Pro	Amersham, Braunschweig
Spectrophotometer U-2000	Hitachi, NY, USA
Thermocycler Trio-Thermoblock™	Biometra, Göttingen
Ultrasonication Apparatus: Sonifier® II Desintegrator Modell 250	Branson, Danburg
Ultra-Turrax T25	Janke&Kunkel/IKA Labortechnik

Consumables

0.5 – 2.0 ml reaction tubes	Sarstedt, Nümbrecht
15 ml sterile tubes and 50 ml centrifugation tubes	Greiner, Nürtingen
Blotting-Paper	Schleicher & Schüll, Dassel
Cell culture flasks from 25 to 175 cm ²	Sarstedt, Newton
Centrifuge Beaker, 15 and 50 ml, Quickseal™	Beckman, Munich
Positively charged nylon membrane porablot NY plus	Macherey & Nagel, Düren
Sterile Filters, 150 ml Bottle Top Filter, 0.45 µm	Nalgene, NY
Syringes and Needles, sterile	Braun Melsungen AG, Melsungen
X-Ray film Hyperfim™ -MP	Amersham, Braunschweig

Chemicals, commercially available kits and solutions

Agarose NEE0	Roth, Heidelberg
Agar-Agar, Bacto-Peptone, Yeast Extract, Glucose, Yeast	Difco Laboratories, Augsburg
Nitrogen Base w/o Amino Acids	
Amino Acids, Antibiotica	Sigma, Deisenhofen
BCA Protein Assay	Pierce
Benchmark™ Prestained Protein Ladder	Life Technologies
Broadrange Prestained Protein Marker	NEB, Schwalbach
DNase I, RNase free	Roche
dNTPs lyophilized	Roth, Heidelberg
ECL Chemiluminescence Kit	Amersham, Braunschweig
EGF, TGFα, aFGF, bFGF	ImmunoTools
H-Insulin	Sigma-Aldrich
Matchmaker Two Hybrid System 3	Clontech, Heidelberg

PBS Dulbecco without Ca ²⁺ /Mg ²⁺	
Pfu Turbo Polymerase	Stratagene
Phusion Proof Reading DNA polymerase	Finnzymes
Protease Inhibitor Complete	Roche
Protease Inhibitors	Applichem
Qiagen PCR Cloning Kit	Qiagen, Hilden
Qiagen Plasmid Midi Kit, QIAprep Spin Miniprep Kit, QIAquick PCR Purification Kit, QIAgen Gelextraction Kit	Qiagen, Hilden
Restriction Enzymes, DNA Modifying Enzymes and T4 DNA Ligase	NEB, Schwalbach
RNase Inhibitor	NEB, Schwalbach
TOPO-TA Cloning [®] KIT, Original TA Cloning Kit, pBAD/Thio expression Kit	Invitrogen, Groningen, Netherlands

All buffers and solutions were made with distilled water, autoclaved and sterile filtrated, respectively. For RNA applications, either DEPC-treated or commercially available RNase-free water was used. For enzymatic reactions, double distilled and autoclaved water was used.

5.2 Oligonucleotides

All oligonucleotides were ordered from Sigma-Aldrich/Sigma-Genosys in lyophilized form and were reconstituted with PCR grade water at a final concentration of 50 µM.

vector	oligonucleotide	
pJG4-5	JG4-5	5' CTTATGATGTGCCAGATTATG
	JG4-5 nest	5' CTCCCGAATTCGGCACGAG
	JG45-3'	5' TTGGAGACTTGACCAAACCT
	JG45-3'nest	5' CTGGCGAAGAAGTCC
pBAD/Thio-TOPO [®]	pBAD forward	5' GCTATGCCATAGCATTTCATCC
	pBAD reverse	5' GACTAAATTAGACATAGTCCG
	Trx forward	5' G TTCCTCGACGCTAACCTG
	pBAD up 60	5' CTGATTTAATCTGTATCAGGC
pCR [®] 2.1 [®] TOPO-TA	Topo M13	5' CAGGAAACAGCTATGACCAT
	Topo T7	5' TACGACTCACTATAGGGCGA
pGADT7	Y2H T7 seq	5' TAATACGACTCACTATAGGGC
	Y2H AD seq	5' AGATGGTGCACGATGCACAG
pGBTK7	Y2H T7 seq	5' TAATACGACTCACTATAGGGC
	Y2H BD seq	5' TTTTCGTTTTAAACCTAAGAGTC
	Y2H BD up	5' TAAGAGAGTCACACTTTAAATTTGTAT
pDrive	pDrive T7	5' TAATACGACTCACTATAGGG
	pDrive SP6	5' ATTTAGGTGACACTATAGAA
pGEX-3x	pGEX-3Xup	5' CGGGAGCTGCATGTGTTCAG
	pGEX-3Xdw	5' GGCAAGCCACGTTTGGTGG

PinPoint™-Xa3	xa-dw	5' TGGTCAAGGAGCGTGACG
	xa-up	5' GACATATTGTCGTTAGAACG
pSecHygroA	T7pSec	5' TAATACGACTCACTATAGGG
	BGH reverse	5' TAGAAGGCACAGTCCGAG
cDNA		
	CD3	5' ATCTCTTGAAAGGATCCTGCAGG
	CD3nest	5' CTCTTGAAAGGATCCTGCAGGACT
	CD3RT	5' ATCTCTTGAAAGGATCCTGCAGGTTTTTTTTTTT TTTTTTTTTTTTTTTTT T26,V= G+C+A
	NUP	5' AGGCAGTGGTAACAACGCAGAGT
	NUP mod	5' GAGGCAGTGGTAACAACGCAGAGT
	SMART I	5' AAGCAGTGGTAACAACGCAGAGTACGCGGGGG GGG
	SMART II	5' AAGCAGTGGTAACAACGCAGAGTACGC (GGG) _{RNA}
	UPM long	5' CTAATACGACTCATCATAGGGCAAGCAGTGGTA ACAACGCAGAGT
	UPM short	5' CTAATACGACTCATCATAGGG
gene		
<i>em10</i>	em10-15	5' AATAAGGTAATCAGTCGATC
	em10-16	5' TTGCTGGTAATCAGTCGATC
<i>em1433</i>	1433-dw	5' ATGGCAGCTATCACCTCTTGG
	1433-up	5' CTG TGA CTTGTCATTCTG
<i>emmkk1</i>	mutMEK dw2	5' CCATATAGCGACAGGTGCCCGTGTGTCCTG GGCCATCCTGTTCTTCAACTCTCCCGACACG
	mutMEK up2	5' CGTGC GGGAGAGTTGAAGAACGACATGGC CCAGAGCAACACGGGCACCTGTCGCTATATGG
	MKK-dw5	5' GTAATATCGAGTTCTGGCTGTG
	MKK-3up	5' GAGTCATCCATCAGTTC CATG
<i>emmkk2</i>	5' EmSor dw Xmal	5' GGATCCCGGGATGTCGGGTCTGACGGACAG
	3' EmSor up Xmal	5' GGATCCCGGGCTTTACGAGCAGTAGCAGCG
	5' EmSor dw	5' GCTGAAGACTGAAATGTGC
	3' EmSor up	5' GTCCATATTC AAATCGACATTAG
	SOR-2.M-Nde1	5' CATATGAGCACTGGACCTGTTGATCTC
	SOR-ohne-EcoR1	5' GAATTCGTATCTTGAGAGCCGCAAG
	SOR-67bp-Nde1	5' CATATGCTGGAGACCGGTGTGGAC
	Sor dw1	5' ATGGTGCTGAAGCACGCCGGTCTG
	Sor dw2	5' AATGCCCGAGCCAATTGTGTCCCG
	Sor up1	5' ATGCATATGTTGGATGTTCCCATCAG
	Sor up2	5' GAACGCCCCATAAAAGCCGACG
	Sor up3	5' GAAATTCCTCAATGCGCTCTCGCTGG
	Sor up4	5' AATTGCCTGAGCCAGCTCGGAG
	Sor-Not1-up	5' GCGGCCGCCTTTACGAGCAGTAGCAG
	Sor-Hind3-dw	5' AAGCTTATGTCGGGTCTGACGGAC
	5' SOR-dw-67-bp	5' CACCTGGAGACCGGTGTG
Sor-M-zwei	5' ATGAGCACTGGACCTGTTG	
Sor-ohne-up	5' GTATCTTGAGAGAGCCGCAAG	

	MEK-MAN2	5' CCCACRAANGARTTNGCCAT
	MEK-MAN1	5' CCYACRAARCTRRTTNGCCAT
	MEK-YGA	5' ATCGTCGGNTTYTAYGGNGC
<i>emmpk1</i>	erk dw2	5' GTTGAGTCGCGAGCACACCTG
	erk up2	5' GGGTCTGCAAATGGGAAGAG
	ERK dw6	5' GAACGTACCTGGAGCAGTTG
	ERK C3'spezifisch	5' GTAATTTTACACAATACAAGCAT
	ERK 3'	5' ACCTGCATCTATAGGCTCAG
<i>emmpk2</i>	Ro3	5' GGCGGTCAAGGGAAGGC
	Roc6	5' GCAAGAAGGATCTCAAGGATGCG
	MPK2-PWP1-dw	5' TTAATTAAGCCATGGCCGATGTAAATGAG
	MPK2-PWP1-up	5' TTAATTAATCACGCGTTGATTGGCG
	Roco3	5' CGGTCGGCCTCCATGGCCAAGCATCACGTT GAATTG
<i>emmpk3</i>	Emmpk3 dw expr	5' GATCATGAACTTGAAAAACATG
	Emmpk3 up expr	5' GGCAATCCACGGACGTG
	EmMPK3-ADBD- BamH1-dw	5' GGATCCATGTGTGTAGGAGTTTCG
	EmMPK3-ADBD- BamH1-CT-dw	5' GGATCCATCCAGAAAGTGAAATTGTGATGG
	MPK3-Pst1-N-up	5' CTGCAGCTCGAAATTGGGAAACGTAGTGG
	MPK3-Pst1-5-3-up	5' CTGCAGCGGCAATCCACGGACG
	MPK3-K43R-dw	5'-Phospho-GTAGCCTTCAAGAAGATTTTTGATGC (HPLC)
	MPK3-K43R-up	5'-Phospho-ATGCTTATTAAGCCGCTTGTACTTTG (HPLC)
<i>emegf</i>	EGF-5'RACE nest	5' GTCTCGGCTATGAAGAGCGCGGAG
<i>emer</i>	ERin-BamH1-dw	5' CGGGATCCAAGCACCGGATATGAAGGACG
	ERin-Pst1-up	5' TCCTGCAGAGGTAGTCTTCTGGCTGCAAC
	EmER-C-dw	5' AATTACAAGGCCAAACGCAG
	EGR-5'-kpn-pSec	5' GATCGGGGTACCCAGCTATCCCTTGCCCCAG
	EmER-N-up	5' GGCCTGATTTTCGAGCAG
	EGR-T-up1	5' CACGGCAAGACTACGAAG
	ERin-Nde1-dw	5' CATATGAATTACAAGGCCAAACGCAGT
	ERin-EcoR1-up	5' GAATTCGTAGTCTTCTGGCTGCAAC
<i>hsaerb-b1</i>	ErbB1-C-dw	5' ATCGCCACTGGGATGGTG
	ErbB1-N-up	5' CATGAAGAGGCCGATCCC
	ErbB1 5'	5' GCCAAGGCACGAGTAACAAG
	ErbB1 3'	5' GCTCCAATAAATTCAGTCTTTG
	ErbB1 5'-Kpn1	5' GTAGTAGGTACCGCACGAGTAACAAGCTCACG
	ErbB1-3' EcoR5	5' GGATATCTGCTTTGTGGCGCGACCCTTAG
	Chi N-Emer up	5' GCCCCACCATCCCAGTGGCGATGGAGGCC CTGATTCGAG
	ErbB1-TM-dw	5' GATGGTGGGGGCCCTCC
	ErbB1-TM-up	5' CATGAAGAGGCCGATCCCCAG
	Chi N-ErbB1-dw	5' CTGGGGATCGGCCTTTCATGAATTACAAGG CGCCAAACGCAGTCG
<i>emfr</i>	FRin-BamH1-dw	5' GGATCCGTCCCCAACGAATG
	FRin-Pst1-up	5' TCTGCAGCGAACTTTGACAGTGTAGCG
	GST-up5'	5' CAGATCCGATTTTGGAGGATG

	5'-GST-dw	5' ATGTCCCCTATACTAGGTTATTG
	3'-GST-FRoverh-up	5' GTGGAGGGTGTGGATGCAGATCCGATTTTG GAGG
	GST-SnaB1-dw	5' TACGTAATGTCCCCTATACTAGG
	3'FRexD-Avr2-up	5' CCTAGGATGGTGTGGTGTATGATG
	EmFRexD-up	5' GTAAGTGTGAGAGACTGTGTGTCATGG
	EmFRexD-dw	5' CATCAACACCCTCCACCCTTCAG
	FRexD-His-up	5' ATGGTGTATGGTGTATGATGGTACTTGAGAGAC ACTGTG
	EmFR-BamH1-Sec- dw	5' CGGATCCGCGCAGTGGGCGTCTTC
	EmFR-Not1-Sec-up	5' CGGGCCGCACCCCTGTAAGAACTTTGACAG
	FGR up1	5' TCGCGACGTAGGTTCTTCGTCA
	FGR up2	5' AATGTCCTTGGAGGCGAGGTAGACC
	FRin-Sfi1-dw	5' GGCCATGGAGGCCCGTCCCCAACGAATG
	FRin-Xma1-up	5' CCCGGGAGAACTTTGACAGTGTAGCG
	FR-BamH1-ohne-dw	5' GGATCCACATCAACACCCTCCACCC
<i>embmx</i>	bmx-dw1	5' GACAACGAAGTGATTGCTG
	bmx-up1	5' GTCGTAGAGCTCCTCAAAAG
	bmx-RACE-up2	5' TGGCGTATATCCTATCCTCGCACTGG
	bmx-RACE-up1	5' GAGTCCCAGCACGCCTGCATCTTG
<i>hsamapk14</i>	hsamapk14 dw - kpn1	5' ATTGGTACCAACAAGACAATCTGGGAGGTG
	hsamapk14 up -hind3	5' CAGTTCGAAAAGGGGTGGTGGCACAAAG
	hsamapk14 dw	5' TTCTACCGGCAGGAGCTG
	hsamapk14 up	5' GGAATCCATCTCTTCTTGG
<i>hsamapk11</i>	hsaMAPK11dw	5' GCTTTACCGGCAGGAG
	hsaMAPK11up	5' GCTCAATCTCCAGGCTG
<i>rnotegf</i>	rat-egf-dw1	5' GACGTTGATGAGTGCCAG
	rat-egf-up1	5' GTTCTCCAATATAGCCAATG
<i>rnofgf1</i>	rat-fgf1-dw1	5' GAGGTTCAATCTGCCTCTAG
	rat-fgf1-up1	5' GTCAGAAGATAACCGGGAG
<i>rnofgf2</i>	rat-fgf2-dw1	5' GCTTCCCGCACTGCC
	rat-fgf2-up1	5' GCTCTTAGCAGACATTGGAAG
<i>rnotgfalpha</i>	rat-tgf-alpha-dw1	5' GGCTGCAGTGGTGTCTC
	rat-tgf-alpha-up1	5' GGCAGTGATGGCCTGCT

5.3 Determination of nucleic acid concentration and purity

The nucleic acid concentration was photometrically determined at a wavelength of 260 nm using the spectrophotometer GeneQuant Pro or NanoDrop 1000. The purity of the nucleic acids was analysed on the basis of the ratios of 260 nm/ 280 nm (for protein impurity) and 260 nm /230 nm (for salt impurity). For molecular biology application, especially for DNA ligation, both ratios were 1.5-2.0. DNA concentration was further estimated by comparing the intensity of ethidium bromide staining between a DNA fragment of unknown concentration with DNA size marker fragments of known concentrations (SmartLadder, Eurogentec).

5.4 RNA procedures

5.4.1 Isolation of total RNA from mammalian cell lines

For isolating total RNA from the immortal cell lines RH- and HEK293, cells grown to confluency were washed with 10 ml prewarmed 1x PBS, detached from the bottom of the flask with 2 ml trypsin/ EDTA for 10 min at 37°C and then resuspended in 8 ml DMEM containing 10% FCS and 1% penicillin/ streptomycin (P/S). The number of viable cells was determined by Trypan blue staining using a Neubauer counting chamber. 1×10^6 cells were used to inoculate a fresh 75 cm² cell culture flask containing 20 ml DMEM including 10% FCS, 1% P/S. After culture for 2 days at 37°C and 5% CO₂, the cells reached approximately 80% of confluency. At this point of time, the cells were harvested (see section 5.9) and pelleted by centrifugation at 4°C (300 rcf, 5 min). The supernatant was discarded and the cells were lysed with 600 µl RLT buffer containing β-mercaptoethanol. All following steps were executed according to the manual of the RNeasy Kit (Qiagen).

5.4.2 Isolation of total RNA from *E. multilocularis* larvae

The metacystode vesicles cultivated under axenic conditions or cultivated in the presence of RH- (see section 5.10) were prepared for RNA isolation by washing three times with prewarmed 1x PBS. For each isolation, vesicles of an approximate total volume of 1 ml were disrupted by resuspending with a 1000 µl pipette and subsequently centrifuged. The pellet was either resuspended in RP1 lysis buffer supplemented with 1% β-mercaptoethanol of the Qiagen RNA isolation Kit or in P1 lysis buffer (Machery-Nagel NucleoSpin RNA/Protein isolation Kit). The subsequent steps were performed according to the manufacturer's recommendations. Total RNA of protoscoleces was gained from *in vivo* cultivated *E. multilocularis* isolates J31, 7030 or Java after sacrificing the Mongolian jird (*M. unguiculatus*) in accordance to the manufacturer's manual of the above mentioned kits. The starting material was approximately 10 µl protoscoleces per RNA isolation.

5.4.3 Decontamination of isolated RNA

To obtain genomic DNA free RNA, RNA preparations were treated with 0.2 U/ µl RNase-free DNase I (Roche) for 1 h at 37°C in the presence of 0.05 M sodium acetate and 0.05 M MgSO₄. Following digestion the RNA was purified in accordance to the purification protocol for RNA isolation of the RNA isolation kit from Qiagen.

5.4.4 First strand cDNA synthesis

The reverse transcription of total RNA into the first strand of cDNA was done using the oligo-dT-primer CD3RT and the Reverse Transcriptase from the Omniscript RT-PCR kit (Qiagen). The manual's instruction was modified as follows. To resolve possible RNA secondary structures and to allow better annealing of the oligonucleotide, up to 2 µg RNA (ad 12 µl with RNase free water) were incubated with CD3RT at a final concentration of 1 µM at 65°C for

10 minutes. After cooling to RT, all remaining components were added. The synthesis took place at 37°C for 90 minutes. The total reaction volume was 20 µl.

5.4.5 Synthesis of SMART cDNA

The synthesis of the SMART (switching mechanism at 5' end of RNA transcript) cDNA was performed with the components of the SMART™ RACE cDNA Amplification kit (Clontech) according to the manufacturer's instructions. This method exploits the property of MMLV-reverse transcriptase to add mostly three to five cytidines to the 3' end of the synthesized first strand. The ligation of the SMART primer (SMART I or/and SMART II) binding to these single stranded cytidines allows the amplification of unknown 5' ends via PCR approaches.

5.5 DNA procedures ---

5.5.1 Isolation of chromosomal DNA from the metacestode larval stage with purification

For the isolation of genomic echinococcal DNA, the metacestode vesicles were cultivated as described in section 10.5. After extensively washing with 1x PBS, the metacestode vesicles were disrupted by pipetting and subsequently pelleted. The supernatant was removed and the pellet was dissolved in lysis buffer (100 mM NaCl, 10 mM Tris-HCl, pH8.0, 50 mM EDTA, pH8.0, 0.5 % SDS, 20 µg/ml RNase A; 1.2 ml per 100 mg pellet) supplemented with 0.1 mg/ml Proteinase K. For total digestion of *Echinococcus* cells, the samples were incubated over night in a 50°C water bath and agitated as necessary. The DNA was extracted by phenol chloroform extraction and subsequently concentrated via ethanol precipitation as follows. One volume of phenol-chloroform-isoamyl-alcohol (25:24:1) was added to the sample solution. Following centrifugation for 25 minutes at 2000 rcf at RT, the upper aqueous phase containing the DNA was transferred into a new tube. After repeating the extraction step, the DNA was precipitated by addition of 0.1 volumes LiCl (stock 5 M; pH4.5) and 2 volumes 96% ethanol. The precipitation mix was incubated over night at -20°C. The following day, the DNA was completely precipitated at 20,000 rcf for 30 minutes at 4°C. The supernatant was removed and, after a washing step with 70% ethanol, the pellet was dried over 24 h at RT. The dried pellet was resuspended in 1x TE buffer (10 mM Tris, 1 mM EDTA pH 8.0).

5.5.2 BrdU-Staining

To analyse a potential proliferatory effect of human EGF and TGF- α , the incorporation of BrdU into *Echinococcus* DNA was detected as described previously [134]. In brief, metacestode vesicles were cultivated in the presence of 1mM BrdU under starvation conditions for 4 days as described in 5.10. Subsequently, the chromosomal DNA was isolated and purified by phenol-chloroform-extraction followed by EtOH precipitation as described in 5.5.1. The DNA content was determined by photometric analysis and the amount of DNA in a total volume of 20 µl was transferred onto a nitrocellulose membrane via

slot blotting. The slot blot chamber was connected with a vacuum pump and the nitrocellulose membrane tightly clamped. To increase the suction force, the membrane was underlaid by approximately 6 Whatman papers. The loading of the samples was carried out in the middle of the slot. After the transfer, the membrane was dried at RT and the DNA was cross linked with UV. To detect the incorporated BrdU, the membrane was blocked with 1% BSA TBST (see section 5.6.7) for 1 h on the seesaw. The incubation with the anti-BrdU antibody took place overnight at 4°C. After three washing steps with TBST, a HRP conjugated anti-mouse antibody was employed as secondary antibody. After 1 h at RT, the membrane was washed three times with TBST. The blot was developed by chemiluminescence and the incorporation of BrdU was detected by exposing the membrane to an X-ray film. Cross reactivity of the anti-BrdU antibody with uridine of the RNA can be excluded due the RNase in the lysis buffer.

5.5.3 DAPI staining of DNA blotted on nitrocellulose membrane

The DNA cross-linked to the nitrocellulose membrane was stained with DAPI nucleic acid stain as additionally control for the amount of transferred DNA. For this, the membrane was first incubated in 0.2 M Tris pH7.5 for 5 min at RT on the seesaw and then for 30 min 0.2 M Tris pH7.5 containing 0.1 M sodium sulfate and 2.5 µg/ ml DAPI. After a washing step with distilled water for 5 min, the membrane was repeatedly rinsed in 0.2 M Tris pH7.5 and than photographed under UV light. The membrane was enclosed in a box after the DAPI staining to avoid the degradation of the light sensitive dye.

5.5.4 Isolation of plasmid DNA from *E. coli*

The isolation of plasmid DNA from *E. coli* strains was performed with the QIAprep® Spin Miniprep kit and the Plasmid Midi kit (both Qiagen).

5.5.5 Gel electrophoresis of DNA

Depending on the size of DNA fragments, the agarose gel was prepared as 0.7% (for fragments larger than 4 kb), 1.0 % (fragments of 0.2 to 7 kb) or 2% (fragments smaller than 0.2 kb) gel. Corresponding amounts of agarose were dissolved by heating in 1x TAE buffer (40 mM Tris, 1 mM EDTA, pH8.0, 0.11% glacial acetic acid ad 1l dH₂O pH8.5). After the cooling down, the agarose TAE solution was poured into a horizontal gel sleigh where loading wells were left by fitting combs. To load the DNA, the samples were mixed with 6x agarose buffer containing 0.25% bromo phenol blue, 0.25% xylene cyanol, 40% saccharose and 30% glycerol. The separation was done at a voltage of 100 V for approximately 20-30 minutes. The separation was estimated by running of the two dyes included in the lading buffer. In a 1% agarose gel, the bromo phenol blue band and the xylene cyanol correspond to a 0.3 kb and 3 kb fragments, respectively. The DNA was visualized by exposing the ethidium bromide stained gel (2 mg/l ethidium bromide in 1xTAE) to UV light.

As marker for the DNA size, SmartLadder (Eurogentec) was utilized.

5.5.6 Purification of DNA

After gel electrophoresis, the bands of interest were excised and the DNA was extracted with the QIAquick[®] gel extraction kit. PCR amplicons or restriction digested DNA were purified using the QIAquick[®] PCR purification kit or the nucleotide removal kit (all Qiagen) according to the manufacturer's recommendations.

5.5.7 DNA precipitation

To precipitate DNA from a sample solution 0.1 volume of 3 M sodium acetate pH5.2 and 2.5 volume of 96% ice-cold ethanol were added and mixed well. After incubation for up to 24 h at -20°C, the DNA was pelleted by centrifugation (30 minutes, 15,000 rpm, 4°C) and the supernatant was removed. After washing with 70% ethanol, the pellet was dried in the speed vac or by air. Finally, the DNA was dissolved in H₂O or 1x TE buffer (10 mM Tris and 1mM EDTA pH8.0).

5.5.8 Sequencing

DNA was sequenced according to the dideoxy method developed by Sanger (1977) in an ABI Prism[™] Sequencer 377 (Perkin Elmer). DNA sample (400 ng of plasmid DNA or 100 ng PCR amplicon) was set up with 5 nM oligonucleotide and 2 µl sequencing mix to a final volume of 10 µl. The PCR programme was performed with 25 cycles of 96°C for 10 seconds, 45°C –60°C for 5 seconds and 72°C for 1 minute. Here, the annealing temperature for the specific primer was calculated with the equation $T_a [^{\circ}\text{C}] = 4x (\text{G+C}) + 2x (\text{A+T}) - 5$. Subsequently, the DNA was precipitated, heated to 90°C for 2 minutes, and separated on polyacrylamide.

5.5.9 Amplification of DNA via PCR

Custom-made oligonucleotides with a defined sequence have been designed were amplified via polymerase chain reaction (PCR) in the Trio-Thermoblock[™] (Biometra). The design of the oligonucleotides was usually carried out for annealing temperature of about 58°C calculated with the equation $T_a [^{\circ}\text{C}] = 4x (\text{G+C}) + 2x (\text{A+T})$. The Taq DNA polymerase (NEB) needs approximately 30 seconds and a temperature of 72°C for the synthesis of 500 nt. Consequently, the cycling conditions were generally as follows: with an initial denaturation for 60 seconds at 94°C, 30 cycles of a denaturation, primer annealing and a elongation step (30 seconds at 94°C, 30 seconds at T_a , 60 seconds/1000 nt at 72°C) and with a final elongation for 10 to 30 minutes at 72°C. The PCR mix comprised 1-5 µl template, 2 µl 10x buffer, 0.2 µl 10 mM dNTPs, 0.2 µl 50 µM oligonucleotide I, 0.2 µl 50 µM oligonucleotide II, 0.2 µl Taq DNA polymerase (2 U/µl) ad a final volume of 20 µl. Besides the non-proof-reading Taq DNA polymerase (NEB), the proofreading enzymes Pfu (Stratagen), Phusion (Finnzymes) and Triple Master (Eppendorf) was used in accordance to the manufacturer's manuals.

5.5.10 Rapid amplification of cDNA ends (RACE)

The rapid amplification of cDNA 5' and 3' ends was carried out by either SMART cDNA or an already present library cDNA (pJG4-5; [74]). A first PCR was carried out using a gene specific primer and a primer complementary to either the 5' end or the 3' end of cDNA. For the nested PCR, a pair of primers was chosen, which binds between the first pair of primers.

5.5.11 Semi-quantitative RT PCR

Total RNA was isolated from *in vitro* cultivated primary cells, metacystode vesicles as well as activated or non-activated protoscolecocytes as described above. cDNA was produced using the Omniscript RT-PCR kit (Qiagen; Hilden, Germany) and oligonucleotide CD3RT according to the manufacturer's instructions. Ten-fold serial dilutions of the cDNA were then used as template for PCRs using primers em10-15 and em10-16 for the constitutively transcribed gene *elp* [76, 81]. Additionally, the primers Roc6 and Ro3 were used for *emmpk2*, SOR-EEF and SOR-IHL for *emmkk2*, MKK-dw5 and MKK-up3 for *emmkk1*, 1433-dw and 1433-up *em14-3-3*. Cycling conditions were 25 cycles of 30 sec at 94°C, 30 sec at 58°C and 30 sec at 72°C. PCR products were simultaneously separated on a 1 % agarose gel and stained with ethidium bromide. The multiplex PCR experiment was performed under unchanged cycling conditions using the primer pairs Roc6 and Ro3 for *emmpk2* and em10-15 and em10-16 for *elp*. Control experiments missing one and two primers or template DNA were included.

5.5.12 TA cloning

PCR products amplified with Taq DNA Polymerase (NEB) or the Triple Master DNA polymerase (Eppendorf) possess an additional 3'A. This overhang is exploited for cloning into the pCR[®]2.1[®] TOPO-TA vector or Original TA cloning vector (both Invitrogen), which possess a complementary 5' T overhang according to the manufacturer's instructions. Both vectors allow blue-white screening to discriminate inserts from religated vectors. PCR products without the 3' A were incubated with Taq DNA polymerase and dATP for 1 h at 72°C to enable TA cloning.

5.5.13 Colony-PCR

The insertion of DNA into the MCS of the corresponding plasmids were analysed via colony PCR approach. The respective colony was picked from the agar plate and resuspended in 30 µl sterile water. 3 µl of the obtained bacteria suspension served as template in the PCR setups (see section 5.5.9). The first denaturation time of the cycle program was extended to ten minutes to disrupt the bacterial cells.

5.5.14 Restriction digest of DNA

All DNA restriction digests were carried out in 20 µl reactions with enzymes purchased from NEB according to the given specifications.

5.5.15 Ligation of DNA fragments

DNA fragments were ligated in 20 μ l reactions using T4 DNA ligase (NEB) by incubating overnight at 16°C. The ligation setup was mixed for a final volume of 20 μ l. For ligation reactions, plasmid and insert DNA were mixed at a ratio of 1:3 (with 100 ng of plasmid). To avoid re-ligation in cloning procedures, the cutted vectors were dephosphorylated at the 5' end by treatment with antarctic phosphatase or CIP (both NEB).

5.6 Protein procedures

5.6.1 Determination of protein concentration

The protein concentration was determined with the BCA Protein Assay Kit (Pierce). Based on the absorbance measured for the protein standards, the protein concentration of the samples was calculated. To this end, reagents A and B were mixed in a ratio of 50: 1 to yield the working solution. 50 μ l of each bovine serum albumin (BSA) standard (50, 100, 200, 400, 600, 800, 1000 und 1200 μ g/ml) and 50 μ l of the protein solution (in 1:5 and 1:10 dilutions) of unknown concentration were mixed with 1 ml working solution. After a 30 min incubation step at 37°C, 150 μ l of each sample were transferred into a 96well plate and the absorption at 540 nm was determined in the ELISA reader Multiscan Ex Primary EIA V.2.1-0 (Thermo).

5.6.2 *In vitro* activity assay with myelin basic protein as substrate

The enzyme activity of the recombinant MAP kinases Hsp38, EmMPK2 and EmMPK3 was determined measuring the transfer of radioactively labelled [γ -³²P]-P onto MBP (Sigma-Aldrich). Equal amounts of purified protein were incubated in kinase buffer (20 mM HEPES pH7.4, 10 mM MgCl₂, 2 mM EGTA, 1 mM DTT, 100 μ M ATP) supplemented with 0.5 mg/ml MBP, 1 μ M leupeptin, 1 μ g/ml aprotinin, 1 μ g/ml pepstatin A, 1 mM PMSF and 4 μ Ci [γ -³²P]-ATP. In some experiments, inhibitor or solvent were also added. After 60 min incubation at 37°C the reaction was stopped by adding 2x stop mix (see below) and boiling for 10 min. The samples were subsequently separated on 15% polyacryl-amid, blotted onto nitrocellulose membranes, and exposed for 48h to x-ray films.

5.6.3 *In vitro* activity assay for the MAPK cascade

Purified recombinant proteins (20 μ l EmMPK1, 10 μ l EmMKK2 and 5 μ l EmRAF/ EmRAS) were mixed and incubated with 60 μ l kinase buffer (20 mM HEPES pH7.4, 150 mM NaCl, 10 mM MgCl₂, 2 mM EGTA, 2 mM EDTA, 1 mM DTT, 1 mM PMSF, 1 mM Na₃VO₄, 500 μ M ATP) for 30 minutes at 30°C. Subsequently, the reaction was stopped by adding equal volumes of 2x stop mix and the samples were boiled for 5 minutes. After separation on 12% poly-acrylamid, the proteins were detected by Western blotting using the corresponding antibodies. Control reactions lacked either one of the proteins or ATP.

5.6.4 Co-immunoprecipitation

250 µl of the purified protein solutions were mixed with equal volumes of 1x TBST buffer (20 mM Tris HCl pH8, 150 mM NaCl, 1% Triton-X 100) containing 1 mM Na₃VO₄, 10 mM NaF, 1 mM PMSF and were incubated for 30 minutes at 4°C under overhead agitation with the anti-thioredoxin antibody at a final dilution of 1:500. Afterwards, 50 µl of slurry agarose G- beads equilibrated with 1x TBST were added. After 4 h, 250 µl of the second protein solution was added without changing the conditions. Protein complexes were allowed to form overnight and precipitated by centrifugation (1 min, 500 rpm). The supernatant with unbound proteins was removed. Unspecific and unbound protein was removed by washing three times with 1x TBST. Finally, equal volumes of 1x TBST and 2x stop mix (see below) containing β-MEtOH were added and the samples were boiled for 5 minutes. After a short spin, the supernatant was analysed by Western blotting.

5.6.5 SDS-PAGE

For the sodium dodecyl sulfate –polyacrylamide gel electrophoresis (SDS-PAGE) the separation chamber Mini-Protean (BIORAD) was used. The acrylamid polymerisation of the resolving gel was initiated by addition of 40 µl TEMED and 120 µl APS and required an incubation of approximately 30 min at RT. For the polymerisation of the stacking gel 40 µl TEMED and 70 µl APS were added. Combs with 10 and 15 wells were used. The described volumes are sufficient to synthesize six Mini gels (100 mm x 75 mm x 1 mm) of the BioRad system. Before loading, the samples were mixed with 2x stop mix and boiled for 5 min. The separation took place at 150 V (approx. 60 mA).

Working solutions

PAA	30% Acrylamid/ 0.8% bis-acrylamid (Roth)
4x Lower-Tris	1.5 M Tris-HCl, pH 8.8 0.4% SDS
4x Upper-Tris	0.5 M Tris-HCl, pH 6.8 0.4% SDS
TEMED	<i>N,N,N',N'</i> -tetramethylethan-1,2-diamin (Merck)
APS	16% ammonium persulfate dissolved in H ₂ O
Running buffer	192 mM glycine 25 mM Tris base 1% SDS
2x stop mix	2 ml 0.5 M Tris-HCl pH 6.8 1.6 ml glycerol 1.6 ml 20% SDS 1.4 ml dH ₂ O 0.4 ml 0.05% (w/v) bromophenol blue 7 µl β-mercaptoethanol/100 µl

Resolving Gel Composition:

5%	7.5%	10%	12%	15%	17.5%	Resolving gel
4 ml	6 ml	8 ml	10 ml	12 ml	14 ml	PAA
6 ml	6 ml	6 ml	6 ml	6 ml	6 ml	4x Lower Tris
14 ml	12 ml	10 ml	8 ml	6 ml	4 ml	dH ₂ O

Stacking Gel Composition:

1.5 ml PAA
2.5 ml 4x Upper-Tris
6.5 ml dH₂O

5.6.6 Coomassie staining of protein gels

The proteins of the PAA gels were stained for approximately 30 min with coomassie staining solution on the seesaw. Bands were visualized by destaining the unspecifically stained gel areas.

Coomassie staining solution	0.25% Coomassie R250 50% methanol 10% glacial acetic acid
Coomassie destaining solution	45% methanol 45% H ₂ O 10% glacial acetic acid

5.6.7 Western blotting

The transfer of the resolved proteins onto nitrocellulose membranes with the Mini Trans-Blot Cell (BIORAD) was carried out for 1 h at 350 mA. After the transfer, the nitrocellulose was blocked for 1 h at RT in blocking buffer (depending on the antibody) and was incubated with the corresponding antibody over night at 4°C on the seesaw. Upon three washing steps for 10 minutes, the membrane was incubated with the secondary antibody solution for 1 h at RT on the seesaw. The washing steps were repeated and the proteins were visualized by chemiluminescence (ECL, Pierce) and exposing to X-ray-films. The films were developed with a Curix 60 automated developer (Agfa).

Western blotting buffer	192 mM glycine 25 mM Tris base 20 % methanol
Blocking buffer	5 % skim milk (SM) or 5 % BSA dissolved in 1x TBST (20 mM Tris, 150 mM NaCl, pH7.5, 0.1% Tween20)
Washing buffer	1xTBS 0.1%Tween20 (TBST)

Primary Antibody	Dilution	Buffer	Firma	Source
anti-Erk1/2	1:1000	5% SM- TBST	Stressgen	rabbit
anti- Erk (pTpY 185/187)	1:1000	5% SM- TBST	Biosource	rabbit
anti-elp	1:1000	5% SM- TBST	mAb2810 [73]	mouse
anti-ERM	1:1000	5% BSA- TBST	Cell Signaling	rabbit
anti-phospho-ERM	1:1000	5% BSA- TBST	Cell Signaling	rabbit
anti-MEK 1/2	1:1000	5% BSA- TBST	Cell Signaling	rabbit
anti-phospho-MEK 1/2 (S221)	1:1000	5% BSA- TBST	Cell Signaling	rabbit
anti-active p38	1:1000	5% TopBlock- or BSA-TBST	Promega	rabbit
anti-phospho-CREB (Ser133)	1:1000	5% BSA- TBST	Cell Signaling	rabbit
anti-phospho-S6 (Ser235/236)	1:1000	5% BSA- TBST	Cell Signaling	rabbit
anti-phospho-tyrosine	1:2000	5% BSA- TBST	Cell Signaling	mouse
anti-GST	1:1000	5% SM- TBST	Santa Cruz Biotechnologies	mouse
anti-HA	1:1000	5% SM- TBST	Santa Cruz Biotechnologies	rabbit
anti-myc	1:1000	5% SM- TBST	Santa Cruz Biotechnologies	mouse
anti-V5	1:5000	5% SM- TBST	Invitrogen	mouse
anti-His	1:1000	5% SM- TBST	Cell signaling	mouse
anti-Biotin - HRP	1:5000	5% SM- TBST	Cell signaling	
anti-BrdU	1:1000	1% BSA- TBST	Sigma-Aldrich	mouse
anti-phospho-histon H3 (Ser10)	1:1000	5% BSA- TBST	Cell signaling	rabbit
anti-phospho-MAPKAPK-2 (Thr334)	1:1000	5% BSA- TBST	Cell signaling	rabbit
anti- MAPKAPK-2	1:1000	5% BSA- TBST	Cell signaling	rabbit
anti-EGF	1:1000	3% SM -PBS	upstate biotechnology	rabbit
Secondary Antibody				
anti- mouse IgG – HRP	1:10 ⁴	blocking buffer	Jackson, ImmunoResearch	
anti-rabbit IgG – HRP	1:5000	blocking buffer	Jackson, ImmunoResearch	

5.7 Working with bacteria

5.7.1 Bacteria strains and media

Bacteria Strains

<i>E. coli</i> DH5 α	Invitrogen	F ⁻ Φ 80dlacZ Δ M15 Δ (lacIZY-argF) U169 <i>recA1 endA1 hsdR17</i> (r _k ⁻ ,m _k ⁻) <i>phoA supE44 thi-1λ gyrA96 relA1 tonA</i>
<i>E. coli</i> TOP10	Invitrogen	F ⁻ <i>mcrA</i> Δ (<i>mrr-hsdRMS-mcrBC</i>) Φ 80lacZ Δ M15 Δ lacX74 <i>recA1 araD139</i> Δ (<i>ara-leu</i>)7697 <i>galU galK rpsL</i> (Str ^R) <i>endA1 nupG</i>
<i>E. coli</i> BL21	Amersham	B F ⁻ , <i>ompT</i> , <i>hsdS</i> (r _B ⁻ ,m _B ⁻), <i>gal</i> , <i>dcm</i>

Media

Luria-Broth (LB)	Invitrogen	
LB agar plates		LB medium with 1.5% Bacto-Agar
SOC	Invitrogen	

All bacteria were incubated at 37°C either in LB- liquid medium or on LB-agar plates supplemented with antibiotics depending on the transformed plasmid. Usually, 100 µg/ ml ampicillin or 50 µg/ ml kanamycin were used.

5.7.2 Chemically competent *E. coli*

Competent bacteria were prepared using the CaCl₂ method as follows. 50 ml LB-medium was inoculated with 1 ml O/N culture of the *E. coli* strain and incubated at 37°C and 225 rpm until an OD₆₀₀ of 0.5 -0.7 was reached (approximately 2-3 h). Subsequently, the culture was separated into 2 aliquots, pelleted at 4000 rpm and 4°C for 10 min. The supernatant was decanted and the pellet directly placed on ice. Each pellet was carefully resuspended in 12 ml ice cold 100 mM CaCl₂ and the centrifugation step was immediately repeated. The resulting pellet was dissolved 1 ml fresh CaCl₂ by gently resuspending and subsequently incubated for 30 up to 60 min on ice. Before freezing the bacteria suspension at -80°C in 50 µl aliquots, glycerol was added to a final concentration of 20%.

5.7.3 *E. coli* transformation

For each transformation, 50 µl competent cells were incubated with plasmid for 30 min on ice followed by a heat shock step (1 min, 42°C). After addition of 300 µl LB-liquid medium, the bacteria were incubated for 1 h at 37°C and 225 rpm. Finally, the bacteria were plated on LB-agar plates supplemented with the corresponding antibiotics (100 µg/ ml ampicillin or 50 µg/ ml kanamycin) and incubated at 37°C over night.

5.7.4 Heterologous expression in *E. coli* and purification of the recombinant proteins

pBAD/Thio-TOPO[®] vector and pBAD/TOPO[®] vector systems

In this work, recombinant Hsap38 MAPK-α, EmMPK2, EmMPK3, EmMKK2 and EmFR were expressed in DH5α using the pBAD/Thio-TOPO[®] vector and pBAD/TOPO[®] vector, respectively (Invitrogen). Both vectors allow the expression of fusion proteins under the control of the inducible *araBAD* promoter (pBAD) with an N-terminal thioredoxin tag which can be cleaved off at the enterokinase site (pBAD/Thio only). A second tag, the V5 epitope, is fused to the C-terminus followed by a 6xHis tag. The former can be used to easily detect the fusion protein with the anti – V5 antibody and the latter to purify the fusion protein under native and denaturing conditions by affinity chromatography. The tags contribute approximately 16 kDa (6 kDa in the case of pBAD/TOPO[®] expression) to the overall size of the fusion protein. For the selection and propagation in *E. coli* an ampicillin resistance and pUC origin of replication are encoded on the plasmid. The transcriptional regulator of the pBAD, AraC, is also encoded on the plasmid.

The corresponding PCR products were cloned into the cloning sites of the pBAD/Thio-TOPO[®] vector and pBAD/TOPO[®] vector via TA cloning according to the manufacturer's instructions (Invitrogen). Positive clones validated by sequencing were used for the over night culture. LB-medium containing 100 µg/ml ampicillin was inoculated 1:200 with the

corresponding starter culture. When the bacteria reached an OD₆₀₀ of 0.5, the protein expression was induced by supplementation of 0.2% L-arabinose into the medium. After incubation for 4 h at 37°C and 225 rpm, the cells were pelleted by centrifugation at 6000 rcf and 20 min at 4°C. The supernatant was discarded and the pellet resuspended in lysis buffer (depending on the purification method). Finally, 5 mg/ ml lysozyme was added and the suspension frozen at -20°C over night.

The recombinant proteins were purified under native and denatured conditions. For the latter purification method, the lysisbuffer contained 500 mM NaCl, 20 mM Na-phosphat-buffer and 6 M guanidine-HCl. Cell debris was removed by centrifugation at 6000 rcf at 4°C for 20 min. The supernatant was transferred to 4 ml slurry Ni beads (ProBond Resin, Invitrogen), which had been equilibrated with lysis buffer. After slow rotation at 4°C over night, the beads were washed three times with 300 ml denaturing wash buffer (500 mM NaCl, 20 mM Na-phosphat-buffer, 8 M Urea, pH5.8). The protein was eluted initially with 6 ml elution buffer (500 mM NaCl, 20 mM Na-phosphat-buffer, 8 M Urea, pH3.8) and subsequently, with 6 ml imidazol elution buffer (300 mM NaCl, 50mM Na-phosphat-buffer, 250 mM imidazol, pH8.0).

For the native purification the procedure was done analogously with the following buffers containing increasing concentrations of imidazol: lysis buffer (300mM NaCl, 50 mM Na-phosphat-buffer pH8.0, 10 mM imidazol), washing buffer (300mM NaCl, 50 mM Na-phosphat-buffer pH8.0, 20 mM imidazol), elution buffer I (300mM NaCl, 50 mM Na-phosphat-buffer pH8.0, 250 mM imidazol), elution buffer II (300mM NaCl, 50 mM Na-phosphat-buffer pH8.0, 500 mM imidazol). The isolated fractions were analysed by Coomassie staining as well as Western blot analysis. The protein containing fractions were pooled and dialysed overnight against 2 l 1x PBS at 4°C.

Recombinant protein	Vector	Purification	Primers used for ORF amplification
EmMPK2	pBAD	native and denatured	p38-5EC / p38-3EC
EmMPK3	pBAD	native	Emmpk3 dw expr/ Emmpk3 up expr
Hsap38 MAPK-α	pBAD	native	hsMAPK14 dw/ hsMAPK14 up
EmMKK2	pBAD and pBad/Thio	native	Sor-67-dw/ Sor-ohne-up
EmFRex	pBAD and pBad/Thio		FRex-dw/ FRex-up
EmNIP	pBAD/Thio	native	TRI-dw/ TRI- up

pGEX-3X Vector System

The pGEX-3X system (Amersham) was used to express recombinant proteins of EmMKK1, EmFRex and EmSkip. The protein expression is under control of the IPTG (isopropyl-β-D-thiogalactopyranoside) inducible tac promoter and leads to proteins with a N-terminally fused glutathione-s-transferase (GST) of *S. japonicum*. The GST- tag increases the size of proteins by 26 kDa and allows the purification on immobilized glutathione.

For the recombinant expression, the LB-medium (100 µg/ ml ampicillin) was inoculated 1:50 with *E. coli* BL21 over night culture and the suspension was shaken at 225 rpm and 37°C until OD₆₀₀ of 0.5. Protein expression was induced by the addition of 1 mM IPTG. After 2 h of further incubation, the culture was pelleted by 6000 rcf and 4°C for 20 min. The supernatant was decanted and the pellet was resuspended in a total volume of 10 ml cold 1x TBS. To brake the bacterial cell walls 5 mg lysozyme were added and the pellets were frozen by

-20°C for 4 h to over night. This step was followed by sonification of the bacterial suspension for at least 5 times for 30 s (continuous output of 4-5, duty-cycle of 40-50%) until the suspension was slightly viscous. After addition of RNase, DNase (each 5 mg/ml) and the protease inhibitors 1 µM pepstatin A, 10 µg/ml aprotinin A, 1 µg/ml leupeptin, 1 mM PMSF, Triton-X-100 was added to a final concentration of 1%. The suspension was incubated for 1 h at 4°C on an overhead agitation wheel and the cell debris was subsequently pelleted by centrifugation at 13000 rpm at 4°C for 30 min. The supernatant was transferred to a fresh 15 ml reaction tube and glutathione sepharose beads that had been previously equilibrated with 1x PBS 1% Triton X-100 were added. After 4 h at 4°C on an overhead agitation wheel, the beads were washed three times with 1x TBS supplemented with 1% Triton – X-100 to remove unbound protein. Bound protein was collected in six fractions by adding three times elution buffer I (25 mM glutathione in 1x TBS) and three times elution buffer II (50 mM glutathione in 1x TBS). Protein containing fractions were pooled, dialyzed overnight against 1x PBS at 4°C and supplemented with the above listed phosphatase and protease inhibitors.

Pinpoint-Xa-3 system

The pinpoint expression vector Xa-3 was used to express and purify the recombinant EmFRex (extracellular domain of EmFR) according to the manufacturer's manual.

5.8 Working with yeast

5.8.1 Yeast strains and media

Yeast strains

AH109	BD Biosciences Clontech	<i>MATa, trp1-901, leu2-3, 112, ura3-52, his3-200, gal4Δ, gal80Δ, LYS2::GAL1_{UAS}-GAL1_{TATA}-HIS3, GAL2_{UAS}-GAL2_{TATA}-ADE2, URA3::MEL1_{UAS}, MEL1_{TATA}-lacZ</i>
Y187	BD Biosciences Clontech	<i>MATa, ura3-52, his3-200, ade2-101, trp1-901, leu2-3, 112, gal4Δ, met⁻, gal80Δ, URA3::GAL1_{UAS}-GAL1_{TATA}-lacZ, MEL1</i>

Media

YPDA	20 g/l Difco Peptone 10 g/l yeast extract 20 g/l Bacto agar (for plates) distilled H ₂ O ad 950 ml	pH 6.5 adjusted by adding 25% HCl; after autoclaving 50 ml of 40% glucose and 3 ml of 1% adenine-hemisulfate solution were added. Both solution were filter sterilized.
SD	6,7 g Difco™ Yeast Nitrogen Base w/o Amino Acids 20 g Difco™ Bacto Agar X g of the corresponding drop out supplement (DOS) (Clontech) lacking the selective amino acid distilled H ₂ O ad 930 ml or 950 ml	pH 6.5 adjusted by adding 25% HCl; after autoclaving 50 ml of 40% glucose

SD - Trp	+ 0.64 g/l Leu/- Trp DOS + 20 ml 50x Leu (5 mg/ 1ml)
SD - Leu	+ 0.64 g/l Leu/- Trp DOS + 20 ml 50x Trp (1mg/ 1ml)
SD - Leu/- Trp	+ 0.64 g/l Leu/- Trp DOS
SD - Leu/- Trp/ -His	+ 0.6 g/l Ade/- His/- Leu/-Trp DOS + 20 mg/l histidine HCl mono- hydrate (Sigma)
SD - Leu/- Trp/ -His/-Ade	+ 0.6 g/l Ade/ - His/ - Leu/ - Trp DOS

5.8.2 Yeast two hybrid analysis

For analysis of protein-protein interactions, the Gal4-based MATCHMAKER system (Clontech) was used. For the expression of proteins of interest fused to the C-terminal end of either the DNA-binding domain or the activation domain of the Gal4 transcription factor, the corresponding reading frames were cloned into pGBKT7 and pGADT7, respectively, and co-transfected into *S. cerevisiae* strain AH109. The construction of EmRAF, Em1433, EmMKK1 and EmMPK1 translational fusions was described by Spiliotis [86]. The EmMPK2 constructs were produced as published by Gelmedin et al. [179]. The ORF for EmMKK2 constructs was amplified from cDNA with the primers SOR-67-Nde1-dw and SOR-ohne-EcoRI and was cloned via the restriction sites NdeI and EcoRI into the yeast vectors. Using the oligonucleotids EmMPK3-ADBD-BamH1-dw and MPK3-Pst1-5-3-up, the complete ORF of EmMPK3 was amplified and cloned via BamHI and PstI into the expression vectors (used in this work). For the cloning of EmMPK3's N-terminus and C-terminus, the primer pairs EmMPK3-ADBD-BamH1-dw and MPK3-Pst1-N-up and EmMPK3-ADBD-BamH1-CT-dw and MPK3-Pst1-5-3-up were employed, respectively.

For the transfection, YPDA was inoculated with AH109 and incubated overnight at 30°C and 200 rpm. For each transformation, 1 ml overnight culture was pelleted and the supernatant discarded. The pellet was washed with 1xPBS and subsequently resuspended in 100 µl of freshly prepared transfection buffer (40% PEG 3350, 200 mM lithium acetate, 100 mM DTT) and mixed with 200 ng DNA of each plasmid. The yeast-suspension was plated on selection plates after incubation at 45°C for 30 minutes. Yeast clones were selected for double transfection on leucin-tryptophan-deficient SD medium for 4 d at 30°C. Protein expression of each clone was confirmed by Western blot analysis. For protein-protein interaction under high stringency conditions, yeasts were selected on leucin-tryptophan-histidin-adenin-deficient (quad) SD plates. Individual yeast colonies were picked and plated repeatedly on quad SD plates for 48 h at 30°C to avoid false positive clones.

5.9 Working with mammalian cell lines

5.9.1 Cell lines and media

Cell lines		ATCC no.	Media
Rat Reuber hepatoma cells	RH-	CRL-1600	Dulbecco's minimal essential medium (DMEM; GIBCO BRL)
Human embryonic kidney cells	HEK293	CRL-1573	DMEM; GIBCO BRL
Human brain-derived endothelial cells	HBMEC		described in [180]

5.9.2 Quantitative live-dead staining of mammalian cell lines

The cell lines RH-, HEK293 and HBMEC were seeded into 24 well plates with 1×10^4 cells per well and incubated in DMEM supplemented with 10% FCS 1% penicillin/ streptomycin under 5% CO₂ atmosphere in presence of DMSO or inhibitor, respectively. After 4 d crystal violet staining was performed according to the established protocol [114]. To this end, the medium was aspirated by a vacuum pump and the cells were washed with 1x PBS. Cells were fixed with 1% glutaraldehyde for 15 min on a seesaw. After three washing steps, the cells were dried at RT and stained with 0.1% crystal violet solution. The staining process was stopped after 30 min and the non-absorbed crystal violet was removed. The cells were washed under microscopical observation. Cells were destained by addition of acetic acid for 5 min. The absorbance measurement at 570 nm of 100 μ l supernatant was measured on a 96 well plate.

5.9.3 Transfection of HEK293 cells

HEK293 cells were transfected with constructs of the vector pSecHygro A encoding EmFR and EmER (see section 3.10). The day prior to the transfection, the medium was removed and the cells were detached by adding 2 ml trypsin/ETDA solution for 5 min at 37°C. The suspension was then mixed with 8 ml DMEM 10% FCS 1% P/S. The number of viable cells was determined by trypan blue staining and counting in a Neubauer chamber. 1×10^6 cells were seeded per well of a 6-well plate containing 3 ml DMEM 10% FCS 1% P/S and incubated overnight at 37°C and 5% CO₂. The next day, the medium was replaced by 4 ml fresh medium and the transfection solution was added drop wise. The transfection solution consisted of 7.5 μ g of plasmid DNA mixed with 62 μ l 2 M CaCl₂ and brought to a final volume of 500 μ l with double distilled water. After mixing, 500 μ l 2x HBS buffer (50 mM HEPES, 1.5 mM Na₂HPO₄, 280 mM NaCl, 10 mM KCl, 12 mM α -D-glucose pH7.1) were added. Then, the suspension was inverted for 2-4 times and incubated for 30 min at RT prior to the addition to the seeded cells. After 7 h, the medium was carefully replaced with fresh medium and the incubation was continued for another 48 h. For the analysis of protein expression by Western blotting, the medium was removed and the cells were lysed in 200 μ l 1xTBS lysis buffer (20 mM Tris, 150 mM NaCl, 1 mM Na₃VO₄, 1 mM EDTA, 10 mM NaF, 1 mM PMSF, 1 μ g/ml aprotinin A, 1 μ g/ml pepstatin hemisulfate, 1 μ M leupeptin, 1% Triton-X 100) under over head agitation for 1 h at 4°C. Cell debris was collected by centrifugation at 15,000 rpm for 15 min.

20 µl of the supernatant were mixed with 2x stop mix. The remaining supernatant was frozen at -20°C for further analysis.

5.10 Working with *E. multilocularis*

5.10.1 *E. multilocularis* isolates

Isolate	Source	Use
H95	primary infection of <i>M. unguiculatus</i> by oncosphere uptake	metacestode cultivation <i>in vitro</i>
Java, 7030, J31	Java monkey as intermediate host, secondary infection of <i>M. unguiculatus</i>	protoscoleces isolation

5.10.2 *In vivo* cultivation of metacestode larvae

The long-term maintainance of *E. multilocularis* metacestodes requires repeated passages in laboratory animals. To this end, Mongolian jirds (*Meriones unguiculatus*) were infected with homogenized larval material by intraperitoneal injection to develop a secondary alveolar echinococcosis. Approximately two month p.i., the larval material was isolated under sterile conditions upon sacrificing the animal with CO₂. The sterility was preserved by working in a sterile bench, repeated substitution of the used sterile instruments and by avoiding the injury of the digestive tract of the animals. Additionally, it was avoided to contaminate the parasite material with fur hair. The isolated parasite tissue was cut into small pieces (1-2 mm slices) and subsequently strained through a metallic tea sieve. The ground material was then washed at least three times with sterile 1x PBS to remove host cells. After this step, the parasite material was treated in different ways depending of the subsequent experiments. For the isolation of protoscoleces, see section 5.10.3. For other applications, the suspension was subsequently incubated in the presence of 10 µl/ml Ciprobay 400 (ciprofloxacin) and/or 100 U/ml penicillin G/ streptomycin for 16 h at 4°C to eliminate any contaminating bacteria. After removal of the antibiotics by repeated washing steps with 1x PBS, 0.3-0.5 ml of the decontaminated suspension were used for injection into a new jird (0.9 µl canula). The decontaminated material was also used to start the cultivation of metacestode larvae *in vitro*.

5.10.3 Isolation and activation of protoscoleces

For the isolation of protoscoleces, the freshly isolated and ground parasitic material (5.10.2) was diluted with 1x PBS to obtain a 1:4 suspension und vigorously shaken for approximately 10 min to release the protoscoleces from the metacestode material. Afterwards, the suspension was firstly sieved through a polyester gauze (pore size 150 µm). Then, the flow through was decanted onto a second polyester gauze (pore size 30 µm). On the top of the gauze, the retained material contained the protoscoleces, which were collected by resuspension in 1x PBS and transfer into a Petri dish (diameter 10 cm). By horizontal rotation of the Petri dish on the working bench, the protoscoleces gathered in the middle and

were subsequently transferred with a 1000 µl pipette to a fresh reaction tube for further applications.

The protoscoleces were activated by mimicking the gastrointestinal passage by adding 0.05% pepsin in DMEM without FCS at pH2. After 30 min at 37°C and careful rotation at 125 rpm, the protoscoleces were allowed to precipitate by gravity and were subsequently washed three times with 1x PBS. Afterwards, the protoscoleces were resuspended in 0.2% sodium taurocholate in DMEM without FCS at pH7.4 and were incubated for another 3 h at 37°C and 125 rpm. After several washing steps, the protoscoleces were prepared according to the use that followed. Both activating solutions (25 ml each for 500-1000 µl protoscoleces solution) were freshly prepared and filter sterilized.

5.10.4 *In vitro* Cultivation of metacestode larvae

The homogenized parasite material isolated from the animal (see section 5.10.2) was subsequently employed for the *in vitro* cultivation system in the absence or presence of host cells as follows [86].

Co-cultivation

1 ml parasite suspension was incubated in 50 ml normal culture medium (see table below) in a 75 cm² flask and the presence of 1x10⁷ freshly trypsinized feeder cells (RH- ; see section 5.9) at 37°C and 5% CO₂ atmosphere. After approximately 10 d, the parasite material was precipitated by gravity and the medium was decanted and replaced. In the following long-term incubation, the medium was replaced weekly by precipitating or percolating through a plastic tea sieve. At each medium replacement, feeder cells were added, but the flask was used repeatedly. At a diameter of 3-5 mm, the metacestode vesicles were used for the experiments.

Axenic cultivation

Co-cultivated metacestode vesicles (diameter approximately 3 mm) were adapted to axenic cultivation conditions by transfer into pre-conditioned medium (A4) supplemented with reducing agents (see table below) [86]. The most critical point for the adaptation is the elimination of contaminating feeder cells. To this end, the vesicles were intensively washed with pre-warmed 1x PBS prior to passage to a fresh culture flask (75 cm²). At every subsequent passage, the same flask was re-used. For 10 ml vesicles, a total volume of 40 ml medium was used. Every 48-72 h of incubation at 37°C under a nitrogen atmosphere, the medium was replaced. After approximately 4 weeks, the vesicles have adapted to the axenic conditions and can be used for experiments.

Media

normal culture medium	DMEM 10% FCS	1% P/S
starvation medium	DMEM 0.2% FCS	1% P/S
pre-conditioned medium (A4)	filter sterilized supernatant of RH- culture (1x10 ⁶ RH- in 20 ml DMEM 10% FCS 1% P/S for 1 week in a 75 cm ² flask)	

axenic culture medium (nitrogen atmosphere) A4 1µl/ml β-MEtOH, 1µl/ml BAT, 1µl/ ml L-Cys 1% P/S

5.10.5 Treatment of the metacystode vesicles

Co-cultivated and axenically cultivated metacystode vesicles with a minimal diameter of 3 mm were used in all experiments. For the analysis of effects of the drugs examined in this work, vesicles were manually picked, extensively washed with 1x PBS, and cultivated in groups of five per well in a 24 well plate. The pre-set culture medium consisted of 1 ml DMEM, 10% FCS and 1% P/S. Vesicles were incubated in presence or absence of the inhibitor in different concentrations and the solvent DMSO. All experiments were repeated four times for each dilution. The viability as indicated by the integrity of the cyst wall was repeatedly examined using an inverted light microscope, in particular upon transfer to the multiwell plates.

The same experimental setups were used for the cultivation under oxidative stress conditions. The induction was carried out for 30 minutes, 2 h and 8 h by supplementing with the following compounds: 50 µM and 200 µM H₂O₂, 1 µM and 10 µM paraquat, 1% and 10% DMSO. For the analysis of the effect of growth factors, metacystode vesicles were incubated under starving condition (DMEM 0.2% FCS 1% P/S) for 4 days prior to the stimulation.

5.10.6 Quantitative measurement of *E. multilocularis* alkaline phosphatase activity

The activity of *E. multilocularis* Alkaline Phosphatase (ALP) was measured after treatment of the *in vitro* cultivated metacystode vesicles using the previously published protocol [113]. In brief, 30 µl of culture supernatant were mixed with 170 µl AP buffer containing 0.5 M ethanolamine, 0.5 mM MgCl₂, pH 9.8, and 1 mg/ml *p*-nitrophenyl phosphate as substrate. The incubation took place at 37°C for 30 min in 96 well plate. The absorbance at 405 nm was measured with the ELISA reader Multiscan Ex Primary EIA V.2.1-0 (Thermo).

5.10.7 Isolation and cultivation of *E. multilocularis* primary cells

E. multilocularis primary cells were obtained from metacystode vesicles, which had been axenically cultivated for two months. The procedure has been published by Spiliotis et al. [86]. After washing three times with 1x PBS, the vesicles were disrupted by sucking into a 10 ml pipette and carefully resuspending. The vesicles were centrifuged for 10 min at 2600 rcf, the supernatant was poured off, and the pellet was resuspended in 8 volumes of pre-warmed trypsin/ EDTA solution. The suspension was subsequently incubated at 37°C under seesawing from time to time until the suspension became turbid. The germinal layer cells were separated from the remaining debris by a two minutes shaking step followed by passage through a 30 µm gaze. The flowthrough containing the germinal layer cells was centrifuged for 10 min and 2200 rcf. The supernatant was decanted and the pellet was carefully resuspended in the leftover supernatant. The resulting cell suspension was taken up in 1x PBS to a total volume of 1 ml. Cells were seeded on 24-well plates at a concentration of 60 µl suspension in 1 ml culture medium per well. Pre-conditioned DMEM (A4) supplemented with 100 U/ ml penicillin G, 100 mg/ ml streptomycin (both Biochrom), 10

mM bathocuproinedisulfonic acid (BAT; Sigma), β -mercaptoethanol (β -MEtOH) and L-cystein (L-Cys) or the hydatide fluid of axenically cultivated vesicles served used as medium. The plates were incubated at 37°C under a nitrogen atmosphere.

5.10.8 Treatment of *E. multilocularis* primary cells

For the drug treatment experiments, the primary cells were isolated and seeded as described in section 5.10.7. Alternatively, the primary cells were seeded into DMEM 10% FCS 1% P/S. For the stimulation with growth factors, the primary cells were starved in DMEM 0.2% FCS 1% P/S for 2, 8 and 24 h upon isolation. The respective stimulus was added for 3 and 24 h. The long-term observation in the presence of growth factors took place in medium containing 1% FCS.

5.10.9 Verification of pure of *Echinococcus* material

To verify the absence of DNA originating from feeder cells, the synthesized echinococcal cDNA was subjected to PCR analysis for the presence of host tubulin cDNA using the primers Tub12up (5' CCCCAAGTGTATGATACTGG) und Tub12ST (5' CTGGGCAGTGCGGCAACCA) [35].

Protein samples were examined for contamination with feeder cells using human specific anti-phospho-CREB (Ser133) or anti-phospho-histon H3 (Ser10) antibodies for the Western blot experiments. Both antibodies do not cross-react with *Echinococcus* proteins as examined (data not shown).

5.11 Computer analyses and statistics

Amino acid sequence comparisons were performed using the basic local alignment research tool (BLAST) software on the nr-aa database collection (<http://blast.genome.jp>). Pileups were constructed employing the software tool BioEdit using the BLOSUM62 matrix. Kinase domain predictions were done as described by Schultz et al. [106] using the simple modular architecture research tool (SMART; <http://smart.embl-heidelberg.de>). Important residues and motifs were predicted by ELM [120]. For statistical analyses, the GraphPad Prism software (GraphPad Software) version 4 was used. Error bars represent the standard deviation. Differences were considered significant for p values below 0.05 indicated by (*), very significant for p between 0.001 to 0.01 (**), extremely significant for p < 0.001 (***) and non-significant for p > 0.5 (ns). Survival curves after drug treatment were compared using the log-rank test. The influences of drugs on metacestode vesicles and mammalian cell lines were analyzed using ANOVA and Tukey's multiple comparison test. For IC₅₀ determination, linear regression was performed according to Pearson's correlation. R² values indicate the 'goodness of fit'. The confidence interval was calculated as 95% in all analyses.

6. Supplements

6.1 Survey of the yeast two hybrid studies

pGBKT7	pGADT7	double trans- formation	interaction middle stringency	interaction high stringency
EmMKK2	x EmRAL	++++	----	---
EmMKK2	x Em14-3-3	++++	+++-	+++-
EmMKK2	x EmRAP	++++	----	---
EmMKK2	x EmMKK1	++++	----	---
EmMKK2	x EmMKK2	++++	----	---
EmMKK2	x EmRAF	++++	++++	+++-
EmMKK2	x EmMPK1	++++	++++	+++-
EmMKK2	x EmMPK2	++++	----	---
EmMKK1	x Em14-3-3	++++	----	---
EmRAL	x EmMKK2	++++	----	---
Em14-3-3	x EmMKK2	++++	++++	+++-
EmRAP	x EmMKK2	++++	----	---
EmMKK1	x EmMKK2	++++	----	---
EmRAF	x EmMKK2	++++	+++-	+++-
EmMPK1	x EmMKK2	++++	++++	++++
EmMPK2	x EmMKK2	++++	----	---
EmMPK3	x EmMKK2	++++	----	---
Em14-3-3	x EmMKK1	++++	----	---
EmRAF	x EmMKK1	++++	+++-	+++-
EmMKK1	x EmRAF	++++	+++-	+++-
EmERin	x EmRAL	++++	++++	++++
EmERin	x EmRAP	++++	++++	++++
EmERin	x Em14-3-3	++++	++++	++++
EmERin	x EmRAF	++++	++++	++++
EmRAL	x EmERin	++++	++++	---
EmRAP	x EmERin	++++	++++	++++
Em14-3-3	x EmERin	++++	++++	++++
EmRAF	x EmERin	++++	++++	+++-
Controls				
p53	x T-Ag	++++	++++	++++
LamC	x T-Ag	++++	----	---
empty	x EmRAL	++++	----	---
empty	x Em14-3-3	++++	----	---
empty	x EmRAP	++++	----	---
empty	x EmMKK1	++++	----	---
empty	x EmMKK2	++++	----	---
empty	x EmRAF	++++	----	---
empty	x EmMPK1	++++	----	---
empty	x EmMPK2	++++	----	---
empty	x EmERin	++++	+++-	+++-
EmRAL	x empty	++++	----	---
Em14-3-3	x empty	++++	----	---
EmRAP	x empty	++++	----	---
EmMKK1	x empty	++++	----	---
EmMKK2	x empty	++++	----	---
EmRAF	x empty	++++	----	---
EmMPK1	x empty	++++	----	---
EmMPK2	x empty	++++	----	---
EmMPK3	x empty	++++	----	---
EmERin	x empty	++++	++++	++++

Tab. 6.1: Protein-protein interactions studied by yeast two hybrid experiments.

6.1 Alignment of Elp

Elp	MLKRSKNKTNKVRVTTAESQLEFEMQKGS LGQDLFDQVVRTIGLREVWYFGIQYIDKDG	60
HsEzrin	-----MPKPINVRVTTMDAELEFAIQPNTTGKQLFDQVVKTIGLREVWYFGLHYVDNKG	55
HsRadixin	-----MPKPINVRVTTMDAELEFAIQPNTTGKQLFDQVVKTIGLREVWYFGLQYVDSKGY	55
HsMoesin	-----MPKTIISVRVTTMDAELEFAIQPNTTGKQLFDQVVKTIGLREVWYFGLQYQDTKGF	55
Elp	PTFLRLDKKISSNDFAPGSEYDFKFMVKFYPENVEEELIQCTITHFYLVQVKS DIMSGKI	120
HsEzrin	PTWLKLDKVVSAQEVKKNPLQFKFRAKFYPEDVAEELIQDITQKLFLLQVKEGILSDEI	115
HsRadixin	STWLKLNKKVTQQDVKKENPLQFKFRAKFFPEDVSEELIQEITQRLFFLQVKEAILNDEI	115
HsMoesin	PTWLKLNKKVTAQDVRKESPLLFKFRKAFYPEDVSEELIQDITQRLFFLQVKEGILNDDI	115
Elp	YCPTDTAVLLAS YACVAKYGPYPDQSCPKS - -LPIDRLITSS - -KEQYDQTD EQWYERIIA	176
HsEzrin	YCPPETAVLLGS YAVQAKFGDYN - KEVHKS GYLSSERLIPQRVMDQHKLT RDQWEDRIQV	174
HsRadixin	YCPPETAVLLAS YAVQAKYGDYN - KEIHKPGYLANDRLLPQRVLEQHKLTKEQWEERIQV	174
HsMoesin	YCPPETAVLLAS YAVQSKYGFN - KEVHKS GYLAGDKLLPQRVLEQHKLNKDQWEERIQV	174
Elp	YYKDHHDMSREDAMVQYLQIAQDLEMYGVETFN IKNKKGTS LVLGVDALGLS IYEPGNLL	236
HsEzrin	WHA EHRGMLKDNAMLEYLKIAQDLEMYG I NYFE IKNKKGTDLWLGVDALGLNIYEKDDKL	234
HsRadixin	WHEEHRGMLREDSMMEYLKIAQDLEMYGVNYFE IKNKKGTDLWLGVDALGLNIYEHDDKL	234
HsMoesin	WHEEHRGMLREDAVLEYLKIAQDLEMYGVNYFS IKNKKGSELWLGVDALGLNIYEQNDRL	234
Elp	DPKIGFPWSEIRNLSFHDKKFI IKPADKSAKEFFFLVLEKSKINKRILALC TGNHELYMRR	296
HsEzrin	TPKIGFPWSEIRNISFNDKKFV IKPIDKKAPDFVFYAPRLRINKRILQLCMGNHELYMRR	294
HsRadixin	TPKIGFPWSEIRNISFNDKKFV IKPIDKKAPDFVFYAPRLRINKRILALCMGNHELYMRR	294
HsMoesin	TPKIGFPWSEIRNISFNDKKFV IKPIDKKAPDFVFYAPRLRINKRILALCMGNHELYMRR	294
Elp	RKSDSIEVQQMKIQAKKEER ELKEAERQR LKKEERLQR - -MENE - QKLRELRAQMVEKESDL	353
HsEzrin	RKPDTEVQQMKAQAREEKHQKQLERQQL ETEKKRRETVEREKEQMMREKEELMLRLQDY	354
HsRadixin	RKPDTEVQQMKAQAREEKHQKQLERAQL ENEKKKREIAEKEKERIEREKEELMERLQKI	354
HsMoesin	RKPDTEVQQMKAQAREEKHQKQMERAMLEN EKKKKREMAEKEKEKIEREKEELMERLQKI	354
Elp	ADMKNKASAYESKIAELEM L LQQR - - - -HARES LQKSS QDKLAEMNRK LKEETAASAEER	409
HsEzrin	EEKTKKARELSEIQRALQLEERKRAQEEAERLEADRMAALRAKEELERQAVDQIKSQ	414
HsRadixin	EEQTIKAQKELEEQRKALELDQERKRAK EEAERLEKERRAAEEAKSATAKQAADQMKNQ	414
HsMoesin	EEQTKKAQQELEEQTRRALELEQERKRAQS EAEKLAKERQEAEEAKEAL LQASRDQKKTKQ	414
Elp	DRLMAQRDEVQREVEAQKVAMAKKEAEKAQ - - - - -AEAELRRMREK HDAKHKSQ - - - -	458
HsEzrin	EQLAAELAEYTAKIALLEEARRRKEDVEEWQHRAKEAQDDL VKTKEELHLVMTAPP PPP	474
HsRadixin	EQLAAELAEFTAKIALLEEA KKKKEEEAT EWQHKAFAAQEDLEKTKEELKTVM SAP PPP	474
HsMoesin	EQLALEMAELTARISQLEMARQKKESEAV EWQQK AQMVQEDLEKTRAE LKTAMSTP - - - -	470
Elp	-----VNGSGDAASQDDES EAK - - - -EL EVIPNVR - RTEESRVTA VSKNETLQTKLANL	507
HsEzrin	PPVYEPVSYHVQESLQDEGA EPTGYS AELSS EGI RDDRNEEKRITEAEKNERVQRQLLTL	534
HsRadixin	PPPVIPTTENEHDEHDENNAEAS - - - AELSN EGVMMNHRSE EERVTE TQKNERVKKQLQAL	531
HsMoesin	- - HVAEPAEN EQDEQDENGAEAS - - - ADLRADAMAKDRSE EERTTEAEKNERVQKHLKAL	525
Elp	KMELSS TRDQSKMRDIDRRHEYNVRE GNDKYKTLRNIRKGNMTCRVEQFESM	559
HsEzrin	SSELS QARDENKRTHNDI IHNENMRQGRDKYKTLRQIRQGNTKQRIDEF EAL	586
HsRadixin	SSELA QARDET KKTQNDV LHAENVKAGRDKYKTLRQIRQGNTKQRIDEF EAM	583
HsMoesin	TSELANARDES KKTANDMI HAENMRLGRDKYKTLRQIRQGNTKQRIDEF ESM	577

Fig. 6.1: Amino acid alignment of Elp and human ERM proteins. Shown are the sequences of Elp (Q05768) and human ezrin (P15311), radixin (P35241), moesin (P26038). The threshold for identical amino acid residues, which are highlighted in white on black background, is set to 60%. Similar residues are shaded in blue. 'P's above the lines mark residues which are modified during the activation process (see sections 3.6.1 and 4)

6.2 Alignment of EmMPK3

EmMPK3	-----MDH ELEK HVCR SFEIVKRI GKGAYGIVWKA KYKRLNK --H VAFKKIFDAF 48
HsErk8	-----MCT-V VDPRIVRRY L LRRLQ LG Q GAYGIVWKA VD RR TGE --V VAIKKIFDAF 48
RnErk7	-----MCAA EVD RHV SQR YL IKRRL GKGAYGIVWKA MD RR TGE --V VAIKKIFDAF 49
CeYPC2	-----MT DDVD TH IHEK FD LQKRL GKGAYGIVWKA YDK RS RE --T VALKKIFDAF 48
ScSLT2	MADK I ERHTFKVFN QDF SV DKRF QL IKEI GHGAYGIVCSA RF FA EAE ED TTVAIKKVT N VF 60
EmMPK3	HNK TDAQRTFRE I V FLREFS GHPN I K LLG VIRAHND---- KDI YLVFE YMETDL H KLI K 104
HsErk8	RDK TDAQRTFRE I T LLQEF GD HPN I IS LLDVIR AEND --- RDI YLVFE FMD TDLNA VI R 104
RnErk7	RDQ TDAQRTFRE I M LLREF GGHPN I R LLD V I PAKND--- RDI YLVFE SMD TDLNA VI R 105
CeYPC2	RNP TDSQRTFRE V M FLQEF G KHPN V IK LYN I FRADND--- RDI YLA FE F MEAD LHN VI K 104
ScSLT2	SKT LL CKR SL RE L KLLR HFR GH KN IT CL YD MD I V F YPDGS ING L YLYE EL MECD M HQI I K 120
EmMPK3	RGN IL RS AHMRY I T YQIL KA KYI HSAD V I HRD LKPSN ILL S DC NA KI CD FGL TR SL SR 164
HsErk8	KG GL LQD VHVRS I F YQL LRAT RF L HSG HVV HRD QKPSN VLLD AN CT V KL CD FGL ARS LG - 163
RnErk7	KGR LL ED I HK RC I F YQL LRAT RF L HSG RV HRD QK PAN VLL DA AC RV KL CD FGLARS LS - 164
CeYPC2	KGS IL KD V HK Q YI M CQL FR A RF LHSG N V L HRD LKPSN VLLD AD CR V KL AD FGL ARS LS 164
ScSLT2	SG Q PL DA HY Q S F TYQ IL CGL K YI HSAD VL H RD LK PGN L LV NA DC Q LK I CD FGLAR GYS - 179
EmMPK3	- CNA PNCKNSVPDFYN PE L TEY VATRWYRA PE ILL SS TY YTK GVDM WS I GC IL AE IF IG K 223
HsErk8	-- DL PEG PE ----- DQA V TEY VATRWYRA PE V LL SS HRY T L GVDM WS L GC IL GE M L R GR 215
RnErk7	-- DF PEG PG ----- GQA L TEY VATRWYRA PE V LL SS RWY T P GVDM WS L GC IL GE M L R GQ 216
CeYPC2	LE D Y PEG QK ----- MPD L TEY VATRWY RS PE ILL A AK RY T KGVDM WS L GC IL AE M L I GR 218
ScSLT2	-- EN PV ENS ----- QF L TEY VATRWYRA PE I MLS Y QG Y T KA I D V WS AG CIL AE F L GG K 230
EmMPK3	AL FP GT ST LN Q LE K I MS I GP KPS RED IL C LR SD Y GAS I L D Q PS I AG RR RL ED V V T PV PE P 283
HsErk8	PL FP GT ST LH Q LE L I LET I PP SE ED LL A LG SG CR AS V L H Q L GS R PR QT LD AL LP PD T SP 275
RnErk7	PL FP GT ST FH Q LE L I LET I PL PS ME EL Q L GS D YS AL I L Q N L GS R PR QT LD AL LP PD T PP 276
CeYPC2	AL FP GS ST IN Q I ER IM NT IA KPS RAD IAS I GS H YAAS V L E K MP QR PK PL D L I T QS Q T 277
ScSLT2	P I F K G KD Y V N Q L N Q I L Q V L G T P DE T L RR I GS K N V Q D Y I H Q L G F I P K V P F V N L Y P N ANS 289
EmMPK3	SAL EM V R GL LN-- PN K RL TA AQA LE H HY V S Q FR DP ESE I V MD H V V PP LS DS Q K L G V S E Y 341
HsErk8	EAL DL LR RL LV F AP D K RL S AT QA L QH PY V Q RF H CP S DE WA RE AD V R PR A HE GV Q LS V PE Y 335
RnErk7	EAL DL LR RL LA F AP D K RL SA E QA L QH PY V Q RF H CP D RE W TR GS D V RL P V H EG D Q LS A PE Y 336
CeYPC2	AA I DM V Q RL L I F AP Q K RL T VE Q CL V HP Y V V Q F HN P S EE P V LN Y E V Y PP L PD H I Q LS I DD Y 337
ScSLT2	QAL DL L EQ ML A FD P Q K R I T V DE A L E H PY LS I W H D PA DE P V CS E K F EF S F ES V N -- DM ED L 347
EmMPK3	RS RL Y DM I LET K S K RP Q M K KL SS SE SE AS KD V S ENG SS V SS ST ST GS ST V SL ED SG ST T 401
HsErk8	RS R V Y Q M I LE CG GS----- SG T S RE K GE PE GV SP ----- SQA H L H K PR AD P QL PS R TP 382
RnErk7	RN RL Y Q M I L ER RR N----- RS P RE ED L GV V AS RA EL RS Q R Q S L K PG V LP Q V LA ET P 389
CeYPC2	RD RL Y EM I DE KK AS F ----- KR I Q HE K IR P ----- 362
ScSLT2	K Q M V I Q EV Q DF RL F VR----- Q PL LE E----- 369
EmMPK3	AAT TTTT ASA ETS AT SP ST V S -- RS R I V AP PS P Q RP I HL SP AK Q RS E K SK P TT V K F Q R GA S 460
HsErk8	VQ GR PR PS Q SS P GH D PA E H ES PR AA KN V PR Q NS A PL L Q T ALL NG ER----- 429
RnErk7	AR K R GP K Q NG H GH D PE H VE ----- VRR Q S SD P LY Q L PP PS G GER----- 429
CeYPC2	----- Y GE D ----- KSR AP IA QA E CS D T D YD----- 383
ScSLT2	----- QR QL L Q Q Q Q Q Q Q Q ----- 386
EmMPK3	CG NGG K V L PK S I SV T W IP N Q EN R K TT R K R Q V Y P D I L V K NS Q Q N H P V RS RR A L GC G DA A I 520
HsErk8	----- PP GA E AP L T L S L V K PS GR GA AP SL TS Q AAA Q V AN 465
RnErk7	----- PP GAT GE PS AP SG V K TH RA V AP SL TS Q AAA Q AA N 465
CeYPC2	----- TAR SL Q RT TS M D KN NS SS H D SS SG T LR ER A AS A ES - 418
ScSLT2	----- QQ Q Q Q PS D V D NG NA AA AS E EN Y P K MA TS NS V AP Q 420
EmMPK3	I TT AP AT MT S T MA T S F TR SH D I PM I LR GN EN H MG S D GN L V R H Y HP GR Q KT T NS GG Y Y EG 580
HsErk8	QAL I R GD WN R GG GV R V AS V Q Q V PP R LP----- PE AR P GR RM F S TS----- 505
RnErk7	QPL I R SD P ARG GG GP RA V G ARR V PS R LP REA ----- PE PR P GR RM F G IS----- 508
CeYPC2	----- RT SK D SN G ----- EM R NG NG N TP SS ----- 438
ScSLT2	Q ES F GI HS Q N L PR ----- HD AD F PP RP Q ES ----- 445
EmMPK3	WRR GG Q RS ASS GP PH PP L PP S LP N P ANT V TH AR L HR AL A AR P W IA 625
HsErk8	----- AL Q G A Q GG AR ALL GG YS Q AY GT V CH SA L GH L PL L EG H V- 544
RnErk7	----- V S Q GA Q GA ARA AL GG YS Q AY GT V CR SA L GR L PL L PG PR A- 547
CeYPC2	----- I K Q RR RS V ER AR L ----- FAN I K PS K I L HP H K L I S NY-- 470
ScSLT2	----- MM EM R PA T GN TAD I PP Q ND NG T LL D LE K E L EF L DR K Y F - 484

Fig. 6.2: Amino acid sequence comparison of EmMPK3 with homologue MAPKs from different phylogenetic origins. Displayed are the sequences of EmMPK3, human Erk8 (Q8TD08), *Rattus norvegicus* Erk7 (Q9Z2A6), *Caenorhabditis elegans* YPC2 (Q11179) and yeast SLT2 (Q00772). Identical amino acid residues are highlighted in white on black background by a threshold at 60%. Similar residues are shaded in blue. 'M' indicates the residue Lys⁴³ of human Erk8 which replacement to Arg resulted in a kinase inactive mutant (see sections 3.9 and 4).

7. List of abbreviations

°C	Grad Celsius	MetOH	methanol
A	Ampère	min	minutes
AA	amino acid	MKK	mitogen activated protein kinase kinase
aFGF	acidic fibroblast growth factor	MV	<u>met</u> acestode <u>ves</u> icles
AP	alkaline phosphatase	Mw	molecular weight
APS	ammonium persulfate	NES	nucleus exclusion sequence
ATP	adenosine triphosphate	ORF	open reading frame
bFGF	basic fibroblast growth factor	P	protoscolices
BMP	bone morphogenetic protein	p.i.	post infection
bp	base pair	PAA	polyacrylamide
cDNA	complementary DNA	P _{act}	activated protoscoleces
Ce	<i>Caenorhabditis elegans</i>	PAGE	polyacrylamide gel electrophoresis
CIP	calf intestine alkaline phosphatase	PBS	phosphate buffered saline
Da	dalton	PCR	polymerase chain reaction
dATP	deoxy ATP	RACE	rapid amplification of cDNA end
Dm	<i>Drosophila melanogaster</i>	Raf	rapidly growing fibrosarcoma
DMEM	Dulbecco's minimal essentiell medium	rATP	ribosomal ATP
DMSO	dimethyl sulfoxide	RH	Reuber hepatoma
DNA	deoxyribonucleic acid	RNA	ribonucleic acid
dNTP	deoxyribonucleotide triphosphate	rpm	rotations per minute
EGF	<u>e</u> pidermal <u>g</u> rowth <u>f</u> actor	RT PCR	reverse transcriptase PCR
Elp	<u>E</u> zrin- <u>R</u> adixin- <u>M</u> oesin <u>l</u> ike <u>p</u> rotein	RT	room temperature
Em	<i>Echinococcus multilocularis</i>	SAPK	stress activated phospho kinase
Erk	extracellular signal regulated kinase	SD	standard deviation
EtOH	ethanol	SDS	sodium dodecyl sulfate
FCS	fetal calf serum	sec	seconds
Fig.	Figure	SM	stop mix
GST	glutathione s-transferase	SMART	<u>s</u> witching <u>m</u> echanism <u>a</u> t 5' end of <u>R</u> NA <u>t</u> ranscript
h	hour	Tab.	Table
H ₂ O ₂	hydrogen peroxide	TBS	Tris buffered saline
HBMEC	human brain microvascular endothelial cell	TBST	TBS Tween
HEK	human embryonic kidney cells	Tc	<i>Taenia crassiceps</i>
Hs	<i>Homo sapiens</i>	TEMED	N, N, N', N'-tetra-methylethylenediamine
JNK	c-Jun N-terminal kinase	TGF-α	transforming growth factor alpha
LM	light microscopy	TGF-β	transforming growth factor beta
M	Mol	UV	ultra violet
MAPK	mitogen activated protein kinase	V	Volt
MBP	myelin basic protein	WB	Western blot
		XI	<i>Xenopus laevis</i>

8. References

1. Gilbert SF: **Developmental Biology**, 6th edn; 2000.
2. Romig T, Dinkel A, Mackenstedt U: **The present situation of echinococcosis in Europe**. *Parasitol Int* 2006, **55** Suppl:S187-191.
3. Hüttner M, Nakao M, Wassermann T, Siefert L, Boomker JDF, Dinkel A, Sako Y, Mackenstedt U, Romig T, Ito A: **Genetic characterization and phylogenetic position of *Echinococcus felidis* (Cestoda: Taeniidae) from the African lion**. *International Journal for Parasitology* 2008, **38**(7):861-868.
4. Hemphill A, Kern P: **Special issue: Experimental studies in echinococcosis**. *Exp Parasitol* 2008, **119**(4):437-438.
5. Romig T, Thoma D, Weible AK: **Echinococcus multilocularis--a zoonosis of anthropogenic environments?** *J Helminthol* 2006, **80**(2):207-212.
6. Eckert J, Conraths FJ, Tackmann K: **Echinococcosis: an emerging or re-emerging zoonosis?** *Int J Parasitol* 2000, **30**(12-13):1283-1294.
7. Deplazes P, Hegglin D, Gloor S, Romig T: **Wilderness in the city: the urbanization of *Echinococcus multilocularis***. *Trends in Parasitology* 2004, **20**(2):77-84.
8. Eckert J, Deplazes P: **Biological, epidemiological, and clinical aspects of echinococcosis, a zoonosis of increasing concern**. *Clin Microbiol Rev* 2004, **17**(1):107-135.
9. Xiao N, Qiu J, Nakao M, Li T, Yang W, Chen X, Schantz PM, Craig PS, Ito A: ***Echinococcus shiquicus* n. sp., a taeniid cestode from Tibetan fox and plateau pika in China**. *International Journal for Parasitology* 2005, **35**(6):693-701.
10. Xiao N, Qiu J, Nakao M, Li T, Yang W, Chen X, Schantz PM, Craig PS, Ito A: ***Echinococcus shiquicus*, a new species from the Qinghai-Tibet plateau region of China: Discovery and epidemiological implications**. *Parasitology International* 2006, **55**(Supplement 1):S233-S236.
11. Gottstein B, Dai WJ, Walker M, Stettler M, Muller N, Hemphill A: **An intact laminated layer is important for the establishment of secondary *Echinococcus multilocularis* infection**. *Parasitol Res* 2002, **88**(9):822-828.
12. Gottstein B, Hemphill A: ***Echinococcus multilocularis*: the parasite-host interplay**. *Exp Parasitol* 2008, **119**(4):447-452.
13. Spiliotis M, Lechner S, Tappe D, Scheller C, Krohne G, Brehm K: **Transient transfection of *Echinococcus multilocularis* primary cells and complete in vitro regeneration of metacystode vesicles**. *Int J Parasitol* 2008, **38**(8-9):1025-1039.
14. Gottstein B, Hemphill A: **Immunopathology of echinococcosis**. *Chem Immunol* 1997, **66**:177-208.
15. Kern P, Bardonnnet K, Renner E, Auer H, Pawlowski Z, Ammann RW, Vuitton DA: **European echinococcosis registry: human alveolar echinococcosis, Europe, 1982-2000**. *Emerg Infect Dis* 2003, **9**(3):343-349.
16. McManus DP, Zhang W, Li J, Bartley PB: **Echinococcosis**. *Lancet* 2003, **362**(9392):1295-1304.
17. Schweiger A, Ammann RW, Candinas D, Clavien PA, Eckert J, Gottstein B, Halkic N, Muellhaupt B, Prinz BM, Reichen J *et al*: **Human alveolar echinococcosis after fox population increase, Switzerland**. *Emerg Infect Dis* 2007, **13**(6):878-882.
18. Deplazes P: **Ecology and epidemiology of *Echinococcus multilocularis* in Europe**. *Parassitologia* 2006, **48**(1-2):37-39.
19. Hubner MP, Manfras BJ, Margos MC, Eiffler D, Hoffmann WH, Schulz-Key H, Kern P, Soboslay PT: ***Echinococcus multilocularis* metacystodes modulate cellular cytokine and chemokine release by peripheral blood mononuclear cells in alveolar echinococcosis patients**. *Clin Exp Immunol* 2006, **145**(2):243-251.

20. Hemphill A, Spicher M, Stadelmann B, Mueller J, Naguleswaran A, Gottstein B, Walker M: **Innovative chemotherapeutical treatment options for alveolar and cystic echinococcosis.** *Parasitology* 2007, **134**(Pt 12):1657-1670.
21. Kocherscheidt L, Flakowski AK, Gruner B, Hamm DM, Dietz K, Kern P, Soboslay PT: **Echinococcus multilocularis: inflammatory and regulatory chemokine responses in patients with progressive, stable and cured alveolar echinococcosis.** *Exp Parasitol* 2008, **119**(4):467-474.
22. Gottstein B, Felleisen R: **Protective immune mechanisms against the metacestode of Echinococcus multilocularis.** *Parasitol Today* 1995, **11**(9):320-326.
23. Zhang W, McManus DP: **Recent advances in the immunology and diagnosis of echinococcosis.** *FEMS Immunology & Medical Microbiology* 2006, **47**(1):24-41.
24. Frosch PM, Geier C, Kaup FJ, Muller A, Frosch M: **Molecular cloning of an echinococcal microtrichal antigen immunoreactive in Echinococcus multilocularis disease.** *Mol Biochem Parasitol* 1993, **58**(2):301-310.
25. Frosch PM, Frosch M, Pfister T, Schaad V, Bitter-Suermann D: **Cloning and characterisation of an immunodominant major surface antigen of Echinococcus multilocularis.** *Mol Biochem Parasitol* 1991, **48**(2):121-130.
26. Vogel M, Gottstein B, Muller N, Seebeck T: **Production of a recombinant antigen of Echinococcus multilocularis with high immunodiagnostic sensitivity and specificity.** *Mol Biochem Parasitol* 1988, **31**(2):117-125.
27. Hemmings L, McManus DP: **The isolation, by differential antibody screening, of Echinococcus multilocularis antigen gene clones with potential for immunodiagnosis.** *Mol Biochem Parasitol* 1989, **33**(2):171-182.
28. Hemmings L, McManus DP: **The diagnostic value and molecular characterisation of an Echinococcus multilocularis antigen gene clone.** *Mol Biochem Parasitol* 1991, **44**(1):53-61.
29. Brehm K, Kern P, Hubert K, Frosch M: **Echinococcosis from every angle.** *Parasitol Today* 1999, **15**(9):351-352.
30. Reuter S, Jensen B, Buttenschoen K, Kratzer W, Kern P: **Benzimidazoles in the treatment of alveolar echinococcosis: a comparative study and review of the literature.** *J Antimicrob Chemother* 2000, **46**(3):451-456.
31. Mathis A, Wild P, Boettger EC, Kapel CM, Deplazes P: **Mitochondrial ribosome as the target for the macrolide antibiotic clarithromycin in the helminth Echinococcus multilocularis.** *Antimicrob Agents Chemother* 2005, **49**(8):3251-3255.
32. Vuitton DA: **The ambiguous role of immunity in echinococcosis: protection of the host or of the parasite?** *Acta Trop* 2003, **85**(2):119-132.
33. Stettler M, Fink R, Walker M, Gottstein B, Geary TG, Rossignol JF, Hemphill A: **In vitro parasitocidal effect of Nitazoxanide against Echinococcus multilocularis metacestodes.** *Antimicrob Agents Chemother* 2003, **47**(2):467-474.
34. Jura H, Bader A, Frosch M: **In vitro activities of benzimidazoles against Echinococcus multilocularis metacestodes.** *Antimicrob Agents Chemother* 1998, **42**(5):1052-1056.
35. Brehm K, Kronthaler K, Jura H, Frosch M: **Cloning and characterization of [beta]-tubulin genes from Echinococcus multilocularis.** *Molecular and Biochemical Parasitology* 2000, **107**(2):297-302.
36. Reuter S, Merkle M, Brehm K, Kern P, Manfras B: **Effect of amphotericin B on larval growth of Echinococcus multilocularis.** *Antimicrob Agents Chemother* 2003, **47**(2):620-625.
37. Reuter S, Buck A, Grebe O, Nussle-Kugele K, Kern P, Manfras BJ: **Salvage treatment with amphotericin B in progressive human alveolar echinococcosis.** *Antimicrob Agents Chemother* 2003, **47**(11):3586-3591.
38. Stettler M, Rossignol JF, Fink R, Walker M, Gottstein B, Merli M, Theurillat R, Thormann W, Dricot E, Segers R *et al*: **Secondary and primary murine alveolar echinococcosis: combined**

- albendazole/nitazoxanide chemotherapy exhibits profound anti-parasitic activity.** *Int J Parasitol* 2004, **34**(5):615-624.
39. Widmann C, Gibson S, Jarpe MB, Johnson GL: **Mitogen-activated protein kinase: conservation of a three-kinase module from yeast to human.** *Physiol Rev* 1999, **79**(1):143-180.
40. McKay MM, Morrison DK: **Integrating signals from RTKs to ERK/MAPK.** *Oncogene* 2007, **26**(22):3113-3121.
41. Dhanasekaran DN, Johnson GL: **MAPKs: function, regulation, role in cancer and therapeutic targeting.** *Oncogene* 2007, **26**(22):3097-3099.
42. Normanno N, De Luca A, Bianco C, Strizzi L, Mancino M, Maiello MR, Carotenuto A, De Feo G, Caponigro F, Salomon DS: **Epidermal growth factor receptor (EGFR) signaling in cancer.** *Gene* 2006, **366**(1):2-16.
43. Higashiyama S, Iwabuki H, Morimoto C, Hieda M, Inoue H, Matsushita N: **Membrane-anchored growth factors, the epidermal growth factor family: beyond receptor ligands.** *Cancer Sci* 2008, **99**(2):214-220.
44. Wong RW, Guillaud L: **The role of epidermal growth factor and its receptors in mammalian CNS.** *Cytokine Growth Factor Rev* 2004, **15**(2-3):147-156.
45. Cohen S: **Isolation of a mouse submaxillary gland protein accelerating incisor eruption and eyelid opening in the new-born animal.** *J Biol Chem* 1962, **237**:1555-1562.
46. Fisher DA, Lakshmanan J: **Metabolism and effects of epidermal growth factor and related growth factors in mammals.** *Endocr Rev* 1990, **11**(3):418-442.
47. Jorissen RN, Walker F, Pouliot N, Garrett TP, Ward CW, Burgess AW: **Epidermal growth factor receptor: mechanisms of activation and signalling.** *Exp Cell Res* 2003, **284**(1):31-53.
48. Dailey L, Ambrosetti D, Mansukhani A, Basilico C: **Mechanisms underlying differential responses to FGF signaling.** *Cytokine Growth Factor Rev* 2005, **16**(2):233-247.
49. Eswarakumar VP, Lax I, Schlessinger J: **Cellular signaling by fibroblast growth factor receptors.** *Cytokine Growth Factor Rev* 2005, **16**(2):139-149.
50. Werner H, Weinstein D, Bentov I: **Similarities and differences between insulin and IGF-I: structures, receptors, and signalling pathways.** *Arch Physiol Biochem* 2008, **114**(1):17-22.
51. Claeys I, Simonet G, Poels J, Van Loy T, Vercammen L, De Loof A, Vanden Broeck J: **Insulin-related peptides and their conserved signal transduction pathway.** *Peptides* 2002, **23**(4):807-816.
52. Zheng CF, Guan KL: **Activation of MEK family kinases requires phosphorylation of two conserved Ser/Thr residues.** *Embo J* 1994, **13**(5):1123-1131.
53. Zheng CF, Guan KL: **Cloning and characterization of two distinct human extracellular signal-regulated kinase activator kinases, MEK1 and MEK2.** *J Biol Chem* 1993, **268**(15):11435-11439.
54. Belanger LF, Roy S, Tremblay M, Brott B, Steff AM, Mourad W, Hugo P, Erikson R, Charron J: **Mek2 is dispensable for mouse growth and development.** *Mol Cell Biol* 2003, **23**(14):4778-4787.
55. Zheng CF, Guan KL: **Cytoplasmic localization of the mitogen-activated protein kinase activator MEK.** *J Biol Chem* 1994, **269**(31):19947-19952.
56. Brott BK, Alessandrini A, Largaespada DA, Copeland NG, Jenkins NA, Crews CM, Erikson RL: **MEK2 is a kinase related to MEK1 and is differentially expressed in murine tissues.** *Cell Growth Differ* 1993, **4**(11):921-929.
57. Dhanasekaran DN, Kashaf K, Lee CM, Xu H, Reddy EP: **Scaffold proteins of MAP-kinase modules.** *Oncogene* 2007, **26**(22):3185-3202.
58. Kolch W: **Meaningful relationships: the regulation of the Ras/Raf/MEK/ERK pathway by protein interactions.** *Biochem J* 2000, **351 Pt 2**:289-305.

59. Kyriakis JM, Avruch J: **Mammalian mitogen-activated protein kinase signal transduction pathways activated by stress and inflammation.** *Physiol Rev* 2001, **81**(2):807-869.
60. Jiang Y, Gram H, Zhao M, New L, Gu J, Feng L, Di Padova F, Ulevitch RJ, Han J: **Characterization of the structure and function of the fourth member of p38 group mitogen-activated protein kinases, p38delta.** *J Biol Chem* 1997, **272**(48):30122-30128.
61. Avitzour M, Diskin R, Raboy B, Askari N, Engelberg D, Livnah O: **Intrinsically active variants of all human p38 isoforms.** *Febs J* 2007, **274**(4):963-975.
62. Enslin H, Raingeaud J, Davis RJ: **Selective activation of p38 mitogen-activated protein (MAP) kinase isoforms by the MAP kinase kinases MKK3 and MKK6.** *J Biol Chem* 1998, **273**(3):1741-1748.
63. Jiang Y, Chen C, Li Z, Guo W, Gegner JA, Lin S, Han J: **Characterization of the structure and function of a new mitogen-activated protein kinase (p38beta).** *J Biol Chem* 1996, **271**(30):17920-17926.
64. Katz M, Amit I, Yarden Y: **Regulation of MAPKs by growth factors and receptor tyrosine kinases.** *Biochim Biophys Acta* 2007, **1773**(8):1161-1176.
65. Bogoyevitch MA, Court NW: **Counting on mitogen-activated protein kinases--ERKs 3, 4, 5, 6, 7 and 8.** *Cell Signal* 2004, **16**(12):1345-1354.
66. Abe MK, Kuo WL, Hershenson MB, Rosner MR: **Extracellular signal-regulated kinase 7 (ERK7), a novel ERK with a C-terminal domain that regulates its activity, its cellular localization, and cell growth.** *Mol Cell Biol* 1999, **19**(2):1301-1312.
67. Abe MK, Saelzler MP, Espinosa R, 3rd, Kahle KT, Hershenson MB, Le Beau MM, Rosner MR: **ERK8, a new member of the mitogen-activated protein kinase family.** *J Biol Chem* 2002, **277**(19):16733-16743.
68. Abe MK, Kahle KT, Saelzler MP, Orth K, Dixon JE, Rosner MR: **ERK7 is an autoactivated member of the MAPK family.** *J Biol Chem* 2001, **276**(24):21272-21279.
69. Coulombe P, Meloche S: **Atypical mitogen-activated protein kinases: structure, regulation and functions.** *Biochim Biophys Acta* 2007, **1773**(8):1376-1387.
70. Tappe D, Frosch M: **Rudolf Virchow and the recognition of alveolar echinococcosis, 1850s.** *Emerg Infect Dis* 2007, **13**(5):732-735.
71. Gottstein B, Tschudi K, Eckert J, Ammann R: **Em2-ELISA for the follow-up of alveolar echinococcosis after complete surgical resection of liver lesions.** *Trans R Soc Trop Med Hyg* 1989, **83**(3):389-393.
72. Ito A, Osawa Y, Nakao M, Horii T, Okamoto M, Itoh M, Yamashita T: **Em18 and Em16, new serologic marker epitopes for alveolar echinococcosis in western blot analysis, are the only two epitopes recognized by commercially available weak positive (cut off) sera for Em2plus-ELISA.** *J Helminthol* 1995, **69**(4):369-371.
73. Hubert K, Cordero E, Frosch M, Solomon F: **Activities of the EM10 protein from Echinococcus multilocularis in cultured mammalian cells demonstrate functional relationships to ERM family members.** *Cell Motil Cytoskeleton* 1999, **42**(3):178-188.
74. Hubert K, Zavala-Góngora R, Frosch M, Brehm K: **Identification and characterization of PDZ-1, a N-ERMAD specific interaction partner of the Echinococcus multilocularis ERM protein Elp.** *Molecular and Biochemical Parasitology* 2004, **134**(1):149-154.
75. Louvet-Vallee S: **ERM proteins: from cellular architecture to cell signaling.** *Biol Cell* 2000, **92**(5):305-316.
76. Brehm K, Jensen K, Frosch P, Frosch M: **Characterization of the genomic locus expressing the ERM-like protein of Echinococcus multilocularis.** *Molecular and Biochemical Parasitology* 1999, **100**(1):147-152.
77. Brehm K, Jensen K, Frosch M: **mRNA trans-splicing in the human parasitic cestode Echinococcus multilocularis.** *J Biol Chem* 2000, **275**(49):38311-38318.

78. Borst P: **Discontinuous transcription and antigenic variation in trypanosomes.** *Annu Rev Biochem* 1986, **55**:701-732.
79. Nilsen TW: **Trans-splicing of nematode premessenger RNA.** *Annu Rev Microbiol* 1993, **47**:413-440.
80. Blaxter M, Liu L: **Nematode spliced leaders--ubiquity, evolution and utility.** *Int J Parasitol* 1996, **26**(10):1025-1033.
81. Brehm K, Wolf M, Beland H, Kroner A, Frosch M: **Analysis of differential gene expression in Echinococcus multilocularis larval stages by means of spliced leader differential display.** *International Journal for Parasitology* 2003, **33**(11):1145-1159.
82. Fernández C, Gregory WF, Loke Pn, Maizels RM: **Full-length-enriched cDNA libraries from Echinococcus granulosus contain separate populations of oligo-capped and trans-spliced transcripts and a high level of predicted signal peptide sequences.** *Molecular and Biochemical Parasitology* 2002, **122**(2):171-180.
83. Hemphill A, Gottstein B: **Immunology and morphology studies on the proliferation of in vitro cultivated Echinococcus multilocularis metacestodes.** *Parasitol Res* 1995, **81**(7):605-614.
84. Jura H, Bader A, Hartmann M, Maschek H, Frosch M: **Hepatic tissue culture model for study of host-parasite interactions in alveolar echinococcosis.** *Infect Immun* 1996, **64**(9):3484-3490.
85. Spiliotis M, Tappe D, Sesterhenn L, Brehm K: **Long-term in vitro cultivation of Echinococcus multilocularis metacestodes under axenic conditions.** *Parasitol Res* 2004, **92**(5):430-432.
86. Spiliotis M: **Untersuchungen zur in vitro Kultivierung und Charakterisierung von MAP-Kinase-Kaskade-Komponenten des Fuchsbandwurmes Echinococcus multilocularis.** *PhD thesis.* 2006.
87. Suga H, Katoh K, Miyata T: **Sponge homologs of vertebrate protein tyrosine kinases and frequent domain shufflings in the early evolution of animals before the parazoan-eumetazoan split.** *Gene* 2001, **280**(1-2):195-201.
88. Suga H, Ono K, Miyata T: **Multiple TGF-[beta] receptor related genes in sponge and ancient gene duplications before the parazoan-eumetazoan split.** *FEBS Letters* 1999, **453**(3):346-350.
89. Gelmedin V, Zavala-Góngora R, Fernández C, Brehm K: **Echinococcus multilocularis: Cloning and characterization of a member of the SNW/SKIP family of transcriptional coregulators.** *Experimental Parasitology* 2005, **111**(2):115-120.
90. Gelmedin V: **Molekulare Charakterisierung von Komponenten des Nukleären-Hormonrezeptor-Signaling beim Fuchsbandwurm Echinococcus multilocularis.** *Diploma Thesis.* 2005.
91. Günthel D: **Molekulare Charakterisierung von Komponenten des nukleären Hormon-Rezeptor-Signalings in Echinococcus multilocularis.** *MDPhD.* 2005.
92. Konrad C, Kroner A, Spiliotis M, Zavala-Góngora R, Brehm K: **Identification and molecular characterisation of a gene encoding a member of the insulin receptor family in Echinococcus multilocularis.** *International Journal for Parasitology* 2003, **33**(3):301-312.
93. Konrad C: **Molecular analysis of insulin signaling mechanisms in Echinococcus multilocularis and their role in the host-parasite interaction in the alveolar echinococcosis.** *PhD thesis.* 2007.
94. Schäfer T: **Molekulare Charakterisierung einer Tyrosinekinase der fibroblast growth factor-Rezeptorfamilie des Fuchsbandwurms Echinococcus multilocularis.** *Diploma Thesis.* 2006.
95. Spiliotis M, Kroner A, Brehm K: **Identification, molecular characterization and expression of the gene encoding the epidermal growth factor receptor orthologue from the fox-tapeworm Echinococcus multilocularis.** *Gene* 2003, **323**:57-65.
96. Zavala-Góngora R, Kroner A, Bernthaler P, Knaus P, Brehm K: **A member of the transforming growth factor-[beta] receptor family from Echinococcus multilocularis is activated by human bone morphogenetic protein 2.** *Molecular and Biochemical Parasitology* 2006, **146**(2):265-271.

97. Graf M: **Charakterisierung einer bisher noch unbekanntenen MAPK aus dem Fuchsbandwurm *Echinococcus multilocularis***. Bachelor thesis. 2006.
98. Spiliotis M, Konrad C, Gelmedin V, Tappe D, Brückner S, Mösch H-U, Brehm K: **Characterisation of EmMPK1, an ERK-like MAP kinase from *Echinococcus multilocularis* which is activated in response to human epidermal growth factor**. *International Journal for Parasitology* 2006, **36**(10-11):1097-1112.
99. Zavala-Góngora R, Derrer B, Gelmedin V, Knaus P, Brehm K: **Molecular characterisation of a second structurally unusual AR-Smad without an MH1 domain and a Smad4 orthologue from *Echinococcus multilocularis***. *International Journal for Parasitology* 2008, **38**(2):161-176.
100. Zavala-Góngora R, Kroner A, Wittek B, Knaus P, Brehm K: **Identification and characterisation of two distinct Smad proteins from the fox-tapeworm *Echinococcus multilocularis***. *International Journal for Parasitology* 2003, **33**(14):1665-1677.
101. Köhler P: **The biochemical basis of anthelmintic action and resistance**. *International Journal for Parasitology* 2001, **31**(4):336-345.
102. Eibl H, Unger C: **Hexadecylphosphocholine: a new and selective antitumor drug**. *Cancer Treat Rev* 1990, **17**(2-3):233-242.
103. Seifert K, Duchene M, Wernsdorfer WH, Kollaritsch H, Scheiner O, Wiedermann G, Hottkowitz T, Eibl H: **Effects of miltefosine and other alkylphosphocholines on human intestinal parasite *Entamoeba histolytica***. *Antimicrob Agents Chemother* 2001, **45**(5):1505-1510.
104. Gasteiger E, Gattiker A, Hoogland C, Ivanyi I, Appel RD, Bairoch A: **ExpASY: The proteomics server for in-depth protein knowledge and analysis**. *Nucleic Acids Res* 2003, **31**(13):3784-3788.
105. Hanks S, Hunter T: **Protein kinases 6. The eukaryotic protein kinase superfamily: kinase (catalytic) domain structure and classification**. *FASEB J* 1995, **9**(8):576-596.
106. Schultz J, Milpetz F, Bork P, Ponting CP: **SMART, a simple modular architecture research tool: identification of signaling domains**. *Proc Natl Acad Sci U S A* 1998, **95**(11):5857-5864.
107. Bell M, Capone R, Pashtan I, Levitzki A, Engelberg D: **Isolation of hyperactive mutants of the MAPK p38/Hog1 that are independent of MAPK kinase activation**. *J Biol Chem* 2001, **276**(27):25351-25358.
108. Bell M, Engelberg D: **Phosphorylation of Tyr-176 of the yeast MAPK Hog1/p38 is not vital for Hog1 biological activity**. *J Biol Chem* 2003, **278**(17):14603-14606.
109. Diskin R, Lebendiker M, Engelberg D, Livnah O: **Structures of p38alpha active mutants reveal conformational changes in L16 loop that induce autophosphorylation and activation**. *J Mol Biol* 2007, **365**(1):66-76.
110. Tanoue T, Nishida E: **Docking interactions in the mitogen-activated protein kinase cascades**. *Pharmacol Ther* 2002, **93**(2-3):193-202.
111. Lee JC, Laydon JT, McDonnell PC, Gallagher TF, Kumar S, Green D, McNulty D, Blumenthal MJ, Heys JR, Landvatter SW *et al*: **A protein kinase involved in the regulation of inflammatory cytokine biosynthesis**. *Nature* 1994, **372**(6508):739-746.
112. Kammerer B, Scheible H, Albrecht W, Gleiter CH, Laufer S: **Pharmacokinetics of ML3403 ({4-[5-(4-fluorophenyl)-2-methylsulfanyl-3H-imidazol-4-yl]-pyridin-2-yl}-(1-phenylethyl)-amine), a 4-Pyridinylimidazole-type p38 mitogen-activated protein kinase inhibitor**. *Drug Metab Dispos* 2007, **35**(6):875-883.
113. Stettler M, Siles-Lucas M, Sarciron E, Lawton P, Gottstein B, Hemphill A: ***Echinococcus multilocularis* alkaline phosphatase as a marker for metacestode damage induced by in vitro drug treatment with albendazole sulfoxide and albendazole sulfone**. *Antimicrob Agents Chemother* 2001, **45**(8):2256-2262.
114. Gillies RJ, Didier N, Denton M: **Determination of cell number in monolayer cultures**. *Anal Biochem* 1986, **159**(1):109-113.
115. Hilgard P, Klenner T, Stekar J, Nossner G, Kutscher B, Engel J: **D-21266, a new heterocyclic alkylphospholipid with antitumour activity**. *Eur J Cancer* 1997, **33**(3):442-446.

116. van Blitterswijk WJ, Verheij M: **Anticancer alkylphospholipids: mechanisms of action, cellular sensitivity and resistance, and clinical prospects.** *Curr Pharm Des* 2008, **14**(21):2061-2074.
117. Croft SL, Snowdon D, Yardley V: **The activities of four anticancer alkyllysophospholipids against *Leishmania donovani*, *Trypanosoma cruzi* and *Trypanosoma brucei*.** *J Antimicrob Chemother* 1996, **38**(6):1041-1047.
118. Kuhlencord A, Maniera T, Eibl H, Unger C: **Hexadecylphosphocholine: oral treatment of visceral leishmaniasis in mice.** *Antimicrob Agents Chemother* 1992, **36**(8):1630-1634.
119. Alessi DR, Saito Y, Campbell DG, Cohen P, Sithanandam G, Rapp U, Ashworth A, Marshall CJ, Cowley S: **Identification of the sites in MAP kinase kinase-1 phosphorylated by p74raf-1.** *Embo J* 1994, **13**(7):1610-1619.
120. Puntervoll P, Linding R, Gemund C, Chabanis-Davidson S, Mattingsdal M, Cameron S, Martin DM, Ausiello G, Brannetti B, Costantini A *et al*: **ELM server: A new resource for investigating short functional sites in modular eukaryotic proteins.** *Nucleic Acids Res* 2003, **31**(13):3625-3630.
121. Siles-Lucas M, Felleisen RS, Hemphill A, Wilson W, Gottstein B: **Stage-specific expression of the 14-3-3 gene in *Echinococcus multilocularis*.** *Mol Biochem Parasitol* 1998, **91**(2):281-293.
122. Spiliotis M, Tappe D, Brückner S, Mösch H-U, Brehm K: **Molecular cloning and characterization of Ras- and Raf-homologues from the fox-tapeworm *Echinococcus multilocularis*.** *Molecular and Biochemical Parasitology* 2005, **139**(2):225-237.
123. Spiliotis M, Brehm K: ***Echinococcus multilocularis*: identification and molecular characterization of a Ral-like small GTP-binding protein.** *Experimental Parasitology* 2004, **107**(3-4):163-172.
124. Orian-Rousseau V, Morrison H, Matzke A, Kastilan T, Pace G, Herrlich P, Ponta H: **Hepatocyte growth factor-induced Ras activation requires ERM proteins linked to both CD44v6 and F-actin.** *Mol Biol Cell* 2007, **18**(1):76-83.
125. Baumgartner M, Sillman AL, Blackwood EM, Srivastava J, Madson N, Schilling JW, Wright JH, Barber DL: **The Nck-interacting kinase phosphorylates ERM proteins for formation of lamellipodium by growth factors.** *Proc Natl Acad Sci U S A* 2006, **103**(36):13391-13396.
126. Yonemura S, Tsukita S: **Direct involvement of ezrin/radixin/moesin (ERM)-binding membrane proteins in the organization of microvilli in collaboration with activated ERM proteins.** *J Cell Biol* 1999, **145**(7):1497-1509.
127. Hanke JH, Gardner JP, Dow RL, Changelian PS, Brissette WH, Weringer EJ, Pollok BA, Connelly PA: **Discovery of a novel, potent, and Src family-selective tyrosine kinase inhibitor. Study of Lck- and FynT-dependent T cell activation.** *J Biol Chem* 1996, **271**(2):695-701.
128. Xu X, Shen J, Mall JW, Myers JA, Huang W, Blinder L, Saclarides TJ, Williams JW, Chong AS: **In vitro and in vivo antitumor activity of a novel immunomodulatory drug, leflunomide: mechanisms of action.** *Biochem Pharmacol* 1999, **58**(9):1405-1413.
129. Liebmann C: **Regulation of MAP kinase activity by peptide receptor signalling pathway: paradigms of multiplicity.** *Cell Signal* 2001, **13**(11):777-785.
130. Boonstra J, Rijken P, Humbel B, Cremers F, Verkleij A, van Bergen en Henegouwen P: **The epidermal growth factor.** *Cell Biol Int* 1995, **19**(5):413-430.
131. Mullhaupt B, Feren A, Fodor E, Jones A: **Liver expression of epidermal growth factor RNA. Rapid increases in immediate-early phase of liver regeneration.** *J Biol Chem* 1994, **269**(31):19667-19670.
132. Giraud AS: **X. Trefoil peptide and EGF receptor/ligand transgenic mice.** *Am J Physiol Gastrointest Liver Physiol* 2000, **278**(4):G501-506.
133. Fausto N, Laird AD, Webber EM: **Liver regeneration. 2. Role of growth factors and cytokines in hepatic regeneration.** *Faseb J* 1995, **9**(15):1527-1536.
134. Knobloch J, Kunz W, Grevelding CG: **Quantification of DNA synthesis in multicellular organisms by a combined DAPI and BrdU technique.** *Dev Growth Differ* 2002, **44**(6):559-563.

135. Wilhelm SM, Carter C, Tang L, Wilkie D, McNabola A, Rong H, Chen C, Zhang X, Vincent P, McHugh M *et al*: **BAY 43-9006 exhibits broad spectrum oral antitumor activity and targets the RAF/MEK/ERK pathway and receptor tyrosine kinases involved in tumor progression and angiogenesis.** *Cancer Res* 2004, **64**(19):7099-7109.
136. Sebolt-Leopold JS, Dudley DT, Herrera R, Van Becelaere K, Wiland A, Gowan RC, Teclé H, Barrett SD, Bridges A, Przybranowski S *et al*: **Blockade of the MAP kinase pathway suppresses growth of colon tumors in vivo.** *Nat Med* 1999, **5**(7):810-816.
137. Koziczak M, Holbro T, Hynes NE: **Blocking of FGFR signaling inhibits breast cancer cell proliferation through downregulation of D-type cyclins.** *Oncogene* 2004, **23**(20):3501-3508.
138. Zaman GJ, Vink PM, van den Doelen AA, Veeneman GH, Theunissen HJ: **Tyrosine kinase activity of purified recombinant cytoplasmic domain of platelet-derived growth factor beta-receptor (beta-PDGFR) and discovery of a novel inhibitor of receptor tyrosine kinases.** *Biochem Pharmacol* 1999, **57**(1):57-64.
139. Fry DW, Bridges AJ, Denny WA, Doherty A, Greis KD, Hicks JL, Hook KE, Keller PR, Leopold WR, Loo JA *et al*: **Specific, irreversible inactivation of the epidermal growth factor receptor and erbB2, by a new class of tyrosine kinase inhibitor.** *Proc Natl Acad Sci U S A* 1998, **95**(20):12022-12027.
140. Baltensperger K, Lewis RE, Woon CW, Vissavajhala P, Ross AH, Czech MP: **Catalysis of serine and tyrosine autophosphorylation by the human insulin receptor.** *Proc Natl Acad Sci U S A* 1992, **89**(17):7885-7889.
141. Saperstein R, Vicario PP, Strout HV, Brady E, Slater EE, Greenlee WJ, Ondeyka DL, Patchett AA, Hangauer DG: **Design of a selective insulin receptor tyrosine kinase inhibitor and its effect on glucose uptake and metabolism in intact cells.** *Biochemistry* 1989, **28**(13):5694-5701.
142. Vicogne J, Cailliau K, Tulasne D, Browaeys E, Yan YT, Fafeur V, Vilain JP, Legrand D, Trolet J, Dissous C: **Conservation of epidermal growth factor receptor function in the human parasitic helminth *Schistosoma mansoni*.** *J Biol Chem* 2004, **279**(36):37407-37414.
143. Haccard O, Lewellyn A, Hartley RS, Erikson E, Maller JL: **Induction of *Xenopus* oocyte meiotic maturation by MAP kinase.** *Dev Biol* 1995, **168**(2):677-682.
144. Lee JC, Kumar S, Griswold DE, Underwood DC, Votta BJ, Adams JL: **Inhibition of p38 MAP kinase as a therapeutic strategy.** *Immunopharmacology* 2000, **47**(2-3):185-201.
145. Askari N, Diskin R, Avitzour M, Capone R, Livnah O, Engelberg D: **Hyperactive variants of p38alpha induce, whereas hyperactive variants of p38gamma suppress, activating protein 1-mediated transcription.** *J Biol Chem* 2007, **282**(1):91-99.
146. Cuenda A, Rousseau S: **p38 MAP-kinases pathway regulation, function and role in human diseases.** *Biochim Biophys Acta* 2007, **1773**(8):1358-1375.
147. Salvador JM, Mittelstadt PR, Guszczynski T, Copeland TD, Yamaguchi H, Appella E, Fornace AJ, Jr., Ashwell JD: **Alternative p38 activation pathway mediated by T cell receptor-proximal tyrosine kinases.** *Nat Immunol* 2005, **6**(4):390-395.
148. Laufer SA, Wagner GK, Kotschenreuther DA, Albrecht W: **Novel substituted pyridinyl imidazoles as potent anticytokine agents with low activity against hepatic cytochrome P450 enzymes.** *J Med Chem* 2003, **46**(15):3230-3244.
149. Gum RJ, McLaughlin MM, Kumar S, Wang Z, Bower MJ, Lee JC, Adams JL, Livi GP, Goldsmith EJ, Young PR: **Acquisition of sensitivity of stress-activated protein kinases to the p38 inhibitor, SB 203580, by alteration of one or more amino acids within the ATP binding pocket.** *J Biol Chem* 1998, **273**(25):15605-15610.
150. Fox T, Coll JT, Xie X, Ford PJ, Germann UA, Porter MD, Pazhanisamy S, Fleming MA, Galullo V, Su MS *et al*: **A single amino acid substitution makes ERK2 susceptible to pyridinyl imidazole inhibitors of p38 MAP kinase.** *Protein Sci* 1998, **7**(11):2249-2255.
151. Rey A, Manen D, Rizzoli R, Ferrari SL, Caverzasio J: **Evidences for a role of p38 MAP kinase in the stimulation of alkaline phosphatase and matrix mineralization induced by parathyroid hormone in osteoblastic cells.** *Bone* 2007, **41**(1):59-67.

152. Caverzasio J, Manen D: **Essential role of Wnt3a-mediated activation of mitogen-activated protein kinase p38 for the stimulation of alkaline phosphatase activity and matrix mineralization in C3H10T1/2 mesenchymal cells.** *Endocrinology* 2007, **148**(11):5323-5330.
153. Wei S, Daniel BJ, Brumlik MJ, Burow ME, Zou W, Khan IA, Wadsworth S, Siekierka J, Curiel TJ: **Drugs designed to inhibit human p38 mitogen-activated protein kinase activation treat *Toxoplasma gondii* and *Encephalitozoon cuniculi* infection.** *Antimicrob Agents Chemother* 2007, **51**(12):4324-4328.
154. Tran Quang C, Gautreau A, Arpin M, Treisman R: **Ezrin function is required for ROCK-mediated fibroblast transformation by the Net and Dbl oncogenes.** *Embo J* 2000, **19**(17):4565-4576.
155. Tamma G, Procino G, Svelto M, Valenti G: **Hypotonicity causes actin reorganization and recruitment of the actin-binding ERM protein moesin in membrane protrusions in collecting duct principal cells.** *Am J Physiol Cell Physiol* 2007, **292**(4):C1476-1484.
156. Krieg J, Hunter T: **Identification of the two major epidermal growth factor-induced tyrosine phosphorylation sites in the microvillar core protein ezrin.** *J Biol Chem* 1992, **267**(27):19258-19265.
157. Ng T, Parsons M, Hughes WE, Monypenny J, Zicha D, Gautreau A, Arpin M, Gschmeissner S, Verveer PJ, Bastiaens PI *et al*: **Ezrin is a downstream effector of trafficking PKC-integrin complexes involved in the control of cell motility.** *Embo J* 2001, **20**(11):2723-2741.
158. Srivastava J, Elliott BE, Louvard D, Arpin M: **Src-dependent ezrin phosphorylation in adhesion-mediated signaling.** *Mol Biol Cell* 2005, **16**(3):1481-1490.
159. Elliott BE, Qiao H, Louvard D, Arpin M: **Co-operative effect of c-Src and ezrin in deregulation of cell-cell contacts and scattering of mammary carcinoma cells.** *J Cell Biochem* 2004, **92**(1):16-28.
160. Steinberg SF: **Distinctive activation mechanisms and functions for protein kinase Cdelta.** *Biochem J* 2004, **384**(Pt 3):449-459.
161. Su YC, Han J, Xu S, Cobb M, Skolnik EY: **NIK is a new Ste20-related kinase that binds NCK and MEKK1 and activates the SAPK/JNK cascade via a conserved regulatory domain.** *Embo J* 1997, **16**(6):1279-1290.
162. Tanaka M, Gupta R, Mayer BJ: **Differential inhibition of signaling pathways by dominant-negative SH2/SH3 adapter proteins.** *Mol Cell Biol* 1995, **15**(12):6829-6837.
163. Thoresen GH, Guren TK, Sandnes D, Peak M, Agius L, Christoffersen T: **Response to transforming growth factor alpha (TGFalpha) and epidermal growth factor (EGF) in hepatocytes: lower EGF receptor affinity of TGFalpha is associated with more sustained activation of p42/p44 mitogen-activated protein kinase and greater efficacy in stimulation of DNA synthesis.** *J Cell Physiol* 1998, **175**(1):10-18.
164. Brabyn CJ, Kleine LP: **EGF causes hyperproliferation and apoptosis in T51B cells: involvement of high and low affinity EGFR binding sites.** *Cell Signal* 1995, **7**(2):139-150.
165. Kamer AR, Sacks PG, Vladutiu A, Liebow C: **EGF mediates multiple signals: dependence on the conditions.** *Int J Mol Med* 2004, **13**(1):143-147.
166. Fanger GR, Widmann C, Porter AC, Sather S, Johnson GL, Vaillancourt RR: **14-3-3 proteins interact with specific MEK kinases.** *J Biol Chem* 1998, **273**(6):3476-3483.
167. Bardwell AJ, Abdollahi M, Bardwell L: **Docking sites on mitogen-activated protein kinase (MAPK) kinases, MAPK phosphatases and the Elk-1 transcription factor compete for MAPK binding and are crucial for enzymic activity.** *Biochem J* 2003, **370**(Pt 3):1077-1085.
168. Biondi RM, Nebreda AR: **Signalling specificity of Ser/Thr protein kinases through docking-site-mediated interactions.** *Biochem J* 2003, **372**(Pt 1):1-13.
169. Xu B, Wilsbacher JL, Collisson T, Cobb MH: **The N-terminal ERK-binding site of MEK1 is required for efficient feedback phosphorylation by ERK2 in vitro and ERK activation in vivo.** *J Biol Chem* 1999, **274**(48):34029-34035.
170. Alessandrini A, Greulich H, Huang W, Erikson RL: **Mek1 phosphorylation site mutants activate Raf-1 in NIH 3T3 cells.** *J Biol Chem* 1996, **271**(49):31612-31618.

-
171. Mansour SJ, Matten WT, Hermann AS, Candia JM, Rong S, Fukasawa K, Vande Woude GF, Ahn NG: **Transformation of mammalian cells by constitutively active MAP kinase kinase.** *Science* 1994, **265**(5174):966-970.
172. Welch DR, Sakamaki T, Pioquinto R, Leonard TO, Goldberg SF, Hon Q, Erikson RL, Rieber M, Rieber MS, Hicks DJ *et al*: **Transfection of constitutively active mitogen-activated protein/extracellular signal-regulated kinase kinase confers tumorigenic and metastatic potentials to NIH3T3 cells.** *Cancer Res* 2000, **60**(6):1552-1556.
173. Cha H, Lee EK, Shapiro P: **Identification of a C-terminal region that regulates mitogen-activated protein kinase kinase-1 cytoplasmic localization and ERK activation.** *J Biol Chem* 2001, **276**(51):48494-48501.
174. Yu C, Bruzek LM, Meng XW, Gores GJ, Carter CA, Kaufmann SH, Adjei AA: **The role of Mcl-1 downregulation in the proapoptotic activity of the multikinase inhibitor BAY 43-9006.** *Oncogene* 2005, **24**(46):6861-6869.
175. Bain J, Plater L, Elliott M, Shpiro N, Hastie CJ, McLauchlan H, Klevernic I, Arthur JS, Alessi DR, Cohen P: **The selectivity of protein kinase inhibitors: a further update.** *Biochem J* 2007, **408**(3):297-315.
176. Delaney AM, Printen JA, Chen H, Fauman EB, Dudley DT: **Identification of a novel mitogen-activated protein kinase kinase activation domain recognized by the inhibitor PD 184352.** *Mol Cell Biol* 2002, **22**(21):7593-7602.
177. Reuter S, Manfras B, Merkle M, Harter G, Kern P: **In vitro activities of itraconazole, methiazole, and nitazoxanide versus Echinococcus multilocularis larvae.** *Antimicrob Agents Chemother* 2006, **50**(9):2966-2970.
178. Kuo WL, Duke CJ, Abe MK, Kaplan EL, Gomes S, Rosner MR: **ERK7 expression and kinase activity is regulated by the ubiquitin-proteasome pathway.** *J Biol Chem* 2004, **279**(22):23073-23081.
179. Gelmedin V, Caballero-Gamiz R, Brehm K: **Characterization and inhibition of a p38-like mitogen-activated protein kinase (MAPK) from Echinococcus multilocularis: antiparasitic activities of p38 MAPK inhibitors.** *Biochem Pharmacol* 2008, **76**(9):1068-1081.
180. Stins MF, Gilles F, Kim KS: **Selective expression of adhesion molecules on human brain microvascular endothelial cells.** *J Neuroimmunol* 1997, **76**(1-2):81-90.

9. Publications

Original articles in peer reviewed journals

Gelmedin V, Spiliotis M, Brehm K

"Molecular Characterization of two mitogen activated protein kinase kinases in the cestode *Echinococcus multilocularis*"

Manuscript in preparation

Gelmedin V, Caballero-Gamiz R, Brehm K

"Characterization and inhibition of a p38-like mitogen activated protein kinase (MAPK) from *Echinococcus multilocularis*: antiparasitic activities of p38 MAPK inhibitors"

Biochem Pharmacol, **2008** Oct 30; 76(9):1068-81

Zavala-Gongora R, Derrer B, **Gelmedin V**, Knaus P, Brehm K.

"Molecular characterisation of a second structurally unusual AR-Smad without an MH1 domain and a Smad4 orthologue from *Echinococcus multilocularis*"

Int J Parasitol, **2007** Feb; 38(2):161-76

Spiliotis M, Konrad C, **Gelmedin V**, Tappe D, Bruckner S, Mosch HU, Brehm K. Characterisation of "EmMPK1, an ERK-like MAP kinase from *Echinococcus multilocularis* which is activated in response to human epidermal growth factor"

Int J Parasitol, **2006** Sep; 36(10-11):1097-112

Gelmedin V, Zavala-Gongora R, Fernandez C, Brehm K.

"*Echinococcus multilocularis*: cloning and characterisation of a member of the SNW/SKIP family of transcriptional coregulators" *Exp Parasitol*, **2005** Oct; 111(2):115-20

Abstracts

Gelmedin V, Caballero-Gamiz R, Brehm K

"EmMPK2, the p38 MAP kinase orthologue of *Echinococcus multilocularis*, as a target for anti-parasitic chemotherapy"

Annual Meeting of the German Society for Parasitology, Hamburg, Germany, **2008** March 4-7

Gelmedin V, Brehm K

"Targeting the signaling cascades of *Echinococcus multilocularis* for the development of anthelmintic drugs"

Status workshop of the German Society for Hygiene and Microbiology, Section "Eukaryotic Pathogens", Würzburg, Germany, **2008** Feb 15-16

Brehm K, Konrad C, Zavala-Gongora R, Spiliotis M, **Gelmedin V**, Hemphill A, Epping K, Schäfer T

"Host hormones and cytokines affect *Echinococcus multilocularis* development through activation of evolutionary conserved receptor tyrosine and receptor serine/ threonine signaling systems"

22nd International Congress of Hydatidology, Athens, Greece, May **2007** 15-19

Gelmedin V, Caballero-Gamiz R, Brehm K

"EmMPK2, the p38 MAPK kinase orthologue from *Echinococcus multilocularis*, as a possible target for anti-parasitic chemotherapy"

Status workshop of the German Society for Hygiene and Microbiology, Section "Eukaryotic Pathogens", Stuttgart, Germany, **2007** Feb 23-24

Brehm K, Spiliotis M, Zavala-Gongora R, Konrad C, **Gelmedin V**, Schäfer T, Epping K

"Hormonal crosstalk between parasite and host in alveolar echinococcosis"

Annual Meeting of the German Society for Hygiene and Microbiology, Würzburg, Germany, Oct 1- 4 **2006**

Gelmedin V, Caballero-Gamiz R, Spiliotis M, Brehm K

"EmMPK2, the p38 MAPK kinase orthologue from *Echinococcus multilocularis*, as a possible target for anti-parasitic chemotherapy"

Annual Meeting of the German Society for Hygiene and Microbiology, Würzburg, Germany, **2006** Oct 1- 4

Schäfer T, **Gelmedin V**, Fernandez C, Brehm K

"Molecular characterization of a fibroblast growth factor receptor orthologue from *Echinococcus multilocularis*"

Annual Meeting of the German Society for Hygiene and Microbiology, Würzburg, Germany, **2006** Oct 1- 4

Gelmedin V, Günthel D, Brehm K.

"Characterisation of nuclear hormone receptor signalling components in *Echinococcus multilocularis*"

Annual Meeting of the German Society for Parasitology, Vienna, Austria, **2006** Feb 22- 25

Brehm K, Spiliotis M, Zavala-Gongora R, Konrad C, Caballero-Gamiz R, Kroner A, **Gelmedin V**

"Receptor kinases and the MAP kinase cascade of *Echinococcus multilocularis* as possible targets for chemotherapy"

6th Drug Development Seminar on Antiparasitic Chemotherapy, Bernhardt-Nocht-Institute for Tropical Medicine, Hamburg, Germany, **2005** April 28 -29

10. Curriculum vitae

- May 2008 to date Research associate
Institute of Hygiene and Microbiology, University of Würzburg, Germany
- Topic: *Host-pathogen interaction: Analysis of mechanisms involved in the crossing of the blood-brain-barrier by Neisseria meningitides*
PI: Alexandra Schubert-Unkmeir
- May 2005 - April 2008 PhD studies
Institute of Hygiene and Microbiology, University of Würzburg, Germany
- Thesis: *Targeting flatworm signaling cascades for the development of novel anthelmintic drugs*
PI: Klaus Brehm
- Funding by the international graduate college Würzburg-Nice 1141:
Signal transduction: where cancer and infections converge
- Oct 1999 – March 2005 Diploma studies
- Undergraduate studies in Biology
Philipps University, Marburg, Germany
- Diploma studies in Microbiology, Biochemistry and Biotechnology
Julius-Maximilians-University, Würzburg, Germany
- Thesis: *Molecular characterization of nuclear hormone receptors from the fox tapeworm Echinococcus multilocularis*
PI: Klaus Brehm
- Sep 1998 - Aug 1999 Voluntary year of social service, Universical Clinic of Freiburg, Germany
- Aug 1985 - June 1998 School education
- Gymnasium Marienschule, Saarbrücken, Germany
Abitur (A-level)
- Grundschule St. Barbara, Saarbrücken, Germany

Würzburg, 2008 December

Verena Gelmedin